# UNIVERSITÉ DE STRASBOURG

***ÉCOLE DOCTORALE 222***

**UMR 7140**

# **THÈSE** présentée par :


## Emma THOMÉE


soutenue le : **20 Septembre 2021**

Pour obtenir le grade de : **Docteur de l'université de Strasbourg**

Discipline/ Spécialité : Chimie

# Development of thermoplastic elastomer microfluidic systems for bio-applications

**THÈSE dirigée par :**

M. HERMANS Thomas — Professeur, Université de Strasbourg

**RAPPORTEURS :**

M. BARET Jean-Christophe — Professeur, Université de Bordeaux

M. MONTEL Fabien — Docteur, Ecole Normale Supérieure de Lyon

---

**AUTRES MEMBRES DU JURY :**

M. ROUET Philippe — Docteur, INSERM Toulouse

Mme. LEBRAS-JASMIN Guénaëlle — Docteur, CEA Paris-Saclay

M. LESHER-PEREZ Sasha Cai — Docteur, Intelligent Optical Systems

Emma THOMÉE

# Development of thermoplastic elastomer microfluidic systems for bio-applications


## Résumé

Depuis son apparition, la technologie microfluidique s'est révélée être un outil puissant en biologie. La manipulation de fluides dans des géométries à l'échelle du micron avec un contrôle fluidique de précision permet l'analyse de cellules cultivées à un débit amélioré et à un coût réduit. Il est nécessaire de trouver de nouveaux matériaux pour le prototypage de dispositifs microfluidiques au-delà du polydiméthylsiloxane (PDMS), afin de combler le fossé entre la microfluidique dans des contextes de recherche à petite échelle et la production industrielle à grande échelle. Les inconvénients associés aux dispositifs en PDMS pour les applications de biologie cellulaire et les organes-sur-puce encouragent la transition vers d'autres matériaux de fabrication. Cette thèse présente une évaluation de nouveaux élastomères thermoplastiques souples et le développement de nouvelles techniques de fabrication pour le prototypage de dispositifs microfluidiques pour des applications biomédicals. Nous démontrons l'utilité des élastomères thermoplastiques souples pour la fabrication transférable de systèmes microfluidiques pour la biologie cellulaire.


**Mots clés :** microfluidique, élastomère thermoplastique, lab-on-a-chip, micro dispositifs biomédicaux, organe-sur-puce


## Résumé en anglais

Since its emergence, microfluidic technology has been demonstrated to be a powerful tool in biology and the life sciences. Manipulation of fluids in micron-scale geometries with precision fluidic control enables analysis of cultured cells at improved throughput and reduced cost. However, there is a need for new materials for microfluidic device prototyping, beyond polydimethylsiloxane (PDMS), to bridge the gap between microfluidics in small-scale research settings and large-scale industrial production. Drawbacks associated with PDMS devices for cell biological applications and organ-on-a-chip are further encouraging a transition to alternative fabrication materials. This thesis presents an evaluation of novel soft thermoplastic elastomers and the development of new fabrication techniques for prototyping of microfluidic devices for bio-applications. We demonstrate the utility of soft thermoplastic elastomers for rapid and transferable device fabrication of microfluidic systems for cell biology research.


**Keywords:** microfluidics, thermoplastic elastomer, lab-on-a-chip, biomedical microdevices, organ-on-a-chip

# Acknowledgements

To my academic supervisor Thomas Hermans for giving me the opportunity to present my work at the University of Strasbourg, and for his guidance throughout this project.

To my co-supervisors (in chorological order): Walter Minnella, Noemi Thomazo and Aurélie Vigne for their continuous support and encouragement every day.

To my co-supervisor, mentor and friend Sasha Cai Lesher-Pérez for providing invaluable advice, ideas and discussions, and for his infinite generosity and enthusiasm to teach and inspire. His scientific guidance has been crucial for the completion of this project as well as for my development as an independent researcher.

To Guénaëlle Lebras-Jasmin, Karla Perez Toralla, Claude Fermon and Lourdes Basabe-Desmonts for welcoming me in their groups during my secondments. It was a privilege to have had the opportunity to learn from them.

To my co-workers and friends, Alex and Alessandra for the great collaborations and discussions and all the good times. I am so grateful to have shared this experience with them and for their friendship.

To Lisa, Jessica, Julia, Christa and the rest of the Elvesys team, for all the support and good times.

To the European Union for the financial support of the Horizon 2020 Marie Sklodowska Curie project, MAMI.

And last but not least, to my flatmate Camille for the year we spent working from home in our tiny Parisian apartment during the COVID-19 pandemic, and to my family and friends for all their love and support.

Thank you!

Emma

# List of abbreviations

| | |
|---|---|
| 2D | two-dimensional |
| 3D | three-dimensional |
| AFM | atomic force microscopy |
| ANOVA | analysis of variance |
| ApoO | apolipoprotein O |
| BSA | bovine serum albumin |
| CHO | Chinese hamster ovarian |
| COP | cyclic olefin polymer |
| COC | cyclic olefin copolymer |
| DI | deionized |
| DMEM | Dulbecco's Modified Eagle Medium |
| E | ethylene |
| EB | ethylene-butylene |
| ECM | extra cellular matrix |
| FEP | fluorinated ethylene- propylene |
| FEPM | tetrafluoroethylene |
| FD | FlexDym™ |
| GFP | green fluorescent protein |
| HDF | human dermal fibroblasts |
| Hf MSC | hair follicle-derived mesenchymal stroma cells |
| HFP | hexafluoropropylene |
| HUVEC | human umbilical vein endothelial cells |
| ICAM-1 | intercellular adhesion molecule 1 |
| ID | inner diameter |

| | |
|---|---|
| IPSC | induced pluripotent stem cells |
| MEMS | microelectromechanical systems |
| OD | outer diameter |
| OOC | organ-on-a-chip |
| OSTE | off-stoichiometry thiole-ene |
| OSTE+ | off-stoichiometry thiole-ene-epoxy |
| PBS | phosphate saline buffer |
| PC | polycarbonate |
| PDMS | polydimethylsiloxane |
| PEEK | poly ether ketone |
| PFA | paraformaldehyde |
| PFPE | perfluoropolyether |
| PMMA | poly (methyl methacrylate) |
| PTFE | polytetrafluoroethylene |
| RE | Reynold |
| ROS | reactive oxygen species |
| RPM | revolutions per minute |
| SEBS | styrene-ethylene-butylene-styrene |
| sTPE | soft thermoplastic elastomer |
| TEER | trans-epithelial/endothelial electrical resistance |
| TFE | tetrafluoroethylene |
| $T_g$ | glass transition temperature |

# Table of Contents

# Chapter 1. Introduction

**Abstract:** In this chapter, a brief introduction to microfluidics and its applications in cell culture and particularly organ-on-a-chip technology are presented. Moreover, we summarize the most common materials used for microfluidic device fabrication, including soft thermoplastic elastomers, and discuss their relative advantages and disadvantages for applications in microfluidic cell culture. Lastly, the aims and scope of the thesis together with a brief outline of the subsequent chapters are presented.

---

Parts of this chapter have been published:

* Dellaquila, A., Thomée, E., McMillan, A., Lesher-Pérez, S. Lung-on-a-chip platforms for modeling diesease pathogenesis, Hoeng, J., Bovard, D., Peitsch, M, Eds. Academic Press, 2020, pp. 133-180.

## 1.1 Introduction to microfluidics

Microfluidics refers to the physical phenomena and research domain involving manipulation of small volumes of fluids, from microliter down to femtoliters, in micron-scale geometries.[1] This is realized using a microfluidic device that incorporate a network of microfluidic channels, in which fluid can be manipulated by the integrated micropumps, capillary flow or external flow controllers such as syringe pumps or pressure controllers. The small geometries of a microfluidic channel result in a large surface-area-to-volume ratio. Thus, the influence of inertial forces will decrease compared to viscous forces, characterized by a low Reynolds number, resulting in highly predictable flows in the laminar regime (**Figure 1.1**).[2] Laminar flows can be leveraged for highly controlled delivery of e.g., chemical reagents, soluble factors or biological samples in and out of the system. The absence of convective forces in slow laminar flows results in mixing by means of diffusion which can be utilized to control mixing of fluids or defined gradients in microfluidic systems. Moreover, the small volumes of fluids inside the systems allow for rapid heat and mass transfer compared to macroscale fluidic systems.

The concept of "miniaturized Total Analysis Systems" (μTAS) was introduced in the early 90s, suggesting that microfluidic technology would enable development of fully integrated systems, μTAS, that could carry out all steps of an assay including sampling, sample preparation and transport, reactions, separation and detection, all inside a microfluidic system.[3] In addition, these systems would be fully automatable and enable massive parallelization of assays for ultra-high throughput. The often-used term "lab-on-a-chip" also refers to miniaturizing and integrating multiple laboratory functions on a microfluidic chip. These concepts have greatly influenced the field of microfluidics and the development towards the advanced microfluidic systems we have today.[4]

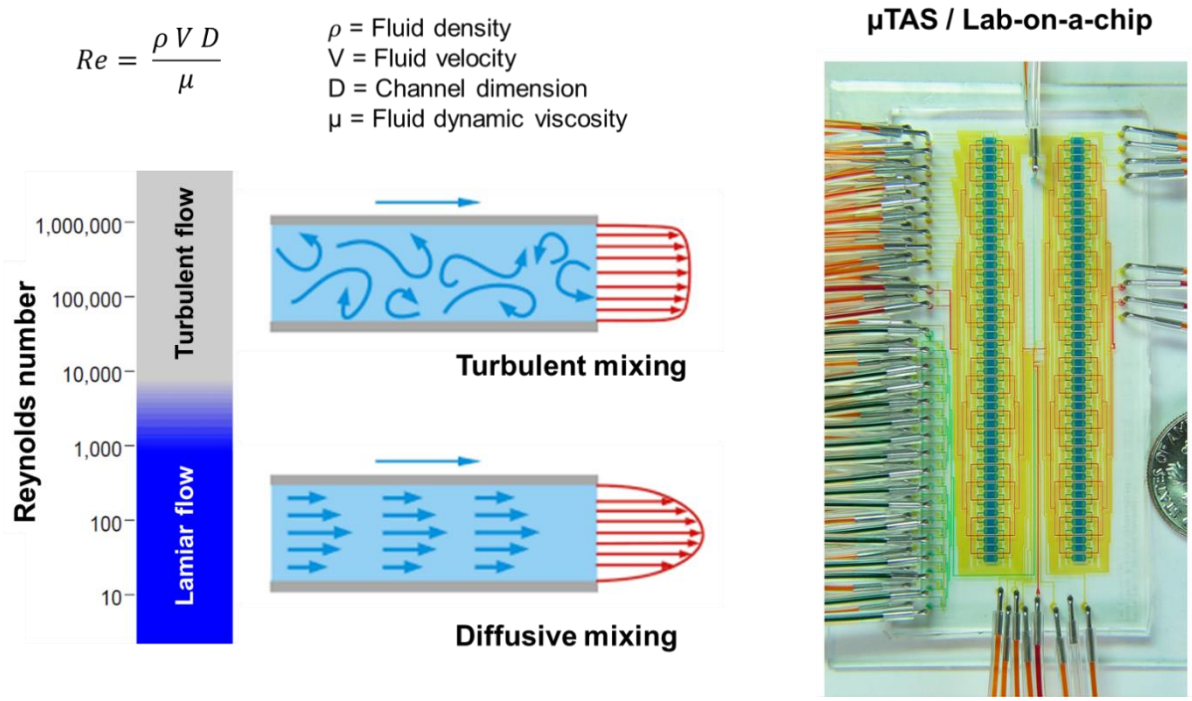


**Figure 1.1** Concepts in microfluidics. (Left) Reynolds number (Re) describes the ratio of inertial forces to viscous forces in a fluid flow. At high Reynolds numbers (Re > 3500) turbulent mixing occurs characterized by irregular movements of fluid particles. At low Reynolds numbers (Re < 2000) fluid flows are laminar, flow particles move in straight lines. As a result, mixing occurs only by diffusion. Laminar flows have a parabolic flow velocity profile with a maximum in the centre of the pipe. (Right) A microfluidic chip and its interconnections. Adapted from Gomez-Sjöberg et al.[5] with permission from American Chemical Society.

Microfluidic tools have gained particular attention in the field of life science, including a wide range of applications for biological analysis such as cell sorting and detection of rare cells [6], point-of-care diagnostics [7], single cell studies [8], DNA analysis [9] and high throughput screening for drug discovery [10]. The functionality of a microfluidic device is largely influenced by the material that makes up the device. In the following section, common materials for fabrication of microfluidic devices will be introduced.

## 1.2 Microfluidic materials and microfabrication

The selection of fabrication material is an important step of the design process of microfluidic devices. Microfluidic materials should be evaluated based on their fabrication processes and their material properties in order to create devices with desired functionalities for the specific application.

In this section we introduce the most common materials for fabrication of microfluidic devices and their respective fabrication processes. Polymers are here categorized into based on their physical properties into three groups – thermosets, elastomers and hard thermoplastics. We distinguish between the popular thermoset siloxane elastomer, PDMS, and thermoplastic elastomer. The material selection process and the relative advantages and disadvantages of the mentioned materials for cell-based applications will be discussed at the end of this chapter.

### 1.2.1 Inorganic materials

The earliest microfluidic devices were fabricated in glass or silicon, directly adopting microfabrication techniques from the semiconductor industry.[11,12] Glass capillaries had been used for chromatography and capillary electrophoresis [13], while silicon was used for fabrication of MEMS [14]. Silicon is transparent to infrared light but not visible light, which is a limitation for microfluidic applications that require optical detection. Glass, however, has excellent optical properties and consequently, silicon-glass hybrid devices are often used.

Microstructures in silica and glass are generally processed with photolithography techniques followed by wet or dry etching.[14,15] Briefly, a thin layer of photoresist is applied to the surface of the substrate and the photosensitive resist is selectively exposed with ultraviolet light through a photomask that transfers the micropattern to the resist. After developing the photoresist, the remaining pattern is used to guide the etching process to create microfluidic features. Glass is an amorphous material, and etching of glass thus results in channels with rounded side walls, while etching of crystalline silicon results in vertical channel walls. Bonding of device layers is commonly achieved through fusion bonding based on the silanol group (-Si-OH) of the silicon surface chemistry.[16]

From a fabrication standpoint, processing of inorganic materials is associated with high material costs and costly fabrication requiring cleanroom facilities of high maintenance, trained staff and dangerous chemicals, making it less accessible than polymer fabrication.[16] Consequently, the resulting devices are costly and not suitable for disposable use. However, for certain applications that require high temperature, pressure, thermal conductivity or chemical resistance, polymers fall short to inorganic materials. Silicon and glass also facilitate the integration of electrodes or electronic circuits and their high stiffness enable fabrication of structures of high-aspect ratios and excellent geometric definition.

### 1.2.2 Thermosets

Thermosets are thermosetting resins that irreversibly crosslink to form a rigid network upon exposure to heat or radiation. Once fully cured, thermosets cannot be reshaped. They are often characterized by high temperature- and solvent resistance, and high stiffness (although the mechanical properties vary greatly between different thermosets). Since before being introduced as microfluidic device materials [17], thermosets, such as SU-8, have been used as negative photoresists (as used in photolithography processes). Microfluidic devices can be fabricated from thermosets by several techniques, including replica molding, photolithography, 3D-printing and reaction injection molding. Thermoset polyesters are among the most used thermosets in microfluidics, and have been used for a range of microfluidic applications such as microchip electrophoresis.[18] Thermoset polyesters are transparent to light in the visible range, but absorbs UV light.[19]

Another alternative group of thermosets for microfluidic device fabrication, perfluoropolyethers (PFPEs) or "Liquid Teflon", were introduced by DeSimone and co-workers.[20] PFPE microfluidic devices are fabricated from an initial, partial UV cure, followed by complete curing to seal the device once it has been assembled. Several of PFPE-based microfluidic studies have been demonstrated, highlighting the value of soft, flexible and organic solvent resistant microfluidic devices.[21–23]

### 1.2.3 PDMS

It was following the introduction of PDMS-based microfluidic devices and its associated fabrication process, soft lithography, by Whitesides and co-workers in the 90s (several years after first devices in glass and silicon) that the field of microfluidics saw its breakthrough.[24,25] PDMS is a siloxane elastomer characterized by long polymer chains, low glass transition temperatures[26] and low shear modulus (250 Pa-range) [27], resulting in a flexible, elastic, rubberlike physical properties. PDMS is a two-part polymer which upon fabrication involves mixing of the monomer base with a crosslinking agent. The process of soft lithography is illustrated in **Figure 1.2**. Briefly, soft lithography involves casting of a liquid polymer over a master mold to replicate the pattern of the mold. The polymer is then cured and peeled off the master mold once fully cured. In the case of PDMS, the curing step can be accelerated through elevated temperatures, to a couple of hours.[28] The master mold can be created though photolithography techniques (as previously described) or micromachining techniques. PDMS can seal irreversibly to itself or to other materials, such as glass and silicone, by exposing the interfacing surfaces to plasma directly before bringing the

surfaces in conformal contact. The process of soft lithography enables prototyping of microfluidic devices at low cost without specialized equipment as required for processing inorganic materials. The historical significance of PDMS highlights the importance of facile and accessible fabrication techniques, that can be performed beyond sophisticated cleanroom facilities, for the scientific progression of microfluidics-based discoveries. Indeed, a significant drawback of PDMS fabrication is that the procedure which involves several manual steps such as mixing, degassing, casting and bonding, cannot straightforwardly be scaled up for high-throughput, industrial production.[29]

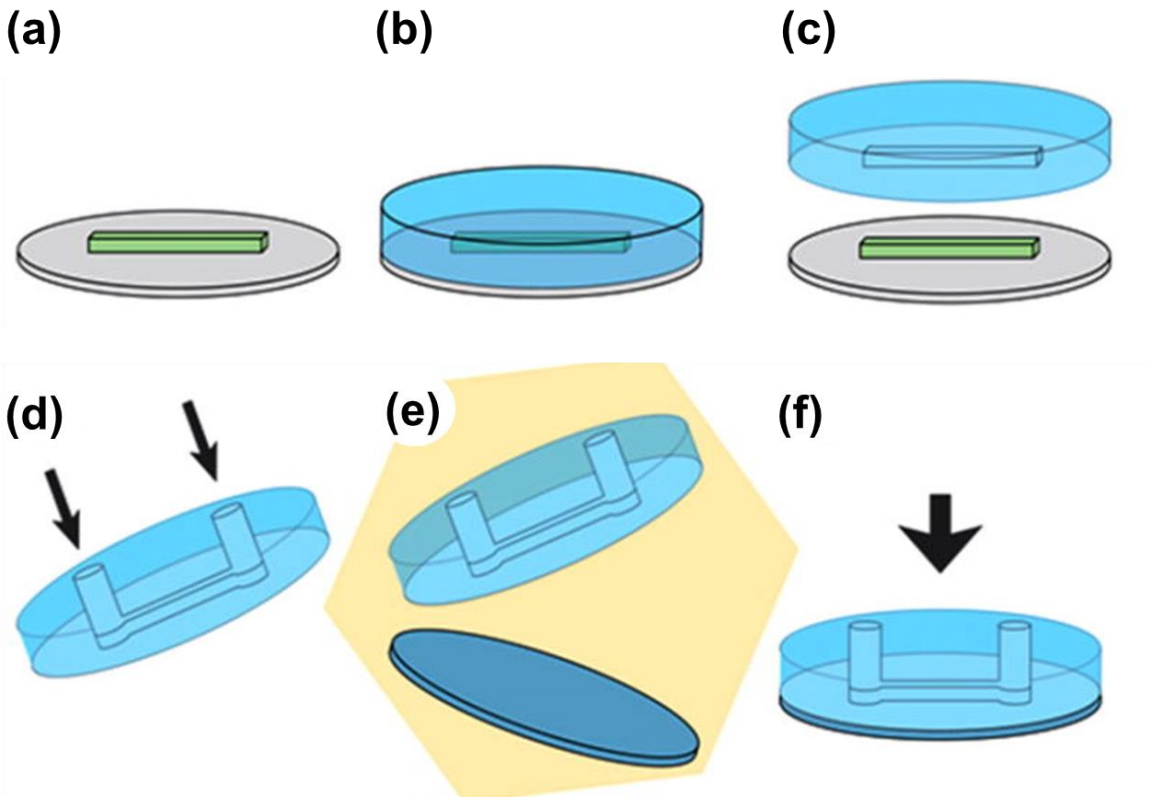


**Figure 1.2** PDMS soft lithography. The process, starting from a microfluidic mold (a), consists of the steps: (b) casting of PDMS over the microfluidic mold, (c) release of the PDMS replica, (d) punching holes for fluid interfacing, (e) plasma surface activation of the two device components (PDMS and a glass slide) and (f) device bonding by placing the plasma activated surfaces in conformal contact. Adapted from Velve-Casquillas et al.[30] with permission from Elsevier.

Importantly in microfluidics, flexible materials enable integration flexible components such as microvalves, micropumps or micromixers to perform complex on-chip manipulations.[31–33] Thin membranes (down to sub-micron scale), fabricated

by spin coating of the uncured polymer, have been central for the development of microfluidic systems for membrane-based cell culture.[34] Furthermore, PDMS has excellent optical transparency down to ~300 nm [35], a property highly desirable in microfluidic assays involving optical readout. Unlike silicon and glass, PDMS is permeable to gases, including oxygen, carbon dioxide and nitrogen [36], a property that has been leveraged to culture living cells that require exchange of gases for respiration in enclosed microfluidic systems [34]. The surface of PDMS is naturally hydrophobic. Surface hydrophobicity is generally an undesired feature could result in, for instance, non-specific adsorption of biomolecules and biofouling, and therefore limits the use of PDMS as analytical devices.[37] Several surface modifications have been suggested to render PDMS surfaces hydrophilic, among them oxygen plasma activation [38] being the most prevalent. However, due to the intrinsic polymer chain mobility, PDMS quickly recovers to a hydrophobic state.[39] PDMS is also largely incompatible with organic solvents[40] and absorbs small hydrophobic molecules [41,42].

### 1.2.4 Hard thermoplastics

Hard thermoplastics, such as polystyrene, polycarbonate (PC) and poly(methyl methacrylate) (PMMA), are readily available at low cost and widely used in industry. Thermoplastics are made up of un-crosslinked polymers, characterized by high stiffness and softening at their characteristic glass transition temperature ($T_g$). At the $T_g$ (unique to each material), thermoplastics are shapable and can be processed through thermo-moulding techniques, such as injection molding and hot-embossing, into microfluidic devices.[43] Alternatively, micromachining techniques, including 3D printing and micro milling, can be used to fabricate microfluidic devices of limited resolution and speed. Thermoplastics retain their shape as they cool down, but unlike PDMS, no curing occurs and thermoplastics can be reheated and reshaped multiple times.[44]

In contrast to replica molding techniques such as PDMS soft lithography, thermomoulding techniques are highly scalable and feasible on industrial scales at low-cost and high throughput. At small scales (such as in research laboratories), however, processing of hard thermoplastics is challenging and not economical. Specialized equipment and expensive molds that can withstand high temperatures are needed.[16] To this end, thermoplastic fabrication is less accessible for prototyping purposed, as a new mold is typically required each time the microchannel features must be changed. Moreover, device sealing is another challenge of thermoplastics microdevice fabrication. Bonding of plastics is commonly performed through thermal

bonding or solvent assisted bonding (or a combination of the two).[45] For thermal bonding, the interfacing surfaces are heated to near the $T_g$ before being pressed together. This enables diffusion of polymer chains over the interface, resulting in a strong bond once the device has cooled.[46,47] Solvent assisted bonding is performed by partly solubilizing the thermoplastic surface with an organic solvent, such as dimethyl sulfoxide, acetone or methanol, before bonding to another surface.[48,49] The intrinsic high stiffness or hard thermoplastics (tensile moduli in the order of ~1–4 GPa [50]), makes it difficult to achieve conformal contact between surfaces. Achieving strong bonding is thus a careful balance between applying enough pressure for thermal diffusion and applying too much pressure that will deform the microstructures. A more straight-forward approach to thermoplastic bonding is adhesive bonding, using solid or liquid adhesives. A few challenges associated with adhesive bonding are ensuring proper alignment of solid adhesive and thermoplastics and preventing liquid adhesives from clogging the channel structures.[45,51]

PMMA, PC and polystyrene are a few, among others, popular traditional thermoplastics for microfluidic device fabrication.[47,52,53] Compared to PDMS, many hard thermoplastics generally show more stable covalently modified surfaces and lower permeability to gases, but they are incompatible with organic solvents.[16] Cyclic olefin (co)polymers (COP/COC) make up a relatively newer class of polymers that has gained popularity presenting promising properties for microfluidic fabrication such as higher chemical resistance, biocompatibility and good optical transparency.[54] Thermoformable perfluorinated polymers, particularly perfluoroalkoxy (Teflon PFA) and fluorinated ethylenepropylene (Teflon FEP) have excellent resistance to organic solvents and anti-fouling properties thanks to their chemical inertness. Despite their high melting temperatures (above 280°C), they can effectively be thermo-processed to fabricate microfluidic devices.[55,56]

### 1.2.5 Soft thermoplastic elastomers

Recent advances in polymer engineering have provided a wide range of elastomers, tailored to meet specific requirements. Soft thermoplastic elastomers (sTPE) is a class of hybrid materials that exhibit both thermoplastic and elastic properties of variable degrees.[57] Due to their thermoplastic properties, sTPEs can be processed by melt processing like thermoplastics.[58–60] They also exhibit elastic behaviour that enable high deformability, similar to conventional (chemically crosslinked) elastomers such as PDMS. Several sTPE formulations are commercially available at low cost and can be purchased in the form of extruded sheets or pellets that can be processed for

microfluidic device fabrication. In contrast to hard thermoplastics, sTPE materials have low stiffness and they are flexible and readily form conformal contact to other surfaces. These properties facilitate microfabrication at laboratory scale compared to hard thermoplastics.

One sTPE formulation has recently been commercialized under the name FlexDym™, and been demonstrated to have properties desirable for a microfluidic material including optical transparency, low absorption of small molecules and low stiffness (Young's modulus of 1.15 MPa).[58,61] FlexDym™ is an oil-free block copolymer, based on molecules of the type S-EB-S, where S is polystyrene and EB is an elastomeric ethylene-butylene. Contrasting both PDMS and hard thermoplastics fabrication, the fabrication of sTPE devices is directly transferable from small- to large scale. Thanks to its flexibility, FlexDym™ can be micropatterned through hot-embossing using the same type of molds as for PDMS fabrication. Moreover, for large scale production, high throughput processing techniques such as roll to roll hot embossing or injection moulding can be envisioned.

The unique properties of sTPE elastomers are provided by their biphasic morphology, where the two phases retain many of the properties of their respective homopolymers. The polystyrene domains, present as a minor part of the total volume, provide the material with structural integrity, while the EB domains provide the elastomeric properties. The copolymer exhibits two distinct $T_g$, a positive $T_g$ (~100 °C) for the stiff polystyrene domains and a negative $T_g$ (~-70 °C) for the EB domains.[62] The negative $T_g$ allows mobility of the polymer chains at room temperature, which enables reversible thermal bonding.[61] Facile thermal bonding at low temperatures is a particularly beneficial characteristic of SEBS elastomers for microfluidic fabrication, as device sealing can be achieved by simple conformal contact at varying bonding time and temperature, without the need for adhesives, solvents or high temperatures.

## 1.3 Microfluidic cell culture

In vitro cell culture was developed in the early twentieth century and has since become an essential concept in the field of life sciences, providing a crucial tool for studying fundamental cell biology, interactions with drugs and development of therapeutics.[63–66] Traditionally, in vitro cell culture is carried out in two-dimensional, static macrosystems such as flasks, petri dishes and well plates made of hard plastics materials. While these platforms effectively enable cultivation of cells in laboratories, they lack the complexity to recreate dynamic aspects of mechanical and biochemical

microenvironments (**Figure 1.3**. e.g., chemical and gaseous gradients, pH, fluid shear stress, extra cellular matrix (ECM), …) of the human body – which are important cues for determining phenotype and cell functionality.[67] Traditional cell culture practices are also labour intensive and involve manual steps that cause cellular and metabolic stress.[67]

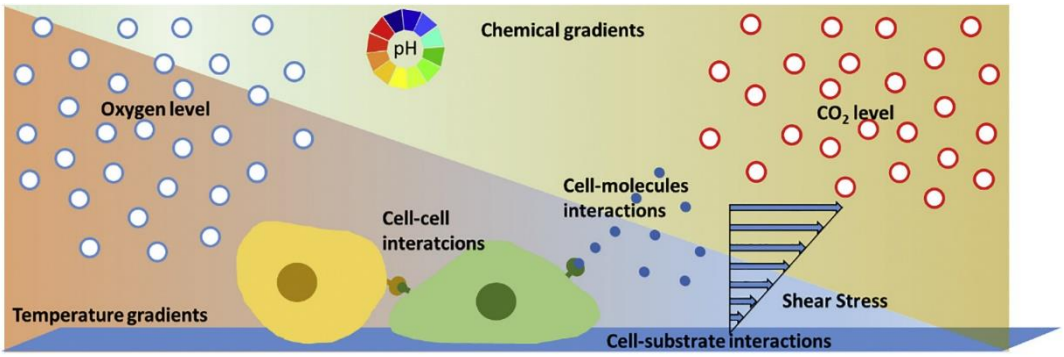


**Figure 1.3**. Graphic illustration of the cell microenvironment including physical (shear stress), biochemical (cell interactions) and physicochemical (pH, oxygen, $CO_2$, temperature) factors. Figure adapted from Coluccio et al.[67] with permission from Elsevier.

Microfluidic approaches to in vitro cell culture provide a number of attractive features. Cultivation, manipulation and analysis of cells in microfluidic systems require lower quantities of cells and biological reagents compared to macroscale culture. This is of particular significance in applications involving cells of limited availability, such as primary cells from patient samples.[68,69] The micro-scale dimensions also open up for new opportunities in single-cell analysis, such as studying cell heterogeneity with high throughput.[70] Moreover, microscale fluid handling allows for automation of assays and on-chip parallelization to reduce time and cost and improve throughput of analyses.[71] The precision of laminal flows and defined microchannel geometries can be leveraged to deliver nutrients, gases, and other soluble factors or mechanical stresses (fluid induced shear stresses) through perfusion with high temporal and spatial precision.[72] These aspects have be utilized to create biochemical and mechanical microenvironments that better recapitulate aspects of the native cellular microenvironment.[73]

The use of microfluidic technology for biomedical research has experienced a significant growth over the past two decades (**Figure 1.4a**). One of the most keenly researched areas within microfluidics at the moment, is what is known as "organ-on-

a-chip" (OOC).[4] After being introduced in the early 2010s [34,74], OOC research has rapidly expanded (**Figure 1.4b**), and in 2016 OOC was listed as a top emerging technology at the World Economic Forum [75].

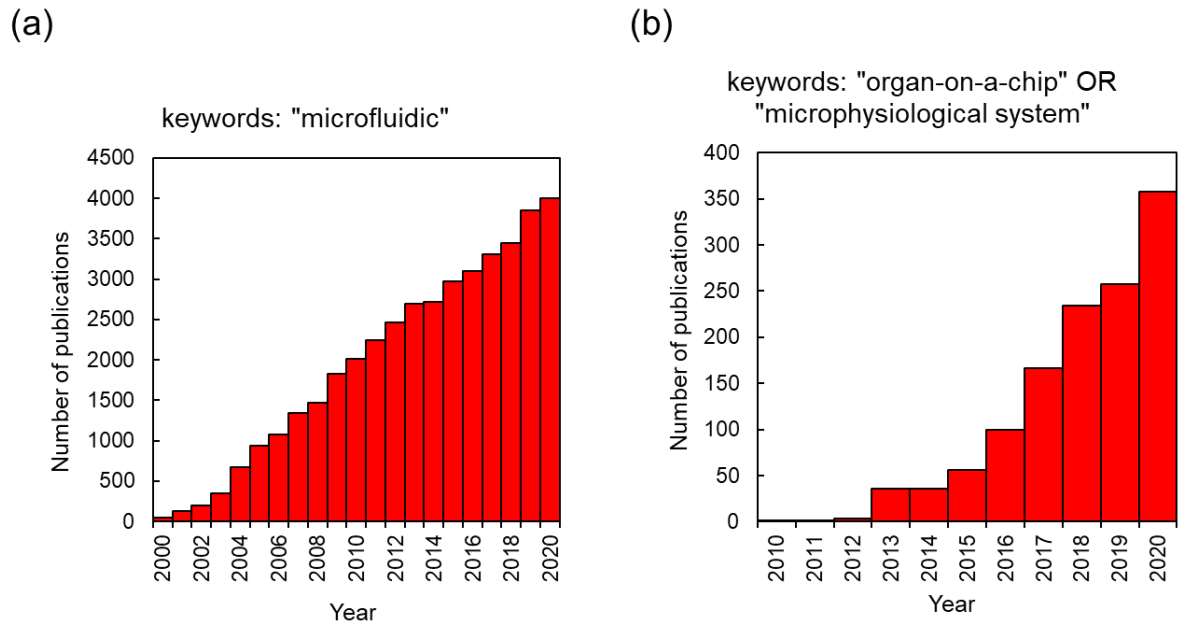


**Figure 1.4** Publication history. A rough estimate of the number of biomedical journal articles published each year on (a) microfluidics (2000-2020) determined by keyword search "Microfluidic" and (b) organ-on-a-chip (2010-2020) determined by keywords search "organ-on-a-chip" OR "microphysiological system", gathered from PubMed.

Despite tremendous efforts from the research community (illustrated by the publication history), OOC still remain a rather inaccessible technology beyond the microfluidics research community.[4,76–78] The technology is still at an early stage and the promises and expectations of the technology are still far beyond the capabilities of current systems.[79]

In this section, we will introduce key concepts in OOC engineering and discuss existing challenges in the progression toward a wider research and industry adoption of OOC technology. The challenges discussed largely extend beyond OOC technology to broader applications of microfluidic systems for cell culture and cell-based assays. Indeed, many challenges stem from the lack of appropriate device fabrication materials that can offer both suitable fabrication procedures and desired device functionalities [80], which will be further discussed throughout this chapter.

### 1.3.1 Organ-on-a-chip systems

OOC are micro-physiological systems that aim to recapitulate structural and functional aspects of human tissues and organs, utilizing microfluidic technology.[81] These advanced in vitro models integrate living human cells on a microfluidic chip and regulate key parameters, such as concentration gradients, shear stresses, tissue interfaces and organ-like architectures, by means of microfluidics and microengineering. A variety of human organ functions have been modelled with OOC technology including, lung [82], gut [83], heart [84], kidney [85], bone [86] and brain [87] among others (**Figure 1.5**).

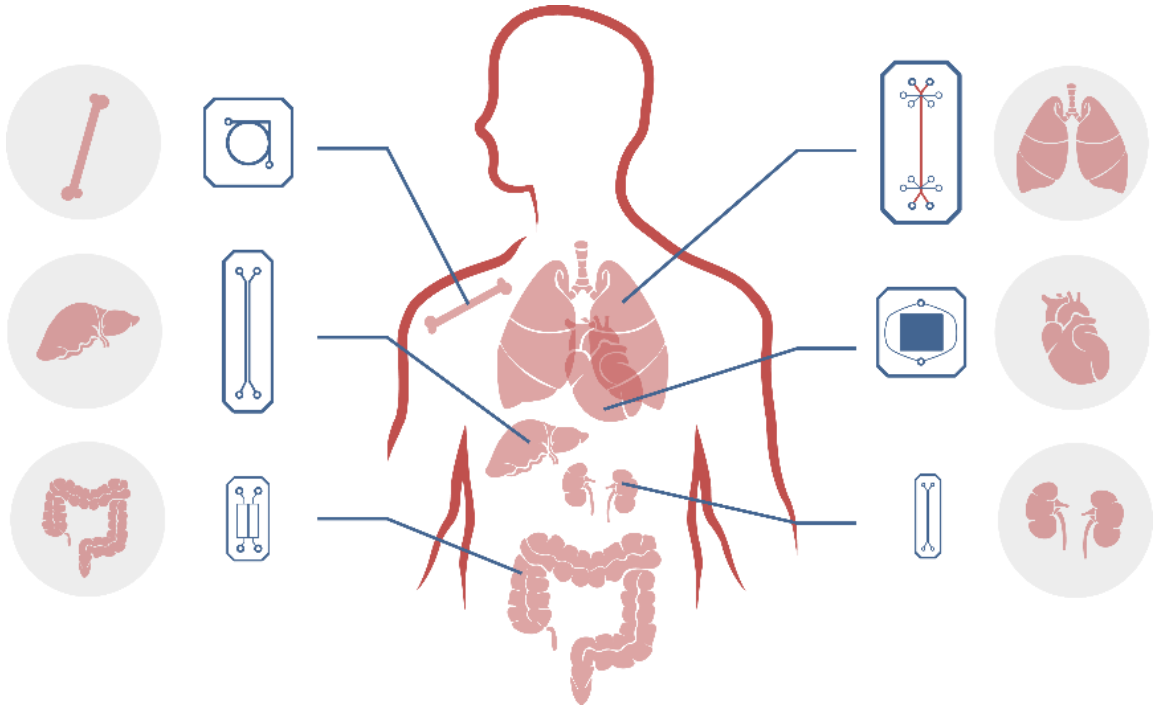

**Figure 1.5** Illustration of human organ-on-a-chip systems, including bone-, liver-, gut-, lung-, heart-, and kidney-on-a-chip models.

The growing interest in OOC systems is largely motivated by their potential to revolutionize drug development pipelines, where new tools to predict clinical outcomes are desperately needed.[88] To date, preclinical validation largely relies on results obtained from animal studies. However, roughly 40% of new drug candidates that pass preclinical evaluation fail clinical trials due to unexpected toxicity in humans.[89] This gap in pre-clinical to clinical translation calls for better methods to predict human responses. Recent breakthroughs in stem cell engineering and generation of induced pluripotent stem cells (iPSC) presents unprecedented

opportunities for more physiologically representative cellular models.[90–93] As iPSCs technology advances, they are likely to be the cellular source for future OOC models.

OOC systems have two defining characteristics: they are made up of multiple cell types that have a three-dimensional, physiologically relevant arrangement, and they incorporate biomechanical forces (such as tissue stretching or haemodynamic shear forces) relevant to the tissue in question.[94] Some of the key design concepts in OOC engineering are presented below:

### i. Mechanically active systems

The first OOC system was introduced by Huh et al. in 2010 and aimed to model the air-liquid interface found at the endothelial-epithelial barrier in human alveoli.[35] With each breath the lung undergoes a volume change that results in complex forces on the alveolar wall that vary in magnitude, direction and frequency. Additionally, surface tension and fluid shear stresses from blood and interstitial flow pose significant mechanical stimulation on the alveolar wall.[95,96]

The OOC system (**Figure 1.6)**, fabricated entirely in PDMS, consisted of two microfluidic channels separated by a thin, porous membrane on which alveolar epithelial cells and microvascular endothelial cells were seeded on opposite sides. After cells had grown to a confluent state, an air-liquid interface was recreated by flowing air through the microchannel on the alveolar side and media on the vascular side. The mechanical strains at the alveolar-capillary interface were modelled by applying vacuum in the parallel side channels to induce a unidirectional cyclic stretching of the elastic membrane. Endothelial cells were additionally stimulated with flow-induced shear stresses that resulted in cell alignment responses, similar to those of the endothelium in vivo[97,98] and differing from cell behaviour in 3D culture systems that do not incorporate an air-liquid interface or mechanical actuation [99].

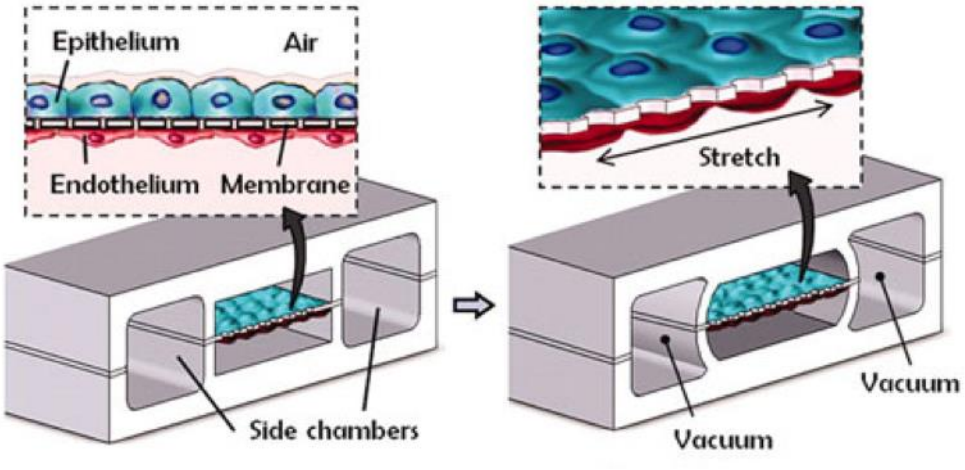


**Figure 1.6** Mechanically active lung-on-a-chip device. The three-layer PDMS device consists of two central chambers separated by a thin porous membrane seeded with alveolar epithelial cells on one side and vascular endothelial cells on the other. An air-liquid interface is established by flowing air in the upper, alveolar channel. As illustrated, vacuum can be applied to the two-side chambers in order to deform the elastic PDMS walls, and thus the membrane. This serves to unidirectionally stretch the cells and simulates the stretching that is undergone during the expansion and contraction of the alveoli in the human body. Adapted from Huh et al.[34] with permission from AAAS.

Pulmonary inflammation response was demonstrated in the OOC system by introduction of the proinflammatory cytokine tumor necrosis factor α (TNFα) in the vascular channel. The inflammatory response of the system was monitored by the endothelial expression of intercellular adhesion molecule 1 (ICAM-1) and subsequent adhesion and transmembrane migration of fluorescently labelled neutrophils. Mechanical strain on the alveolar membrane did not affect the immune response. However, when silica nanoparticles were used as a stimulant, the inclusion of mechanical strain resulted in increased expression of ICAM-1, similarly to observations in murine lungs and consistent with in vivo evidence – suggesting that nanoparticle toxicity attributable to cross-membrane absorption [100].

This system highlights how elastomeric materials are utilized to develop active components in microfluidic devices to create functional features that elicit organ-level responses in vitro. OOC systems have similarly been used to model in other mechanically active body barriers, such as of the gut [101], aorta [102], musculoskeletal system [103] and skin [104].

## ii. Organotypic tissue architectures

A key feature of OOC models is creating organotypic tissue architectures containing multiple cell types. One example demonstrating a biological complexity and innovative design toward mimicking in vivo biology was presented by Barkal et al.[105] (**Figure 1.7**) in 2017. Their model of the terminal bronchiole was based on a fibroblast and collagen gel matrix that supported monolayers of epithelial and endothelial cells.

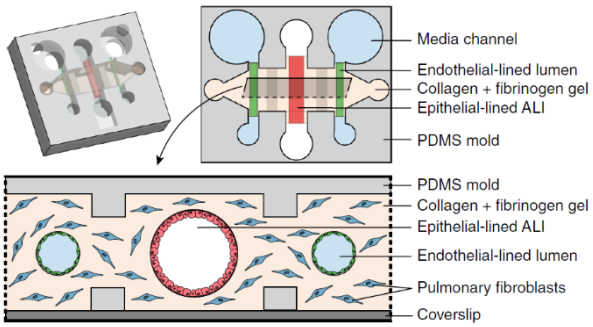


**Figure 1.7** Organotypic lung-on-a-chip device featuring two media-filled endothelial-lined lumens and one central epithelial-lined lumen, where an air-liquid interface is present. The lumens run through a collagen and fibrinogen gel matrix, incorporating pulmonary fibroblasts. Adapted from Barkal et al.[105] with permission from Springer Nature.

To fabricate channel with circular cross-sections, PDMS rods were encased in the hydrogel matrix and after their removal, three parallel channels remained, one to model the bronchial airway and two to model vascular capillaries. The biologically relevant geometry resulted in distinctly different cell behaviour compared to cultures of flat monolayers [106]. Moreover, channel sizes could be controlled to match the average dimensions of human terminal bronchioles and adjacent capillaries [107,108]. This organotypic system could model the complex immunoinflammatory environment of the lung under two different pathological conditions. Pathogens could be inserted into the bronchial lumen to study responses from direct pathogen contact. Alternatively, a complementary microbial culture insert was designed to be positioned over air-exposed surface the OOC model to facilitate host-pathogen communication via bacteria and fungi-derived volatile compounds, which has been shown to produce unique host infection responses [109,110]. Such phenomena have particular relevance in patients with cystic fibrosis colonized by multiple microbial species.[111]

### iii. Multi-organ systems

The OOC systems highlighted in the sections above have focused on modelling features of one specific organ. "Body-on-a-chip" or "human-on-a-chip" systems are multi-organ systems that aim to provide systemic insight into the interaction of multiple organs in the body.[112–114] Multi-organ system usually have a modular design where individual OOC platforms are interconnected by microfluidic tubing [115,116], or alternatively, the different compartments can be integrated on the same microfluidic chip [117,118]. "Plug-and-play" systems have also been demonstrated where different organs can be inserted or removed on demand.[119,120] The interest in multi-organ systems is largely related to their potential use in drug development processes where they could act as a tool for understanding complex mode of actions e.g., in the field on immune-cancer therapy.[121] Multi-organ systems can potentially be a suitable tool for in vitro adsorption, distribution, metabolism, and elimination (ADME) modelling, as could mimic the pharmacokinetic/pharmacodynamic (PK/PD) conditions of drug candidates in vivo.[94] Such interplay between multiple organs has previously only been associated with animal in vivo experiments that frequently fail to predict human responses.[122,123] A number of multi-organ systems have been presented, constituting various different organ models. For instance, a liver-lung system that represented bronchial epithelial cells at an air-liquid interface and liver spheroids was developed to study toxicity of inhaled aerosols.[115] Another model presented crosstalk between four different organ models representing the liver, lung, kidney and adipose tissue.[116]

## 1.3.2 Current challenges in organ-on-a-chip engineering

In the previous section we presented some of the accomplishments and key microfluidic design concepts that define OOC engineering. The development of these systems illustrates the ongoing efforts of creating OOC systems to model diseases, predict clinical outcomes and evaluate drug efficacy. However, technical challenges remain. With increasing device complexity, design and usability aspects become increasingly important factors. To date, fabrication and manipulation of OOC systems largely rely on manual manipulation by experts in the field. More robust and user-friendly devices, and improved capabilities of integration with existing laboratory techniques and know-how are aspects that require further consideration to facilitate the transfer of devices from developers to end-users. The technology could also greatly benefit from implementation of standards with regards to fabrication, device

design, interfacing, cell sources and readouts, etc., in order to facilitate communication between stakeholders and accelerate development and validation processes.[124,125] Looking at the MEMS industry, standardization of materials, high-throughput manufacturing processes and system-integration have enabled the ubiquitous technologies we have today. Further work around parallelization, automation and on-chip monitoring is also required for the technology to excel.

A main challenge in OOC engineering is finding suitable materials for device fabrication.[88,126,127] The majority of OOC systems presented have been fabricated from PDMS.[126] The importance of PDMS in the field of OOC can be attributed to its convenience for prototyping and device fabrication in research laboratories, but also its beneficial material properties such as optical transparency, high elasticity and gas permeability.[128] However, as previously mentioned, PDMS device fabrication is not feasible in high-throughput, as would be required for industrial production. PDMS devices also require surface modifications, often oxygen plasma treatment followed by a protein coating, to improve hydrophilicity and promote cell attachment.[77] However, due to the polymer chain mobility in PDMS, it quickly recovers to a hydrophobic state after oxygen plasma hydrophilization.[39] The question of shelf life is typically not an issue in research laboratories (beyond the burden of having to use the device within a couple of hours after preparation), but for commercialization it poses significant limitations.

PDMS also has a number of inherent drawbacks that limits its performance for OOC applications. Firstly, the absorption of small molecules, such as drugs, cell signalling and dye compounds, by PDMS devices is problematic in studies involving soluble factors, where absorption can alter critical concentrations and results in misinterpretations of results.[129–131] This severely limiting the utility of OOC systems in drug screening, cell signalling, and cell-drug interactions studies such as PK/PD modelling, which are key areas that OOC technology can address. For instance, Regehr et al. showed that estrogen levels in cell culture media were depleted due to absorption into PDMS channels [131], and Su et al. observed differences in cellular responses to the drug fluoxetine (Prozac®) in PDMS devices compared to polystyrene devices, supposedly due to compound absorption [130]. Strategies to chemically modify the PDMS surface to minimize absorption have been introduced, e.g. by parylene coatings [132]. However, such modifications must remain stable throughout the experiment, which may run over several weeks.[133,134]

Another potential drawback of PDMS is related to the inertness of the material. Cured PDMS contain residual un-crosslinked PDMS oligomers that can diffuse freely throughout the material and leach out into the fluid in the microfluidic channel. The

issue of leaching and its potential impacts, on for instance cell viability, is not fully clear.[77] Regehr et al. showed that oligomers can leach out of PDMS devices and incorporate into the membranes of cells cultured in devices.[131]

The high permeability of PDMS to gases can also be a problem in certain cases. Thin PDMS devices (in the range ~200 µm) have shown to produce hyperoxic microenvironments that may induce cellular stress.[135,136] In general, diffusion of oxygen and carbon dioxide through microfluidic walls is considered advantageous for applications in cell culture in order to ensure sufficient gas levels for cellular respiration. However, high permeability to water vapor can also cause undesirable effects, such as fluid evaporation and formation of air bubbles in microchannels. While evaporation also occurs in macro-scale cell culture systems, its effects are more significant on the microscale due to small fluid volumes and high surface-area-to-volume ratio. Evaporation can cause: microchannels to completely dry out, formation of air bubbles, or result in shifts in osmolarity.[137]

From a research point of view, these aspects of PMDS devices are difficult to monitor and may introduce additional uncertainties to the microfluidic experiments. From an industrial point of view, these material properties entail a number of back-end processing steps, such as surface modifications, in order to manufacture devices of desired functionality. The issues around up-scaling and back-end processing associated with PDMS manufacturing make most microfluidic companies refrain from PDMS, resulting in a barrier between academia and industry.[76,138] Whether this is a challenge for academia or for industry to tackle is a topic frequently debated within the microfluidics community.

### 1.3.3 Novel materials in organ-on-a-chip research

The need for new materials beyond PDMS for OOC fabrication has been widely acknowledged, and also broadly applies to other biomedical applications of microfluidic devices.[77,94,127,139,140] Transferable prototyping procedures and better adoption of concepts around scalable manufacturing, standardization and system-integration thinking at the prototyping stage could help bridging the gap between academia and industry.[141]

Thermoplastic materials are excellent options from a large-scale fabrication point of view, and many thermoplastics are more inert, have improved resistance to small molecules, more stable surface hydrophilization and lower water vapor permeability, compared to PDMS. There have been many successful demonstrations of

thermoplastic OOC systems fabricated from, for instance, PC [142–145], COP/COC [146,147] and PMMA [148,149]. However, OOC functionality often requires flexible components, such as stretchable membranes for recapitulation of tissue elasticity [96] or cell orientation induced via topological cues [150]. Moreover, the stiffness of hard thermoplastics greatly differs from that of soft, native ECM.

As previously mentioned, prototyping of thermoplastics is also inaccessible on laboratory scales. To address this issue, OOC systems have been fabricated from a 3D-printable UV-curable polymer, Veroclear, that simulates PMMA.[151–153] An innovative Veroclear liver-gastrointestinal tract multi-organ system with integrated Ag/AgCl electrodes to measure the transepithelial resistance (TEER) across the gastrointestinal tract layer was demonstrated.[118] However, the fabrication process is limited in terms of throughput, as five hours was required for 3D printing of one Veroclear device.[154]

An interesting new group of thermosets was recently introduced for applications in microfluidics are off-stoichiometry thiol-ene (OSTE) and off-stoichiometry thiol-ene-epoxy (OSTE+) materials.[155] OSTE materials have elastomeric properties after an initial UV-curing step, which enable facile demolding after the micropatterning step. The OSTE materials can then be heat-cured to tune the mechanical properties to render the material stiff (~ 1 GPa). This enabled fabrication of monolithic devices that contain both flexible and stiff components. OSTE materials can also be processed with injection molding, which enable high-throughput fabrication of microfluidic devices.[156] A lung-on-a-chip system fabricated from OSTE materials was recently presented.[157] The devices demonstrated promising features in terms of improved fabrication methodology and small molecule absorption compared to PDMS. However, further improvements of the material's optical transmission, particularly reduced light scattering, are required to improve its performance as a material for OOC research.

Another OOC platform from a novel, promising material, tetrafluoroethylene (FEPM) elastomer, was recently introduced by Sano et al.[139] They demonstrated formation of a tissue-tissue interface on a thin, stretchable ECM membrane inside a device fabricated from FEPM. The FEPM devices showed improved resistance to three small hydrophobic drugs and a relatively streamlined fabrication process involving mixing of precursor materials, press-curing at 160 °C for 30 minutes followed by a second curing step at 200 °C for 2 hours and bonding through elastomeric self-sealing at room temperature.

To date, there are no demonstrations OOC systems using styrene-based copolymers such as SEBS. Domansky et al.[59] explored the use of SEBS copolymers for fabrication

of microfluidic devices by injection molding. The devices were fabricated completely from SEBS elastomers and the design was replicated the from the OOC model by Huh et al.[34] (illustrated in **Figure 1.6**). They demonstrated that SEBS elastomers are well-suited for high throughput fabrication of devices of a typical OOC geometry, including fabrication of a porous membrane of ~30 µm thickness. The device was tested to withstand 0.5 million 0-20% stretch cycles under combined wet and dry conditions, simulating the intended use of the devices for recapitulating cyclical physiological motion of e.g., the alveoli in the lung.

For devices with complex functionality, such as OOC systems, it is clear that no material can satisfy every requirement. It has been recognized that the ideal OOC system may require multiple materials, for instance a combination of thermoplastics, elastomers and a cell interacting component, such as a hydrogel. In this section we have merely highlighted a few promising examples of novel materials for OOC fabrication. Several more extensive reviews have been published on the topic, including both the structural materials of the devices as well as materials in the context of cell contact.[127,158,159] In **Table 1.1**, we identified and outlined material properties desired for an ideal OOC prototyping material. Based on the identified criteria, we evaluated different materials for creating successful OOC devices (**Table 1.2**).

**Table 1.1 Device material criteria for successful OOC prototyping**

| | |
|---|---|
| **Low cost** | Low-cost raw materials are advantageous. |
| **Facile prototype fabrication** | Accessible and cheap fabrication on laboratory scales is highly advantageous. |
| **Transferability of fabrication** | A fabrication methodology that can be transferred to large-scale production is highly advantageous. |
| **Mechanical flexibility** | Flexibility (low stiffness) is desirable in order to create mechanically active components and facilitate chip interfacing. It can however also cause undesirable effects such as mechanical deformation to the channel. |
| **Oxygen permeability** | In general, high oxygen permeability of OOC devices is preferred. However, for certain studies, e.g., cellular hypoxia, a controlled low-oxygen environment is desired. |
| **Biocompatibility** | Biocompatibility is a strict requirement for all OOC device materials. |
| **Optical transparency** | High optical transparency in the visible and near-UV range is critical for real-time on-chip imaging and fluorescent spectroscopy of cells inside the devices. Low material autofluorescence is likewise desired. |
| **Surface chemistry** | Hydrophilic surfaces are generally ideal to promote cell attachment and facilitate fluid flow, alternatively having the potential for surface modification to alter surface charges or hydrophobicity. |
| **Absorption** | Absorption of small molecules is undesirable and limits the device use for certain applications, such as PK/PD modelling, cell-cell signalling, drug discovery, etc. |
| **Inertness** | Leaching of material can have undesirable effects, such as cytotoxic effects on cells. |
| **Sterilization** | Methods for effective sterilization are necessary. |

**Table 1.2 General comparison of fabrication materials for OOC devices**

| | | PDMS | Hard Thermoplastics | Inorganic materials | Thermosets | sTPE |
|---|---|---|---|---|---|---|
| Fabrication | **Raw material cost** | Low | Low | High | Low | Low |
| | **Accessible prototyping** | Yes | No | No | Yes | Yes |
| | **High throughput fabrication** | No | Yes | Yes | Yes | Yes |
| | **Channel resolution** | < 50 nm | < 50 nm | 10 nm | < 50 nm | < 50 nm |
| | **High aspect ratio** | Not feasible | Feasible | Feasible | Feasible | Not feasible |
| | **Ease of micro-structuring** | Easy, slow | Moderate, fast | Difficult, slow | Easy, fast | Easy, fast |
| | **Ease of bonding** | Moderate | Moderate | Difficult | Easy | Easy |
| | **Recyclability** | Not recyclable | Recyclable | Not recyclable | Not recyclable | Recyclable |
| Material Properties | **Elasticity** | Elastic | Rigid | Rigid | Tuneable | Elastic |
| | **Tuneable mechanical properties** | Yes | No | No | Yes | No |
| | **Absorption of small molecules** | High | Low | Low | Low | Low |
| | **Chemical resistance** | Low/ moderate | Moderate | High | High | Low/ moderate |
| | **Gas permeability** | High | Low | Low | Low | Moderate |
| | **Optical transparency** | High | High | High (glass) | Moderate | Moderate-High |
| | **Biocompatibility/bio-inertness** | Moderate | High | High | High | High |
| Applications | **Potential for chemical modification** | High | Moderate | High/ Moderate | High | Moderate |
| | **Potential for integration of electrodes** | Low/ Moderate | Moderate | High | Moderate | Low/ Moderate |
| | **Potential for Multiplexing/ valves** | High | Low | Low | High | High |

## 1.4 Aims and scope of thesis

As outlined throughout this chapter, there is a need for new prototyping material for microfluidic device fabrication to bridge the current gap between microfluidics in small-scale research settings and large-scale industrial production. Drawbacks associated with PDMS devices for cell biological applications and OOC technology are encouraging a transition to alternative materials. To this end, sTPE materials have been introduced as promising candidates to replace PDMS as a prototyping material. Their unique combination of thermoplastic and elastic properties enables accessible and cost-effective device fabrication in research laboratory settings, while also providing a feasible scope for large-scale industrial production. Biocompatible and transparent sTPE formulations are particularly well suited for fabrication of microfluidic devices for use in the field of cell biology and OOC. However, relatively limited use of such materials in the context of microfluidics have been presented.

*The aim of this industrial PhD project is to evaluate the potential of two novel sTPE formulations: FlexDym™ and Fluoroflex as materials for prototyping of microfluidic devices in the context of cell culture studies as a step toward implementation in OOC technology, by means of material and microfluidic characterization and proof-of-concept studies.*

**Chapter 2** presents the material and microfluidic characterization of two novel sTPE formulations: FlexDym™ and Fluoroflex for applications in microfluidic cell culture, as a first step toward implementation for OOC technology. We evaluate cell-material interactions and critical material properties, such as gas permeability and small molecule absorption, and investigate the influence of static and perfusion conditions on cancer cell proliferation.

In **chapter 3** we employ the strategies for sTPE-based microfluidic cell culture, developed in chapter 2, for investigating cardiac myoblast physiology. The sTPE system is validated against a PDMS system of equivalent design and a macro-scale system. A microfluidic circuit for automated administration of soluble factors to microfluidic cell culture sTPE-devices is developed together with tools, in the form of application notes, to facilitate implementation of sTPE microfluidic devices and microfluidic fluid handling in cell biology laboratories.

**Chapter 4** introduces novel microfabrication strategies for the development of a composite sTPE device for membrane-based cell culture. The fabrication methodology

enables high-throughput and cost-effective fabrication of a "barrier model", a design commonly used for OOC devices. The self-sealing properties for microfluidic bonding of the sTPE were evaluated through a series of delamination tests. By this method we characterized the pressure capacity of the devices under simulated cell culture use. Proof-of-concept cell studies are also presented.

**Chapter 5** provides a broader perspective and outlook on the work presented in this thesis. sTPE materials are discussed in the context of OOC engineering and the necessary next steps toward sTPE-based OOC systems are outlined.

## 1.5 References


1. Venkatesan, S., Jerald, J., Asokan, P. & Prabakaran, R. A Comprehensive Review on Microfluidics Technology and its Applications. in *Lecture Notes in Mechanical Engineering* 235–245 (2020).
2. Beebe, D. J., Mensing, G. A. & Walker, G. M. Physics and applications of microfluidics in biology. *Annu. Rev. Biomed. Eng.* **4**, 261–286 (2002).
3. Manz, A., Graber, N. & Widmer, H. M. Miniaturized total chemical analysis systems: A novel concept for chemical sensing. *Sensors Actuators B Chem.* **1**, 244–248 (1990).
4. Convery, N. & Gadegaard, N. 30 years of microfluidics. *Micro Nano Eng.* **2**, 76–91 (2019).
5. Gómez-Sjöberg, R., Leyrat, A. A., Pirone, D. M., Chen, C. S. & Quake, S. R. Versatile, Fully Automated, Microfluidic Cell Culture System. *Anal. Chem.* **79**, 8557–8563 (2007).
6. Shields 4th, C. W., Reyes, C. D. & López, G. P. Microfluidic cell sorting: a review of the advances in the separation of cells from debulking to rare cell isolation. *Lab Chip* **15**, 1230–1249 (2015).
7. Sachdeva, S., Davis, R. W. & Saha, A. K. Microfluidic Point-of-Care Testing: Commercial Landscape and Future Directions . *Frontiers in Bioengineering and Biotechnology* **8**, 1537 (2021).
8. Mazutis, L. *et al.* Single-cell analysis and sorting using droplet-based microfluidics. *Nat. Protoc.* **8**, 870–891 (2013).
9. Khandurina, J., McKnight, T. E., Jacobson, S., Waters, L., Foote, R., Ramsey, J. Integrated System for Rapid PCR-Based DNA Analysis in Microfluidic Devices. *Anal. Chem.* **72**, 2995–3000 (2000).
10. Du, G., Fang, Q. & den Toonder, J. M. J. Microfluidics for cell-based high throughput screening platforms—A review. *Anal. Chim. Acta* **903**, 36–50 (2016).
11. Abgrall, P. & Gu, A. Lab-on-chip technologies : making a microfluidic network and coupling it into a complete microsystem — a review. (2007).
12. Whitesides, G. M. The origins and the future of microfluidics. *Nature* **442**, 368–373 (2006).
13. Woolley, A. T. & Mathies, R. A. Ultra-high-speed DNA fragment separations using microfabricated capillary array electrophoresis chips. *Proc. Natl. Acad. Sci. U. S. A.* **91**, 11348–11352 (1994).
14. Jensen, K. F. Silicon-Based Microchemical Systems: Characteristics and Applications. *MRS Bull.* **31**, 101–107 (2006).
15. Lin, C.-H., Lee, G.-B., Lin, Y.-H. & Chang, G.-L. A fast prototyping process for fabrication of microfluidic systems on soda-lime glass. *J. Micromechanics Microengineering* **11**, 726–732 (2001).
16. Ren, K., Zhou, J. & Wu, H. Materials for microfluidic chip fabrication. *Acc. Chem. Res.* **46**, 2396–2406 (2013).
17. Jackman, R. J., Floyd, T. M., Ghodssi, R., Schmidt, M. A. & Jensen, K. F. Microfluidic systems with on-line UV detection fabricated in photodefinable epoxy. *J. Micromechanics Microengineering* **11**, 263–269 (2001).

18. Vickers, J. A. *et al.* Thermoset polyester as an alternative material for microchip electrophoresis/electrochemistry. *Electrophoresis* **28**, 1123–1129 (2007).
19. Kim, J., deMello, A. J., Chang, S.-I., Hong, J. & O'Hare, D. Thermoset polyester droplet-based microfluidic devices for high frequency generation. *Lab Chip* **11**, 4108–4112 (2011).
20. Rolland, J. P., Van Dam, R. M., Schorzman, D. A., Quake, S. R. & DeSimone, J. M. Solvent-Resistant Photocurable "Liquid Teflon" for Microfluidic Device Fabrication. *J. Am. Chem. Soc.* **126**, 2322–2323 (2004).
21. Liao, S., He, Y., Chu, Y., Liao, H. & Wang, Y. Solvent-resistant and fully recyclable perfluoropolyether-based elastomer for microfluidic chip fabrication. *J. Mater. Chem. A* **7**, 16249–16286 (2019).
22. Bong, K. W., Lee, J. & Doyle, P. S. Stop flow lithography in perfluoropolyether (PFPE) microfluidic channels. *Lab Chip* **14**, 4680–4687 (2014).
23. Vitale, A. *et al.* Direct Photolithography of Perfluoropolyethers for Solvent-Resistant Microfluidics. *Langmuir* **29**, 15711–15718 (2013).
24. Duffy, D. C., McDonald, J. C., Schueller, O. J. & Whitesides, G. M. Rapid Prototyping of Microfluidic Systems in Poly(dimethylsiloxane). *Anal. Chem.* **70**, 4974–4984 (1998).
25. McDonald, J. C. *et al.* Fabrication of microfluidic systems in poly(dimethylsiloxane). *Electrophoresis* **21**, 27–40 (2000).
26. Clarson, S. J., Dodgson, K. & Semlyen, J. A. Studies of cyclic and linear poly(dimethylsiloxanes): 19. Glass transition temperatures and crystallization behaviour. *Polymer (Guildf).* **26**, 930–934 (1985).
27. Lötters, J. C., Olthuis, W., Veltink, P. H. & Bergveld, P. The mechanical properties of the rubber elastic polymer polydimethylsiloxane for sensor applications. *J. Micromechanics Microengineering* **7**, 145–147 (1997).
28. Clarson, S. J. & Semlyen, J. A. *Siloxane polymers*. (Prentice Hall, 1993).
29. Capulli, A. K. *et al.* Approaching the in vitro clinical trial: engineering organs on chips. *Lab Chip* **14**, 3181–3186 (2014).
30. Velve-Casquillas, G., Le Berre, M., Piel, M. & Tran, P. T. Microfluidic tools for cell biological research. *Nano Today* **5**, 28–47 (2010).
31. Unger, M. A., Chou, H. P., Thorsen, T., Scherer, A. & Quake, S. R. Monolithic microfabricated valves and pumps by multilayer soft lithography. *Science* **288**, 113–116 (2000).
32. Balagaddé, F. K., You, L., Hansen, C. L., Arnold, F. H. & Quake, S. R. Long-term monitoring of bacteria undergoing programmed population control in a microchemostat. *Science* **309**, 137–140 (2005).
33. Huang, B. *et al.* Counting Low-Copy Number Proteins in a Single Cell. *Science (80-. ).* **315**, 81 LP – 84 (2007).
34. Huh, D. *et al.* Reconstituting organ-level lung functions on a chip. *Science* **328**, 1662–1668 (2010).
35. Martin, S. & Bhushan, B. Transparent, wear-resistant, superhydrophobic and superoleophobic poly(dimethylsiloxane) (PDMS) surfaces. *J. Colloid Interface Sci.* **488**, 118–126 (2017).
36. Merkel, T. C., Bondar, V. I., Nagai, K., Freeman, B. D. & Pinnau, I. Gas sorption, diffusion, and permeation in poly(dimethylsiloxane). *J. Polym. Sci. Part B Polym. Phys.* **38**, 415–434 (2000).
37. Shin, S., Kim, N. & Hong, J. W. Comparison of Surface Modification Techniques on Polydimethylsiloxane to Prevent Protein Adsorption. *BioChip J.* **12**, 123–127 (2018).
38. Bhattacharya, S., Datta, A., Berg, J. M. & Gangopadhyay, S. Studies on surface wettability of poly(dimethyl) siloxane (PDMS) and glass under oxygen-plasma treatment and correlation with bond strength. *J. Microelectromechanical Syst.* **14**, 590–597 (2005).
39. Eddington, D. T., Puccinelli, J. P. & Beebe, D. J. Thermal aging and reduced hydrophobic recovery of polydimethylsiloxane. *Sensors Actuators B Chem.* **114**, 170–172 (2006).
40. Lee, J. N., Park, C. & Whitesides, G. M. Solvent Compatibility of Poly(dimethylsiloxane)-Based Microfluidic Devices. *Anal. Chem.* **75**, 6544–6554 (2003).
41. Wang, J. D., Douville, N. J., Takayama, S. & ElSayed, M. Quantitative Analysis of Molecular

Absorption into PDMS Microfluidic Channels. *Ann. Biomed. Eng.* **40**, 1862–1873 (2012).
42. Toepke, M. W. & Beebe, D. J. PDMS absorption of small molecules and consequences in microfluidic applications. *Lab Chip* **6**, 1484–1486 (2006).
43. Becker, H. & Gärtner, C. Polymer microfabrication technologies for microfluidic systems. *Anal. Bioanal. Chem.* **390**, 89–111 (2008).
44. Boone, T. D. *et al.* Plastic advances microfluidic devices. *Anal. Chem.* **74**, 78A-86A (2002).
45. Tsao, C.-W. & DeVoe, D. L. Bonding of thermoplastic polymer microfluidics. *Microfluid. Nanofluidics* **6**, 1–16 (2009).
46. Li, J., Chen, D. & Chen, G. Low-Temperature thermal bonding of PMMA microfluidic chips. *Anal. Lett.* **38**, 1127–1136 (2005).
47. Wang, Y., Chen, H., He, Q. & Soper, S. A. A high-performance polycarbonate electrophoresis microchip with integrated three-electrode system for end-channel amperometric detection. *Electrophoresis* **29**, 1881–1888 (2008).
48. Ogończyk, D., Węgrzyn, J., Jankowski, P., Dąbrowski, B. & Garstecki, P. Bonding of microfluidic devices fabricated in polycarbonate. *Lab Chip* **10**, 1324–1327 (2010).
49. Zhou, P., Young, L. & Chen, Z. Weak solvent based chip lamination and characterization of on-chip valve and pump. *Biomed. Microdevices* **12**, 821–832 (2010).
50. Gencturk, E., Mutlu, S. & Ulgen, K. O. Advances in microfluidic devices made from thermoplastics used in cell biology and analyses. *Biomicrofluidics* **11**, 51502 (2017).
51. Neils, C., Tyree, Z., Finlayson, B. & Folch, A. Combinatorial mixing of microfluidic streams. *Lab Chip* **4**, 342–350 (2004).
52. Shaegh, S. A. M. *et al.* Rapid prototyping of whole-thermoplastic microfluidics with built-in microvalves using laser ablation and thermal fusion bonding. *Sensors Actuators, B Chem.* **255**, 100–109 (2018).
53. Young, E. W. K. *et al.* Rapid prototyping of arrayed microfluidic systems in polystyrene for cell-based assays. *Anal. Chem.* **83**, 1408–1417 (2011).
54. Nunes, P. S., Ohlsson, P. D., Ordeig, O. & Kutter, J. P. Cyclic olefin polymers: Emerging materials for lab-on-a-chip applications. *Microfluidics and Nanofluidics* **9**, 145–161 (2010).
55. Ren, K., Dai, W., Zhou, J., Su, J. & Wu, H. Whole-Teflon microfluidic chips. *Proc. Natl. Acad. Sci. U. S. A.* **108**, 8162–8166 (2011).
56. Ren, K. N. *et al.* Soft-lithography-based high temperature molding method to fabricate whole Teflon microfluidic chips. in *14th International Conference on Miniaturized Systems for Chemistry and Life Sciences, Groningen, The Netherlands* 554–556 (2010).
57. Chen, Q., Liang, S. & Thouas, G. A. Elastomeric biomaterials for tissue engineering. *Prog. Polym. Sci.* **38**, 584–671 (2013).
58. Salmon, H., Rasouli, M. R., Distasio, N. & Tabrizian, M. Facile engineering and interfacing of styrenic block copolymers devices for low-cost, multipurpose microfluidic applications. *Eng. Reports* **n/a**, e12361 (2021).
59. Domansky, K. *et al.* SEBS elastomers for fabrication of microfluidic devices with reduced drug absorption by injection molding and extrusion. *Microfluid. Nanofluidics* **21**, (2017).
60. Roy, E., Geissler, M., Galas, J. C. & Veres, T. Prototyping of microfluidic systems using a commercial thermoplastic elastomer. *Microfluid. Nanofluidics* **11**, 235–244 (2011).
61. Lachaux, J. *et al.* Thermoplastic elastomer with advanced hydrophilization and bonding performances for rapid (30 s) and easy molding of microfluidic devices. *Lab Chip* **17**, 2581–2594 (2017).
62. Roy, E., Pallandre, A., Zribi B., Horny M-C., Delapierre F., Cattoni A., Overview of Materials for Microfluidic Applications. *Adv Microfluid-New Appl Biol Energy, Mater Sci*. (2016)
63. Verma, A., Verma, M. & Singh, A. Animal tissue culture principles and applications. *Anim. Biotechnol.* 269–293 (2020).
64. Maiorella, B., Inlow, D., Shauger, A. & Harano, D. Large-Scale Insect Cell-Culture for Recombinant Protein Production. *Bio/Technology* **6**, 1406–1410 (1988).
65. Miller, A. J. & Spence, J. R. In Vitro Models to Study Human Lung Development, Disease and

Homeostasis. *Physiology* **32**, 246–260 (2017).
66. Hilleman, M. R. Vaccines in historic evolution and perspective: a narrative of vaccine discoveries. *Vaccine* **18**, 1436–1447 (2000).
67. Coluccio, M. L. *et al.* Microfluidic platforms for cell cultures and investigations. *Microelectron. Eng.* **208**, 14–28 (2019).
68. Berthier, E., Surfus, J., Verbsky, J., Huttenlocher, A. & Beebe, D. An arrayed high-content chemotaxis assay for patient diagnosis. *Integr. Biol. (Camb).* **2**, 630–638 (2010).
69. Nagrath, S. *et al.* Isolation of rare circulating tumour cells in cancer patients by microchip technology. *Nature* **450**, 1235–1239 (2007).
70. Brouzes, E. *et al.* Droplet microfluidic technology for single-cell high-throughput screening. *Proc. Natl. Acad. Sci. U. S. A.* **106**, 14195–14200 (2009).
71. El-Ali, J., Sorger, P. K. & Jensen, K. F. Cells on chips. *Nature* **442**, 403–411 (2006).
72. Hung, P. J., Lee, P. J., Sabounchi, P., Lin, R. & Lee, L. P. Continuous perfusion microfluidic cell culture array for high-throughput cell-based assays. *Biotechnol. Bioeng.* **89**, 1–8 (2005).
73. Meyvantsson, I. & Beebe, D. J. Cell Culture Models in Microfluidic Systems. *Annu. Rev. Anal. Chem.* **1**, 423–449 (2008).
74. Huh, D., Hamilton, G. A. & Ingber, D. E. From 3D cell culture to organs-on-chips. *Trends Cell Biol.* **21**, 745–754 (2011).
75. Cann, O. These are the top 10 emerging technologies of 2016 | World Economic Forum. *World Economic Forum* (2016).
76. Sackmann, E. K., Fulton, A. L. & Beebe, D. J. The present and future role of microfluidics in biomedical research. *Nature* **507**, 181–189 (2014).
77. Berthier, E., Young, E. W. K. & Beebe, D. Engineers are from PDMS-land, biologists are from polystyrenia. *Lab on a Chip* **12**, 1224–1237 (2012).
78. Blow, N. Microfluidics: the great divide. *Nat. Methods* **6**, 683–686 (2009).
79. Bhatia, S. N. & Ingber, D. E. Microfluidic organs-on-chips. *Nat. Biotechnol.* **32**, 760–772 (2014).
80. Ramadan, Q. & Zourob, M. Organ-on-a-chip engineering: Toward bridging the gap between lab and industry. *Biomicrofluidics* **14**, 41501 (2020).
81. Mosig, A. S. Organ-on-chip models: new opportunities for biomedical research. *Futur. Sci. OA* **3**, FSO130–FSO130 (2016).
82. Stucki, A. O. *et al.* A lung-on-a-chip array with an integrated bio-inspired respiration mechanism. *Lab Chip* **15**, 1302–1310 (2015).
83. Kim, H. J. & Ingber, D. E. Gut-on-a-Chip microenvironment induces human intestinal cells to undergo villus differentiation. *Integr. Biol.* **5**, 1130–1140 (2013).
84. Kobuszewska, A., Jastrzębska, E., Żukowski, K. & Brzózka, Z. Simulation of hypoxia of myocardial cells in microfluidic systems. *Sci. Rep.* **10**, (2020).
85. Jang, K.-J. *et al.* Human kidney proximal tubule-on-a-chip for drug transport and nephrotoxicity assessment. *Integr. Biol.* **5**, 1119–1129 (2013).
86. Mansoorifar, A., Gordon, R., Bergan, R. C. & Bertassoni, L. E. Bone-on-a-Chip: Microfluidic Technologies and Microphysiologic Models of Bone Tissue. *Adv. Funct. Mater.* **31**, 2006796 (2021).
87. Yu, F., Selva Kumar, N. D., Choudhury, D., Foo, L. C. & Ng, S. H. Microfluidic platforms for modeling biological barriers in the circulatory system. *Drug Discov. Today* **23**, 815–829 (2018).
88. Ma, C., Peng, Y., Li, H. & Chen, W. Organ-on-a-Chip: A New Paradigm for Drug Development. *Trends Pharmacol. Sci.* **42**, 119–133 (2021).
89. Van Norman, G. A. Limitations of Animal Studies for Predicting Toxicity in Clinical Trials: Is it Time to Rethink Our Current Approach? *JACC Basic to Transl. Sci.* **4**, 845–854 (2019).
90. Yu, J. *et al.* Induced Pluripotent Stem Cell Lines Derived from Human Somatic Cells. *Science (80-. ).* **318**, 1917 LP – 1920 (2007).
91. Takahashi, K., Okita, K., Nakagawa, M. & Yamanaka, S. Induction of pluripotent stem cells from fibroblast cultures. *Nat. Protoc.* **2**, 3081–3089 (2007).
92. Takahashi, K. *et al.* Induction of Pluripotent Stem Cells from Adult Human Fibroblasts by

Defined Factors. *Cell* **131**, 861–872 (2007).
93. Sayed, N., Liu, C. & Wu, J. C. Translation of Human-Induced Pluripotent Stem Cells: From Clinical Trial in a Dish to Precision Medicine. *J. Am. Coll. Cardiol.* **67**, 2161–2176 (2016).
94. Low, L. A., Mummery, C., Berridge, B. R., Austin, C. P. & Tagle, D. A. Organs-on-chips: into the next decade. *Nat. Rev. Drug Discov.* **20**, 345–361 (2021).
95. Fredberg, J. J. & Kamm, R. D. STRESS TRANSMISSION IN THE LUNG: Pathways from Organ to Molecule. *Annu. Rev. Physiol.* **68**, 507–541 (2006).
96. Guenat, O. T. Incorporating mechanical strain in organs-on-a-chip : Lung and skin. **042207**, (2018).
97. Iba, T. & Sumpio, B. E. Morphological response of human endothelial cells subjected to cyclic strain in vitro. *Microvasc. Res.* **42**, 245–254 (1991).
98. Thodeti, C. K. *et al.* TRPV4 Channels Mediate Cyclic Strain–Induced Endothelial Cell Reorientation Through Integrin-to-Integrin Signaling. *Circ. Res.* **104**, 1123–1130 (2009).
99. Pampaloni, F., Reynaud, E. G. & Stelzer, E. H. K. The third dimension bridges the gap between cell culture and live tissue. *Nat. Rev. Mol. Cell Biol.* **8**, 839–845 (2007).
100. Nel, A., Xia, T., Mädler, L. & Li, N. Toxic Potential of Materials at the Nanolevel. *Science (80-. ).* **311**, 622–627 (2006).
101. Kim, H. J., Li, H., Collins, J. & Ingber, D. Contributions of microbiome and mechanical deformation to intestinal bacterial overgrowth and inflammation in a human gut-on-a-chip. *Proc. Natl. Acad. Sci.* **113**, 201522193 (2015).
102. Lundin, V. *et al.* YAP Regulates Hematopoietic Stem Cell Formation in Response to the Biomechanical Forces of Blood Flow. *Dev. Cell* **52**, 446-460.e5 (2020).
103. Sheyn, D. *et al.* Bone-chip system to monitor osteogenic differentiation using optical imaging. *Microfluid. Nanofluidics* **23**, 99 (2019).
104. Lim, H. *et al.* Development of wrinkled skin-on-a-chip (WSOC) by cyclic uniaxial stretching. *J. Ind. Eng. Chem.* **68**, (2018).
105. Barkal, L. J. *et al.* Microbial volatile communication in human organotypic lung models. *Nat. Commun.* **8**, (2017).
106. Bischel, L. L. *et al.* The importance of being a lumen. *FASEB J. Off. Publ. Fed. Am. Soc. Exp. Biol.* **28**, 4583–4590 (2014).
107. Anderson, A. E. & Foraker, A. G. Relative dimensions of bronchioles and parenchymal spaces in lungs from normal subjects and emphysematous patients. *Am. J. Med.* **32**, 218–226 (1962).
108. Hansen, J. E. & Ampaya, E. P. Human air space shapes, sizes, areas, and volumes. *J. Appl. Physiol.* **38**, 990–995 (1975).
109. Briard, B., Heddergott, C. & Latgé, J.-P. Volatile Compounds Emitted by Pseudomonas aeruginosa Stimulate Growth of the Fungal Pathogen Aspergillus fumigatus. *MBio* **7**, e00219 (2016).
110. Koo, S. *et al.* A breath fungal secondary metabolite signature to diagnose invasive aspergillosis. *Clin. Infect. Dis. An Off. Publ. Infect. Dis. Soc. Am.* **59**, 1733–1740 (2014).
111. Amin, R., Dupuis, A., Aaron, S. D. & Ratjen, F. The effect of chronic infection with Aspergillus fumigatus on lung function and hospitalization in patients with cystic fibrosis. *Chest* **137**, 171–176 (2010).
112. Renggli, K., Rousset, N., Lohasz, C., Nguyen, O. T. P. & Hierlemann, A. Integrated Microphysiological Systems: Transferable Organ Models and Recirculating Flow. *Adv. Biosyst.* **3**, 1900018 (2019).
113. Rogal, J., Probst, C. & Loskill, P. Integration concepts for multi-organ chips: how to maintain flexibility?! *Futur. Sci. OA* **3**, FSO180–FSO180 (2017).
114. Ronaldson-Bouchard, K. & Vunjak-Novakovic, G. Organs-on-a-Chip: A Fast Track for Engineered Human Tissues in Drug Development. *Cell Stem Cell* **22**, 310–324 (2018).
115. Bovard, D. *et al.* A lung/liver-on-a-chip platform for acute and chronic toxicity studies. *Lab Chip* **18**, 3814–3829 (2018).
116. Zhang, C., Zhao, Z., Abdul Rahim, N. A., van Noort, D. & Yu, H. Towards a human-on-chip:

Culturing multiple cell types on a chip with compartmentalized microenvironments. *Lab Chip* **9**, 3185–3192 (2009).
117. Imura, Y., Sato, K. & Yoshimura, E. Micro Total Bioassay System for Ingested Substances: Assessment of Intestinal Absorption, Hepatic Metabolism, and Bioactivity. *Anal. Chem.* **82**, 9983–9988 (2010).
118. Esch, M. B., Ueno, H., Applegate, D. R. & Shuler, M. L. Modular, pumpless body-on-a-chip platform for the co-culture of GI tract epithelium and 3D primary liver tissue. *Lab Chip* **16**, 2719–2729 (2016).
119. Maass, C. *et al.* Establishing quasi-steady state operations of microphysiological systems (MPS) using tissue-specific metabolic dependencies. *Sci. Rep.* **8**, 8015 (2018).
120. Edington, C. D. *et al.* Interconnected Microphysiological Systems for Quantitative Biology and Pharmacology Studies. *Sci. Rep.* **8**, 4530 (2018).
121. Renggli, K. & Frey, O. Chapter 12 - Design and engineering of multiorgan systems. in (eds. Hoeng, J., Bovard, D. & Peitsch, M. C. B. T.-O.) 393–427 (Academic Press, 2020).
122. Mak, I. W., Evaniew, N. & Ghert, M. Lost in translation: animal models and clinical trials in cancer treatment. *Am. J. Transl. Res.* **6**, 114–118 (2014).
123. Matthews, R. A. J. Medical progress depends on animal models - doesn't it? *J. R. Soc. Med.* **101**, 95–98 (2008).
124. Piergiovanni, M., Leite, S. B., Corvi, R. & Whelan, M. Standardisation needs for organ on chip devices. *Lab Chip* (2021).
125. Zhang, B., Korolj, A., Lai, B. F. L. & Radisic, M. Advances in organ-on-a-chip engineering. *Nat. Rev. Mater.* **3**, 257–278 (2018).
126. Probst, C., Schneider, S. & Loskill, P. High-throughput organ-on-a-chip systems: Current status and remaining challenges. *Curr. Opin. Biomed. Eng.* **6**, 33–41 (2018).
127. Campbell, S. B. *et al.* Beyond Polydimethylsiloxane: Alternative Materials for Fabrication of Organ-on-a-Chip Devices and Microphysiological Systems. *ACS Biomater. Sci. Eng.* (2020).
128. Campbell, S. *et al.* Beyond polydimethylsiloxane: Alternative materials for fabrication of organ on a chip devices and microphysiological systems. *ACS Biomater. Sci. Eng.* acsbiomaterials.0c00640 (2020).
129. Roman, G. T., Hlaus, T., Bass, K. J., Seelhammer, T. G. & Culbertson, C. T. Sol-gel modified poly(dimethylsiloxane) microfluidic devices with high electroosmotic mobilities and hydrophilic channel wall characteristics. *Anal. Chem.* **77**, 1414–1422 (2005).
130. Su, X. *et al.* Microfluidic cell culture and its application in high-throughput drug screening: cardiotoxicity assay for hERG channels. *J. Biomol. Screen.* **16**, 101–111 (2011).
131. Regehr, K. J. *et al.* Biological implications of polydimethylsiloxane-based microfluidic cell culture. *Lab Chip* **9**, 2132–2139 (2009).
132. Sasaki, H., Onoe, H., Osaki, T., Kawano, R. & Takeuchi, S. Parylene-coating in PDMS microfluidic channels prevents the absorption of fluorescent dyes. *Sensors Actuators B-chemical - Sens.* **150**, 478–482 (2010).
133. Shirure, V. S. & George, S. C. Design considerations to minimize the impact of drug absorption in polymer-based organ-on-a-chip platforms. *Lab Chip* **17**, 681–690 (2017).
134. van Meer, B. J. *et al.* Small molecule absorption by PDMS in the context of drug response bioassays. *Biochem. Biophys. Res. Commun.* **482**, 323–328 (2017).
135. Gewandter, J. S., Staversky, R. J. & O'Reilly, M. A. Hyperoxia augments ER-stress-induced cell death independent of BiP loss. *Free Radic. Biol. Med.* **47**, 1742–1752 (2009).
136. Tang, Y. *et al.* CYP1B1 and endothelial nitric oxide synthase combine to sustain proangiogenic functions of endothelial cells under hyperoxic stress. *Am. J. Physiol. Physiol.* **298**, C665–C678 (2009).
137. Heo, Y. S. *et al.* Characterization and resolution of evaporation-mediated osmolality shifts that constrain microfluidic cell culture in poly(dimethylsiloxane) devices. *Anal. Chem.* **79**, 1126–1134 (2007).
138. Volpatti, L. R. & Yetisen, A. K. Commercialization of microfluidic devices. *Trends Biotechnol.* **32**,

347–350 (2014).
139. Sano, E. *et al.* Tetrafluoroethylene-propylene elastomer for fabrication of microfluidic organs-on-chips resistant to drug absorption. *Micromachines* **10**, (2019).
140. Hirama, H. *et al.* Glass-based organ-on-a-chip device for restricting small molecular absorption. *J. Biosci. Bioeng.* **127**, 641–646 (2019).
141. Becker, H. Mind the gap! *Lab Chip* **10**, 271–273 (2010).
142. Miller, P. G. & Shuler, M. L. Design and demonstration of a pumpless 14 compartment microphysiological system. *Biotechnol. Bioeng.* **113**, 2213–2227 (2016).
143. Chen, H. J., Miller, P. & Shuler, M. L. A pumpless body-on-a-chip model using a primary culture of human intestinal cells and a 3D culture of liver cells. *Lab Chip* **18**, 2036–2046 (2018).
144. Bale, S. S. *et al.* A thermoplastic microfluidic microphysiological system to recapitulate hepatic function and multicellular interactions. *Biotechnol. Bioeng.* **116**, 3409–3420 (2019).
145. Winkler, T. E., Feil, M., Stronkman, E. F. G. J., Matthiesen, I. & Herland, A. Low-cost microphysiological systems: feasibility study of a tape-based barrier-on-chip for small intestine modeling. *Lab Chip* **20**, 1212–1226 (2020).
146. Moore, N. *et al.* A multiplexed microfluidic system for evaluation of dynamics of immune-tumor interactions. *Lab Chip* **18**, 1844–1858 (2018).
147. Theobald, J. *et al.* Liver-Kidney-on-Chip To Study Toxicity of Drug Metabolites. *ACS Biomater. Sci. Eng.* **4**, 78–89 (2018).
148. Humayun, M., Chow, C.-W. & Young, E. W. K. Microfluidic lung airway-on-a-chip with arrayable suspended gels for studying epithelial and smooth muscle cell interactions. *Lab Chip* **18**, 1298–1309 (2018).
149. Yen, D. P., Ando, Y. & Shen, K. A cost-effective micromilling platform for rapid prototyping of microdevices. *Technology* **4**, 234–239 (2016).
150. Feinberg, A. W. *et al.* Muscular thin films for building actuators and powering devices. *Science* **317**, 1366–1370 (2007).
151. Singh, M. *et al.* 3D printed conformal microfluidics for isolation and profiling of biomarkers from whole organs. *Lab Chip* **17**, 2561–2571 (2017).
152. Esch, M. B. *et al.* Multi-cellular 3D human primary liver cell culture elevates metabolic activity under fluidic flow. *Lab Chip* **15**, 2269–2277 (2015).
153. Wang, Y. I. & Shuler, M. L. UniChip enables long-term recirculating unidirectional perfusion with gravity-driven flow for microphysiological systems. *Lab Chip* **18**, 2563–2574 (2018).
154. Ong, L. J. Y. *et al.* A 3D printed microfluidic perfusion device for multicellular spheroid cultures. *Biofabrication* **9**, 45005 (2017).
155. Sticker, D., Geczy, R., Häfeli, U. O. & Kutter, J. P. Thiol–Ene Based Polymers as Versatile Materials for Microfluidic Devices for Life Sciences Applications. *ACS Appl. Mater. Interfaces* **12**, 10080–10095 (2020).
156. Sandström, N. *et al.* Reaction injection molding and direct covalent bonding of OSTE+ polymer microfluidic devices. *J. Micromechanics Microengineering* **25**, 75002 (2015).
157. Rimsa, R. *et al.* Lung on a Chip Development from Off-Stoichiometry Thiol-Ene Polymer. *Micromachines* **12**, (2021).
158. Hassan, S., Heinrich, M., Cecen, B., Prakash, J. & Zhang, Y. S. 26 - Biomaterials for on-chip organ systems. in *Woodhead Publishing Series in Biomaterials* 669–707 (2020).
159. Wang, H. *et al.* Global, regional, and national life expectancy, all-cause mortality, and cause-specific mortality for 249 causes of death, 1980–2015: a systematic analysis for the Global Burden of Disease Study 2015. *Lancet* **388**, 1459–1544 (2016).

# Chapter 2. Evaluating novel thermoplastic elastomers for applications in microfluidic cell culture

**Abstract:** In this chapter we demonstrate that two novel soft thermoplastic elastomers: FlexDym™ and Fluoroflex, are suitable for fabrication of microfluidic devices with applications in cell studies. Microfabrication protocols and proof-of-concept studies of microfluidic cell culture are developed, for the two materials respectively. Characterization of relevant material parameters including, gas permeability, wettability, small molecule absorption, biocompatibility and cell adhesion are presented.

## Contributions

The writing and the majority of the experimental work presented in this chapter was done by Emma Thomée. Gas permeability measurements and data analysis were performed by Dr. Raymond Thür (KU Leuven, Belgium). Oxygen plasma treatments were performed by Dr. Guénaëlle Jasmin-Lebras (CEA Paris-Saclay). Revision was done by Emma Thomée, Dr. Aurélie Vigne and Dr. Sasha Cai Lesher-Pérez.

## 2.1 Introduction

Since its proliferation starting in the late 1990s, microfluidic techniques for cell biology have progressed from foundational demonstrations of technological capabilities [1–3] to advanced biological models addressing fundamental questions in biology [4–6]. One branch in the state-of-the-art of microfluidics for biology is what has become known as "organ-on-chip" (OOC) technologies. These OOC platforms aim to leverage the precision control of fluid flow and unparalleled integration and analysis capabilities that are offered by microfluidic techniques in order to recreate the physical makeup and functionality of living human organ units.[7] In chapter 1 we discussed how OOC technology has positioned itself as a potential paradigm changer in drug development pipelines.

Currently, PDMS is the most used fabrication material for microfluidic devices used for cell culture and OOC applications.[8,9] Thanks to its low, stiffness and consequent facile handling and affordable molding process, PDMS devices of complex structures can be created without specialized equipment or know-how.[10] The elastomeric properties of PDMS have been leveraged to create integrated components for fluid handling such as fluid valves [11], or stretchable membranes for delivery of mechanical forces to cellular layers as commonly utilized in OOC technology [12]. Moreover, PDMS is biocompatible [13], gas permeable [14] and has excellent optical properties [15]. These aspects make it a desired material choice for OOC studies, where evaluation though fluorescent microscopy and flexible components for mechanical actuation are often necessary. In chapter 1, we outlined a number of drawbacks of PDMS that limit its use for OOC applications, the most prevalent of which are small molecule absorption [16], hydrophobic recovery [17] and poor transferability of fabrication [18]. Recent critical reviews highlight that OOC technology could greatly benefit from new, non-absorbent, optically transparent elastomers that offer facile prototyping and mechanical flexibility, as alternative materials to PDMS.[9,19]

Recent advances in polymer engineering have provided a wide range of elastomers that can be tailored to meet specific requirements. Flexible elastomers such as polyester elastomers [20], poly(octamethylene maleate (anhydride) citrate) scaffolds [21,22] and tetrafluoroethylene-propylene [23] have been implemented for applications in microfluidic cell culture. In terms of processability, (soft) thermoplastic elastomers (sTPE) are a group of hybrid elastomers that present unprecedented opportunities for microfluidic device fabrication. Thanks to their unique combination of elastomeric and thermoplastic properties, sTPE enable accessible fabrication of microfluidic devices on both small and large scale.[24–26] On small laboratory scales, the soft physical

properties of sTPEs allow for facile prototyping by means of soft-embossing against microfluidic mold, while on a larger scale, thermoforming by high-throughput techniques such as injection molding or roll to roll hot-embossing can be envisioned. sTPE materials with similar flexibility and elasticity to PDMS, optical transparency, low absorption and similar chemical properties to polystyrene have been developed, and might be a potential candidate for replacing PDMS.[24,27–29]

In this chapter, we evaluate the potential of two such novel sTPE materials, FlexDym™ and Fluoroflex, as prototyping materials for microfluidic cell culture devices. The study serves as a first step toward assessing their suitability for OOC fabrication. FlexDym™ is a commercially available, optically transparent SEBS block copolymer that was recently introduced for microfluidic device fabrication.[27,30,31] While sTPE microfluidic devices have been used for cell culture applications [29,32], there has been limited published data associated with FlexDym™ and its implementation in cell culture systems. To our knowledge, two different FlexDym™ formulations have been previously reported in only two instances with cell culture work. The first one showed yeast cells cultured on FlexDym™ sheets to demonstrate reduced absorption of a chemical division inhibitor due to FlexDym™'s materials properties.[27] The second one used a different, spin-coating formulation, FlexDym™SC, that supported culture of endothelial progenitor cells over four days.[33]

Fluoroflex is a fluoroelastic terpolymer Poly(TFE-ter-E-ter HFP) derived from an extruded fluorocarbon blend and has been developed by the creators of FlexDym™. Fluoroflex was recently demonstrated to be processable by hot-embossing and have similar self-sealing properties to its sister-polymer FlexDym™, but the fluorinated formulation was shown to exhibit enhanced resistance to organic solvents.[28] Fluoroflex devices have been developed for applications in droplet-based chemistry microfluidics.[28] There has, however, not been any previous demonstrations using Fluoroflex for bio-applications.

In this chapter we develop strategies for sTPE-based microfluidic cell culture. The study aims to serves as a reference and practical guide for future adoption of the two materials for microfluidic cell culture (throughout this thesis and beyond), and to facilitate transition from PDMS to sTPE.

## 2.2 Results and Discussion

In the first part of this study, we developed protocols for microfabrication and interfacing of FlexDym™ and Fluroflex microfluidic devices.

Secondly, we characterized selected material parameters of FlexDym™ and Fluoroflex: wettability, hydrophilization and hydrophobic recovery, oxygen and carbon dioxide permeability and small molecule absorption. The material characterization aimed to fill existing knowledge gaps needed to better understand the potential of the sTPE materials for microfluidic cell culture uses. Other critical characteristics of FlexDym™ and Fluoroflex as microfluidic materials, such as optical transparency, mechanical properties, solvent compatibility and surface morphology have been characterized elsewhere and were not considered in this study.[27,28] To leverage the wide knowledge base existing around microfluidic cell culture in PDMS-based devices, the material parameters are characterized in direct comparison to PDMS in the interest of facilitating a transfer from PDMS to sTPE materials.

The material characterization part is followed by an evaluation of material interactions with living cells for the two sTPE materials respectively. One of the most critical aspects when designing a microfluidic cell culture platform, wheatear cells are in direct or indirect contact with the device material, is undoubtedly ensuring that the device is biocompatible and does not induce non-desired effects on cell viability or cell functionality. We evaluated physical and chemical surface modification strategies in order to promote cell attachment and performed a quantitative study to demonstrate the biocompatibility of the two materials. Cell were found to attach selectively to plasma treated surfaces of FlexDym™, which was exploited to develop a method for spatially controlled cell immobilization for applications in cell patterning.

The last section is dedicated to practical implementation of FlexDym™ and Fluoroflex for microfluidic cell culture studies. Cell culture in enclosed microfluidic chambers of FlexDym™ and Fluoroflex devices has not been previously demonstrated. Thus, as a proof-of-concept, we developed experimental procedures for microfluidic cell culture in sTPE devices, and demonstrated on-chip culturing of HeLa cells in FlexDym™ and Fluoroflex devices to study the influence of static and dynamic perfusion conditions on cell proliferation.

### 2.2.1 sTPE microfabrication

**Hot-embossing**

Fabrication protocols were derived and used to fabricate microfluidic devices in FlexDym™ and Fluoroflex for experiments presented throughout this dissertation. If not otherwise mentioned, the microfluidic devices were monolithic, i.e., the same material make up the entire device.

FlexDym™ and Fluoroflex were micro-molded from extruded sheets or pellets by hot-embossing in under 2 minutes. FlexDym™ and Fluoroflex exhibit melting temperatures of approximately 120 °C and 210-220 °C, respectively, and the optimal molding temperatures were found to be 150 °C for FlexDym™ and 220 °C for Fluoroflex. The hot-embossing molding procedure of Fluoroflex is illustrated **Figure 2.1**, and the same procedure, changing only the molding temperature, can be used to mold FlexDym™. Alternatively, a protocol for hot-embossing of FlexDym™ using a vacuum-assisted heat press (Sublym100™, Eden Tech). The protocol for FlexDym™ molding using the vacuum-assisted heat press is outlined in section 2.4.2. Fluoroflex molding, however, had to be performed using the manual heat-press due to the molding temperature of Fluoroflex (220 °C) exceeding the maximum temperature capacity of the vacuum-assisted heat press.

The molding technique is highly compatible with soft lithography expertise and equipment already existing in microfluidics laboratories (apart from the additional need of a heat press). No specialized master mold is required for sTPE hot-embossing. Molds commonly used for PDMS replica molding, made from SU-8[27], epoxy[27] and dry film photoresists (such as the Ordyl® dry film mold used in this work) can be used.

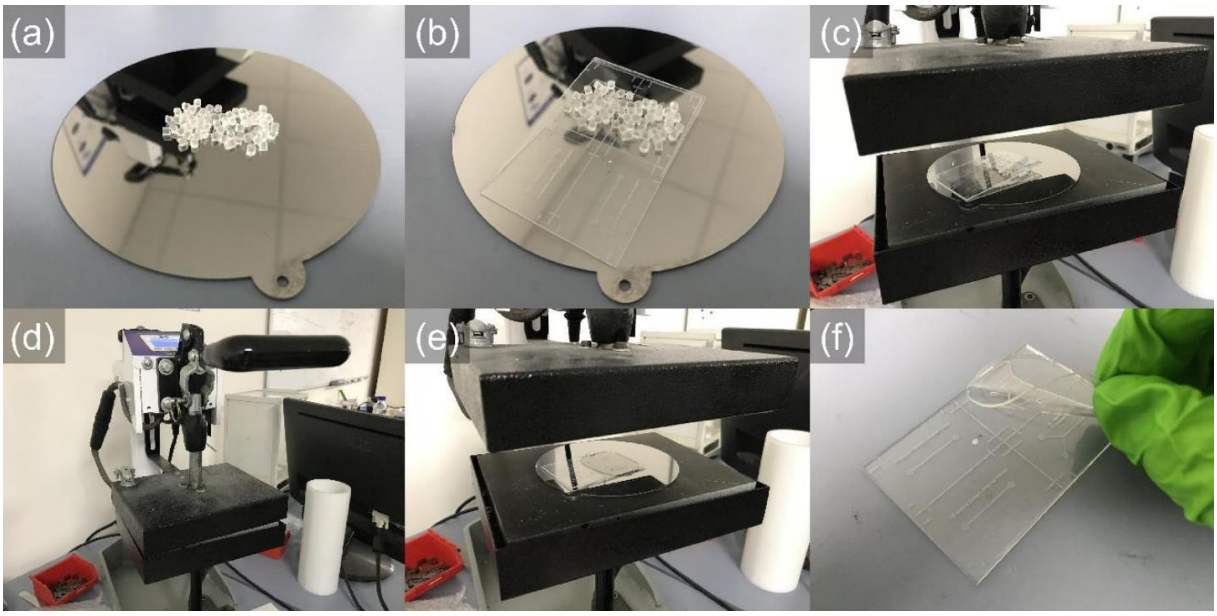


**Figure 2.1** sTPE hot embossing. (a) Raw sTPE pellets (Fluoroflex shown) are placed on a flat, smooth surface used as a counter-plate for hot embossing (nickel-cobalt plate shown). (b) A microfluidic master mold (Ordyl® dry film photo resist on glass) is placed atop the pellets. Note that only half of the mold is being used in this instance. (c) The assembly is placed on a manual heat press with both plates heated to 220 °C. (d) The upper plate is brought into contact with the assembly and left for 15 s while the assembly is allowed to heat, before pressure is manually applied for 15 s to thermoform the melted pellets. (e) After the upper plate is lifted, the hot embossing assembly is removed from the press and separated from the counter-plate using tweezers and isopropanol to ease separation. (f) Finally, the micropatterned sTPE sheet can be removed from the mold for subsequent manipulation. Adapted from ref.[28] with permission from Wiley-VCH GmbH.

### Chip bonding and interfacing

The soft elastomeric properties allowed for facile punching of access holes and conformal contact for device sealing through reversible thermal fusion bonding. A strong seal was formed following a 2 h baking at 85 °C for FlexDym™ and at room temperature for Fluoroflex. Neither of the sTPE required any additional adhesives or plasma activation for device sealing. FlexDym™ bonding is further characterized and discussed in chapter 4.

Micropatterned sTPE sheets resulted in rather thin substrates (~ 1 mm in thickness). For this reason, interfacing microfluidic tubing required an additional connector solution. In contrast to PDMS devices, which can be fabricated with sufficient thickness to interface tubing directly into an access port, sTPE devices represent an additional fabrication step for interfacing. In collaboration with Eden Tech, we

developed and evaluated methods for interfacing sTPE microfluidic chips with external flow control setup. Two satisfactory solutions were derived and commercialized by Eden Tech. For FlexDym™ devices, an industrially manufactured conical FlexDym™ connector could be thermally bonded over the access holes of a FlexDym™ device and microfluidic tubing could be inserted into the connector thanks to its elastomeric properties (**Figure 2.2a**). This solution represented a system completely fabricated in FlexDym™. A second, more robust solution, based on commercial thermoplastic luer lock connectors and double-sided adhesive O-ring stickers, was compatible with both FlexDym™ and Fluoroflex chips (**Figure 2.2b**). In addition, the luer connectors could serve as medium reservoir for static cell culture. Both connector solutions could withstand 2 bar of pressure.

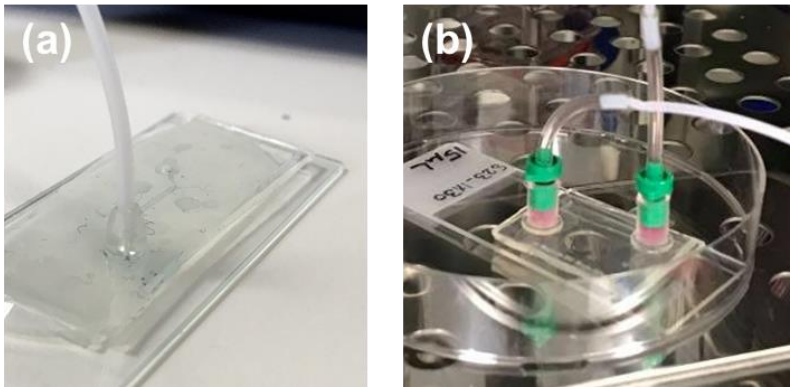


**Figure 2.2** Interfacing sTPE microfluidic chips. Photographs showing (a) a conical FlexDym™ connector thermally bonded to a FlexDym microfluidic chip and (b) thermoplastic luer lock connectors bonded to a FlexDym™ chip using double-sided adhesives.

## 2.2.2 Oxygen and carbon dioxide permeability

Access to oxygen and effective removal of carbon dioxide is of high importance to cell culture.[34] High permeability to oxygen and carbon dioxide through the walls of a microfluidic cell culture chamber enables oxygenation and pH control from the surrounding environment. The oxygen and carbon dioxide permeability values of FlexDym™ and PDMS at 37 °C were experimentally quantified and are presented in **table 2.1**. The FlexDym™ permeability to oxygen and carbon dioxide were found to be 26.17 ± 0.59 Barrer (mean ± standard deviation) and 104.0 ± 1.8 Barrer respectively. PDMS was found to have an oxygen permeability of 674.8 ± 23.3 Barrer and a carbon dioxide permeability of 3381 ± 100 Barrer. The values are in agreement (although in

the lower end) with permeabilities of PDMS reported in literature, found in the ranges ~600-800 Barrer for oxygen and ~3250-3800 Barrer for carbon dioxide.[14,35] Other SEBS formulations have permeabilities reported in the ranges ~33-61 Barrer for oxygen and ~8.6-8.9 Barrer for carbon dioxide.[24]

**Table 2.1. Gas permeability data of PDMS and FlexDym™ at 37 °C**
**Value from McMillan et al.[28], collected at 35 °C.

| | Oxygen permeability (Barrer) | Carbon dioxide permeability (Barrer) |
|---|---|---|
| **PDMS** | 674.8 ± 23.3 | 3381 ± 100 |
| **FlexDym™** | 26.17 ± 0.59 | 104.0 ± 1.8 |
| **Fluoroflex** | 4.04 ± 0.79** | |

Our experimental results represent a 25 times lower oxygen permeability and a 32 times lower carbon dioxide permeability of FlexDym™ compared to PDMS. The oxygen permeability of Fluoroflex has previously been determined to 4.04 ± 0.79 Barrer (quantified at 35°C and 6 bar feed pressure), which represents a 10-fold lower permeability compared to FlexDym™.[28]

While high oxygen and carbon dioxide permeabilities are generally considered an advantage in order to minimize cellular stress, high permeability to water vapor is typically problematic in gas permeable devices as it can cause evaporation of media even in humidified cell culture incubators.[36] The relatively lower gas permeabilities of FlexDym™ and (particularly) Fluoroflex could provide greater opportunity of the sTPEs to be used for hypoxic cell culture or studies requiring a controlled oxygen environmental on a device-level.

### 2.2.3 Small molecule absorption

The uptake of small molecules, such as drugs, dye compounds or signalling molecules, from a solution into the bulk of the microfluidic chip material is an important consideration in microfluidic experiments. Absorption could have a significant impact on the experimental readouts, in the form of as cross-contamination, higher background signal or reduced solute concentration resulting in inaccurate dose-response interpretations.[16] To assess small molecule absorption of FlexDym™ in comparison to PDMS, rhodamine B solution was incubated in microfluidic channels of

FlexDym™ and PDMS for 0, 1, 6 and 24 hours and analysed by fluorescent microscopy. Rhodamine B (log P value = 2.43-2.44, molecular mass = 479 Da) has been shown to be a suitable drug surrogate for assessing susceptibility of polymers to absorption of drugs.[37]

Minimal absorption was observed in the FlexDym™ devices (**Figure 2.3c**) in contrast to the PDMS devices that showed a widening and increased intensity of the line profile (**Figure 2.3b**), indicating absorption into the PDMS bulk on the sides of the channels. Subsequent washing of the channels with DI water, reduced the fluorescent signal in FlexDym™ devices to almost 0 (**Figure 2.3a**). While a small fluorescent signal remained, it was minimal in comparison to PDMS (**Figure 2.3a**). Likewise, Fluoroflex has previously been demonstrated to be resistant to rhodamine B absorption up to 24 hours.[28] Although a quantitative study of would be necessary to determine the degree of absorption/adsorption of a given molecule and weather it would have an impact on a given experimental outcome, these results indicate that FlexDym™ and Fluoroflex devices would hold a significant advantage over PDMS for microfluidic studies involving small molecules.

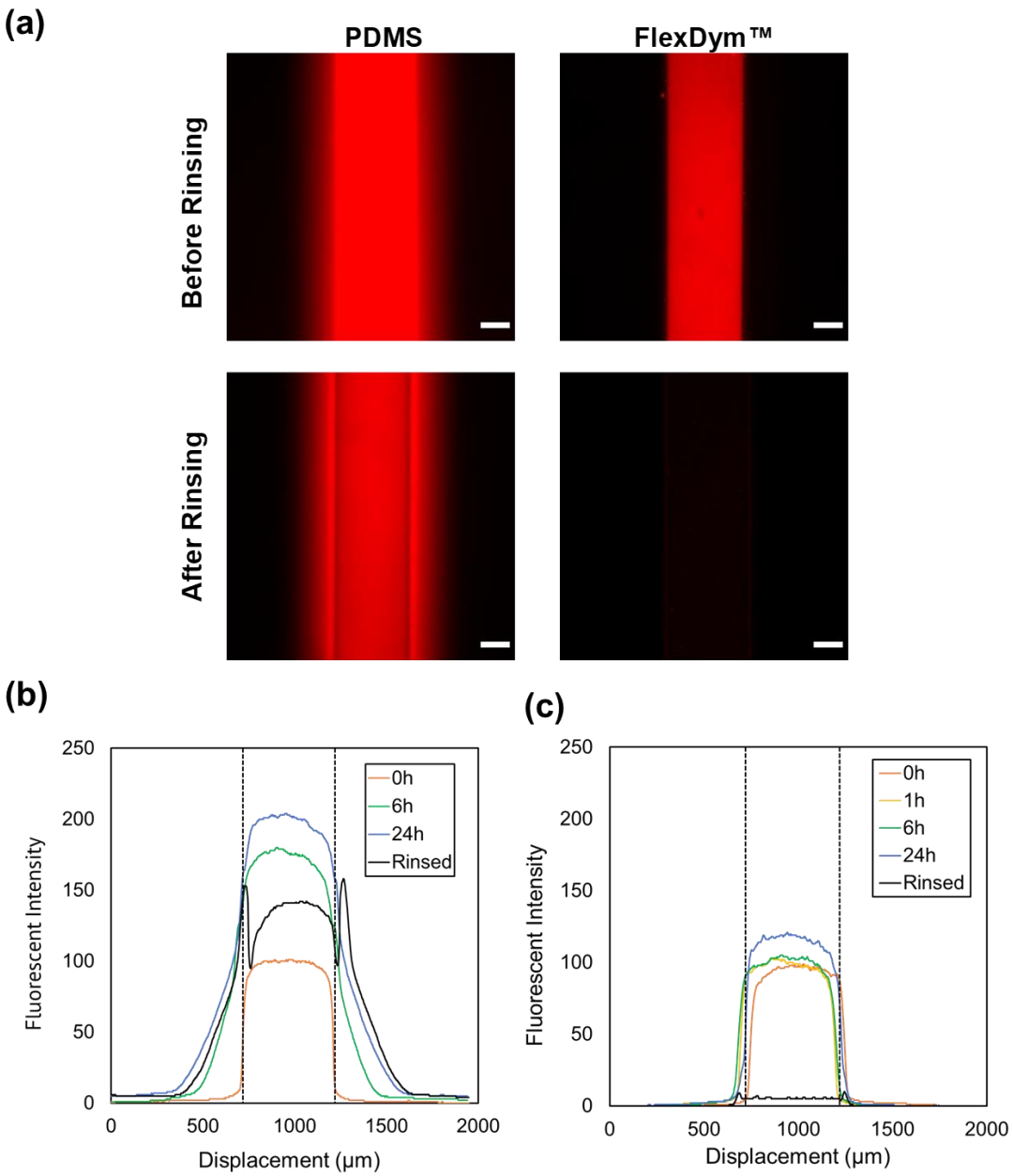


**Figure 2.3.** Characterization of Rhodamine B uptake in PDMS and FlexDym™ microchannels (500 μm x 55 μm). (a) Fluorescent images of PDMS and FlexDym™ channels containing 100 μM Rhodamine B in water after 24 h of incubation The same channels were reimaged after rinsing with 10 mL DI water (exposure time 100 ms). (a) and (b) show the corresponding line profiles of Rhodamine B incubation for 0, 1, 6 and 24 hours in the PDMS and FlexDym™ channel respectively (exposure time 50 ms). The dashed lines mark the position of the channel walls. Scale bars 200 μm.

### 2.2.4 Hydrophilization and hydrophobic recovery

To characterize the surface wettability of FlexDym™ and Fluoroflex, we performed goniometer measurements to determine the static contact angle of sessile drops of water (in air) on pristine polymer samples. Pristine FlexDym™ and Fluoroflex exhibited static contact angles of $\Theta_{water}$= 100 ± 4 ° (mean ± standard deviation) and $\Theta_{water}$= 105 ± 3 °, respectively. The values obtained were in agreement with previously reported values of advancing and receding contact angle of FlexDym™ of 105 ± 4 ° and 88 ± 4 °, respectively[27], and the static contact angle of Fluoroflex 105 ± 1.2 ° [28]. The static contact angles of FlexDym™ and Fluroflex are comparable to pristine PDMS, which has values reported in the range 100-115 ° [13,38–40]. Hydrophobic material characteristics and microfluidic behaviour similar to PDMS would thus be expected, such as poor capillary flow, susceptibility to protein adsorption and poor cell adhesion.[41]

Hydrophilization of naturally hydrophobic polymers by oxygen plasma has been widely utilized, for instance, to improve cell attachment density [42–44], control adsorption of proteins [45,46] and improve biocompatibility [39,47]. To evaluate surface hydrophilization by oxygen plasma, FlexDym™ and Fluoroflex samples were exposed to oxygen plasma treatment for 2, 5 or 10 minutes, at power of 100 W. The plasma parameters were selected based on previous AFM investigations that showed no morphological changes on FlexDym™ surfaces after 10 minutes of plasma treatment with the given parameters.[27] Samples were stored dry in room temperature and analysed by goniometry within 3 h after plasma exposure. 10 min of oxygen plasma treatment resulted in complete surface wetting of FlexDym™, while 2 and 5 minutes of treatment resulted in a significant reduction in contact angle to values of 71 ± 3 ° and 49 ± 5 ° respectively (**figure 2.4a**). These results contrast previously reported data of FlexDym™ samples of equivalent plasma conditions and aging time, that resulted in static contact angles below 40 ° for all treatment times.[27] Fluoroflex samples remained hydrophobic even after the longest plasma treatment time (10 minutes), which resulted in a slight reduction in contact angle to 98 ± 3 °. Fluoropolymers are characterized by high inertness, low surface energy and low adhesive properties. Effects of oxygen plasma treatment on the wettability of another fluoropolymer, PTFE, has been reported to be dependent on the plasma conditions, where high power plasma (300 W) resulted in super hydrophobic surfaces, moderate power plasma resulted in hydrophilic surfaces, and low power plasma (< 50 W) resulted in substantially unchanged surfaces.[48] A more extensive investigation into the wettability behaviour of Fluoroflex was outside the scope of this study.

Oxygen plasma hydrophilization of PDMS has been widely studied [13,17,38,42,49–52], and shown to initially reduce the contact angle to hydrophilic values, followed by a rapid hydrophobic recovery when stored dry in contact with ambient air. The recovery time of PDMS varies greatly between studies, from hours [53] to days [40,54], while FlexDym™ has been reported to remain hydrophilic for up to 96 hours after plasma treatment.[27] To evaluate if the hydrophilicity lasted beyond 96 hours, the recovery of the static contact angle of FlexDym™ samples that had been exposed to oxygen plasma for 2, 5 or 10 minutes and stored dry at ambient conditions from the point of hydrophilization up to 14 days was analysed. The results are presented in **figure 2.4b**. FlexDym™ does not fully recover to its initial hydrophobicity within 14 days, but appears to reach a saturation limit about 20 ° degrees lower than the initial contact angle for all three plasma exposure times. Likewise, other SEBS formulations have been shown to have a more stable hydrophilization than PDMS and to undergo a hydrophobic recovery over 3-4 days after plasma treatment.[32] The EB domain of FlexDym™ exhibit a negative glass transition temperature ($T_{g,\,EB} \simeq 50\,°C$) resulting in mobile polymer chains above this temperature.[27] The polymer chain mobility at room temperature is believed to be one reason for the hydrophobic recovery. However, unlike PDMS, where un-crosslinked polymers are free to diffuse, the EB chain mobility in FlexDym™ is restricted by covalent bonds to thermally stable polystyrene domains, which could explain the slower hydrophobic recovery compared to PDMS.

The slower hydrophobic recovery of FlexDym™ compared to PDMS has practical advantages, such as dry storage of samples in room temperature up to several days after plasma treatment.

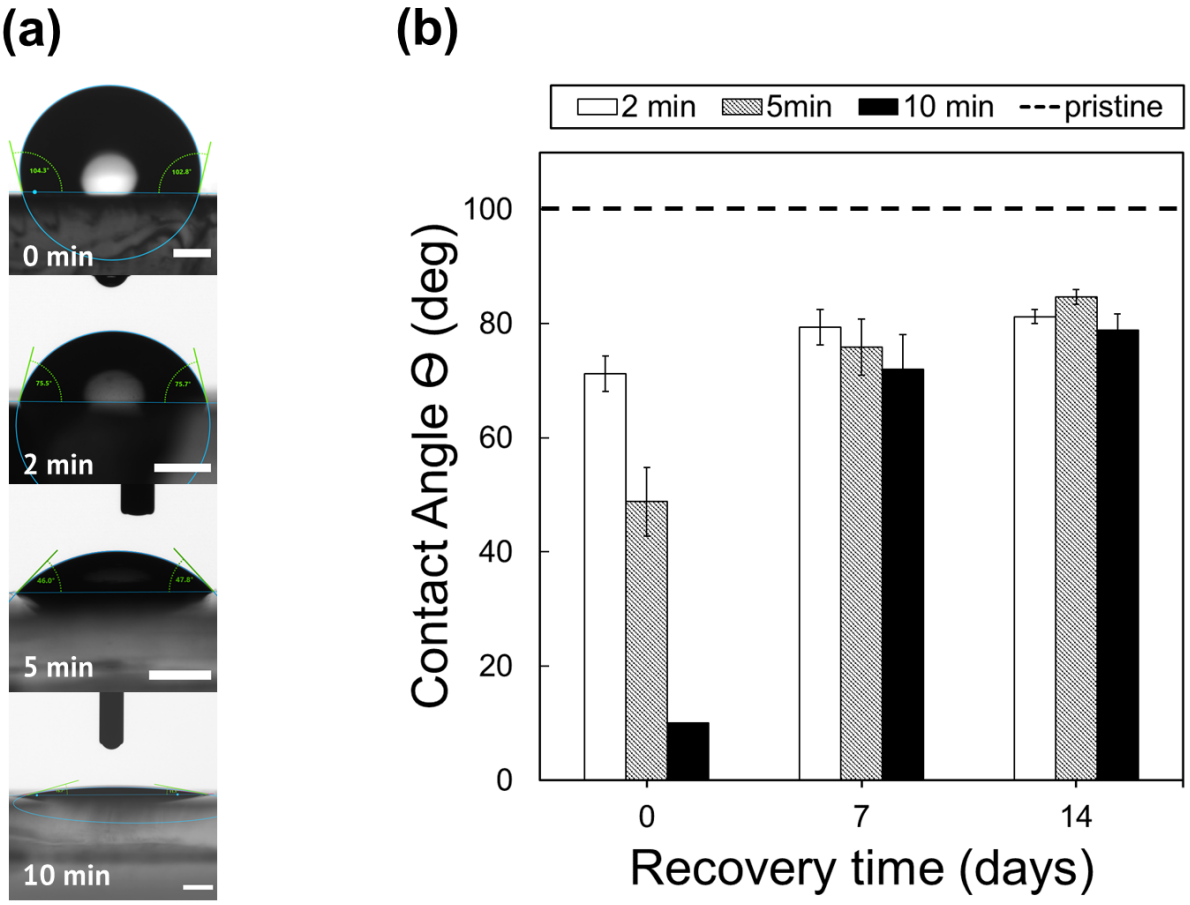


**Figure 2.4.** Static contact angle of DI water on FlexDym™ (a) and FlexDym™ treated with oxygen plasma (20 sccm, 50 mT and 100 W) for 2, 5 or 10 minutes. Scale bars 1 mm. (b) shows the evolution of the static contact angle of DI water on FlexDym™ surfaces treated with oxygen plasma for 2, 5 or 10 minutes. The dashed line represents the value of pristine FlexDym™ without plasma treatment. Average values of 5 measurements are shown and error bars represent one standard deviation.

### 2.2.5 Surface modifications for cell adhesion and proliferation

Achieving good cell attachment that support proliferation and healthy cell morphologies is a key element for the success of implementing a new a material in cell culture systems. Indeed, cell adhesion to a substrate may vary greatly between cell types and may require different surface modifications of the substrate.

We characterized the adhesion and growth of CHO cells in serum-containing culture media on pristine FlexDym™ and Fluoroflex substrates. Results showed that, in comparison to the control tissue culture plates (**Figure 2.5a-c**), CHO cells poorly adhered to pristine FlexDym™ (**Figure 2.5d-e**). After 48 hours, only a low number of

cells had adhered to the samples and most of the cells remained in a rounded morphology. Surface hydrophilization with oxygen plasma treatment for 2 minutes (**Figure 2.5g-h**) was sufficient to achieve a good cell adhesion to FlexDym™ and enhance cell growth, at a rate comparable to the control tissue culture plate substrates. Poly-d-lysine is a chemically synthesized protein with a net positive charge that is commonly used as a coating to improve cell attachment to a substrate by promoting electrostatic interaction with negatively charged ions of the cell membrane.[55] Poly-d-lysine treatment alone did not improve cell adhesion on FlexDym™ substrates (**Figure 2.5j-l**). However, when used in combination with oxygen plasma treatment (**Figure 2.5m-o)**, cell adhesion was significantly improved compared to un-treated samples. A collagen I protein coating also enhanced cell adhesion to FlexDym™ (**Figure 2.5p-r)**. In vivo, collagen is a main component of the extra cellular matrix. While the mechanism of interaction between collagen and cells in tissue is not fully understood, collagen likely interacts with receptors on the cell membrane which could highly influence the adhesion and proliferation of cells.[56]

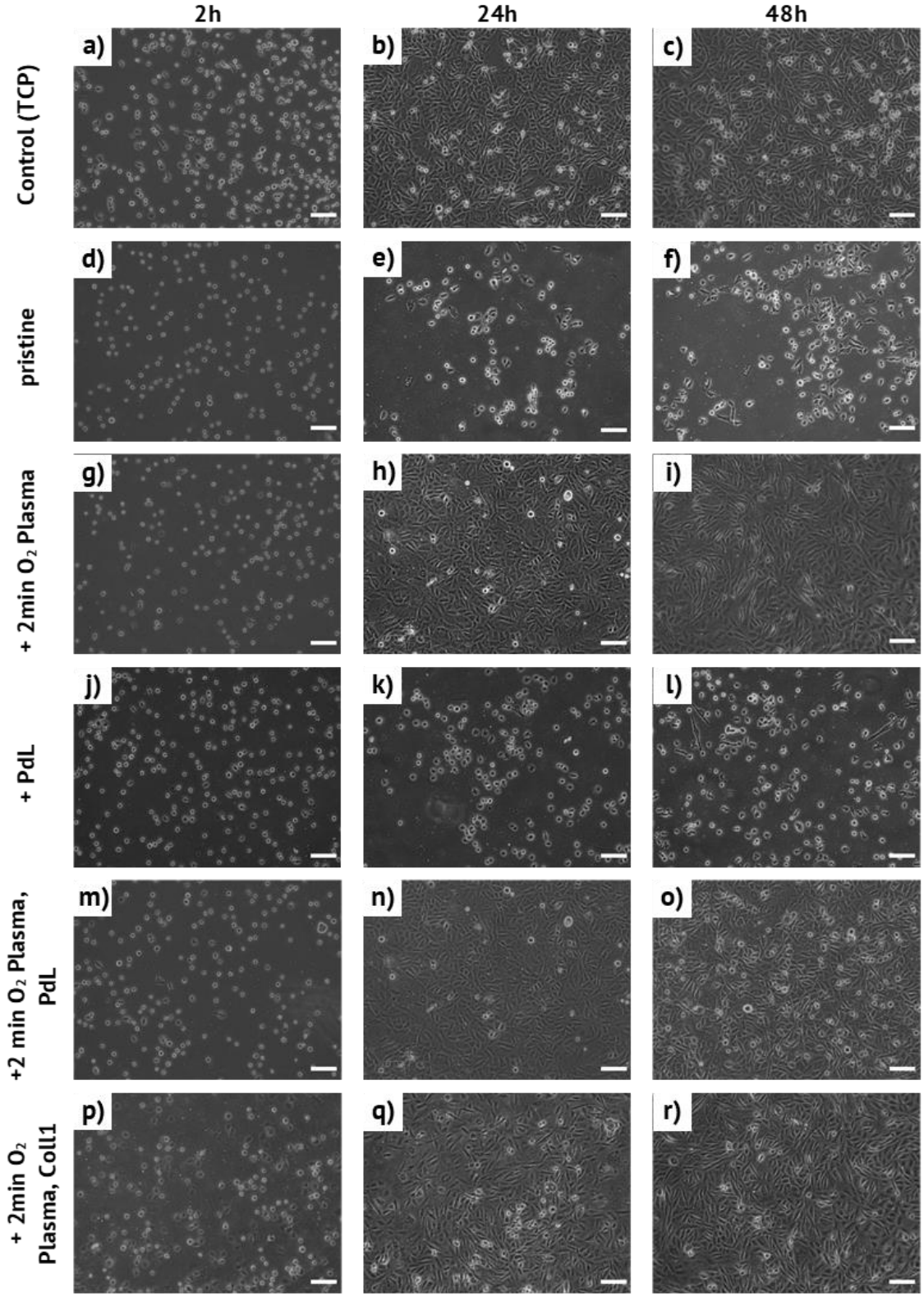


**Figure 2.5.** Comparison of CHO adhesion and proliferation on FlexDym™ and treated surfaces: Phase contrast images of CHO cells, 2, 24 and 48 hours after cell seeding on (a-c) TCP surface (control), (d-f) pristine FlexDym™ and Flexdym™ treated with (g-i) $O_2$ plasma for 2 minutes, (j-l) poly-d-lysine, (m-o) $O_2$ plasma for 2 minutes + poly-d-lysine, (p-r) $O_2$ plasma for 2 minutes + Collagen I. Scale bars 100 µm.

Likewise, we found that plasma treatment was sufficient modification to enable cell attachment and proliferation on FlexDym™ surfaces by a number of cell types: cancerous cell lines (HeLa), cardiac myoblasts (h9c2), hair follicle derived mesenchymal stroma cells (hF MSC) and endothelial cells (HUVEC) (**Figure 2.6.**).

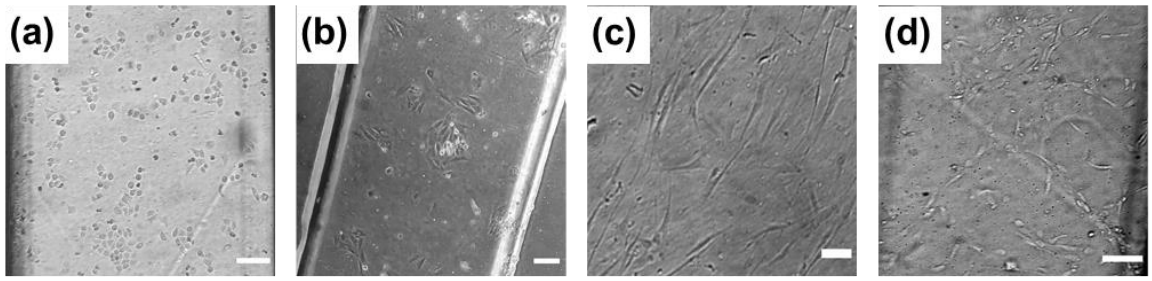


**Figure 2.6.** Cell adhesion on FlexDym™. Brightfield images of (a) HeLa cells, (b) cardiac myoblasts (h9c2), (c) hair follicle derived mesenchymal stroma cells (hf MSC) and (d) endothelial cells (HUVEC) adhered on air plasma treated FlexDym™ surfaces. Scale bars 100 µm.

Interestingly, pristine Fluoroflex supported CHO cell proliferation to a larger extent (**Figure 2.7d-f**) than FlexDym™. Oxygen plasma treatment (**Figure 2.7g-i**) and collagen I coating (**Figure 2.7j-l**) appeared to result in a slightly higher number of cells attached at 15 hours compared to pristine Fluoroflex, and similar to the control group (**Figure 2.7a-c**). After 96 hours, a high cell density was observed for all culture conditions.

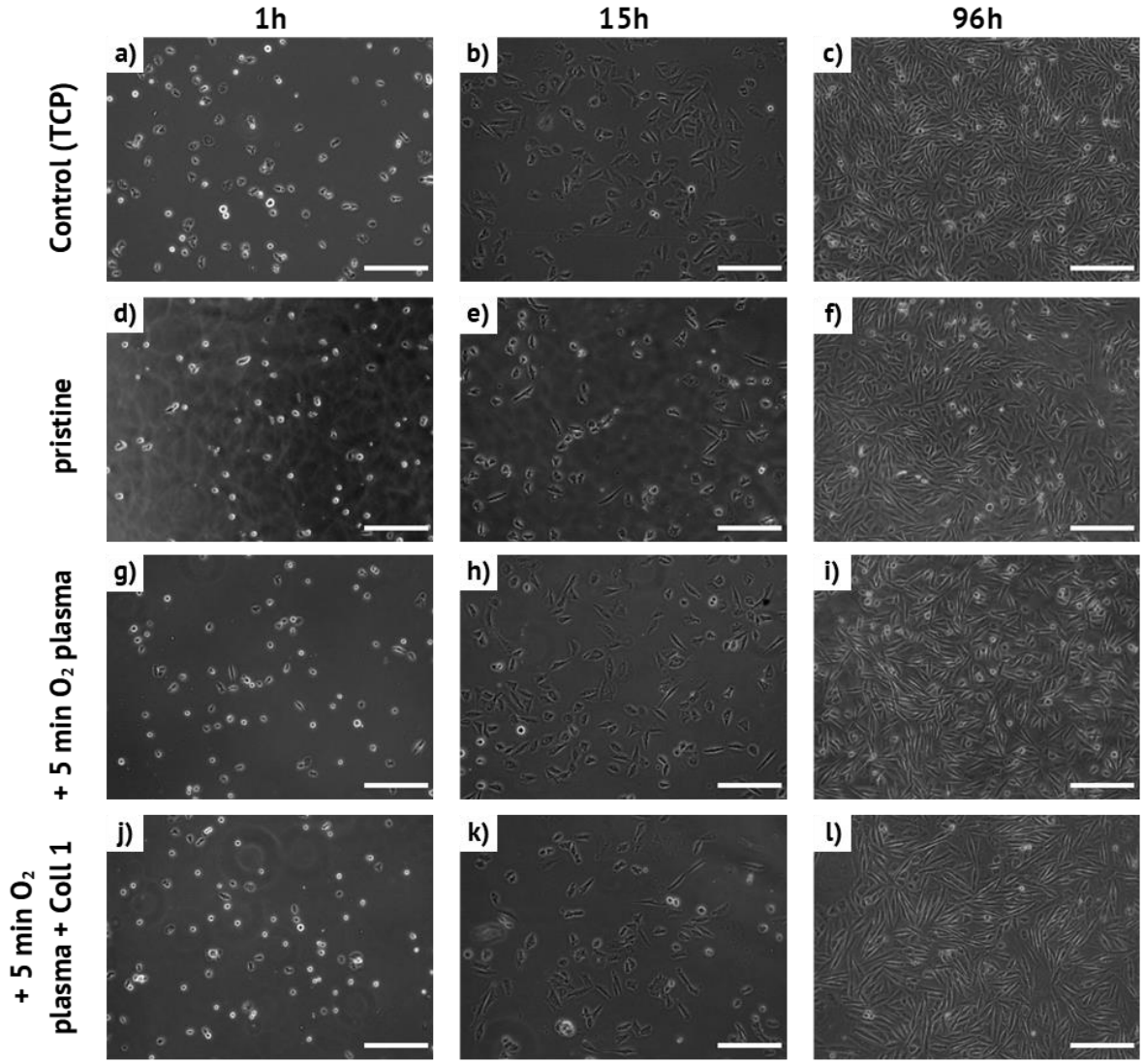


**Figure 2.7.** Comparison of CHO adhesion and proliferation on Fluoroflex and treated surfaces: Phase contrast images of CHO cells, 1, 15 and 96 hours after cell seeding on (a-c) TCP surface (control), (d-f) pristine Fluoroflex and Fluoroflex treated with (g-i) $O_2$ plasma for 5 minutes and (j-l) $O_2$ plasma for 5 minutes + Collagen I. Scale bars 100 µm.

## 2.2.6 Cell patterning in FlexDym™ microfluidic channels

Controlled cell immobilization on micron-scale is of importance in a variety of fields including tissue engineering, biosensors and OOC engineering. Commonly, cell patterning is conducted on stiff substrates such as glass or polystyrene. However, patterns of elastic substrates might be of interest for studies such as cell communication via sensing of substrate interaction under controlled spatial arrangements.[57] Cell patterning techniques based on soft lithography, such as microcontact printing, can effectively produce cell patterns down to single micron

scales.[10] However, such patterned surfaces are generally not compatible with microfluidic device fabrication steps where the device assembly requires surface plasma activation for bonding. Attempts to generate patterned cell culture within microfluidic devices have been described previously based on bonding techniques such plasma bonding [58] or magnetic clamping of device [59].

Based on our previous findings that showed that cell adhesion was poor to pristine FlexDym™ but significantly improved after plasma treatment, we hypothesized that selective plasma treatment could be utilized to achieve spatial control of cells to FlexDym™ substrates. A simple cell patterning technique based on air plasma lithography for selective hydrophilization without the need for any protein surface modifications or blocking steps was developed and used to achieve controlled spatial organization of cells on FlexDym™ substrates (**Figure 2.8**). This technique works exclusively for FlexDym™ as cell did not selectively adhere to plasma-treated Fluoroflex surfaces.

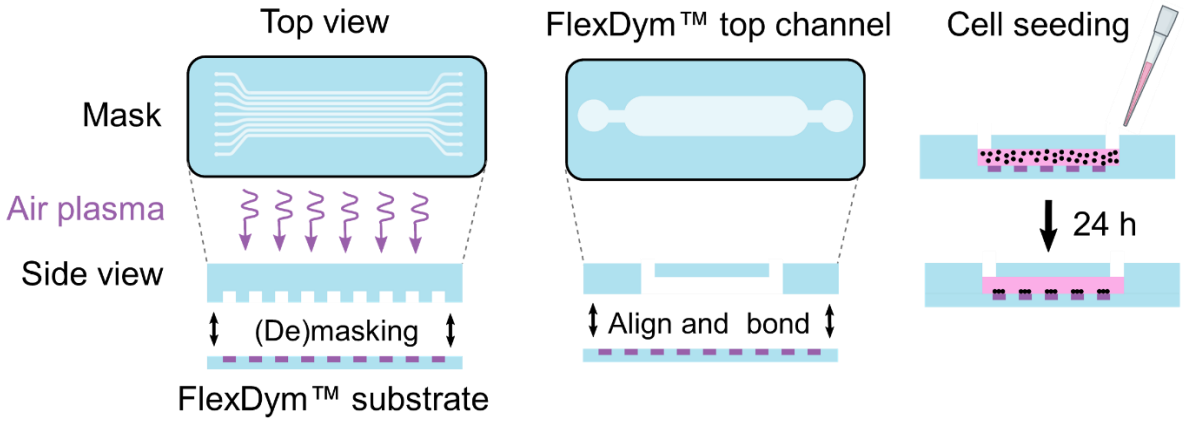


**Figure 2.8.** Cell patterning of FlexDym substrates. Schematic outline of the patterned method developed for confining HeLa cells in microfluidic devices of FlexDym™. The left panel (step 1-3) shows the principle for selective air plasma exposure to create a heterogeneous substrate with non-oxidized region and oxidized regions for cell adhesion. The right panel (step 4-6) shows the process of bonding a Flexdym™ channel to the heterogeneous FlexDym™ substrate to create a microfluidic device. Cell seeding in the channel result in cell adhesion exclusively to the oxidized regions.

Parallel stripes of width 300 µm were hydrophilized with air plasma for 10 minutes. After 15-24 hours of culture, HeLa cells were found to adhere and spread selectively on the parallel stripes (**Figure 2.9a**). A high cell density was obtained in the plasma treated areas, while the non-treated areas remained largely free from cells – apart

from a low number of scattered cells **Figure 2.9d**). After cells had reached a confluent state, they started to outgrowth of the patterned areas (**Figure 2.9b-c**). The same technique applied to PDMS substrates resulted in very poor cell adhesion (**Figure 2.9e**).

The pattern could straightforwardly be integrated inside a microfluidic channel by thermally bonding a FlexDym™ channel to the patterned substrate before cell seeding (**Figure 2.9f**). Thanks to the stable hydrophilization, a strong bond could be achieved from room temperature bonding for 2 hours without compromising the surface hydrophilicity. This simple method to achieve spatial control of cell attachment could potentially serve as tool when designing cell-based microfluidic assays.

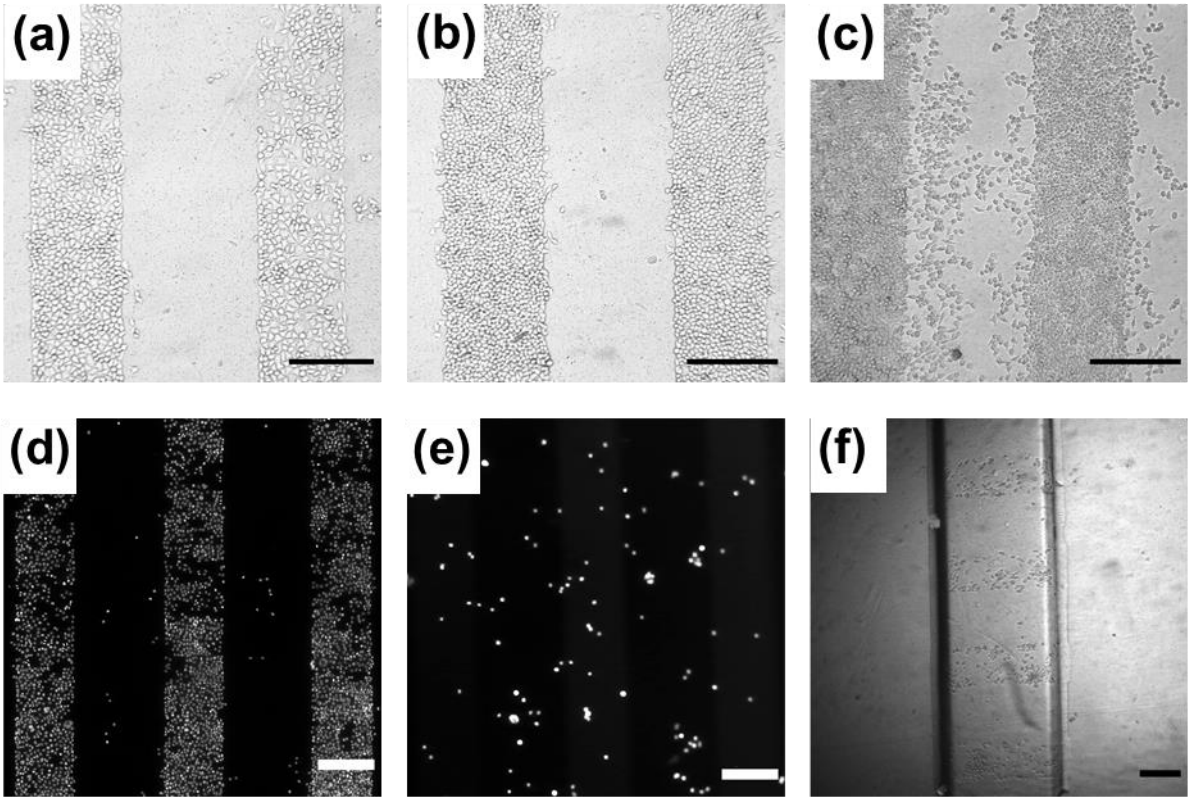


**Figure 2.9.** Cell patterning of HeLa cells on FlexDym™ substrates. Brightfield images showing cell growth on heterogenous FlexDym™ substrates for 1 day (a), 2 days (b) and 3 days (c). Fluorescent images of fixed cell nuclei stained with DAPI on heterogenous FlexDym™ (d) versus PDMS (e) substrates, 1 day after cell seeding. (f) Demonstration of cell patterning (300 µm wide stripes aligned perpendicular to channel) in a microfluidic channel of width 800 µm and height 140 µm. Scale bars 300 µm.

## 2.2.7 Biocompatibility

A LIVE/DEAD in vitro cytotoxicity assay of HeLa cells grown in direct contact with FlexDym™ and Fluoroflex polymers was performed to determine if the materials exerted a cytotoxic effect on the cells. Cells grown on FlexDym™, Fluoroflex and tissue culture plates (TCP, positive controls) were stained with calcein AM and propidium iodide after 3, 24 and 48 hours of culture. **Figure 2.10a** shows representative images of the stained viable (green) and dead (red) cells, and the merged images. The data showed that most cells remained alive after being cultured on the polymers for 48 hours. Quantification of the percentage of viable cells confirmed cell viability over 90% for all experimental conditions (**Figure 2.10b**). There was no significant difference in cell viability of cell growth on either of the sTPE compared to the control substrate, at any of the time points. It was therefore concluded that both FlexDym™ and Fluoroflex showed high biocompatibility and are suitable materials for use in cell culture systems.

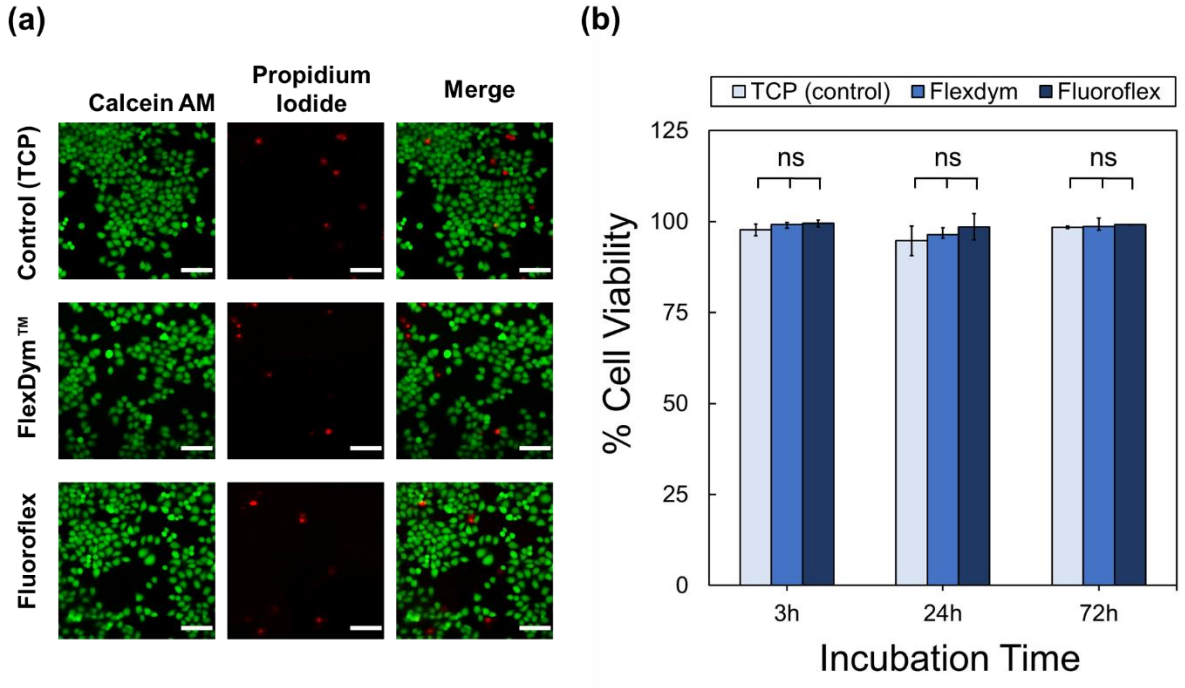


**Figure 2.10.** LIVE/DEAD cell viability staining and quantification of HeLa cells. (a) Fluorescent microscopy images of viable cells stained with calcein AM (green) and dead cells stained with propidium iodide (red) on TCP (control), FlexDym™ and Fluoroflex substrates after 24 h of incubation. Scale bars 200 µm. (b) A high cell viability (> 90%) was observed for cells grown of TCP, FlexDym™ (FD) and Fluorflex (FF) after 3, 24 and 72 h of incubation. Ns indicates no statistical difference ($p > 0.05$, $n = 3$ for each data set, error bars represent one standard deviation).

### 2.2.8 Dynamic cell culture in sTPE devices

Complete procedures for cell culture studies in sTPE devices were developed, including protocols for channel surface treatment, sterilization, cell seeding, medium exchange and on-chip imaging. The protocols are presented in the form a commercial application note, presented in Appendix 1 – How to grow cells in a FlexDym™ microfluidic channel. The experimental flow control setup developed for dynamic cell culture is illustrated in Figure 2.11.

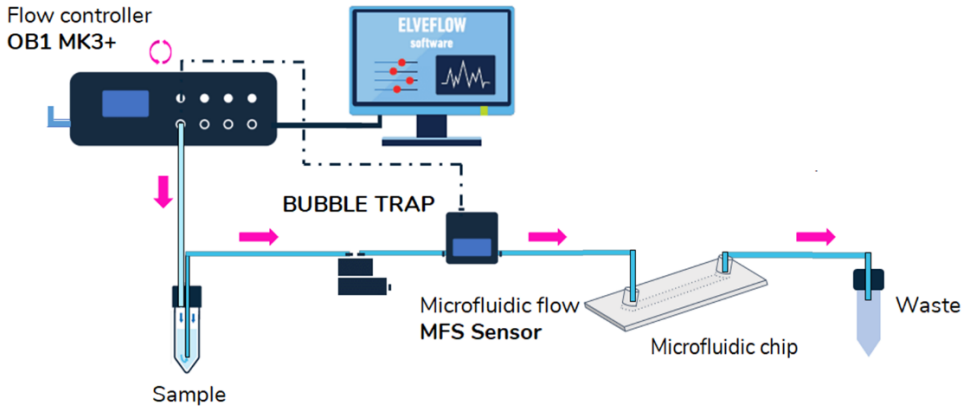


**Figure 2.11.** Schematic of the microfluidic flow control setup utilized for dynamic microfluidic cell culture. The setup consisted of an OB1 MK3+ pressure controller, an inline bubble trap and flow sensor. The circuit was controlled using Elveflow ESI Software.

As a demonstration of microfluidic cell culture in sTPE devices, we investigated the influence of static and dynamic perfusion conditions on HeLa cell proliferation and morphology. The microfluidic cell culture devices in FlexDym™ or Fluroflex had a rectangular microchamber of cross-section 150 x 800 µm, similar to geometries of perfusion microsystems described in literature [60–64]. This design enabled a symmetrical flow profile for even supply culture media and a highly uniform cell density across the entire micro-culture chamber (as seen in **Figure 2.12)**. Both culture conditions, dynamic perfusion and static (with and without manual exchange of media), were evaluated for both device materials. Starting at 24 hours, the dynamic systems were subjected to a constant flow at a flow rate of 3 µL/min, corresponding to a wall shear stress of 0.16 dyne/cm$^2$. This value falls within the range of typical shear stresses reported for culture of cancer cells in perfusion bioreactors.[65,66]

It was found that the FlexDym™ and Fluoroflex devices both supported adhesion of HeLa cells in enclosed microfluidic chambers, and could sustain cell attachment for

48 hours under regular media exchanges or constant perfusion (**Figure 2.12**). Under perfusion, cells in both devices exhibited similar morphologies to cells cultured in tissue culture plates.

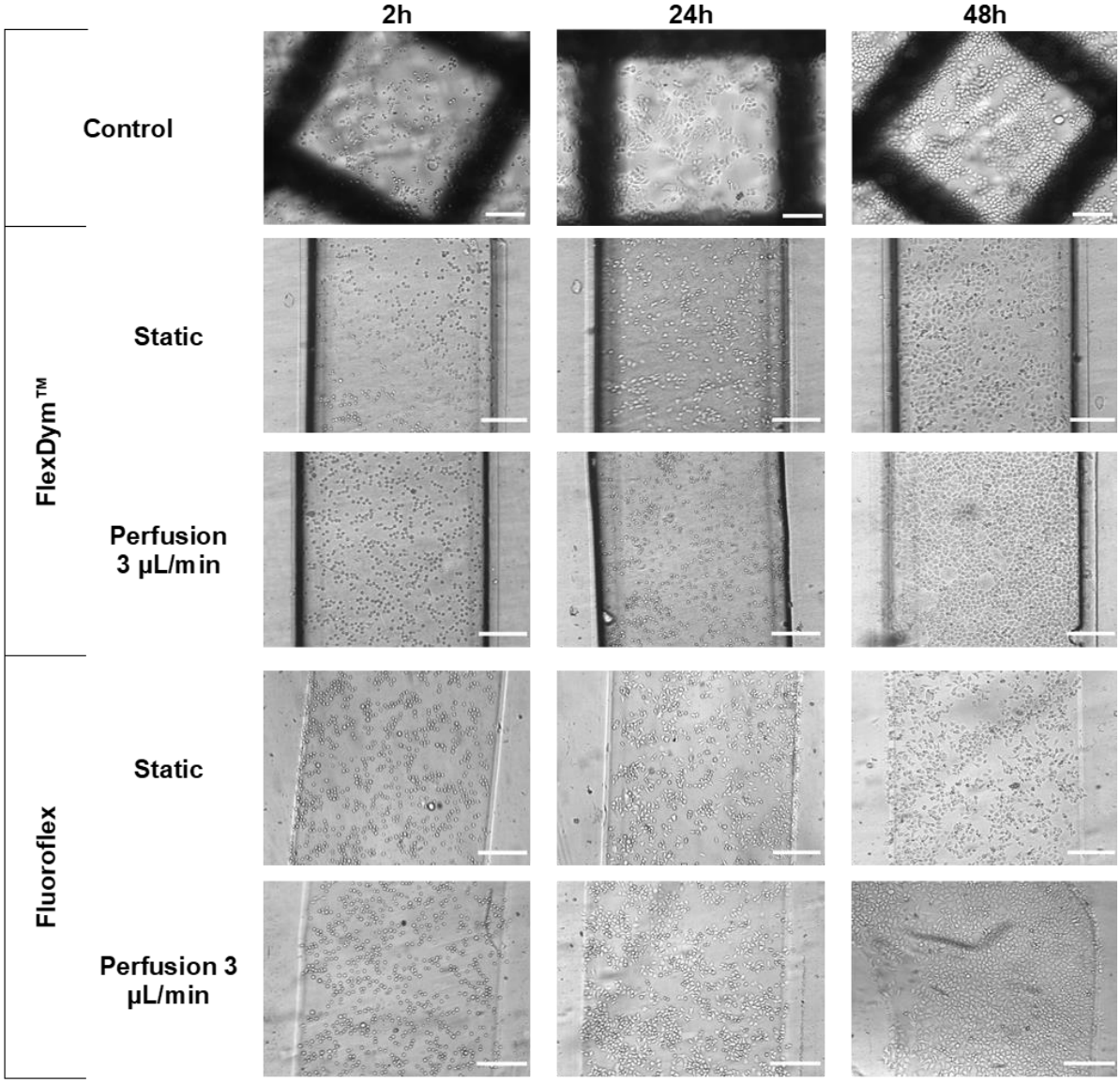


**Figure 2.12.** Microfluidic HeLa cell culture under static and dynamic perfusion (at 3 µl/min) conditions. Representative brightfield images of macroscale controls (6-well plate) and microfluidic cell culture chambers of FlexDym™ and Fluroflex devices at 2, 24 and 48 hours after cell seeding. Scale bars 200 µm.

**Figure 2.13a** shows the normalized cell proliferation over 48 hours of culture in macro-systems (6-well plates). Culture in macro-systems led to an increase in HeLa cell numbers. Similarly, culture in the microfluidic devices of both FlexDym™ and Fluoroflex under perfusion conditions resulted in an increase in cell numbers after 48 hours (**Figure 2.13b-c**), suggesting active proliferation in the devices. After 48 hours,

the cells had reached a confluent state throughout the entire microculture chamber in all perfusion devices. In the static devices (both FlexDym™ and Fluoroflex), we observed no statistically significant increase in cell number after 48 hours of culture. It was thus concluded that perfusion of culture media was required to ensure cellular growth in the sTPE microfluidic devices. Previous studies have reported that cell proliferation is slower in microsystems compared to macrosystems for a range of cell types.[1,63,67] The observations could be attributed to a number of factors such as culture volume, volume densities in the media or surface area-to-volume ratios.

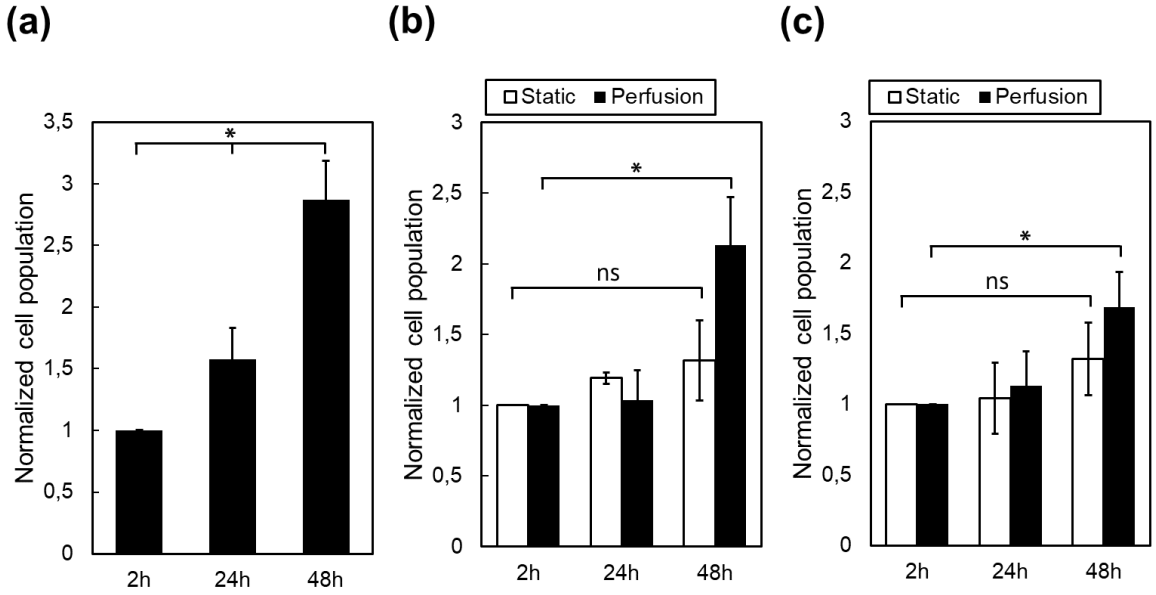


**Figure 2.13** HeLa cell culture under static and dynamic perfusion conditions. (a) HeLa cell proliferation in standard method macro-culture (6-well plates). HeLa cell proliferation in microfluidic devices of (b) FlexDym™ and (c) Fluoroflex under static and dynamic conditions. Ns indicates no statistical difference, * indicates a statistical difference ($p > 0.05$, $n = 3$ for each data set, error bars represent standard error).

Lastly, we wanted to confirm that sTPE devices could support cell adhesion and viability for an extended period, as OOC experiments may run for several days or weeks. We therefore seeded devices with HeLa cells at a lower cell density ($10^5$ cells/mL), and incubated the cells in static conditions and 3 µL/min perfusion conditions in Fluoroflex and FlexDym™ devices for up to 5 days (**Figure 2.14**). During long term cell culture, it appears that Flouroflex deivces in static conditions supported cell viability but grew slower compared to under dynamic conditions, indicated by a significantly lower cell density in static devices compared to dynamic devices after 5

days. This may be attributed to the low gas permeability of Fluoroflex. We observed no evident difference between static and dynamic FlexDym™ devices.

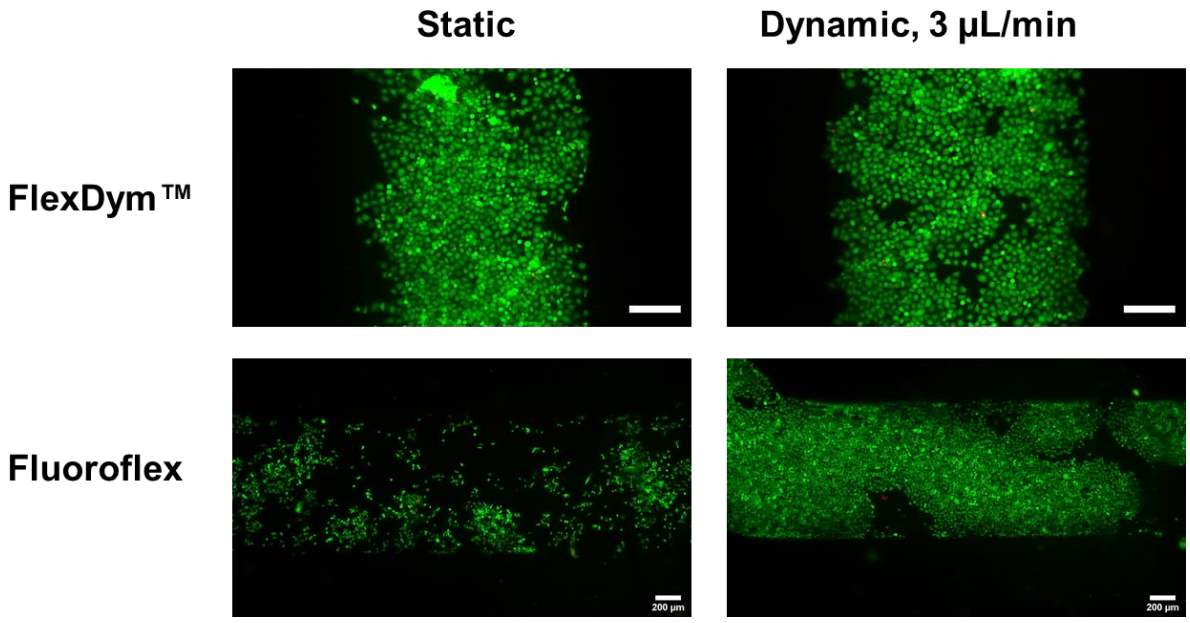


**Figure 2.14** Representative fluorescent microscopy images of HeLa cells cultured in FlexDym™ and Fluoroflex devices, under static conditions and constant perfusion of media at 3 µL/min, over the course of 5 days. Viable cells are stained with calcein AM (green) and dead cells are stained with propidium iodide (red). HeLa cells have grown to a high confluency in all devices, except the static Fluroflex device. A high cell viability is observed in all devices. Scale bars represent 200 µm.

While Fluroflex was developed to target chemistry applications, we demonstrated that the material also is well suited for cell biology applications. To date, Fluoroflex has not been commercialized and we therefore focused our efforts on FlexDym™ devices only from this point forward. Nevertheless, following demonstrations of cell attachment to pristine Fluoroflex, high chemical combability [28] and reversible bonding which can be utilized for modular microfluidics, we believe Fluoroflex to be a promising candidate for substituting PDMS also in bio-devices. A clear disadvantage of Fluoroflex compared to FlexDym™ was that FlexDym™ channels effectively could be hydrophilized by oxygen plasma which enabled passive capillary flow, while Fluoroflex devices required active pumping.

## 2.3 Experimental methods

### 2.3.1 Fabrication of master molds

Master molds used for the fabrication of microfluidic devices in Flexdym™, Fluoroflex and PDMS were fabricated by a photolithography process, using Ordyl® SY 300 dry film negative photoresist (55 µm thickness, ElgaEurope s.r.l., Milan, Italy) on 75 x 50 mm borosilicate glass slides (Corning Inc., Corning, NY, USA). The process, described below, was performed in a ventilated fume hood to minimize human exposure to chemicals and exposure of the mold to dust particles. The glass slides were cleaned with acetone and isopropanol in a sonicator (Elmasonic S 10, Elma Schmidbauer GmbH, Singen, Germany), and dehydrated on a hotplate (Thermo Fisher Scientific, Waltham, MA, US) for 20 minutes at 120˚C. After cleaning and dehydration, a sheet of photoresist was laminated onto the glass slide with a thermal laminator (325R6, FalconK, France) at 120 ˚C and roller speed 4. Multiple sheets of photoresist, successively laminated on top of each other, were used to create molds with thicker features. The photoresist was exposed to UV light (365 nm, 23.3 mW $cm^{-2}$) through a photomask using an exposure masking UV LED lamp (UV-KUB 2, Kloé, Montpellier, France). The exposure times for one, two and three layers of photoresists were optimized to 2 seconds, 6 seconds, and 11 seconds, respectively. The photomasks of the microfluidic designs used in this work were created using AutoCAD software for computer-aided design (Autodesk, Inc. San Rafael, CA, USA), and printed by Selba S.A (Versoix, Switzerland). After UV-exposure, the molds were developed with a solvent blend (Ordyl® SY Developer, ElgaEurope s.r.l., Milan, Italy) for approximately 10 minutes under light agitation to remove unexposed sections of the photoresist. The process was finished with a hard bake on a hotplate at 120 °C for 30 minutes.

### 2.3.2 Fabrication of microfluidic devices in FlexDym™

**Hot embossing**

Extruded sheets of FlexDym™ polymer of thickness 1.3 mm were purchased from Eden Tech SAS (Paris, France). The FlexDym™ sheets were cut with scissors to the size of the master mold, and manually placed on top of the mold. A clean polished metal plate (e.g., a nickel-cobalt plate) was used as a counter plate during the hot embossing. The entire assembly (mold- FlexDym™-counter plate) was placed in vacuum assisted heat-press (Sublym100 ™, Eden Tech, Paris, France) and subjected to an isothermal hot embossing cycle of 2 minutes at 150 ˚C and 0.7 bar applied

pressure (corresponding to approximately 6.5 bar of pressure normalized to the area of the mold). The hot-embossing procedure could alternatively be performed using a manual heat press, as shown in **figure 2.1**. The final thickness of the FlexDym™ was controlled to 1.1 mm by using 2.3 mm spaces between the plates of the heat-press. After the hot-embossing cycle, the FlexDym™ was left to cool down in room temperature for 1 minute, before peeling off the FlexDym™ sheet from the microfluidic mold. The separation was facilitated by applying a few drops isopropanol between the mold and the FlexDym™ sheet. 1 mm access holes were punched with a steel hole puncher (Eden Tech SAS, Paris, France). Device layers of FlexDym™ without microfluidic features were created though the same process, using a clean, flat glass slide instead of a microfluidic mold. This was necessary, as the purchased sheets FlexDym™ have poor optical transparency due to a surface roughness resulting from the extrusion process.

### Bonding

Bonding of FlexDym™ layers to create a FlexDym™ monolithic device was achieved by manually putting the FlexDym™ surfaces in conformal contact. Reversible adhesion occurred immediately upon contact between the polymer surfaces. However, the layers could easily be separated again, for instance to correct for poor alignment. To achieve strong sealing between the layers, the devices were baked in a forced convection oven (DKN612C, Yamoto Scientific Co. Ltd., Tokyo, Japan) for 2 hours at 85 °C.

### Interfacing

Three types of fluid connectors were used in this work to interface the FlexDym™ chips with microfluidic tubing. The first generation FlexDym™ connectors were molded from FlexDym™ pellets (Eden Tech SAS, Paris, France) using a custom made metallic mold, by melting the pellets to shape at 215 °C for 1 hour in an oven. After letting the mold cool down in room temperature, separation of the mold was facilitated with a few drops of isopropanol. The connectors were heated on a hotplate at 150 °C for 10 seconds and immediately fixed on top of the FlexDym™ chip. A second generation conical FlexDym™ connectors (Eden Tech SAS, Paris, France) were similarly baked on a silicon wafer on a hotplate at 150°C for 10 seconds to flatten and smoothen their bottom surface. Immediately after baking, the connectors were fixed on top of the access holes of the microfluidic chip. Light pressure was applied for 10 s to seal the connector to the chip. For cell culture experiments, topas female luer lock connectors (ChipShop, Jena, Germany) were attached to the FlexDym™ device using biocompatible, double-sided adhesive (Eden Tech SAS, Paris, France). Propylene male

luer connectors (ChipShop, Jena, Germany) were used to interface the female luer lock connectors with microfluidic tubing.

### 2.3.3 Fabrication of microfluidic devices in Fluoroflex

A sample of Fluoroflex raw material in an extruded pellet form was provided by Dr. Emmanuel Roy (Eden Tech SAS, Paris, France). Thermoforming of Fluoroflex pellets was performed using a manual heat press (DC8, Geo Knight & Co Inc. Brockton, MA, USA), by placing 5-10 pellets between the microfluidic mold (or a flat glass slide to obtain un-patterned Fluorflex sheets) and a polished metal counter plate. The assembly was placed in the heat-press, pre-heated to 220°C, for 15 s before manually applying pressure (approximated to 5 bar) via the lever arm of the heat-press for 20 s. After releasing the pressure, the assembly was left to cool for 1 minute before demolding. Separation of the Fluoroflex from the mold and counter plate was facilitated with a few drops of isopropanol. 1mm access holes were punched with a steel hole puncher (Eden Tech SAS, Paris, France). Bonding of Fluorflex layers to create a monolithic Fluoroflex microfluidic device was achieved by putting the Fluoroflex surfaces in conformal contact and leaving the device to seal for 2 hours in room temperature. To interface the Fluoroflex device with microfluidic tubing, topas female luer lock connectors (ChipShop, Jena, Germany) and double-sided adhesive (Eden Tech SAS, Paris, France) were used, similarly to FlexDym™ devices.

### 2.3.4 Fabrication of microfluidic devices in PDMS

In this work, microfluidic devices comprising a micro-molded PDMS layer bonded to either a glass microscope slide (25 mm x 75 mm) or to a flat PDMS layer, were used. The devices were fabricated through soft lithography techniques from 2-part liquid PDMS polymer (Sylgard 184, Dow Corning, Midland, MI, USA). Liquid PDMS base and crosslinker were mixed at a ratio 10: 1 (base: crosslinker, w/w) and degassed under vacuum for 30 minutes. The mixture was casted over the master mold, and cured in an oven at 80 °C for 2 hours. After curing, the PDMS was peeled off the mold and access holes were punched using biopsy punchers.

Before bonding, the glass slides were cleaned with acetone and isopropanol in an ultrasonic bath sonicator (Elmasonic S 10, Elma Schmidbauer GmbH, Singen, Germany) and dehydrated on a hotplate at 150 °C for 5 minutes. PDMS was irreversibly bonded to glass slides by activating both surfaces with air plasma for 2 minutes (400 mTorr, 30W, PDC-002, Harrick Plasma, Ithaca, NY, USA), and placing the activated

surfaces in conformal contact with each other. After sealing, the devices were left on a hotplate at 120 °C for 30 minutes. The same procedure was used to irreversibly bond PDMS to another PDMS surface, with an additional step of leaving the PDMS pieces under vacuum pressure (200 mTorr) for 5 minutes before turning on the plasma.

### 2.3.5 Oxygen and carbon dioxide permeability measurements

The oxygen and carbon dioxide gas permeabilities of FlexDym™ and PDMS were measured in a custom built high-throughput gas separation setup (HTML, Leuven, Belgium) that enabled simultaneous measurements of 16 membrane coupons at variable feed pressures, temperatures and gas compositions (the setup has been described previously by Khan et al.[68]). An isochoric method was applied, where permeate gas was accumulated in a 75 $cm^3$ cylinder and the change in pressure over time inside the cylinder was monitored by a pressure sensor ((MKS Baratron®, MKS Instruments, Andover, MA, USA). FlexDym™ membranes of 250 µm thickness were purchased from Eden Tech SAS (Paris France). PDMS membranes of thickness 150 ± 9 µm were fabricated by spin coating 10:1 PDMS (base: crosslinker, Sylgard™ 184) at an initial step of 10 s at 500 rpm and a subsequent 30 seconds step at 514 rpm and 300 rpm $s^{-1}$ acceleration (Spin 150 spin coater, SPS-Europe B.V., Putten, Netherlands). The PDMS films were cured in an oven (DKN612C, Yamoto Scientific Co. Ltd., Tokyo, Japan) for 2 hours at 80 °C. Measurements were performed on membrane coupons of an effective permeation area of 1.91 $cm^2$, at 6 bar feed pressure and 37 °C to simulate the temperature used for cell culture. The gas permeabilities of the materials were calculated from the following equation:

$$P_i = 10^{10} \times \frac{V \times V_m \times L}{P_{up} \times A \times R \times T} \times \frac{dp}{dt}$$

Where $P_{i\ (i = oxygen,\ carbon\ dioxide)}$ is the gas permeability (Barrer), V is the downstream volume ($cm^3$), $V_m$ is the molar volume (L/mol), A is the membrane permeation area ($cm^2$), L the membrane thickness (µm), T the operating temperature (K), pup the upstream pressure (bar), R the gas constant (0.082 L atm/mol K) and dp/dt the pressure increase (Torr/s).

### 2.3.6 Rhodamine B absorption assay

Monolithic microfluidic devices were fabricated in PDMS and FlexDym™, containing a 500*55 µm straight microchannel and bonded to a flat bottom layer of PDMS and

FlexDym™ respectively (according to described fabrication protocols in section 3.4.4.). Channels were filled with 100 mM rhodamine B dye in water (Sigma-Aldrich, St. Louis, MO, USA) and incubated in room temperature for 1, 3, 6 and 24h (n=3 for each condition). After incubation the devices were imaged with the rhodamine B dye in the channel with a fluorescent microscope (Zeiss Axio Observer Z1, Carl Zeiss AG, Oberkochen, Germany). The channel was subsequently washed by flushing 10 mL of DI water for 10 minutes through the channel, and the device was re-imaged. Light intensity and exposure time were kept constant for all devices and images. Images were analyzed in ImageJ software[69].

### 2.3.7 Hydrophilization and hydrophobic recovery

Oxygen plasma hydrophilization of FlexDym™ surfaces and the subsequent hydrophobic recovery were characterized by static contact angle measurements of water droplets in air. Samples of FlexDym™ were exposed to oxygen plasma treatment (PDC-002, Harrick Plasma, Ithaca, NY, USA) for 2, 5 or 10 minutes, at a gas flow of 20 sccm, pressure of 50 mTorr and a power of 100 W. The plasma treated samples were stored dry, in room temperature for 3 hours, 7 days or 14 days before contact angle measurement were performed using the sessile drop method. A drop shape analyser (Krüss, Hamburg, Germany) was used to dispose a 2 µL drop of DI water on the polymer surface, followed by capture of the static contact angle every second for 30 s. Contact angles were determined from the ellipse Tangent-1 fitting method by the software ADVANCE (Krüss, Hamburg, Germany). An average value of the left and right contact angle over the 30 measurements was obtained, and reported values are the average value of 3-5 samples for each experimental condition ± standard deviation. Contact angles near the limit of complete surface wetting, around 10 ° or less, could not be reliably measured and those samples were defined simply as experiencing “complete wetting” and presented by an arbitrarily chosen value of 10 °.

### 2.3.8 Cell culture

Human HeLa cells (ATCC® CCL-2™, Manassas, VA, USA) were grown in high glucose Dulbecco’s Modified Eagle’s Medium (DMEM) (Thermo Fisher Scientific) supplemented with 10% (v/v) fetal bovine serum (FBS, Thermo Fisher Scientific) and 1% (v/v) penicillin-streptomycin (Thermo Fisher Scientific). Chinese hamster ovarian (CHO) cells (ATCC®, Manassas, VA, USA) were grown in Ham F-12 nutrient mixture (Thermo Fisher Scientific) supplemented with 10% (v/v) FBS, 1% (v/v) MEM non-

essential amino acids (100X, Sigma-Aldrich, St. Louis, MO, USA), 1% (v/v) penicillin-streptomycin and 1% (v/v) L-glutamine (Thermo Fisher Scientific). All cells were maintained at sub-confluent levels in appropriate cell culture dishes in humidified incubators at 37°C and 5% $CO_2$.

### 2.3.9 Surface modifications for cell adhesion

1x1 cm pieces of FlexDym™ and Fluoroflex were cut with scissors and placed in individual wells of a 24-well plate. The polymer samples were cleaned with scotch tape and soaked in 70% ethanol for 24 hours for sterilization prior to experiments. Oxygen plasma treatment was performed for a duration of 2 or 5 minutes (400 mTorr, 30 W, PDC-002, Harrick Plasma, Ithaca, NY, USA). Samples were wetted and stored in sterile water directly after the plasma treatment, and used the same day. 22 µg/mL rat-tail collagen I (Sigma Aldrich) diluted in sterile water or 20 µg/mL poly-D-lysine (Sigma Aldrich) diluted in sterile water were used to coat the polymer surfaces. The coatings were added to cover the polymer surface of pristine polymer or oxygen-plasma treated polymers, and incubated for 1 hour at 37 °C. The coatings were rinsed off and the polymer surfaces were washed three times with PBS, directly followed by cell seeding. CHO cells were harvested from culture dishes by incubation in trypsin/EDTA (Thermo fisher Scientific, Waltham, MA, USA) for 2 minutes at 37 °C, centrifugation at 1500 rpm (Megafuge 16R Heraeus, Thermofisher Scientific) for 10 minutes at 4 °C, and resuspended in fresh culture media to a concentration of $10^4$ cells/mL. 0.5 mL of CHO cell suspension was added to each well, and the plate was incubated at 37°C/5% $CO_2$. Empty wells were used as negative controls, and the experiment was performed in triplicates. Living cells were imaged in situ using a phase-contrast microscope (EVOS XL Core, Invitrogen), 1, 24 and 48/96 hours after seeding.

### 2.3.10 Cell viability assay

To evaluate if contact with FlexDym™ and Fluoroflex materials induced a cytotoxic effect on cells, a two-color discrimination LIVE/DEAD assay was performed on cells cultured on the respective polymers. 1 cm x 1 cm pieces of FlexDym™ and Fluoroflex were manually cut and placed in independent wells of a 24-well plate. Prior to cell culture, the polymer pieces were soaked in 70% ethanol overnight and treated with air plasma for 5 minutes (400 mTorr, 30W, PDC-002, Harrick Plasma, Ithaca, NY, USA). HeLa cells were harvested from culture flasks by incubation with trypsin/EDTA for 2 minutes. 0.5 mL of HeLa cell suspension at concentration of $10^4$ cells/mL in culture media were added to each well a top the polymer and incubated in 37°C/5% $CO_2$ for 3,

24 or 72h. Empty wells were used as negative controls. At each time point, samples of each polymer (n=3) were sacrificed for analysis. After gently aspirating the culture media, the cells were incubated for 30 minutes at 37 °C in a staining solution containing 0.5 µM Calcein-AM (GFP, Falcon® Corning, Corning, NY, USA) to label living cells and 3 µM propidium iodide (TRITC, Biotium, Fremont, CA, USA) to label dead cells, diluted in warm PBS. The cells were imaged in the staining solution with a fluorescent microscope (Zeiss Axio Observer Z1, Carl Weiss AG, Oberkonchen, Germany). The number of living (nLIVE) and dead cells (nDEAD) were counted and cell viability percentage was defined from the following formula:

$$Viability\ (\%) = \frac{nLIVE}{nLIVE + nDEAD} \times 100$$

The experimental data were presented as mean standard deviation from of 3 different samples with at least 1000 cells per sample for each experimental condition. One-way analysis of variance (ANOVA) was applied to compare the difference in cell viability between the culture conditions at each time point. P values of less than 0.05 ($p < 0.05$) were considered statistically significant.

### 2.3.11 Plasma lithography for cell patterning

A sheet of FlexDym™ was micropatterned with a serpentine channel with a cross section of 300 µm x 55 µm thorough hot embossing (according to protocol in chapter 2), punched to create one access hole, and thermally bonded to a flat sheet of FlexDym™ for 5 minutes at room temperature. The room temperature bonding enabled formation a tight but reversible seal, and facile separation of the different layers. The device was exposed to air plasma for 10 minutes (200 mTorr, 30 W, Harrick Plasma, Ithaca, NY, USA), resulting in plasma exposure of the channel area (through the access hole) while the bonded areas remained shielded and unexposed to plasma. The micropatterned FlexDym™ layer was carefully peeled off with tweezers and put aside. HeLa cells were seeded on the flat FlexDym™ sheet that had been exposed to plasma in selected areas, at a concentration of $10^5$ cells/mL or $10^6$ cells/mL. After 24 h, the media was aspirated and the cells on the FlexDym™ substrate were rinsed 3 times with PBS, before fixation with 4% PFA and nuclei staining with 10 µg/mL DAPI for 10 minutes in order to evaluate the patterning efficacy. Other samples were kept

for up to 72 hours to evaluate the pattern stability. Similarly, PDMS surfaces were pattered with cells following the same procedure.

To integrate a plasma etched substrate within a microfluidic channel, a layer of FlexDym™ containing a rectangular channel of dimensions 800 µm x 150 µm x 18 mm (fabricated through hot-embossing according to procedure in chapter 2) was placed in conformal contact with the plasma etched FlexDym™ surface. The device was bonded in ambient temperature for 2 hours before cell seeding. The procedure in outlined in **Figure 2.8**.

### 2.3.12 Microfluidic cell culture

Monolithic FlexDym™ and Fluoroflex devices with a rectangular culture chamber of dimensions 800 µm x 150 µm x 18 mm were fabricated according to previously described protocols. Female luer lock connectors (Eden Tech SAS, Paris, France) were fixed on the channel inlet and outlet. Prior to cell experiments, the microfluidic devices were rinsed with 70 % ethanol, dried with compressed air and treated with air plasma for 10 minutes (400 mTorr, 30 W, Harrick Plasma, Ithaca, NY, USA). HeLa cells were harvested from culture flasks by trypsination with trypsin/EDTA (Thermo fisher Scientific, Waltham, MA, USA). 10 µL of cell suspension at a concentration of $10^6$ cells/mL was added to each microfluidic channel with a micropipette. The devices were incubated in a humidified cell culture incubator at 37 °C and 5% $CO_2$. Approximately 1 hour after seeding, 20 µL of fresh culture media was added to each luer lock reservoir to ensure a sufficient volume that would not dry out overnight due to evaporation. 24 hours after seeding, the devices were connected to the microfluidic flow control setup that enabled constant perfusion of culture media through a microfluidic device. The flow control setup consisted of a OB1® MK3+ pressure controller (0–2000 ± 0.1 mbar) and an in-line thermal flow sensor (MFS3, -0–80 µL/min ± 5% m.v.) and computer control via Elveflow® Smart Interface software. The components were connected to the fluid reservoir and the microfluidic chip with polytetrafluoroethylene tubing (all microfluidic equipment from Elveflow®, Elvesys SAS, Paris, France). A constant flow rate of 3 µL/min was applied, continuously providing the system with fresh culture media. In the case of static culture conditions, the media in the system was manually refreshed with a micropipette every 24 hours. The fluid induced shear stress experienced by the cells was calculated by the following equation describing the wall shear stresses, $\tau_w$, of laminar Newtonian fluids in a closed rectangular geometry:

$$\tau_w = \frac{6\mu Q}{bh^2},$$

Where $\mu$ is the dynamic viscosity of the fluid (culture media with 10 % serum, 0.93 mPa.s at 37 °C [70]), $Q$ is the fluid flow rate, $b$ is the channel width and $h$ is the channel height.[71]

Cell were imaged with an inverted brightfield microscope in the devices at time points 0, 15 and 48 hours, and the number of cells in the devices were counted at each time point to monitor the cell growth in the devices. To account for small variations in cell seeding concentration, the cell growth was normalized to the initial seeding density at time point 2 hours, according to equation (X):

$$Normalized\ cell\ growth = Number\ of\ cells\ at\ \frac{Number\ of\ cells\ at\ 2\ h\ /\ 24\ h/48\ h}{Number\ of\ cells\ at\ 2\ h}$$

ANOVA was applied to compare the change in cell population between the time points and the two materials. P values of less than 0.05 ($p < 0.05$) were considered statistically significant.

## 2.4 Conclusions

In this chapter, we have demonstrated that two novel sTPE materials, FlexDym™ and Fluoroflex, are well-suited for fabrication of microfluidic devices with applications in cell biology such as OOC studies. Both materials offer a streamlined fabrication methodology that enables cost and time effective prototyping of microfluidic devices. Unlike PDMS soft lithography procedures, sTPE processing is transferable across fabrication scales, which could be an important step towards bridging the gap between research laboratories and industry [72].

In addition, FlexDym™ and Fluoroflex can address a number of problems associated with PDMS devices for biological studies. Importantly, both sTPE materials showed reduced absorption to small molecules compared to PDMS, and neither of the sTPE required protein coatings for cell attachment, as is typically necessary for cell attachment to PDMS. The sTPE materials showed excellent biocompatibility. FlexDym™ could be effectively hydrophilized by oxygen plasma treatment which

showed prolonged stability compared to PDMS, although not beyond 7 days. A low-power plasma treatment step of 2 minutes was sufficient to promote cell attachment. Plasma treatment of Fluoroflex showed minimal reduction in surface hydrophobicity, however, cells could adhere and grow on native Fluoroflex surfaces.

Further, it was demonstrated that sTPE devices were suitable for on-chip dynamic cell culture experiments. We presented complete procedures for performing dynamic cell culture in sTPE devices, including chip interfacing with flow control instrumentation, cell seeding in microfluidic devices and on-chip culture under constant perfusion of culture media. It was demonstrated that FlexDym™ and Fluoroflex devices could support HeLa cell culture in enclosed microfluidic channels for up to 5 days, an important first step toward implementation of the materials for perfusion-based microfluidic cell studies and OOC studies.

In the quest for flexible, optically transparent materials that offer facile fabrication opportunities, FlexDym™ and Fluroflex are promising candidates for a wide range of microfluidic bio-assays, including OOC technology.

## Acknowledgements

We thank Dr. Karla Perez Toralla (LERI, CEA Paris-Saclay) and Dr. Anne Wijkhusien (LERI, CEA Paris-Saclay) for providing CHO cells and for their assistance during cell experiments, Dr. Guénaëlle Jasmin-Lebras (LNO/SPEC, CEA Paris-Saclay) for supervision and for performing oxygen plasma treatments, Marion Callau (LIONS, CEA Paris-Saclay) for access and training to the goniometer, Dr. Raymond Thür (KU

Leuven, Belgium) for performing gas permeability measurements, Dr. Sasha Cai Lesher-Pérez (Elvesys) and Dr. Vivien Lacour (Eden Tech) for feedback and support.

## 2.5 References


1. Yu, H., Alexander, C. M. & Beebe, D. J. Understanding microchannel culture: Parameters involved in soluble factor signaling. *Lab Chip* **7**, 726–730 (2007).
2. Takayama, S. *et al.* Subcellular positioning of small molecules. *Nature* **411**, 1016 (2001).
3. Hung, P. J. *et al.* A novel high aspect ratio microfluidic design to provide a stable and uniform microenvironment for cell growth in a high throughput mammalian cell culture array. *Lab Chip* **5**, 44–48 (2005).
4. Sudo, R. *et al.* Transport-mediated angiogenesis in 3D epithelial coculture. *FASEB J.* **23**, 2155–2164 (2009).
5. Cavnar, P. J., Berthier, E., Beebe, D. J. & Huttenlocher, A. Hax1 regulates neutrophil adhesion and motility through RhoA. *J. Cell Biol.* **193**, 465–473 (2011).
6. Song, J. W. & Munn, L. L. Fluid forces control endothelial sprouting. *Proc. Natl. Acad. Sci. U. S. A.* **108**, 15342–15347 (2011).
7. Bhatia, S. N. & Ingber, D. E. Microfluidic organs-on-chips. *Nat. Biotechnol.* **32**, 760–772 (2014).
8. Probst, C., Schneider, S. & Loskill, P. High-throughput organ-on-a-chip systems: Current status and remaining challenges. *Curr. Opin. Biomed. Eng.* **6**, 33–41 (2018).
9. Hassan, S., Heinrich, M., Cecen, B., Prakash, J. & Zhang, Y. S. 26 - Biomaterials for on-chip organ systems. in *Woodhead Publishing Series in Biomaterials* (eds. Vrana, N. E., Knopf-Marques, H. & Barthes, J. B. T.-B. for O. and T. R.) 669–707 (Woodhead Publishing, 2020).
10. Xia, Y. & Whitesides, G. M. SOFT LITHOGRAPHY. *Annu. Rev. Mater. Sci.* **28**, 153–184 (1998).
11. Unger, M. A., Chou, H. P., Thorsen, T., Scherer, A. & Quake, S. R. Monolithic microfabricated valves and pumps by multilayer soft lithography. *Science* **288**, 113–116 (2000).
12. Guenat, O. T. Incorporating mechanical strain in organs-on-a-chip : Lung and skin. **042207**, (2018).
13. Mata, A., Fleischman, A. J. & Roy, S. Characterization of polydimethylsiloxane (PDMS) properties for biomedical micro/nanosystems. *Biomed. Microdevices* **7**, 281–293 (2005).
14. Merkel, T. C., Bondar, V. I., Nagai, K., Freeman, B. D. & Pinnau, I. Gas sorption, diffusion, and permeation in poly(dimethylsiloxane). *J. Polym. Sci. Part B Polym. Phys.* **38**, 415–434 (2000).
15. Deguchi, S., Hotta, J., Yokoyama, S. & Matsui, T. S. Viscoelastic and optical properties of four different PDMS polymers. *J. Micromechanics Microengineering* **25**, 97002 (2015).
16. Toepke, M. W. & Beebe, D. J. PDMS absorption of small molecules and consequences in microfluidic applications. *Lab Chip* **6**, 1484–1486 (2006).
17. Eddington, D. T., Puccinelli, J. P. & Beebe, D. J. Thermal aging and reduced hydrophobic recovery of polydimethylsiloxane. *Sensors Actuators B Chem.* **114**, 170–172 (2006).
18. Capulli, A. K. *et al.* Approaching the in vitro clinical trial: engineering organs on chips. *Lab Chip* **14**, 3181–3186 (2014).
19. Campbell, S. B. *et al.* Beyond Polydimethylsiloxane: Alternative Materials for Fabrication of Organ-on-a-Chip Devices and Microphysiological Systems. *ACS Biomater. Sci. Eng.* (2020).
20. Davenport Huyer, L. *et al.* One-Pot Synthesis of Unsaturated Polyester Bioelastomer with Controllable Material Curing for Microscale Designs. *Adv. Healthc. Mater.* **8**, e1900245 (2019).
21. Lai, B. F. L. *et al.* InVADE: Integrated Vasculature for Assessing Dynamic Events. *Adv. Funct. Mater.* **27**, 1703524 (2017).
22. Zhao, Y. *et al.* A Platform for Generation of Chamber-Specific Cardiac Tissues and Disease Modeling. *Cell* **176**, 913-927.e18 (2019).
23. Sano, E. *et al.* Tetrafluoroethylene-propylene elastomer for fabrication of microfluidic organs-

on-chips resistant to drug absorption. *Micromachines* **10**, (2019).
24. Domansky, K. *et al.* SEBS elastomers for fabrication of microfluidic devices with reduced drug absorption by injection molding and extrusion. *Microfluid. Nanofluidics* **21**, (2017).
25. Borysiak, M. D. *et al.* Simple Replica Micromolding of Biocompatible Styrenic Elastomers
26. Roy, E., Geissler, M., Galas, J. C. & Veres, T. Prototyping of microfluidic systems using a commercial thermoplastic elastomer. *Microfluid. Nanofluidics* **11**, 235–244 (2011).
27. Lachaux, J. *et al.* Thermoplastic elastomer with advanced hydrophilization and bonding performances for rapid (30 s) and easy molding of microfluidic devices. *Lab Chip* **17**, 2581–2594 (2017).
28. McMillan, A. H. *et al.* Self-sealing thermoplastic fluoroelastomer enables rapid fabrication of modular microreactors. *Nano Sel.* **n/a**, (2021).
29. Guillemette, M. D., Roy, E., Auger, F. A. & Veres, T. Rapid isothermal substrate microfabrication of a biocompatible thermoplastic elastomer for cellular contact guidance. *Acta Biomater.* **7**, 2492–2498 (2011).
30. Roy, E. *et al.* From cellular lysis to microarray detection, an integrated thermoplastic elastomer (TPE) point of care Lab on a Disc. *Lab Chip* **15**, 406–416 (2015).
31. Case, D. J., Liu, Y., Kiss, I. Z., Angilella, J.-R. & Motter, A. E. Braess's paradox and programmable behaviour in microfluidic networks. *Nature* **574**, 647–652 (2019).
32. Borysiak, M. D. *et al.* Simple replica micromolding of biocompatible styrenic elastomers. *Lab Chip* **13**, 2773–2784 (2013).
33. Lachaux, J. *et al.* Soft Thermoplastic Elastomer for Easy and Rapid Spin-Coating Fabrication of Microfluidic Devices with High Hydrophilization and Bonding Performances. *Adv. Mater. Technol.* **4**, 1800308 (2019).
34. Tiede, L. M., Cook, E. A., Morsey, B. & Fox, H. S. Oxygen matters: tissue culture oxygen levels affect mitochondrial function and structure as well as responses to HIV viroproteins. *Cell Death Dis.* **2**, e246 (2011).
35. Robb, W. L. Thin silicone membranes- their permeation properties and some applications. *Ann. N. Y. Acad. Sci.* **146**, 119–137 (1968).
36. Heo, Y. S. *et al.* Characterization and resolution of evaporation-mediated osmolality shifts that constrain microfluidic cell culture in poly(dimethylsiloxane) devices. *Anal. Chem.* **79**, 1126–1134 (2007).
37. Domansky, K. *et al.* Clear castable polyurethane elastomer for fabrication of microfluidic devices. *Lab Chip* **13**, 3956–3964 (2013).
38. Bhattacharya, S., Datta, A., Berg, J. M. & Gangopadhyay, S. Studies on surface wettability of poly(dimethyl) siloxane (PDMS) and glass under oxygen-plasma treatment and correlation with bond strength. *J. Microelectromechanical Syst.* **14**, 590–597 (2005).
39. Rhodes, N. P., Wilson, D. J. & Williams, R. L. The effect of gas plasma modification on platelet and contact phase activation processes. *Biomaterials* **28**, 4561–4570 (2007).
40. Murakami, T., Kuroda, S. & Osawa, Z. Dynamics of Polymeric Solid Surfaces Treated with Oxygen Plasma: Effect of Aging Media after Plasma Treatment. *J. Colloid Interface Sci.* **202**, 37–44 (1998).
41. Gökaltun, A., Kang, Y. B. (Abraham), Yarmush, M. L., Usta, O. B. & Asatekin, A. Simple Surface Modification of Poly(dimethylsiloxane) via Surface Segregating Smart Polymers for Biomicrofluidics. *Sci. Rep.* **9**, (2019).
42. Ozcan, C., Zorlutuna, P., Hasirci, V. & Hasirci, N. Influence of Oxygen Plasma Modification on Surface Free Energy of PMMA Films and Cell Attachment. *Macromol. Symp.* **269**, 128–137 (2008).
43. Khorasani, M. T. & Mirzadeh, H. Effect of oxygen plasma treatment on surface charge and wettability of PVC blood bag—In vitro assay. *Radiat. Phys. Chem.* **76**, 1011–1016 (2007).
44. Dewez, J.-L. *et al.* Adhesion of mammalian cells to polymer surfaces: from physical chemistry of surfaces to selective adhesion on defined patterns. *Biomaterials* **19**, 1441–1445 (1998).
45. Tsougeni, K., Petrou, P. S., Tserepi, A., Kakabakos, S. E. & Gogolides, E. Nano-texturing of poly(methyl methacrylate) polymer using plasma processes and applications in wetting control

and protein adsorption. *Microelectron. Eng.* **86**, 1424–1427 (2009).
46. Schmalenberg, K. E., Buettner, H. M. & Uhrich, K. E. Microcontact printing of proteins on oxygen plasma-activated poly(methyl methacrylate). *Biomaterials* **25**, 1851–1857 (2004).
47. Chu, P. K., Chen, J. Y., Wang, L. P. & Huang, N. Plasma-surface modification of biomaterials. *Mater. Sci. Eng. R Reports* **36**, 143–206 (2002).
48. Zanini, S., Barni, R., Pergola, R. & Riccardi, C. Modification of the PTFE wettability by oxygen plasma treatments: Influence of the operating parameters and investigation of the ageing behaviour. *J. Phys. D. Appl. Phys.* **47**, 325202 (2014).
49. Wang, L., Sun, B., Ziemer, K. S., Barabino, G. A. & Carrier, R. L. Chemical and physical modifications to poly(dimethylsiloxane) surfaces affect adhesion of Caco-2 cells. *J. Biomed. Mater. Res. - Part A* **93**, 1260–1271 (2010).
50. Berdichevsky, Y., Khandurina, J., Guttman, A. & Lo, Y.-H. UV/ozone modification of poly(dimethylsiloxane) microfluidic channels. *Sensors Actuators B Chem.* **97**, 402–408 (2004).
51. Jahangiri, F., Hakala, T. & Jokinen, V. Long-term hydrophilization of polydimethylsiloxane (PDMS) for capillary filling microfluidic chips. *Microfluid. Nanofluidics* **24**, (2020).
52. Jokinen, V., Suvanto, P. & Franssila, S. Oxygen and nitrogen plasma hydrophilization and hydrophobic recovery of polymers. *Biomicrofluidics* **6**, (2012).
53. Ginn, B. T. & Steinbock, O. Polymer surface modification using microwave-oven-generated plasma. *Langmuir* **19**, 8117–8118 (2003).
54. Morra, M. *et al.* On the aging of oxygen plasma-treated polydimethylsiloxane surfaces. *J. Colloid Interface Sci.* **137**, 11–24 (1990).
55. Zuchowska, A. *et al.* Adhesion of MRC-5 and A549 cells on poly(dimethylsiloxane) surface modified by proteins. *Electrophoresis* **37**, 536–544 (2016).
56. Zhou, J., Khodakov, D. A., Ellis, A. V & Voelcker, N. H. Surface modification for PDMS-based microfluidic devices. *Electrophoresis* **33**, 89–104 (2012).
57. Bose, S., Dasbiswas, K. & Gopinath, A. Substrate mediated elastic coupling between motile cells modulates inter–cell interactions and enhances cell–cell contact. *bioRxiv*. 434234 (2021).
58. Rhee, S. W. *et al.* Patterned cell culture inside microfluidic devices. *Lab Chip* **5**, 102–107 (2005).
59. Foncy, J. *et al.* Dynamic inking of large-scale stamps for multiplexed microcontact printing and fabrication of cell microarrays. *PLoS One* **13**, (2018).
60. Tourovskaia, A., Figueroa-Masot, X. & Folch, A. Differentiation-on-a-chip: A microfluidic platform for long-term cell culture studies. *Lab Chip* **5**, 14–19 (2005).
61. Meissner, R., Eker, B., Kasi, H., Bertsch, A. & Renaud, P. Distinguishing drug-induced minor morphological changes from major cellular damage via label-free impedimetric toxicity screening. *Lab Chip* **11**, 2352–2361 (2011).
62. Pasirayi, G. *et al.* Low cost microfluidic cell culture array using normally closed valves for cytotoxicity assay. *Talanta* **129**, 491–498 (2014).
63. Kobuszewska, A. *et al.* Heart-on-a-Chip: An Investigation of the Influence of Static and Perfusion Conditions on Cardiac (H9C2) Cell Proliferation, Morphology, and Alignment. *SLAS Technol.* **22**, 536–546 (2017).
64. Jastrzebska Jedrych, E., Grabowska-Jadach, I., Chudy, M., Dybko, A. & Brzozka, Z. Multi-function microsystem for cells migration analysis and evaluation of photodynamic therapy procedure in coculture. *Biomicrofluidics* **6**, 44116 (2012).
65. Lee, P. J., Hung, P. J., Rao, V. M. & Lee, L. P. Nanoliter scale microbioreactor array for quantitative cell biology. *Biotechnol. Bioeng.* **94**, 5–14 (2006).
66. Kim, L., Toh, Y.-C., Voldman, J. & Yu, H. A practical guide to microfluidic perfusion culture of adherent mammalian cells. *Lab Chip* **7**, 681–694 (2007).
67. Paguirigan, A. L. & Beebe, D. J. From the cellular perspective: exploring differences in the cellular baseline in macroscale and microfluidic cultures. *Integr. Biol. (Camb).* **1**, 182–195 (2009).
68. Khan, A. L., Basu, S., Cano-Odena, A. & Vankelecom, I. F. J. Novel high throughput equipment for membrane-based gas separations. *J. Memb. Sci.* **354**, 32–39 (2010).
69. Schindelin, J. *et al.* Fiji: An open-source platform for biological-image analysis. *Nature Methods*

**9**, 676–682 (2012).
70. Poon, C. Measuring the density and viscosity of culture media for optimized computational fluid dynamics analysis of <em>in vitro</em> devices. *bioRxiv* 2020.08.25.266221 (2020).
71. Kim, L., Vahey, M. D., Lee, H.-Y. & Voldman, J. Microfluidic arrays for logarithmically perfused embryonic stem cell culture. *Lab Chip* **6**, 394–406 (2006).
72. Ramadan, Q. & Zourob, M. Organ-on-a-chip engineering: Toward bridging the gap between lab and industry. *Biomicrofluidics* **14**, 41501 (2020).

# Chapter 3. Thermoplastic elastomer microfluidic platform for automated combinatorial treatment of cardiac cells

**Abstract:** In this chapter we present a sTPE-based microfluidic system for investigating cardiomyoblast physiology. Compared to the PDMS system, sTPE systems represent a more streamlined protocol for cell seeding, reduced media evaporation from the culture chamber and improved compatibility with lipid cellular staining. A microfluidic circuit that enables fully automated microfluidic assays, as a first step toward high-throughput investigations of heart physiology, is presented.

## Contributions

The writing and the majority of the experimental work presented in this chapter was done by Emma Thomée. Microfabrication of PDMS devices was done by Emma Thomée and Louise Courtaillac (La Maison de la mitochondrie, Toulouse), H9C2 cell cultures were maintained by Dr. Fatima Smih (La Maison de la mitochondrie, Toulouse), and H9C2 microfluidic cell culture experiments were done by Emma Thomée, Louise Courtaillac and Dr. Fatima Smih. Confocal imaging of cardiac cells was performed by Dr. Fatima Smith. The microfluidic circuit and application notes were developed by Emma Thomée. Revision was done by Emma Thomée and Dr. Aurélie Vigne.

## 3.1 Introduction

Cardiovascular diseases are the leading cause of death worldwide.[1] With modern lifestyle and the increasing prevalence of obesity contributing to an increase in heart diseases, there is an urgent need for novel therapies and an increased fundamental understanding of underlying mechanisms of cardiac dysfunctions.[2] A new apolipoprotein, apolipoprotein O (ApoO) was recently discovered and found to be overexpressed in the heart of diabetic patients.[3] In silico, in vivo and in vitro studies revealed that ApoO localize in the mitochondria and induce a cascade of events leading to cardiomyopathy.[4] It has been suggested that Caveolin-3 (Cav-3) expression is positively correlated to ApoO-induced metabolic stress.[5] A further understanding of how the expression of these proteins relate to changes in cardiac function may reveal insights in cardiac pathophysiology and novel therapeutic strategies for cardiac injury.

Preclinical research into cardiac pathophysiology and new therapeutics rely heavily on in vitro models.[6] However, traditional in vitro models represent largely simplified models, as the complex dynamics of the heart, including electrical signalling and mechanical stresses, cannot be modelled.[7] In fact, the most common cause of drug withdrawal from the market are cardiac electrophysiological dysfunction and muscle damage, which highlight the limitation of traditional vitro models in evaluating cardiac effects.[8] Microfluidics, and specifically OOC technology, can provide a number of advantages to cardiac research. Continuous or pulsatile media perfusion to cells can provide supply of nutrient and relevant shear stresses.[9] Microenvironmental conditions have been shown to affect morphology, proliferation, alignment and differentiation of rat embryonic cardiomyocytes (H9C2 cells) in microfluidic systems.[10,11] Moreover, cardiomyocytes in vivo are subjected to continuous contractions and relaxations of the heartbeat. Heart-on-a-chip systems have established aspects of the heart including electromechanical stimulation[12–15], contraction [16–18], 3D tissue organization [13,15,19–21] and cardiac-vascular interactions [14,15,22]. The capability of controlling oxygen levels in microfluidic devices has been utilized to study hypoxia-indued myocardial injury.[23–25] In short, this new group of in vitro models presents a promising step toward testing cardiotoxicity and evaluation cardiac pathophysiology in more human-relevant models in a high throughput fashion, addressing the current needs in drug development pipelines.[26]

Despite evident advantages of microfluidics as a tool for cardiac research, microscale techniques have not been widely implemented in biology laboratories.[27–30] It has been highlighted by many that the microfluidic community needs to focus more on the challenges associated with integration, standardization and market appeal rather

than further demonstrations of highly advanced functionality.[30–32] The "clash of cultures" between biologists and engineers over the choice of microfluidic materials and problems associated with PDMS for biological assays are also often pointed out as factors contributing to the limited adoption of microfluidics for cell biology research.[28,30,33] sTPE materials have been introduced aiming to bridge the material gap between rigid thermoplastics and PDMS by offering improved bio-inertness, facile prototyping and capability of high throughput fabrication.[34]

Main goals of an industrial PhD project are to conduct market-driven research and development and to develop in depth technical expertise based on the commercial needs of the company. Following market research to gain understanding of the target market, a range of marketing tools can be employed to reach the target market and bridge the gap between the innovation and the final user. Application notes, describing specific use cases of a product in order to show the potential customer how and for what scenarios the given product may be used, provide an effective marketing tool for high-tech start-up companies.[35] We identified research cell biology laboratories as a target end user of microfluidic instrumentation and developed a strategy based on application notes to market microfluidic flow control instruments by making microfluidics more accessible for novel users in the field of cell biology.

In this chapter, we develop sTPE-based microfluidic strategies for investigating cardiac myoblast physiology and the interaction between ApoO and Cav-3 in cardiac myoblasts. Moreover, we develop a microfluidic platform for automated administration of soluble factors to microfluidic cell culture devices. Based on the observation and experience from the previous chapter around cell culture in microfluidic devices together with this study, we developed tools, in the form of application notes, to facilitate implementation of sTPE microfluidic devices and robotic fluid handling in cell biology laboratories.

## 3.2 Results and Discussion

The first two sections describe the implementation of a FlexDym™ microfluidic device for culturing cardiac myoblasts, based on the proof-of-concept studies and derived protocols presented in chapter 2. We first compare attachment and microscale culture of cardiac myoblasts in FlexDym™ devices to PDMS devices. After having derived appropriate protocols, we use the microfluidic systems to perform a palmitate-treatment to the cells and study the physiological effects. The results presented here represent the development of on-chip assays, optimization of experimental

parameters and implementation of a FlexDym™-based microfluidic system for cardiac research. Analysis of the remaining samples to complete the study is currently ongoing at the La Maison de la mitochondrie in Toulouse, France.

The second part of this study describes the development and validation of a versatile microfluidic flow control system for dynamic cell culture. Protocols for automation of the cardiac cell-based assay using the flow control system is presented. Complete practical guides to microfluidic cell culture in sTPE devices and automation of microfluidic cell culture assays using Elveflow flow control systems are presented in the form of application notes in Appendix 2 – Microfluidic cell staining.

### 3.2.1 H9C2 myoblast culture in sTPE microfluidic devices

Firstly, we evaluated the capabilities of culturing H9C2 cells in microfluidic devices of FlexDym™ (**Figure 3.1a-b**). To this end, we monitored H9C2 growth in the devices daily, and compared attachment, morphology and proliferation of cells cultured in FlexDym™ devices to PDMS devices and petri dishes. H9C2 cells used in this study were transfected to overexpress the protein Caveolin-3-GFP (referred to as Cav-3 cells) or Caveolin-3-GFP and ApoO (referred to as Cav-3-ApoO cells).

H9C2 cell culture in PDMS devices has been demonstrated previously, where the substrates for cell attachment were modified glass [10,23,24] or PDMS [11,36]. We seeded Cav-3 ApoO cells in PDMS-glass and monolithic FlexDym™ devices at a seeding density of ~300 cells/mm$^2$, directly after air plasma hydrophilization of the channels. 24 hours after seeding, cells in FlexDym™ devices (**Figure 3.1d**) had attached similarly to the cells in the control petri dishes (**Figure 3.1c**). Flattened cells with a characteristic elongated shape were observed. A few unattached cells remained floating in FlexDym™ devices. The formation of cell clusters indicated active proliferation in FlexDym™ devices. In PDMS devices, a significantly higher number of unattached cells remained in a rounded morphology (**Figure 3.1e**).

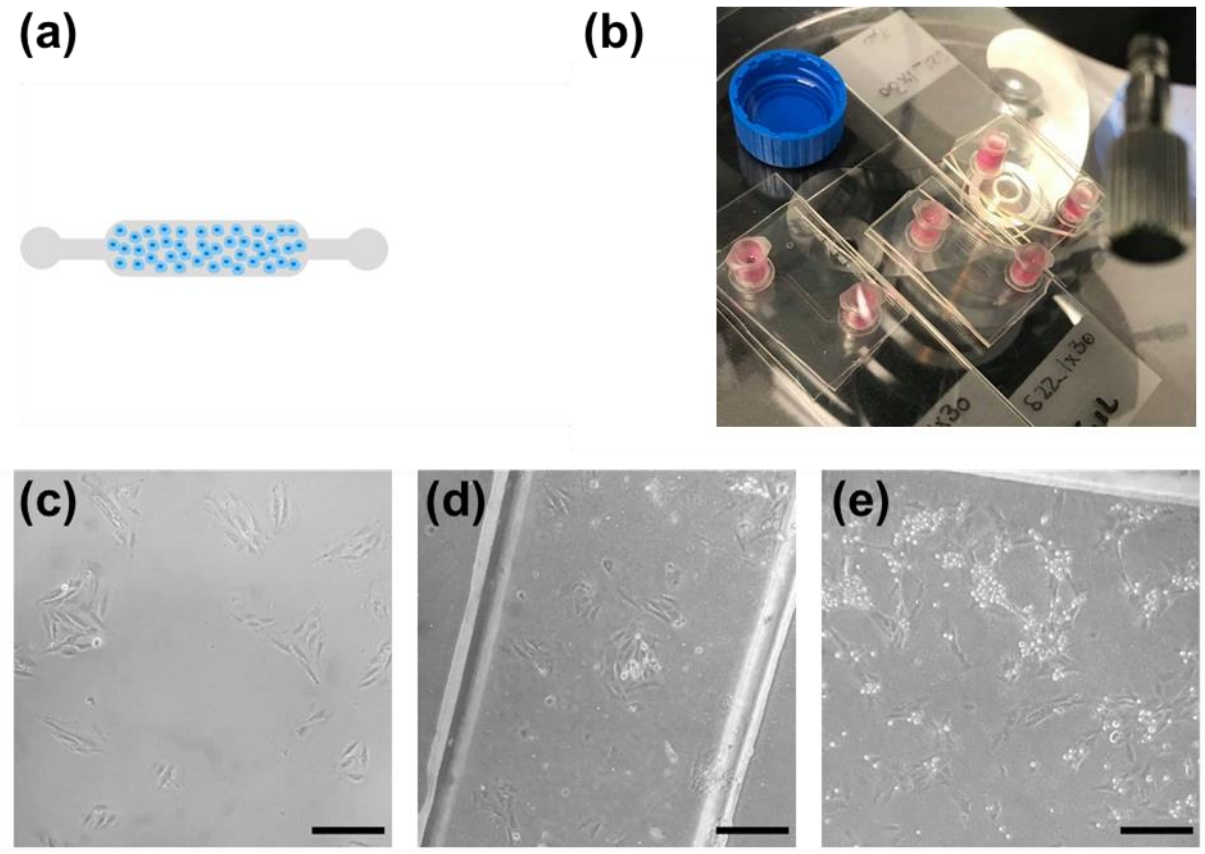


**Figure. 3.1.** H9C2 (Cav-3 ApoO) microfluidic cell culture. Schematic sketch of the (a) microfluidic systems and (b) Photograph of three sTPE devices during a cell culture experiment (here the sTPE devices are placed on top of glass microscope slides during microscopic observation). Representative brightfield images of H9C2 (Cav-3 ApoO) myoblasts cultured for 24 h in (c) petri dish, (d) FlexDym™ microfluidic devices and (e) PDMS microfluidic devices. Scale bars 200 µm.

After 96 hours under static conditions, and media exchange every 24 hours, very few cells remained in the PDMS chips (**Figure 3.2b**), while attached cells with elongated morphologies were still observed in FlexDym™ devices (**Figure 3.2a**). It was concluded that FlexDym™ devices could support H9C2 culture for up to 4 days without the need for surface coatings, while the PDMS devices could not. Thus, for subsequent experiments, a poly-d-lysine coating was used for all PDMS devices to improve cell adhesion to the glass bottom of the PDMS devices. While these results in the PDMS devices were anticipated and can be improved by surface modification techniques such as ECM coatings, it nevertheless means that an additional experimental step is required.[37,38] Depending on the coating method, this additional step adds from one hour up to one day to the device preparation time.

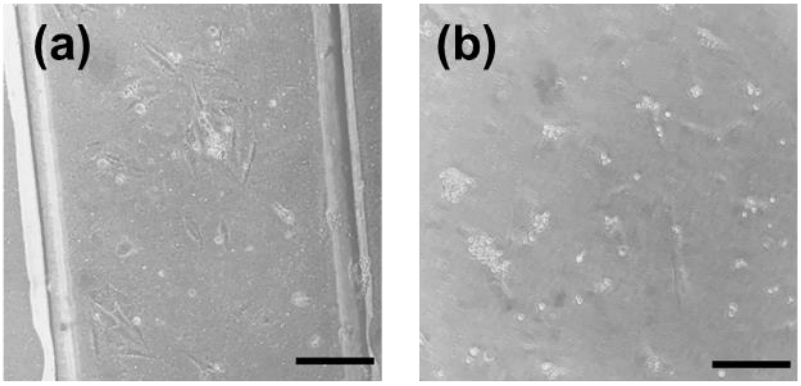


**Figure 3.2.** H9C2 (Cav-3 ApoO) cell culture. Representative brightfield images of H9C2 (Cav-3 ApoO) myoblasts cultured for 96 h in (a) FlexDym™ microfluidic devices and (b) PDMS microfluidic devices. Scale bars 200 µm.

In this study, experiments were performed in static conditions with manual exchange of media in the microchannels once per day. While cells could be maintained this way for up to 96 hours, manual media exchanges in microfluidic devices are laborious and may cause stress to the cells due to the hydraulic pressure resulting from inserting and removing the micropipette tip, as well as the shear stress resulting from a high flow rate generated by manual pipetting. Flow induced shear stress in an inherent part of flow through a microfluidic channel.[39] External flow controllers can be used to manipulate fluids in microfluidic channels with more precise control of the flow rate and the resulting shear stresses. Other microfluidic geometries may also be considered. For example, a common design of heart-on-a-chip systems in literature contain a culture chamber with lateral perfusion channels separated by micropillar.[10,15,24]

In chapter 2 we characterized the oxygen and carbon dioxide permeabilities of FlexDym™. Although we found that FlexDym™ was significantly less permeable to both gases, this did not pose problems for culturing cells in this work. However, for certain channel geometries or flow regimes, a more involved gas control protocol to maintain appropriate oxygen levels inside the device may be needed.

### 3.2.2 Palmitate-induced lipotoxicity in microfluidic devices

To investigate the interaction between ApoO and Cav-3 and to evaluate the fitness of FlexDym™ devices for studying cardiac myoblast physiology, we studied fatty acid-induced alterations in Cav-3 and Cav-3 ApoO cells. Saturated fatty acids, including palmitate, have been shown to induce apoptosis in cardiac myocytes.[40–43] The reduction of cells due to apoptosis is a contributing factor to myocardial dysfunction and heart failure.[44] In vitro studies have revealed that ApoO-expressing cardiac

myoblasts rapidly accumulate palmitate, resulting in a 120% increase in basal intracellular fatty acids compared to control cells.[4] The study also showed that the production of reactive oxygen species (ROS) was also enhanced.

Cav-3 ApoO and Cav-3 cells were cultured in microfluidic devices of PDMS and FlexDym™ as well as in LabTek® chambers (as macro-scale controls). 24 hours after seeding, cells were treated with palmitate (conjugated to BSA (bovine serum albumin) and supplemented in culture media at 100 µM) for 15 hours in the devices. Internal negative controls for all types of devices and cell types were incubated in culture media without palmitate for 15 hours.

Devices containing Cav-3 ApoO cells treated with palmitate were analysed with fluorescent microscopy (**Figure 3.3b** and **Figure 3.4**). The GFP-tagged protein Cav-3 generated a fluorescent signal that was visible in the FlexDym™ devices and LabTek®, but could not be distinguished in the PDMS devices. A rise in Cav-3 levels and translocation to the mitochondria induced by ApoO metabolic stress was expected [5], but not distinguishable from the fluorescent images at this magnification. Apoptotic cells, identified as those with a nucleus exhibiting brightly stained condensed chromatin or fragments as opposed to normal cells with nuclei exhibiting chromatin with an organised structure, were observed in the devices from Hoechst 33342 fluorescent staining (**Figure 3.3a**). We examined the mitochondrial ROS levels after treatment with palmitate by MitoSOX as a fluorescent probe for the presence of superoxide in mitochondria of live cells. As shown in **Figure 3.3b**, generation of superoxide in mitochondria was observed in Cav-3 ApoO cells after treatment with palmitate in LabTek®, PDMS and FlexDym™ devices.

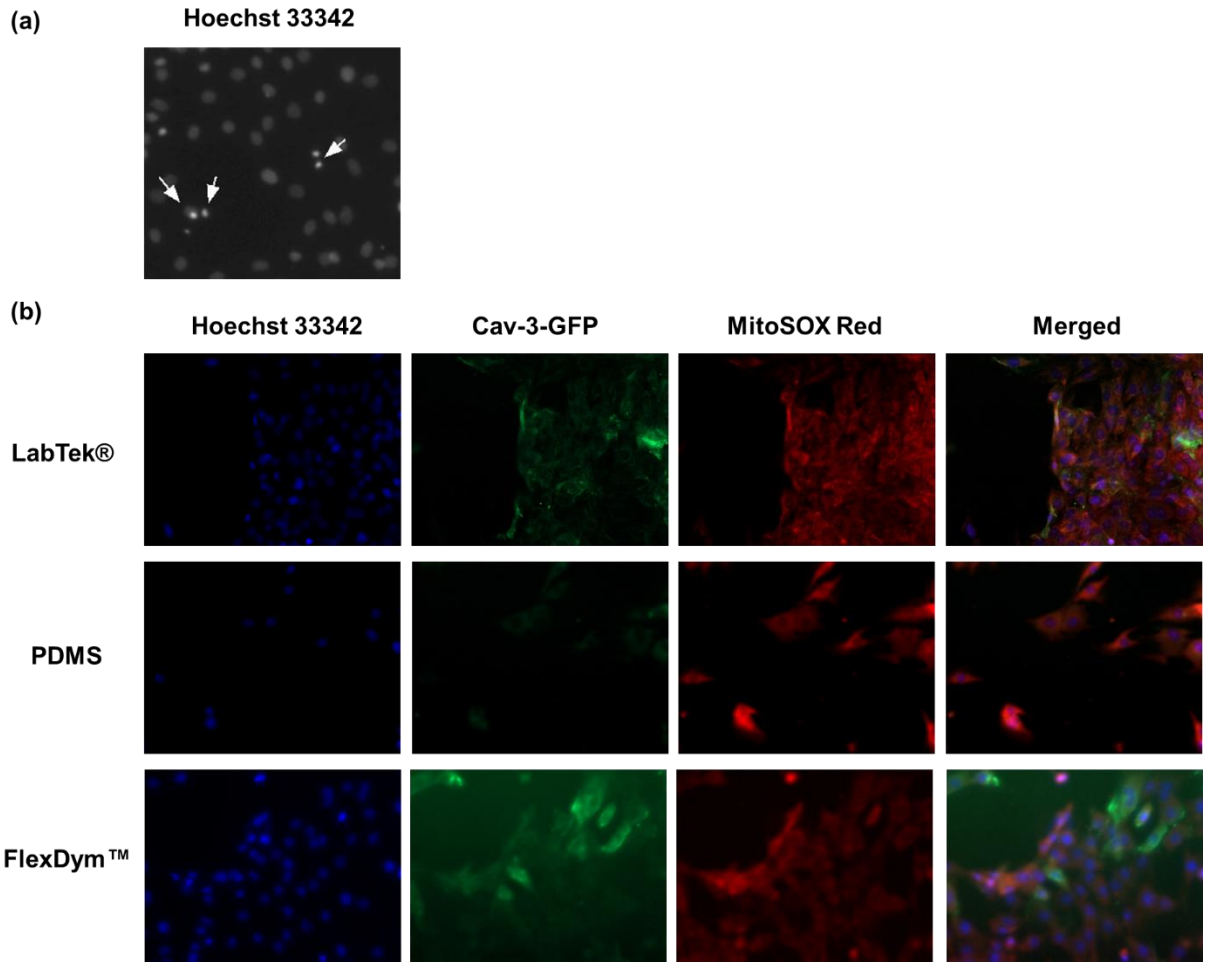


**Figure 3.3.** Palmitate treatment of Cav-3 ApoO cells in microfluidic devices. (a) Cell apoptosis, indicated with arrows, was determined by Hoechst 33342 nuclei staining. (b) Representative fluorescent images of Cav-3 ApoO cells after treatment with palmitate in LabTek®, PDMS and FlexDym™ devices, showing nuclei (blue), Cav-3 (green) and superoxide in mitochondria (red). Magnification 20X.

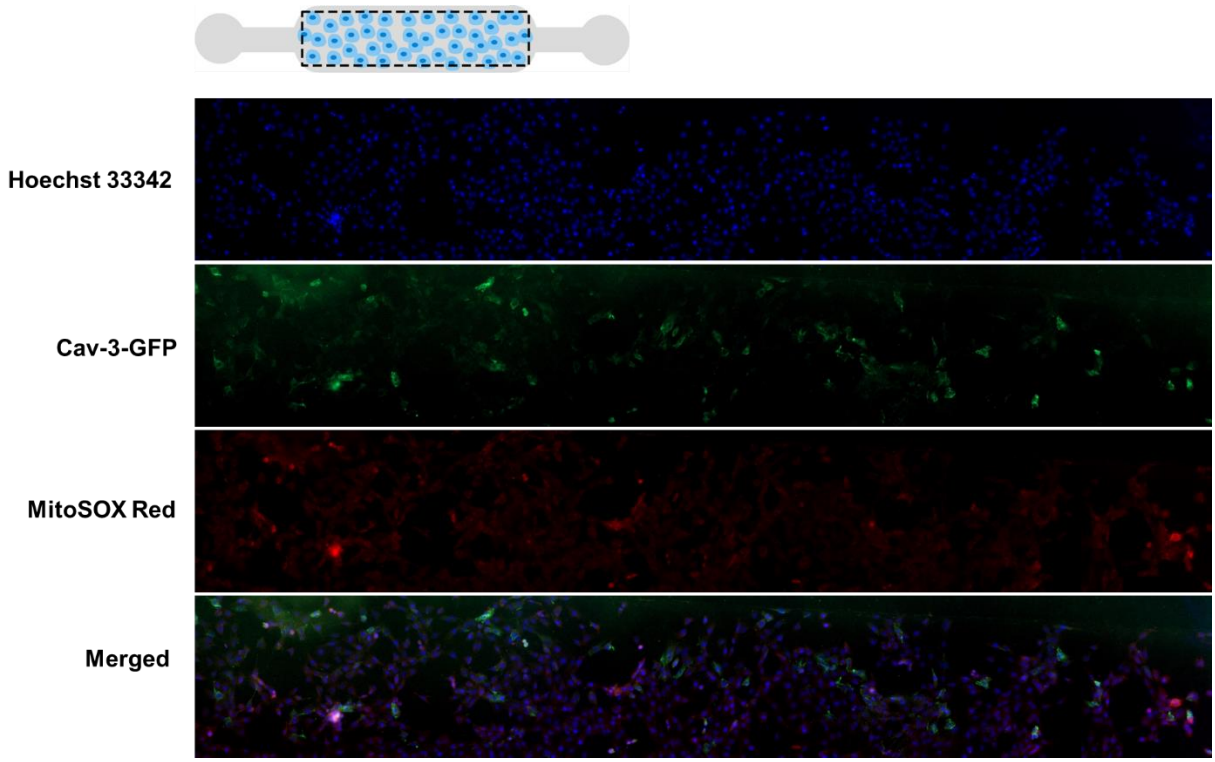


**Figure 3.4** Panorama images showing the entire cell culture chamber (illustrated by dashed in the schematic sketch of the microfluidic device) of a FlexDym™ microfluidic device. Representative images of Cav-3 ApoO cells after palmitate treatment in FlexDym™ devices, showing nuclei (blue), Cav-3 (green) and superoxide in mitochondria (red). Magnification 10X.

Whether the apoptosis and ROS generation were elevated by palmitate could not be quantitatively determined without comparative analysis with negative control samples. Likewise, analysis of Cav-3 cells is necessary to compare the effects of ApoO over expression.

We concluded that the FlexDym™ devices fulfilled the requirements for the given study. However, to improve imaging quality, a flat hard plastic bottom layer could be used that would keep the cells better in plane to facilitate high resolution imaging. Compared to PDMS devices, FlexDym™ devices had practical advantages, including not requiring surface coatings and showing significantly slower media evaporation during static culture.

The evaluation and potential implementation of FlexDym™-based microfluidic devices for the study of cardiac myoblast physiology is motivated by need for alternative prototyping materials to PDMS, due to the well-known drawbacks of PDMS.[45–48] Absorption of hydrophobic molecules by PDMS is a critical concern when conducting studies involving fatty acids, and for quantitative studies involving dye molecules. The absorption of lipids, including palmitic acid (the fatty acid component

of palmitate), into PDMS devices was recently characterized by Yang et al.[49] They found that incubation of palmitic acid at an initial concentration of 167 µM for 24 hours in a PDMS microfluidic device resulted in 53.7% compound absorption. A *n*-dodecyl β-D-maltoside + Matrigel coating mitigated the absorption to 40.9%, which however still meant that almost half of the palmitic acid absorbed. The apoptotic effect of palmitate (increase in caspase-3 activity) in ApoO-expressing cells was shown to dramatically increase with increasing concentrations of palmitate compared to control cells.[4] The dose dependency of palmitate highlights the importance of keeping control of the solute concentration in the microfluidic systems. While the previous studies on palmitic acid are not directly relevant for our study, as we used BSA-conjugated palmitate, it is nevertheless important to keep these inherent limitations of absorption and adsorption by the microfluidic devices in mind during assay development. The absorption of hydrophobic molecules in FlexDym™ devices has not been quantified. It was shown in Chapter 2 that FlexDym™ absorbed significantly less Rhodamine B compared to PDMS. We also compared the absorption of the fluorescent lipophilic membrane dye DIL (Dil$C_{18}$, Invitrogen) in FlexDym™ and PDMS devices. Fluorescent lipid markers, such as DIL, AdioRed, Oil red O and nile red are known to be largely incompatible with PDMS due to absorption, resulting in a high background fluorescence and high signal-to-noise ratio.[49–52] Surface modification strategies, such as PTFE coatings [51], paraffin wax coatings [53], or chemical modification using transition metal sol-gel methods [54], have been employed to minimize the absorption of lipid stains and shown to significantly reduce the background fluorescent signal during cellular lipid imaging.

To evaluate the compatibility of FlexDym™ with cellular lipid staining, DIL stain was incubated for 1 hour in a PDMS channel and a FlexDym™ channel before generously washing off the stain with ethanol and DI water. As seen in **Figure 3.5**, PDMS absorbed DIL to a larger extent than FlexDym™, indicated by a widening in line profile and residual fluorescent signal after washing in the PDMS device. While, the resistance to lipophilic molecules was not characterized in depth, these results indicate that FlexDym™ might be more resistant to lipid absorption and adsorption.

To avoid static incubation in the microfluidic devices we developed a microfluidic circuit with capability of controlled delivery of palmitate and staining solutions.

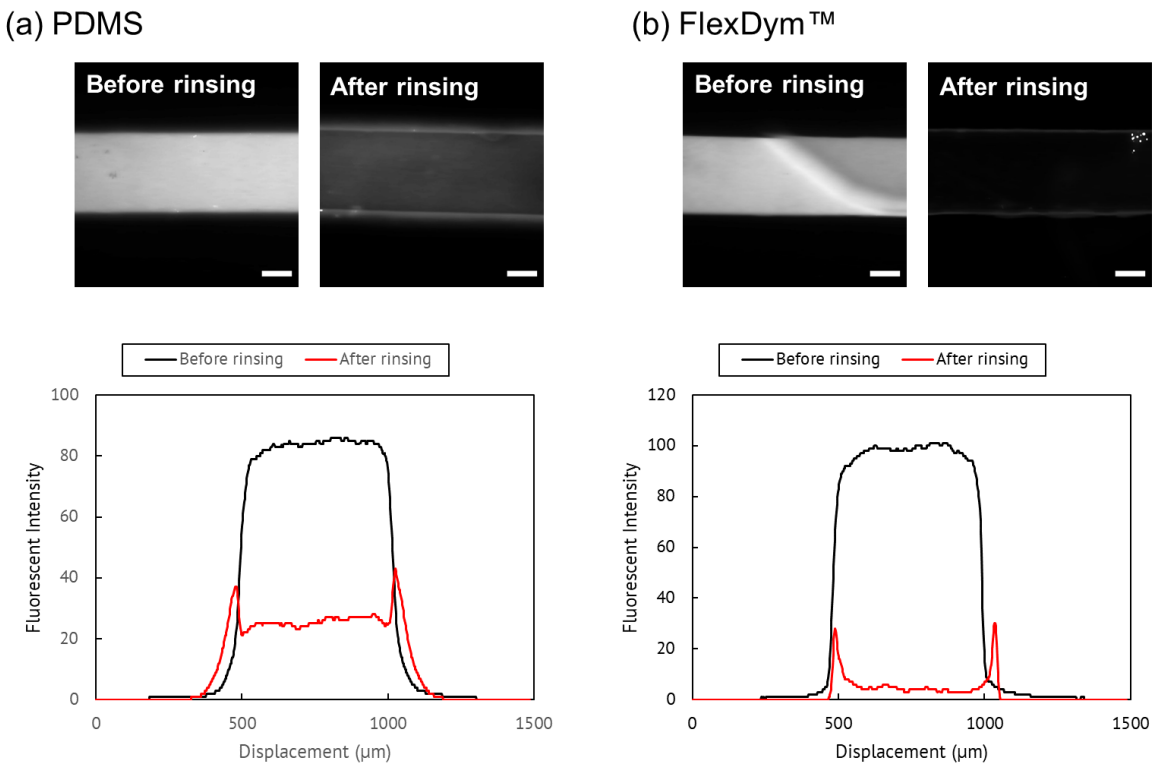


**Figure 3.5.** Characterization of DIL fluorescent stain uptake in PDMS and FlexDym™ microchannels (500 μm x 55 μm). Fluorescent images of (a) PDMS and (b) FlexDym™ channels containing 2 mg/mL DIL in 70% ethanol. The same channels were reimaged after 1 h incubation followed by rinsing with 10 mL 70% ethanol and 10 mL of DI water (exposure time 100 ms). Below are the corresponding line profiles before and after incubation and washing. Scale bars 200 μm.

While more inert materials might be ultimately desired, we believed FlexDym™ to be a better prototype material compared to PDMS for this specific study. Taking the cost into consideration, we estimated the raw material costs for fabrication of one device. Raw material for one PDMS chip was estimated to cost ~2 € while raw material for one FlexDym™ device was estimated to cost ~2.5 €. It should be noted that additional fluid connectors and adhesives are needed to interface a FlexDym™ device, adding a cost of 2.9 € per connector (Eden Tech, Luer lock connector kit). Based on the results presented in Chapter 4, unlike for PDMS, we believe that FlexDym™ material can be reprocessed and reused for prototyping purposes up to at least 3 times which would reduce the raw material costs by 25 %. Compared to commercial chips such as the μ-Slide I 0.4 Luer ibiTreat (IBIDI) that can be purchased for ~ 25 € per piece, or the Nunc™ LabTek™ II Chamber Slide™ system (4 wells, LabTek™, Thermo Scientific™) that can be purchased for ~ 10 €, both FlexDym™ and PDMS devices represent significantly cheaper alternatives for prototyping.

### 3.2.3 Design and validation of an automated flow control platform

We developed a microfluidic circuit capable of administering drug solutions and fluorescent stains to microfluidic cell culture devices in FlexDym™ for automated cell treatment in a high-throughput fashion (**Figure 3.6**). The setup was designed to be compatible with microfluidic chips having one inlet and one outlet, a common design among commercially available microfluidic chips. While components such as valves and manifolds can effectively be integrated on-chip, this modular approach with off-chip components enable connection of generic, commercially available microfluidic chips without the need for custom made microfluidic designs. Thus, complex microfluidic operations are made accessible to laboratories that do not have know-how or access to facilities for microfabrication.

The microfluidic platform (further detailed in section 3.3.8) consisted of a bidirectional rotary valve that allowed for sequential liquid injection of up to 10 different fluids, with capability of automatization and further parallelization with employment of multiple valves and manifolds. Flow rate was monitored by an in-line flow sensor and an in-line bubble trap prevented potential air bubbles from reaching and damaging the sample. A 3/2 valve was connected in line after the rotary valve for purging of liquids at high flow rate without passing in the microfluidic devices. This enabled the option of adding a staining liquid or light/temperature-sensitive reagent immediately before it is needed, as large air plugs that may appear in the tubing when connecting a reservoir can effectively be flushed out. The possibility to flush the system at high flow rate without passing over the cells also saves time, reduces reagent dilution and minimizes the risk of cross contaminations. The valve was considered necessary in this setup as the low flow rates required in order to not damage the cells result in very slow assay time and a high degree of axial mixing during sequential injections. The level of automation is easily programmable and can be adapted by the user, and the setup is compatible with live cell imaging.

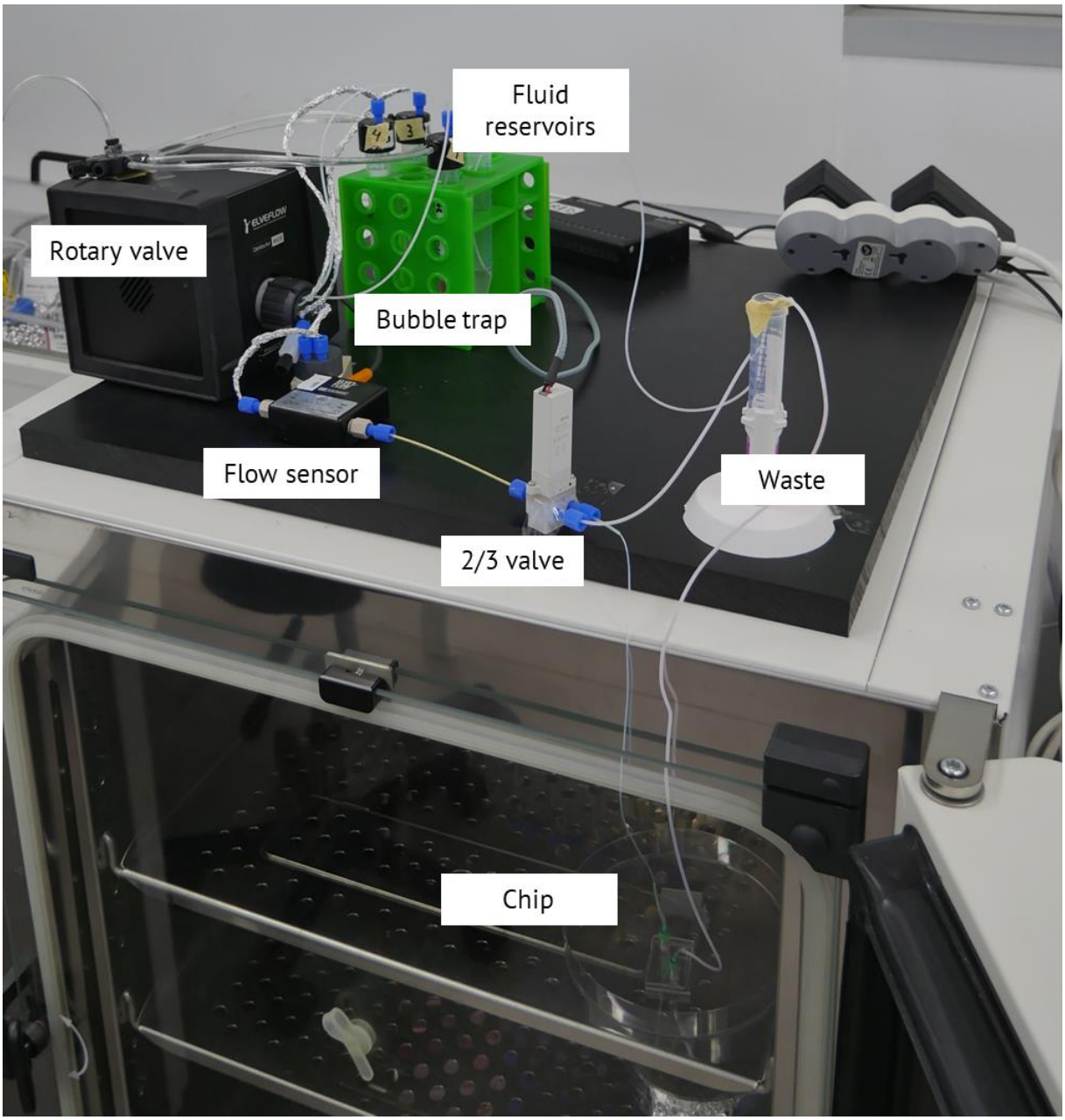


**Figure 3.6.** Photograph of microfluidic flow control platform consisting of a OB1 pressure controller (not seen in figure), fluid reservoirs, a rotary valve, a flow sensor, a bubble trap, a 2/3-way valve and a sTPE microfluidic chip. The microfluidic chip containing cells resides in a cell culture incubator with controlled temperature (37°C) and $CO_2$ level (5%).

A sequence for automation of the experiment conducted in section 3.2.2 was developed. Cells were seeded manually with a pipette and were incubated to adhere for 24 hours in the devices, before connecting the devices to the microfluidic platform. Palmitate treatment, staining and washing steps were fully automated (Table 3.1), with connection of the stain reservoirs being the only manual step required by the user. If additional fluorescent probes or fixation of cells is desired, such steps could easily be added to the end of the program without the need of changing any

experimental setup. Although the automated protocol was developed for treating H9C2 cells with palmitate, MitoSOX and Hoechst 33342 staining, we validated the protocol using HeLa cells with two fluorescent probes of the same incubation times: propidium iodide and Hoechst 33342. This was in order to economize the use of precious fluorescent probes, such as MitoSOX. After manual seeding in FlexDym™ devices, cells were left for 24 hours to adhere in the devices. At 24 hours after cell seeding, 15 hours of palmitate non-static incubation was simulated, by intermittent flow, refreshing the media in the channel once per hour for 15 hours. Directly afterwards, the channel was filled with propidium iodide and incubated for 10 minutes. After 10 minutes, the channel was washed with PBS and subsequently filled with Hoechst 33342 and incubated for 10 minutes. Lastly, the channel was washed with PBS and observed under a fluorescent microscope (**Figure 3.7b**). The protocol is summarized in **Figure 3.7a.**

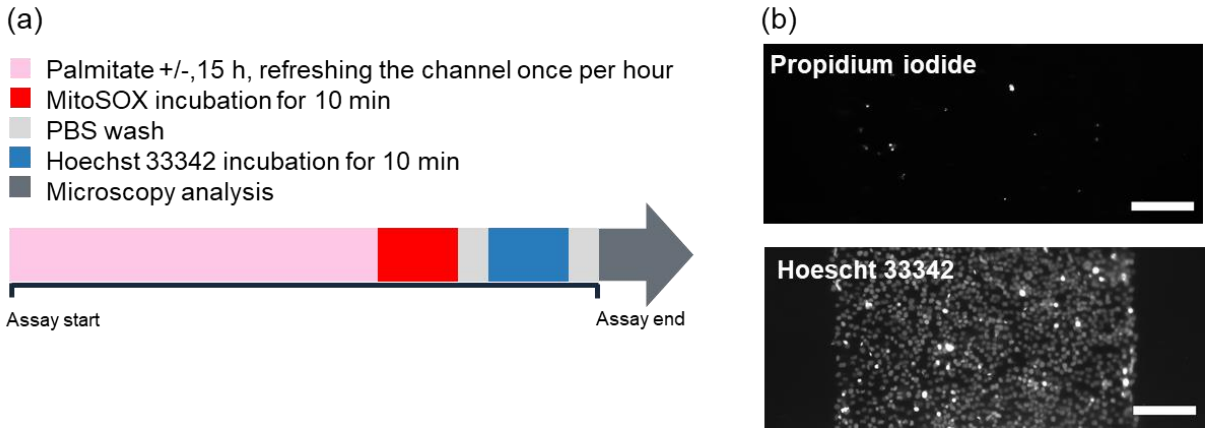


**Figure 3.7.** Automation of protocols. (a) Summary of sequential fluid injections for automation of palmitate assay and analysis, including steps +/- palmitate treatment, MitoSOX staining, Hoechst 33342 staining and PBS washing steps. (b) Fluorescent images resulting from validation of the protocol using Palmitate -, propidium iodide and Hoechst 33342 staining of HeLa cells in FlexDym™ microfluidic devices. Scale bars represent 200 µm.

The total time of the automated assay was 15 hours + 62 minutes compared to approximately 15 hours + 30 minutes for manual staining. Looking at one device, the automated staining protocol was thus slower than performing the staining and washing steps manually. The automated protocol can however be further optimized. We used a slow flow rate of 3 µL/min to minimize the shear stress acting on the cells. However, we believe the flow rate possibly could be increased to around 10 µL/min, as manual pipetting often inevitably exposes the cells to much higher flow rates. The slow filling time of the chip was also attributed to the large dead volume in the connector relative to the channel volume. An improved connector solution without a

large dead volume would further increase assay speed and would be considered necessary in order to use the system for fast liquid switches. With the use of a manifold connected before the chip, the automated protocol allows for simultaneous treatment of up to 10 identical devices without changing the protocol or increasing the assay time. Considering manual manipulation of 10 devices, we estimate additional 10 minutes per device which would result in a total time of 15 hours + 120 minutes. Further time savings can thus be envisioned when dealing with a large number of devices, which is often inevitable taking into consideration that each experimental condition should be performed in at least triplicates. For an experiment including manual manipulation of 10 devices, a time delay of approximately 90 minutes between treating the first and the last device must also be accounted for. While a difference of 90 minutes may not be significant for an incubation time of 15 hours, it may be significant for experiments involving shorter incubation times and the time difference will likely proportionally increase for assay involving multiple steps.

It is also relevant to compare the volumes of reagents used and wasted, as fluorescent probes often are costly and purchased in very small quantities. For the automated protocol, we used 160 µL of each stain compared to 20 µL for manual pipetting per device. The extra volume used in the automated protocol was due to the internal volume of the microfluidic circuit. The sequence was constructed based on the timing between the valve and the chip, assuming that the given liquid had reached the point of the valve. The entire system up until the valve was thus filled with the given liquid. However, the protocol can be further optimized in terms of reagent consumption by injecting a smaller volume of the staining solution and then using PBS to push the liquid plug of stain up until the valve. Alternatively, the 160 µL can be used to stain multiple devices. Another advantage of automating the procedure is that the devices do not need to be taken out of the incubation, thus reducing stress to the cells and light exposure to light-sensitive fluorescent probes. Random variations due to manual manipulations can also be minimized.

The microfluidic circuit with automation capabilities is highly versatile, and timings and duration of fluidic delivery can be adjusted on demand. Similar concepts of automated assays have been developed for high throughput dynamic studies of, e.g., single-cell immune dynamics [55], combinatorial drug screening of tumor organoids [56] and dynamic cues for cellular differentiation [57]. While the ultimate goal may be total integration of the logic components of the microfluidic circuit on the chip, as demonstrated in the studies mentioned, this would require highly sophisticated microfluidic devices and extensive system validation. The “plug-and-play” approach

we present in this chapter represents an accessible solution for sequential injection that is compatible with commercially available microfluidic chips and can easily be integrated in a biology laboratory. The setup is thus ideal for prototyping purposes and could potentially contribute to making microfluidics more accessible beyond specialized microfluidics research laboratories.

## 3.3 Experimental

### 3.3.1 Fabrication

Microfluidic molds were fabricated from photolithography using Ordyl® SY300 dry film negative photoresist on borosilicate glass slides, according to protocols described in chapter 2. The same molds were used for fabrication of both FlexDym™ and PDMS devices. Devices contained one cell culture chamber of 800 µm width × 110 µm height × 20 mm length. Hot embossing was performed in a vacuum-assisted heat press for 2 min at 150 °C and 0.7 bar applied pressure to micropattern FlexDym™ sheets (Eden Tech, Paris, France) according to fabrication protocol in chapter 2). PDMS devices were fabricated from 10: 1 (base:crosslinker) PDMS polymer (Sylgard 184, Dow Corning, Midland, MI, USA) and glass microscope slides (25 mm × 75 mm) according to the protocol described in chapter 2. For coating of PDMS devices, poly-d-lysine (Sigma Aldrich) in DI water was used at a concentration of 100 µg/mL. Devices were incubated with the poly-d-lysine solution in the channels for 1 hour at 37°C. After incubation, the poly-d-lysine solution was rinsed off with sterile water and the devices were left to dry in 37°C overnight.

### 3.3.2 Cell culture

Transfected H9c2 rat cardio myoblasts over-expressing the protein Caveolin-3-GFP (Cav-3 cells) or Caveolin-3-GFP and ApoO (Cav-3-ApoO cells) were provided by Dr. Fatima Smih (La Maison de la mitochondrie, Toulouse, France). ApoO-Cav-3 and Cav-3 cells were grown in high glucose DMEM supplemented with 10 % (v/v) FBS, 1% (v/v) penicillin-streptomycin and 1 % (v/v) G418 (Life Technologies, Carlsbad, CA, USA). All cells were maintained at sub-confluent levels in appropriate cell culture dishes in humidified incubators at 37°C and 5 % $CO_2$.

### 3.3.3 Cell culture in microfluidic devices

ApoO-Cav-3 and Cav-3 cells were harvested from culture dishes with 1 mL of trypsin/EDTA, incubated for 2 minutes. Cell suspensions were centrifuged at 1500 rpm (239 xg) and resuspended in fresh culture media to a concentration of $2.5\times10^6$ cells $mL^{-1}$. 20 µL of cell suspension (ApoO-Cav3 or Cav3) was introduced in the devices (Flexdym™ devices, PDMS devices and LabTek wells) through the inlet hole with a pipette, directly subsequent to plasma treatment of the Flexdym™ devices and within 24 hours of coating the PDMS devices with poly-d-lysine. The devices were kept for 24 hours in a humidified cell culture incubator at 37 °C and 5 % $CO_2$.

### 3.3.4 Palmitate treatment

BSA-conjugated palmitate (provided by Dr. Fatima Smih) was prepared to a concentration of 100 µM in culture medium. At 24 hours after cell seeding, the culture media in devices of each device type (Cav3 Flexdym™ (n=3), Cav3 PDMS (n=2), Cav3 IBIDI (n=1), Cav3 LabTek (n=2), ApoO Flexdym™ (n=3), ApoO PDMS (n=2), and ApoO LabTek (n=2)) was replaced with the 100 µM palmitate (in DMEM) and incubated at 37 °C, 5 % $CO_2$ for 15 hours. The culture media in non-treated negative control devices were simultaneously replaced with fresh culture media (Cav3 Flexdym™ (n=3), Cav3 PDMS (n=2), Cav3 LabTek (n=2), ApoO Flexdym™ (n=3), ApoO PDMS (n=2) and ApoO LabTek (n=2)).

### 3.3.5 Reactive oxygen species assessment

MitoSOX red superoxide indicator was diluted to 5 µM in HBSS (supplemented with calcium and magnesium), according to recommendations by the manufacturer (Invitrogen). The MitoSOX red solution was applied to the cells in the devices and incubated in dark for 10 minutes at 37 °C, before rinsing with PBS 3 times.

### 3.3.6 Nuclear staining with Hoechst 33342

Cells in the microfluidic devices were fixed by filling the channels with 4 % paraformaldehyde for 10 minutes and followed by washing the channels with PBS 3 times. Hoechst 33342 nuclear stain (1 µg/mL in PBS) was applied to the cells in the devices for 10 minutes in dark, ambient conditions. The devices were then washed with PBS 3 times and kept in dark at 4 °C until observation under fluorescent microscope).

### 3.3.7 DIL absorption assay

Monolithic microfluidic devices were fabricated in PDMS and FlexDym™, containing a 500*55 µm straight microchannel and bonded to a flat bottom layer of PDMS and FlexDym™ respectively. Channels were filled with 2 mg/mL DIL fluorescent dye (Invitrogen) in 70 % ethanol and incubated in room temperature for 1 hour (n=3 for each condition). Before incubation the devices were imaged with the DIL dye in the channel with a fluorescent microscope (Zeiss Axio Observer Z1, Carl Zeiss AG, Oberkochen, Germany). The channel was subsequently incubated (kept in dark) at room temperature and washed by flushing 10 mL of 70 % ethanol and 10 mL of DI water through the channels, and the devices were re-imaged. Light intensity and exposure time were kept constant for all devices and images. Images were analyzed in ImageJ software[58].

### 3.3.8 Microfluidic setup

A microfluidic circuit that enabled cell culture in microfluidic devices under perfusion and temporally controlled delivery of soluble factors to the culture chambers was developed. The setup allowed for connection sequential fluid injection of up to 10 different fluids, and simultaneous analysis of up to 10 separate microfluidic devices. The fluid reservoirs were connected to a manifold with equal fluidic resistance in all branches, which delivered fluids to a valve multiplexer (MUX Distributor). The manifold was pressurized by an OB1® MK3+ pressure controller (0–2000 ± 0.1 mbar). A 3/2-way valve was connected in line after the valve multiplexer enabling purging of liquids at high flow rate without passing the microfluidic devices, therefore minimizing the risk of cross contaminations and preventing large air plugs in the system from reaching the samples (as may appear in the tubing when a liquid reservoir is connected). The flow rate was controlled by an in-line thermal flow sensor (MFS3, -0–80 µL/min ± 5 % m.v.) and an in-line bubble trap removed potential air bubbles from damaging the samples (all microfluidic setup was from Elveflow®, Elvesys SAS, Paris, France). All components of the system were controlled by Elveflow® smart interface (ESI) software.

### 3.3.9 Assay automation

A program sequence for sequential fluid injection to automate the microfluidic assays in section 3.3.4 – 3.3.6 was creating using Elveflow® ESI Software (Elveflow, Paris, France). The program sequence is outlined in Table 3.1.

**Table 3.1. Outline of program sequence developed for combinatorial treatment with palmitate, MitoSOX and Hoescht 33342 of cardiac cells**

**MUX distributor positions:**
Position 1 (pos 1) = DMEM culture media
Position 2 (pos 2) = PBS buffer
Position 3 (pos 3) = Stain #1, MitoSOX
Position 4 (pos 4) = Stain #2, Hoechst 33342
Position 5 (pos 5) = dead-end channel
**Valve configurations controlled by MUX wire:**
Normally open (NO) = to chip
Normally closed (NC) = to waste

| Step | Protocol | Program sequence |
|---|---|---|
| 1. Palmitate +/- treatment | [1] Purging system with palmitate/DMEM at 80 µL/min for 2 min<br>[2] Filling of chip with Palmitate/DMEM at 3 µL/min for 10 min<br>[3] zero flow 55 min<br>[4] perfusion 3 µL/min for 5 min<br>[5] loop (step [3] and [4]) 15 times | (1) MUX wire set NC<br>(2) MUX dist set pos 1<br>(3) OB1 config 80 µL/min<br>(4) timing 2 min<br>(5) OB1 config 3 µL/min<br>(6) MUX wire set NO<br>(7) timing 10 min<br>(8) MUX dist set pos 5<br>(9) OB1 config 0 µL/min<br>(10) timing 55 min<br>(11) MUX dist set pos 1<br>(12) OB1 config 3 µL/min<br>(13) timing 5 min<br>(14) go to step 8 – loop 15 times |
| 2. MitoSOX staining | [6] Purging system with stain #1 at 80 µL/min for 2 min<br>[7] Filling chip with stain #1 at 3 µL/min for 10 min<br>[8] Incubation in stain #1 for 10 min | (15) MUX wire set NC<br>(16) MUX dist set pos 3<br>(17) OB1 config 80 µL/min<br>(18) timing 2 min<br>(19) MUX dist set pos 2<br>(20) OB1 config 3 µL/min<br>(21) MUX wire set NO<br>(22) timing 10 min |
| 3. PBS rinsing | [9] Purging system with PBS at 80 µL/min for 2 min<br>[10] Filling chip and flushing with PBS at 3 µL/min | (23) MUX wire set NC<br>(24) OB1 config 80 µL/min<br>(25) timing 2 min<br>(26) OB1 config 3 µL/min<br>(27) MUX wire set NO<br>(28) timing 11 min |
| 4. HOECHST 33342 staining | [11] Purging system with stain #2 at 80 µL/min for 2 min<br>[12] Filling chip with stain #2 at 3 µL/min for 10 min<br>[13] Incubation in stain #2 for 10 min | (29) MUX wire set NC<br>(30) MUX dist set pos 4<br>(31) OB1 config 80 µL/min<br>(32) timing 2 min<br>(33) OB1 config 3 µL/min<br>(34) MUX dist set pos 2<br>(35) MUX wire set NO<br>(36) timing 10 min |
| 5. PBS rinsing | [14] Repeat step [9] and [10] | (37) MUX wire set NC<br>(38) OB1 config 80 µL/min<br>(39) timing 2 min<br>(40) OB1 config 3 µL/min<br>(41) MUX wire set NO<br>(42) timing 11 min |

**Total protocol time: 15 h + 62 min**

## 3.4 Conclusions and outlook

This chapter describes the design and proof-of-concept evaluation of a sTPE-based microfluidic device and an automated fluid control platform for high-throughput investigations of cardiomyoblast physiology. We evaluated sustained cell attachment of cardiomyoblasts in sTPE devices compared to PDMS devices and performed an on-chip palmitate treatment. In cardiomyoblasts transfected with Cav-3-GFP and ApoO, physiological effects of apoptosis and production of ROS were observed. To our knowledge, this is the first time a physiological effect on cells has been observed in FlexDym™-based microfluidic devices. Compared to PDMS systems, sTPE-based systems demonstrated a more streamlined protocol for cell seeding

We also developed a microfluidic circuit for controlled high-throughput delivery of soluble factors to FlexDym™ devices. The platform was implemented in a biology laboratory, and could effectively treat 10 devices simultaneously with capability of further parallelization. A fully automated protocol was developed and validated for overnight treatment with palmitate and subsequent staining with two fluorescent probes and washing steps without user interference.

Ongoing experiments are conducted to extend the biological study in sTPE microfluidic devices. Side-by-side comparison of palmitate uptake and its effects on cardiac cells overexpressing ApoO and cells expressing ApoO on physiological level, is expected to reveal how the localization of Cav-3 expression, apoptosis and generation of mitochondrial ROS is influenced by ApoO. Parallel experiments are performed in sTPE microfluidic systems, PDMS microfluidic systems and LabTek™ macro-systems to further validate the sTPE systems against conventional techniques. We expect ApoO to induce mitochondrial dysfunction, and consequently enhanced mitochondrial respiration, oxidative phosphorylation and fatty acid metabolism. These events, leading to accumulation of fatty acids in the cells, is hypothesized to induce apoptosis due to lipotoxicity. ApoO induced metabolic stress is expected to lead to a rise in Cav-3 levels and translocation to the mitochondria. Cav-3 is thought to be involved in mitochondrial homeostasis and act as a cardiac protector for ApoO-induced metabolic stress.

Looking further, a second-generation FlexDym™-based microfluidic device could be envisioned. For studies on mitochondria metabolism, control of oxygen levels in the microfluidic systems would be highly desirable as it would enable detection of a reduction in oxygen levels resulting from enhanced metabolism. While the high oxygen permeability of PDMS does not permit such functionalities, we believe that a hybrid device made of FlexDym™ and a less permeable material such as PMMA or COP

could be envisioned to this end. In chapter 2 we characterized the oxygen permeability of FlexDym™ which was found to be 25 times lower than PDMS, and in chapter 3 we showed that FlexDym™ can form a strong seal to a number of materials including PMMA and COP. Furthermore, integration of oxygen sensors in microfluidic devices has been previously demonstrated to effectively monitor cellular oxygen consumption rates.[59,60]


## Acknowledgements

We thank Dr. Fatima Smih, Dr. Philippe Rouet and Louise Courtaillac at La Maison de la mitochondrie, Toulouse for their engagement and assistance with cell culture experiments, and Dr. Jessica Ayache (Elvesys) for valuable feedback and assistance.


# 3.5 References


1. Organization, W. H. *Global status report on noncommunicable diseases 2014*. (World Health Organization).
2. Plump, A. Accelerating the pulse of cardiovascular R&D. *Nat. Rev. Drug Discov.* **9**, 823–824 (2010).
3. Lamant, M. *et al.* ApoO, a novel apolipoprotein, is an original glycoprotein up-regulated by diabetes in human heart. *J. Biol. Chem.* **281**, 36289–36302 (2006).
4. Turkieh, A. *et al.* Apolipoprotein O is mitochondrial and promotes lipotoxicity in heart. *J. Clin. Invest.* **124**, 2277–2286 (2014).
5. Caubère, C. Molecular and functional interactions between Apolipoprotein O and Caveolin 3 in the heart.Implication in the development of metabolic disorder-associated cardiomyopathy. in (2013).
6. Kettenhofen, R. & Bohlen, H. Preclinical assessment of cardiac toxicity. *Drug Discov. Today* **13**, 702–707 (2008).
7. Ma, Q., Ma, H., Xu, F., Wang, X. & Sun, W. Microfluidics in cardiovascular disease research: state of the art and future outlook. *Microsystems Nanoeng.* **7**, 19 (2021).
8. Gussak, I., Litwin, J., Kleiman, R., Grisanti, S. & Morganroth, J. Drug-induced cardiac toxicity: emphasizing the role of electrocardiography in clinical research and drug development. *Journal of electrocardiology* **37**, 19–24 (2004).
9. Thompson, C. L., Fu, S., Heywood, H. K., Knight, M. M. & Thorpe, S. D. Mechanical Stimulation: A Crucial Element of Organ-on-Chip Models . *Frontiers in Bioengineering and Biotechnology* **8**, 1426 (2020).
10. Kobuszewska, A. *et al.* Heart-on-a-Chip: An Investigation of the Influence of Static and Perfusion Conditions on Cardiac (H9C2) Cell Proliferation, Morphology, and Alignment. *SLAS Technol.* **22**, 536–546 (2017).
11. Giridharan, G. A. *et al.* Microfluidic Cardiac Cell Culture Model (μCCCM). *Anal. Chem.* **82**, 7581–7587 (2010).
12. Pavesi, A. *et al.* Controlled electromechanical cell stimulation on-a-chip. *Sci. Rep.* **5**, 11800 (2015).
13. Veldhuizen, J., Cutts, J., Brafman, D. A., Migrino, R. Q. & Nikkhah, M. Engineering anisotropic human stem cell-derived three-dimensional cardiac tissue on-a-chip. *Biomaterials* **256**, 120195

(2020).
14. Maoz, B. M. *et al.* Organs-on-Chips with combined multi-electrode array and transepithelial electrical resistance measurement capabilities. *Lab Chip* **17**, 2294–2302 (2017).
15. Mathur, A. *et al.* Human iPSC-based Cardiac Microphysiological System For Drug Screening Applications. *Sci. Rep.* **5**, 8883 (2015).
16. Agarwal, A., Goss, J. A., Cho, A., McCain, M. L. & Parker, K. K. Microfluidic heart on a chip for higher throughput pharmacological studies. *Lab Chip* **13**, 3599–3608 (2013).
17. Pires de Mello, C. P. *et al.* Microphysiological heart–liver body-on-a-chip system with a skin mimic for evaluating topical drug delivery. *Lab Chip* **20**, 749–759 (2020).
18. Oleaga, C. *et al.* Multi-Organ toxicity demonstration in a functional human in vitro system composed of four organs. *Sci. Rep.* **6**, 20030 (2016).
19. Schneider, O., Zeifang, L., Fuchs, S., Sailer, C. & Loskill, P. User-Friendly and Parallelized Generation of Human Induced Pluripotent Stem Cell-Derived Microtissues in a Centrifugal Heart-on-a-Chip. *Tissue Eng. Part A* **25**, 786–798 (2019).
20. Parsa, H., Wang, B. Z. & Vunjak-Novakovic, G. A microfluidic platform for the high-throughput study of pathological cardiac hypertrophy. *Lab Chip* **17**, 3264–3271 (2017).
21. Kujala, V. J., Pasqualini, F. S., Goss, J. A., Nawroth, J. C. & Parker, K. K. Laminar ventricular myocardium on a microelectrode array-based chip. *J. Mater. Chem. B* **4**, 3534–3543 (2016).
22. Weng, K.-C. *et al.* Human Induced Pluripotent Stem-Cardiac-Endothelial-Tumor-on-a-Chip to Assess Anticancer Efficacy and Cardiotoxicity. *Tissue Eng. Part C. Methods* **26**, 44–55 (2020).
23. Ren, L. *et al.* Investigation of Hypoxia-Induced Myocardial Injury Dynamics in a Tissue Interface Mimicking Microfluidic Device. *Anal. Chem.* **85**, 235–244 (2013).
24. Kobuszewska, A., Jastrzębska, E., Żukowski, K. & Brzózka, Z. Simulation of hypoxia of myocardial cells in microfluidic systems. *Sci. Rep.* **10**, (2020).
25. Martewicz, S. *et al.* Reversible alteration of calcium dynamics in cardiomyocytes during acute hypoxia transient in a microfluidic platform. *Integr. Biol. (Camb).* **4**, 153–164 (2012).
26. Ribas, J. *et al.* Cardiovascular Organ-on-a-Chip Platforms for Drug Discovery and Development. *Appl. Vitr. Toxicol.* **2**, 82–96 (2016).
27. Paguirigan, A. L. & Beebe, D. J. Microfluidics meet cell biology: bridging the gap by validation and application of microscale techniques for cell biological assays. *Bioessays* **30**, 811–821 (2008).
28. Berthier, E., Young, E. W. K. & Beebe, D. Engineers are from PDMS-land, Biologists are from Polystyrenia. *Lab Chip* **12**, 1224–1237 (2012).
29. Blow, N. Microfluidics: the great divide. *Nat. Methods* **6**, 683–686 (2009).
30. Torino, S., Corrado, B., Iodice, M. & Coppola, G. PDMS-Based Microfluidic Devices for Cell Culture. *Inventions* **3**, (2018).
31. Mohammed, M., Haswell, S. & Gibson, I. Lab-on-a-chip or Chip-in-a-lab: Challenges of Commercialization Lost in Translation. *Procedia Technol.* **20**, 54–59 (2015).
32. Reyes, D. R. *et al.* Accelerating innovation and commercialization through standardization of microfluidic-based medical devices. *Lab Chip* **21**, 9–21 (2021).
33. Mukhopadhyay, R. When PDMS isn't the best. What are its weaknesses, and which other polymers can researchers add to their toolboxes? *Anal. Chem.* **79**, 3248–3253 (2007).
34. Roy, E. Overview of Materials for Microfluidic Applications. in (ed. Pallandre, A.) Ch. 15 (IntechOpen, 2016).
35. Popovic, D. Modelling the marketing of high-tech start-ups. *J. Targeting, Meas. Anal. Mark.* **14**, 260–276 (2006).
36. Genchi, G. G. *et al.* Bio/non-bio interfaces: A straightforward method for obtaining long term PDMS/muscle cell biohybrid constructs. *Colloids Surfaces B Biointerfaces* **105**, 144–151 (2013).
37. Akther, F., Yakob, S. B., Nguyen, N.-T. & Ta, H. T. Surface Modification Techniques for Endothelial Cell Seeding in PDMS Microfluidic Devices. *Biosensors* **10**, (2020).
38. Siddique, A., Meckel, T., Stark, R. W. & Narayan, S. Improved cell adhesion under shear stress in PDMS microfluidic devices. *Colloids Surfaces B Biointerfaces* **150**, 456–464 (2017).
39. Hattori, K., Sugiura, S. & Kanamori, T. Microfluidic perfusion culture. *Methods Mol. Biol.* **1104**,

251–263 (2014).
40. Wei, C., Li, Y., Zheng, H., Tong, Y. & Dai, W. Palmitate induces H9c2 cell apoptosis by increasing reactive oxygen species generation and activation of the ERK1/2 signaling pathway. *Mol Med Rep* **7**, 855–861 (2013).
41. Miller, T. A. *et al.* Oleate prevents palmitate-induced cytotoxic stress in cardiac myocytes. *Biochem. Biophys. Res. Commun.* **336**, 309–315 (2005).
42. Hickson-Bick, D. L., Buja, L. M. & McMillin, J. B. Palmitate-mediated alterations in the fatty acid metabolism of rat neonatal cardiac myocytes. *J. Mol. Cell. Cardiol.* **32**, 511–519 (2000).
43. de Vries, J. E. *et al.* Saturated but not mono-unsaturated fatty acids induce apoptotic cell death in neonatal rat ventricular myocytes. *J. Lipid Res.* **38**, 1384–1394 (1997).
44. Haunstetter, A. & Izumo, S. Apoptosis: basic mechanisms and implications for cardiovascular disease. *Circ. Res.* **82**, 1111–1129 (1998).
45. Torres-Alvarez, D. & Aguirre-Soto, A. Polydimethylsiloxane chemistry for the fabrication of microfluidics—Perspective on its uniqueness, limitations and alternatives. *Mater. Today Proc.* (2020).
46. Toepke, M. W. & Beebe, D. J. PDMS absorption of small molecules and consequences in microfluidic applications. *Lab Chip* **6**, 1484–1486 (2006).
47. Paguirigan, A. L. & Beebe, D. J. From the cellular perspective: exploring differences in the cellular baseline in macroscale and microfluidic cultures. *Integr. Biol. (Camb).* **1**, 182–195 (2009).
48. Campbell, S. B. *et al.* Beyond Polydimethylsiloxane: Alternative Materials for Fabrication of Organ-on-a-Chip Devices and Microphysiological Systems. *ACS Biomater. Sci. Eng.* (2020).
49. Yang, J. *et al.* Integrated gut–liver-on-a-chip platform as an <em>in vitro</em> human model of non-alcoholic fatty liver disease. *bioRxiv* 2020.06.10.141606 (2020).
50. Hirama, H. *et al.* Glass-based organ-on-a-chip device for restricting small molecular absorption. *J. Biosci. Bioeng.* **127**, 641–646 (2019).
51. Yao, J. *et al.* Optimization of PTFE Coating on PDMS Surfaces for Inhibition of Hydrophobic Molecule Absorption for Increased Optical Detection Sensitivity. *Sensors (Basel, Switzerland)* **21**, (2021).
52. Nianzhen Li, Schwartz, M. & Ionescu-Zanetti, C. PDMS compound adsorption in context. *J. Biomol. Screen.* **14**, 194–202 (2009).
53. Sasaki, H., Onoe, H., Osaki, T., Kawano, R. & Takeuchi, S. Parylene-coating in PDMS microfluidic channels prevents the absorption of fluorescent dyes. *Sensors Actuators B-chemical - Sens. ACTUATOR B-CHEM* **150**, 478–482 (2010).
54. Roman, G. T. & Culbertson, C. T. Surface Engineering of Poly(dimethylsiloxane) Microfluidic Devices Using Transition Metal Sol–Gel Chemistry. *Langmuir* **22**, 4445–4451 (2006).
55. Junkin, M. *et al.* High-Content Quantification of Single-Cell Immune Dynamics. *Cell Rep.* **15**, 411–422 (2016).
56. Schuster, B. *et al.* Automated microfluidic platform for dynamic and combinatorial drug screening of tumor organoids. *Nat. Commun.* **11**, (2020).
57. Zhang, C. *et al.* Ultra-multiplexed analysis of single-cell dynamics reveals logic rules in differentiation. *Sci. Adv.* **5**, eaav7959 (2019).
58. Schindelin, J. *et al.* Fiji: An open-source platform for biological-image analysis. *Nature Methods* **9**, 676–682 (2012).
59. Krenger, R., Cornaglia, M., Lehnert, T. & Gijs, M. A. M. Microfluidic system for Caenorhabditis elegans culture and oxygen consumption rate measurements. *Lab Chip* **20**, 126–135 (2020).
60. Grist, S. M., Chrostowski, L. & Cheung, K. C. Optical Oxygen Sensors for Applications in Microfluidic Cell Culture. *Sensors* **10**, (2010).

# Chapter 4. Rapid fabrication of membrane-integrated thermoplastic elastomer microfluidic devices

**Abstract:** Leveraging the advantageous properties of soft thermoplastic elastomers, this work presents the facile and rapid fabrication of composite membrane-integrated microfluidic devices consisting of Flexdym™ polymer and commercially available porous polycarbonate membranes. The three-layer devices can be fabricated in under 2.5 hours, consisting of a 2 minutes hot embossing cycle, conformal contact between device layers and a low-temperature baking step. The soft thermoplastic elastomer bonding integrity is characterized and composite devices are shown to comfortability withstand pressures and flow rates corresponding to typical device use for cell culture experiments. Proof-of-concept cell culture studies are presented, followed by an investigation into the capability of FlexDym™ material recycling.

---

Parts of this chapter have been published:

* McMillan, A., Thomée, E., Dellaquila, A., Nassman, H., Segura, T., Lesher-Pérez, S. Rapid Fabrication of Membrane-Integrated Thermoplastic Elastomer Microfluidic Devices. *Micromachines* **11**, (2020). 

## Contributions

Microfabrication, delamination experiments and data analysis were performed by Emma Thomée, Dr. Alexander McMillan (Elvesys) and Alessandra Dellaquila (Elvesys). Microfluidic cell culture experiments and data analysis were performed by Hussam Nassam (Duke University) and Sasha Cai Lesher-Pérez (Elvesys). Polymer recycling experiments and data analysis were performed by Emma Thomée. Writing was done by Emma Thomée and revision was done by Emma Thomée and Dr. Aurélie Vigne.

## 4.1 Introduction

Cell culture on thin, porous membranes has been shown useful for studying cell-cell signalling, cell filtration and cell migration, in both static [1–5] and dynamic microfluidic models [6–8]. One branch of the state-of-the-art membrane-based cell culture is OOC technology, which has been of attention to much research. Often, OOC systems principally consist of two microfluidic chambers separated by a thin, porous membrane. Cells can be cultured on both sides of the membrane to generate tissue-tissue interfaces that simulate critical physiological barriers, such as the blood-brain barrier [9], liver [10], the epithelial-endothelial membranes in the lung [11], kidney [12] and gut [13], among other human organs and tissues [14–16].

The device fabrication process becomes increasingly important when complex device geometries, such as the non-trivial contraction of membrane-integrated devices, are desired. Indeed, many cutting edge microfluidic membrane-models have been based on PDMS for fabrication of both the device and the membrane.[17] Fabrication of thin, porous PDMS membranes is a time-consuming, cumbersome process that requires know-how and delicate handling.[18] The manual fabrication process is also prone to poor reproducibility resulting in batch-to-batch variations, and undesired issues such as blocking of pores or tearing of membranes which limit the throughput of fabrication.[18–21] While PDMS device fabrication is relatively easy, its multi-step process involving manual steps of mixing, degassing, curing and bonding cannot be straightforwardly scaled up for high-throughput fabrication.[22] Thus, for industrial implementations, the fabrication of PDMS devices as used in research laboratories must be reimagined which may have side-effects on the material and experimental outcomes. To circumvent problems associated with membrane fabrication, commercially available track-etched porous membranes have been employed for membrane-based cell culture devices. Such membranes are available in various biocompatible materials, thicknesses (down to 7 µm [23]), pore sizes and porosities.[24]

The use of hard thermoplastic materials, such as polystyrene, PC, PMMA and COP, for microfluidic fabrication can address some of the limitations associated with PDMS. Furthermore, the wealth of industrial knowledge around processing of thermoplastics can be leveraged for high-throughput fabrication of thermoplastic microfluidic devices through melt-processing techniques.[25] Thermoplastics are low-cost materials and have demonstrated promising utility for microfluidic device fabrication.[26–29] Moreover, unlike cured PDMS, thermoplastic materials can generally be recycled and re-molded into new parts. The aspect of sustainability and the environmental impact of a product, is an increasingly important factor that should be considered as early as

possible during the product development process. However, due to their rigidity (of tensile moduli in the order of ~1–4 GPa[30]), processing of thermoplastics on a small scale is less accessible than PDMS fabrication and requires expertise, expensive molds, and process-intensive bonding and interfacing to fluidic setups.

sTPE materials provide a unique combination of high-throughput processing of thermoplastics with the flexibility and prototyping-fabrication of elastomers such as PDMS.[31–33] In chapter 2, we demonstrated that two novel sTPE materials, FlexDym™ and Fluoroflex, had desirable properties for applications in microfluidic cell culture. However, out of the two, only FlexDym™ is commercially available and accessible in larger quantities. FlexDym™ has also been shown to be rapidly processable through hot-embossing in less than 2 minutes with common microfluidic molds and to have adhesive and cohesive bonding properties that allow for facile sealing of microfluidic devices without the need for adhesives or plasma treatment.[34] In contrast to both PDMS and hard thermoplastics, the transferability of FlexDym™ fabrication allows for rapid prototyping in research laboratory settings, as well as feasible scaling up of fabrication processes for industry adoption, without the need to alter the material.

In this chapter, we present a composite membrane-integrated microfluidic device based on FlexDym™ polymer and porous PC membranes for use in membrane-based cell culture. The device is fabricated entirely from off-the-shelf components.

## 4.2 Results and Discussion

In the first section, the development of a rapid and scalable protocol for fabrication of membrane-integrated sTPE microfluidic devices is presented. A microfluidic setup for automated delamination testing was developed and used to characterize the bonding strength of the microfluidic devices in order to assess the integrity of the devices. Additional characterization of FlexDym™ bonding strength to other materials has also been included in the chapter, to give scope for implementation of FlexDym™ in composite devices composed of other common microfluidic materials. Flow characteristics in the PC composite devices were also characterized for practical translation of the device pressure capabilities to flow rates. Moreover, cell attachment and the capability of the devices to support long-term cell culture (up to 7 days) was confirmed, giving a proof-of-concept for membrane-based microfluidic cell culture. Lastly, we investigated if material from composite FlexDym™-PC devices that had been used for basic microfluidic cell culture experiments could be recycled and used to fabricate a new microfluidic device. Selected material properties of recycled

FlexDym™ polymer were characterized to assess whether the recycling process impacted the material in a way that was detrimental to the intended device functionality.

### 4.2.1 Composite device fabrication

A protocol for fabrication of three-layered composite FlexDym™-PC-FlexDym™ microfluidic devices was developed. The procedure, beginning from the molding step, is outlined in **Figure 4.1**.

The developed fabrication protocol resulted in devices in under 2.5 hours. Compared to equivalent membrane-integrated devices in PDMS, this presents a significant improvement on the production time, and the time savings are multiplied for fabrication of multiple devices. A single master mold can be used to fabricate multiple FlexDym™ devices in parallel, as it is only needed for the 2-minutes hot-embossing step. For PDMS molding, however, the master mold is needed for the most time-intensive step of the fabrication – the slow curing of the base polymer-crosslinker mixture that typically requires 1-4 hours baking or 48 hours in room temperature [35,36].

Porous PC membranes similar to the Isopore™ membranes used in this study have effectively been used in microfluidic cell culture studies and OOC applications.[9,37,38] They represent an accessible option to custom-made membranes, and crucially, they retain the spontaneous FlexDym™ self-sealing interaction, for facile interfacing of composite layers. In literature, microfluidic barrier model platforms of PDMS often comprise thin, homemade, porous membranes in PDMS. Their complex fabrication processes are limited in accessibility, reproducibility and high-throughput aspects. The possibility to mechanically stretch the PC membranes to deliver mechanical stimuli (e.g., desirable for modelling the alveolar interface in lung-on-chip systems [11,39]) was not evaluated. However, the intrinsic stiffness of PC suggests difficulties in achieving stretching of relevant scale. A more elastic material would thus be optimal for studies involving mechanical stretching of the membrane. Another potential drawback of using track-etched membranes is their micro-scale thickness, which can limit diffusion and cell-cell contact from one side of the membrane to the other.[40,41] Moreover, the more significant thickness of the thermoplastic membranes and their material properties reduces optical clarity, notably for bright field observation. The development of ultra-thin nano-scale membranes showing improved optical transparency, permeability and cell contact has recently advanced [40], but they are yet not readily available.


A
B
C
D
E
F
G
H
I
J
K
L
M
N
O
P
Q
R
S
T
U

**Figure 4.1.** Photos demonstrating the step-by-step fabrication process of a PC membrane-integrated FlexDym™ device. (a) Extruded FlexDym™ sheets (covered by red protective layers of Teflon) were cut to appropriate size (50 × 75 mm). (b-c) The FlexDym™ sheet was placed on a microfluidic mold (d) and a counter plate for hot-embossing (here a plain glass slide) was placed on top of the FlexDym™. (e) The assembly was placed on top of the lower metal plate in a vacuum heat press together with four spacers surrounding it for control of final thickness. (f) The upper metal plate of the heat-press was placed on top, (g) and the 2 minutes hot-embossing cycle at 150 °C was run. (h) The mold-FlexDym™-counter plate assembly was removed from the vacuum heat press (i) and the glass counter plate was removed using wafer tweezers and isopropanol to facilitate separation. (j) The micropatterned FlexDym™ sheet was peeled off the mold using tweezers (k) and the sheet was cut to appropriate device size with scissors. (l-m) Access holes were punched in the top FlexDym™ layer with a steel hole punch. (n) A PC membrane (covered by blue protective films) was cut to size with scissors, (o-q) and layered with conformal contact over the channel of the top layer of FlexDym™. The PC membrane covered the top channel but leaves the access ports to the lower channel unobstructed. (r-s) Using a stereoscope for alignment, the second FlexDym™ layer was placed on top of the membrane such that the two channels are superimposed and the access holes align. Light adhesion occurs immediately, but can be reversed to correct for misalignment. (t) The device was baked in an oven for 2 hours at 80 °C. (u) Final device, ready for cell culture use. Reproduced from ref.* (see page 1) with permission from MDPI.

The composite device presented here is made entirely from off-the-self components, allowing rapid fabrication of entire devices with minimal investment and planning, in contrast to PDMS devices. The device fabrication is accessible at laboratory scale, but also represents a transferable process. At small lab-scale, the procedure shares equipment and know-how from soft lithography (only requiring the addition of a heat press). The thermoplastic properties of FlexDym™ gives scope for scaling up the fabrication for manufacturing of large quantities in a highly reproducible manner through injection molding or roll to roll hot embossing using the same material. This transferability between lab and industrial-scale is in sharp contrast to both PDMS and hard thermoplastic microfluidics.

### 4.2.2 Automated delamination testing

An experimental setup for delamination tests to evaluate the integrity of bonding between layers of microfluidic devices was created, consisting of a microfluidic "delamination device" design and an automated microfluidic circuit. The deamination device, presented in **figure 4.2a-c**, comprised two disconnected channels separated by a gap of varying distances. As pressure was applied to the input channel, no fluid could flow except in cases where delamination over the gap occurred, i.e., the bond at the gap separated and consequently allowed fluid passage from the input to the output channel. The distance of the gap could be varied to investigate the bonding characteristics of small features, and better understand the minimum feature sizes attainable with the given material. This could be significant where thin channel walls or micropillars are desired.

Delamination devices were connected to the microfluidic setup (**Figure 4.2d**, ensuring that no bubbles were present in the system. Using the Elveflow® Smart Interface software, the input channel was pressurized by a stepwise pressure profile from 0 to 2000 mbar gauge pressure, in steps of 50 mbar each step lasting 30 seconds. The in-line flow and pressure data were logged by the sensors, and the system was programmed to stop the pressure sequence at a detection of leak. A leak was indicated by a sudden increase to a non-zero flow rate and a drop in pressure at the device inlet. A single program execution allowed for sequential testing of up to ten devices (number of ports of the valve multiplexer), and the synchronized logging of data from both the sensors as well as the pressure controller itself offered redundancy to reduce erroneous results and allowed for the precise confirmation of the moment and pressure at which delamination occurred. As soon as a delamination event was detected, a feedback loop cut a testing cycle short and switched devices.

Through sequential testing of multiple devices without user interference, this setup represents a streamlined and robust method for burst testing, regulated by feedback from real-time pressure and flow rate data (**Figure 4.3**). Indeed, the testing could be further parallelized with the use of multiple sensors for higher-throughput testing.

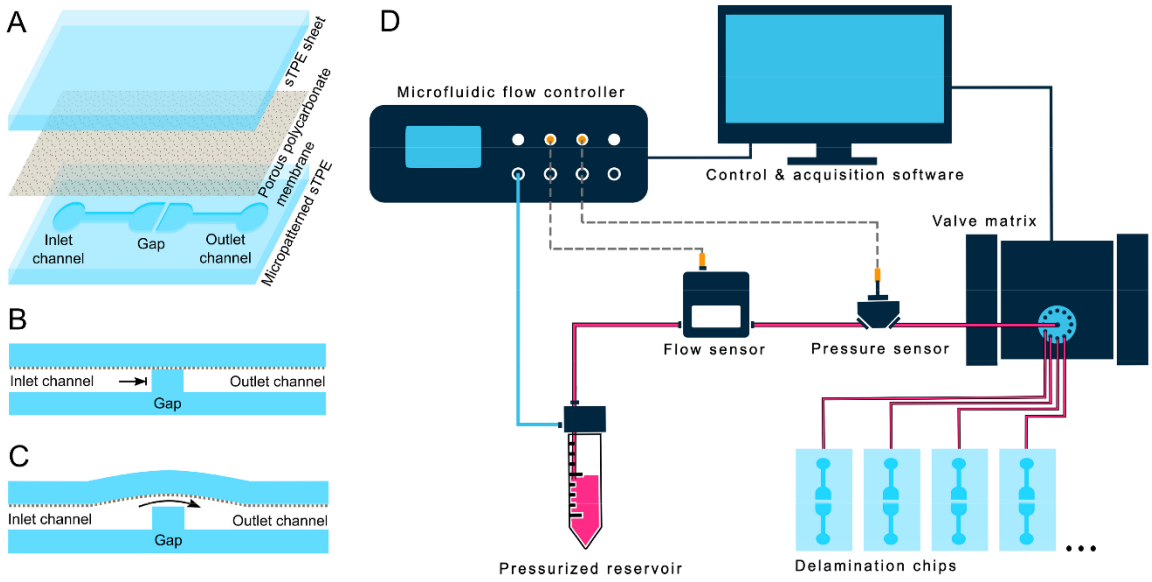


**Figure 4.2.** (a) Expanded view of the microfluidic chip design for delamination tests, consisting of two disconnected channels separated by a gap of varying distances. The inlet channel is increasingly pressurized, with no flow occurring until the delamination of test substrate from the FD gap structure occurs, at which point fluid crosses the gap into the outlet channel. (b) And (c) respectively show cross sections of the gap portion of the device before and after delamination. (d) Schematic of the automated delamination testing setup utilizing flow and pressure sensors and a valve matrix in series with a water-filled reservoir pressurized by a pressure controller. Continuous data logging and sensor feedback allowed the sequential testing of the pressure capacities of up to 10 microfluidic devices with no user monitoring. Reproduced from ref.* (see page 1) with permission from MDPI.

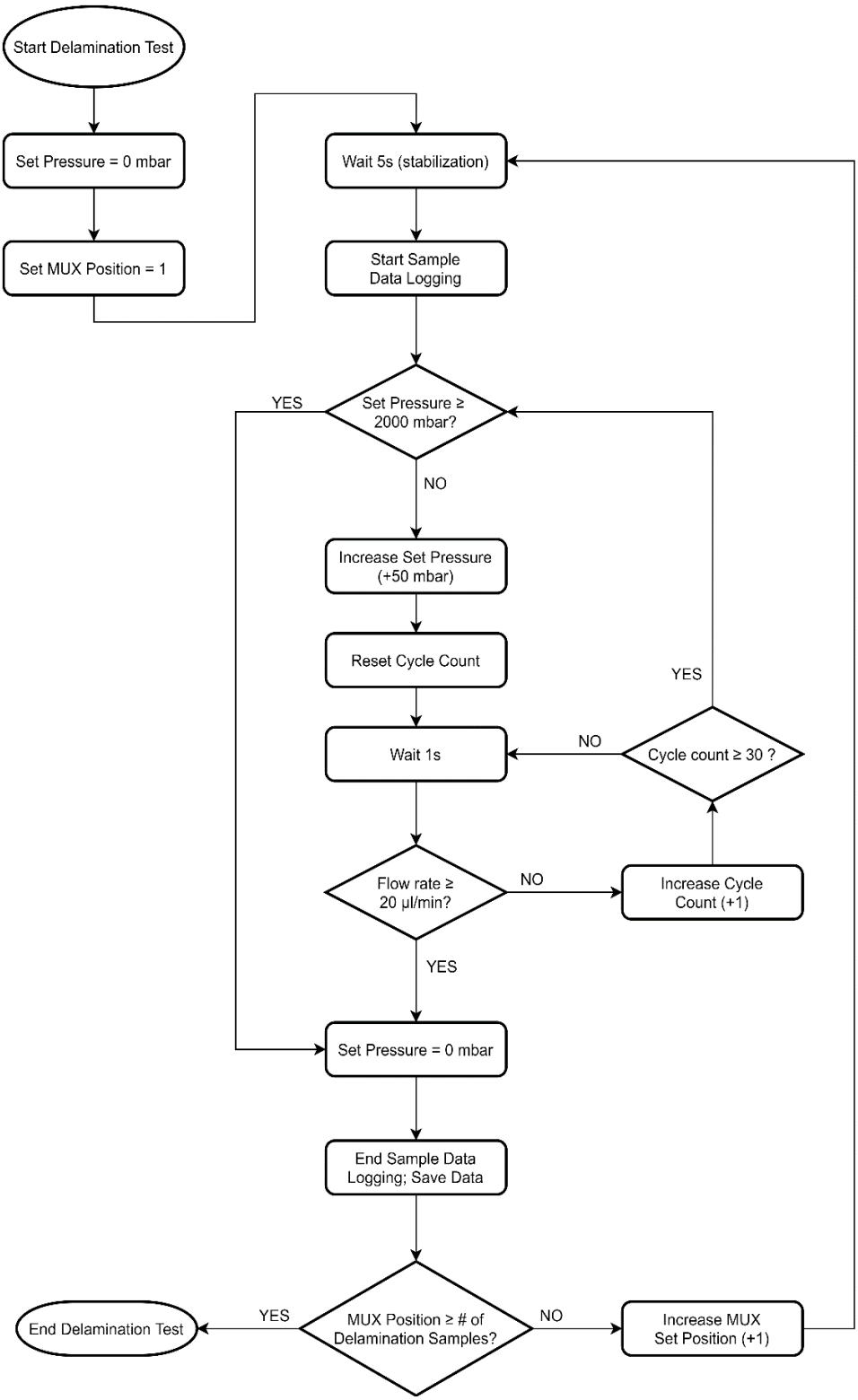


**Figure 4.3**. Logic flowchart of the automated delamination testing setup programmed in the Elveflow Smart Interface software. The sequence uses feedback from a flow sensor in order to detect device delamination (i.e. leak in the system) and stop the pressurization cycle before switching to the subsequent sample. Reproduced from ref.* (see page 1) with permission from MDPI.

Effective sealing to prevent leaks is an integral part of microfluidic device design and remains a challenge facing the microfluidics community when evaluating new materials.[42] While no standardized method specific to microfluidic applications exist, a wide variety of techniques have been employed to assess sealing techniques, including flow rate-based evaluation in flow-through channels and the pressurization of closed channels, both commonly relying on optical detection of leaks.[43–51] Such systems for leak/burst tests remain low throughput in comparison to the automated delamination system presented here. Another advantage of the delamination systems is that the dynamics of delamination is considered on a smaller scale, as opposed to leaking from a device channel toward the exterior of the device (often representing millimetres or centimetres of bonding distance before a leak/burst occurs). The technique to assess bonding proposed here is thus more representative in a microfluidic context and higher through-put than existing methods.

### 4.2.3 FlexDym™ bonding strength

**FlexDym™-polycarbonate bonding strength**

While microfluidic cell culture typically does not involve high flow rates and high pressures inside the microfluidic system, the robustness of a microfluidic device greatly depends on its capacity to withstand leaks. To this end, a series of delamination tests were carried out to evaluate the bonding integrity of the composite FlexDym™-PC devices. Delamination devices containing a PC membrane (of design shown in **Figure 4.2a-c**) with varying gap sizes were used to evaluate the minimum bonding distance to achieve sufficient and reliable bonding. The pressure capacities of the delamination devices are presented in **Figure 4.4a**, showing an increase from 529 ± 318 mbar (mean ± standard deviation) with a gap distance of 100 µm to 1802 ± 186 mbar with a gap distance of 1000 µm (noting that a maximum testing pressure of 2000 mbar was used, which, accounting for some pressure drop between the pressure controller and the devices, corresponded to a maximum pressure of ~1880 measured at the devices). The positive trend showed high variability across the range of gap distances tested. High variability was apparent for gap distances of 100 and 200 µm for both devices with and without a membrane. This might be due to limitations of the fabrication protocol using tweezers to ensure conformal contact at the gap at small gap distances. Devices lacking a membrane overall showed a higher pressure-capacity, ~1500 mbar and above at all gap distances, compared to membrane-devices. For gap distances of 300 µm and above, results are consistent with the bulk pressure capacity found by Lachaux et al. when using a similar bonding protocol.[34] At a bonding distance

of 1 mm, FlexDym™-PC devices frequently withstood the maximum testing pressures of 2 bar. This gap distance represents microfluidic channels that do not contain micro-scale structures such as thin walls, and is more analogous to bulk microfluidic burst testing in literature.[43–47,49–51] After delamination, minor spontaneous resealing at the gap was observed when pressurization was released. Although outside the scope of this work, such phenomenon could be interesting for applications in normally-closed valves responding to varying pressure profiles, such as seen in microfluidic circuits and logics [52,53].

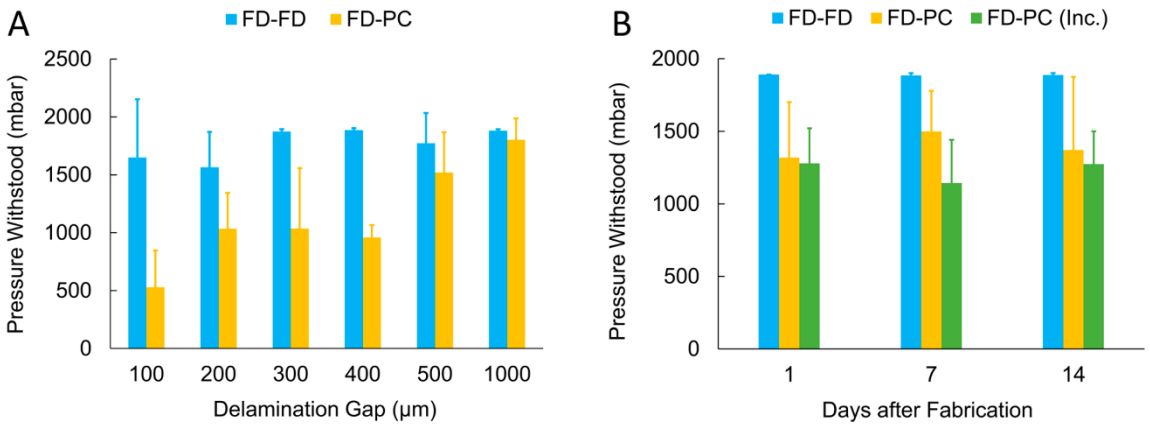


**Figure. 4.4.** Pressure delamination testing. (a) FlexDym™-polycarbonate (FD-PC) and FlexDym™- FlexDym™ (FD-FD) bonding evaluation through pressure delamination testing of devices with gap distances from 100 to 1000 µm. FD-PC devices show reduced bonding strength compared to FD-FD bonding, but reliably withstand pressures of 500 mbar at gap distances of 200 µm and above. (b) Pressure delamination testing of FD-FD and FD-PC devices (fixed 400 µm gap distance) at 1, 7 and 14 days after fabrication. An additional set of FD-PC devices was aged in high humidity, 37 °C incubation conditions (Inc.), which revealed no significant impact on the device sealing due to time post-fabrication or incubation conditions (n=5 devices per dataset; error bars represent one standard deviation). Reproduced from ref.* (see page 1) with permission from MDPI.

Delamination devices lacking a membrane could withstand higher pressure capacity compared to membrane-devices. This likely indicates a greater material interaction of FlexDym™ with itself compared to with PC. The bonding of SEBS block copolymers depends on the mobility of EB polymer chains at the bonding interface [54], and as PC does not contain the same EB chains it follows that the interaction at the interface is weaker. PC also has a higher glass transition temperature, around 150 °C, that is not

reached at the bonding temperature of 80 °C which could reduce the bonding due to polymer chain immobility.

To further evaluate the device integrity in context of microfluidic cell culture use, we performed a complementary series of delamination tests using devices of 400 µm gap distance with and without incubation at 37 °C and high humidity (simulating cell culture incubation conditions) for up to 14 days (**Figure 4.4b**). The study aimed to evaluate if any bonding degradation occurred as a result of the incubation conditions over time. A gap distance of 400 µm was selected as this was the largest gap size that frequently delaminated within the test pressure range. FlexDym™-PC devices after 14 days of aging in incubation conditions withstood pressures of 1274 ± 225 mbar, as compared to 1280 ± 241 mbar and 1319 ± 382 mbar one day after fabrication, with and without incubation conditions, respectively. No statistically significant difference in device integrity of FlexDym™-PC devices was observed resulting from time after fabrication or exposure to cell culture conditions (ANOVA: $F(5, 24) = 0.61$, $p = 0.69$, see section 4.3.2 for details).

We also investigated the bonding performance with pressurization over longer time periods. Microfluidic cell culture typically involves long-term continuous or pulsatile perfusion for transport of nutrients, waste and soluble factors.[55] Thus, delamination devices of gap distance 400 µm were subjected to constant pressure as well as cyclic pressure for 10 hours. No delamination occurred resulting from pressurization at 500 mbar for 10 hours, nor at cyclic pressurization (0 to 500 mbar, 0.2 Hz, 10,000 cycles), demonstrating robust and reproducible performance under realistic working conditions.

Studies on device integrity of membrane-integrated microfluidic devices for cell culture in PDMS have not been directly reported. Analogous PDMS devices with an integrated thermoplastic membrane typically use a PDMS glue/mortar method [43] or chemical surface modification for covalent bonding [56] that result in cross-linked or covalent bonds. PDMS devices comprising a PDMS membrane often utilize oxygen plasma bonding between PDMS slabs and PDMS porous membranes.[11,13,18,20,21] Burst testing conducted in PDMS-PDMS plasma bonded devices have revealed that the resulting covalent Si-O-Si bonds generally withstand pressures between 2 and 3 bar [51,57], but can range between approximately 0.7 and 4 bar depending on the oxygen plasma parameters.[50] PDMS-PDMS sealing without plasma activation has been shown to leak at pressures above ~400 mbar.[57]

**FlexDym™ bonding to other materials**

Hypothesising that the adhesive properties of FlexDym™ could be utilized to create sufficiently strong steals to other thermoplastics, we investigated the bonding strength to a number of materials (glass, FlexDym™, polystyrene petri dish, PMMA, COP and PDMS) bonded under different time- and temperature conditions. Indeed, these materials are not of relevance for characterization of the PC membrane-integrated device, but could be of interest for development of hybrid devices in the context of OOC beyond this study.

Delamination devices consisted of a delamination design of gap distance 1000 µm bonded to a flat substrate of the test material (glass, FlexDym™, polystyrene petri dish, PMMA, COP and PDMS). The pressure capacities of the composite devices under different bonding conditions are presented in **Figure 4.5**. The maximum test pressure of 2 bar (corresponded to a pressure of ~1880 at the devices, accounted for some pressure drop across the microfluidic circuit), was withstood by FlexDym™ bonded to all materials except glass and PDMS at bonding temperature of 85 °C for 2 hours. The study did not attempt to find the ultimate delamination pressure beyond 2000 mbar. Indeed, a pressure of 2000 mbar was assumed to be largely sufficient to withstand flow rates corresponding to most biological microfluidic experiments, and the low stiffness of FlexDym™ did not support higher pressures without experiencing large deformation of the channel dimensions. The results highlight great versatility and potential of FlexDym™ to be used in combination with other materials to create hybrid devices through facile bonding. To glass and PDMS, however, relatively lower bonding strengths were observed after bonding at 85 °C for 2 hours, 562 ± 110 mbar (mean ± standard deviation) and 1375 ± 177 mbar, respectively. Poor polymer interactions across the interfaces resulted in complete delamination that instantly spread over the entire bonding area at the point of delamination. Room temperature bonding for only 5 minutes was sufficient to create a seal to FlexDym™ and to petri dishes that could comfortably withstand pressures around 700 mbar, and leaving the chip at room temperature of 2 hours resulted in an average bond strength above 1000 mbar.

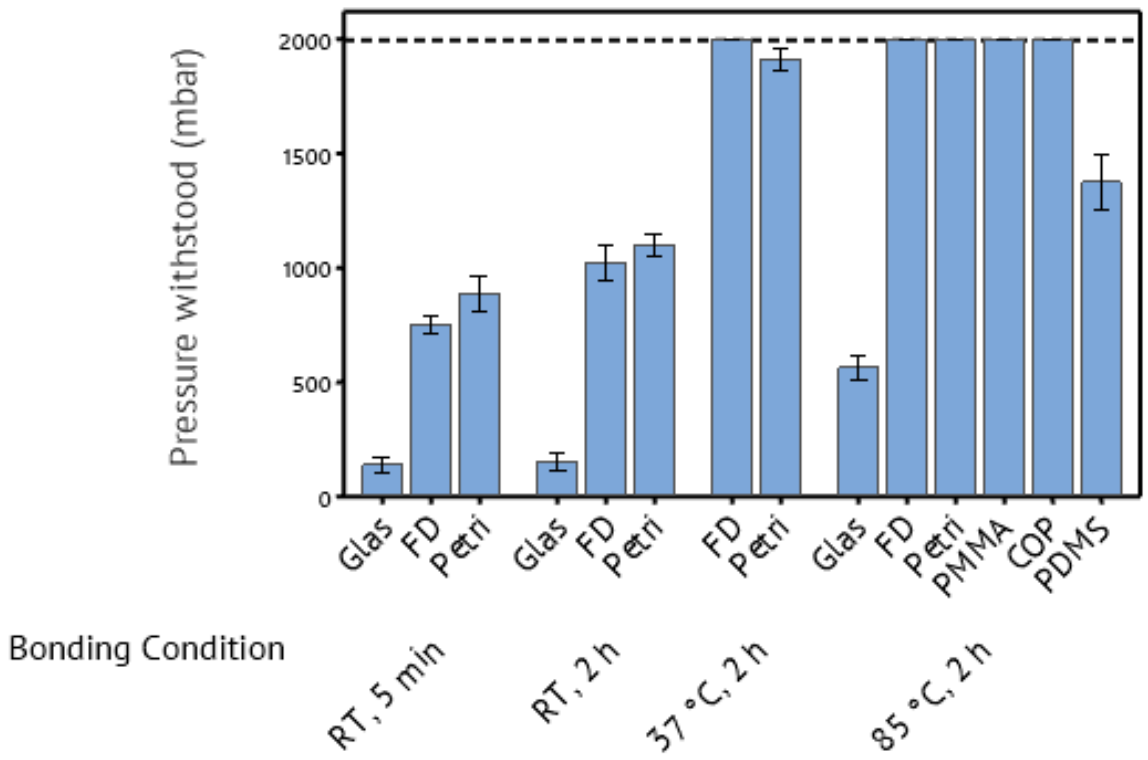


**Figure 4.5**. Evaluation of FlexDym™ bonding to glass, FlexDym™ (FD), petri dish, PMMA, COP and PDMS through pressure delamination testing of devices with gap distances 1000 µm. The dashed line represents the maximum test pressure (2000 mbar). The reported values are average values of 5 devices per dataset, and error bars represent the standard error.

Salmon et al. recently reported that leaving a monolithic chip in room temperature for 72 hours resulted in an equivalent bonding quality to baking at 80 °C.[58] The time and temperature dependency of bond strength and spontaneous bonding below the melting temperature (120 °C) [34] could be explained by the polymer chain mobility of the EB phase at the surface being sufficiently long and mobile to produce conformal contact to the counterpart surface, with a mobility that is accelerated at the increase of temperature.[59]

### 4.2.4 Flow-Pressure correlation

The influence of fluid induced shear stress experienced by the cells in the devices is a critical factor that must be considered during the design and fabrication stage. Shear stress has been demonstrated to impact a range of cellular functions such as differentiation, drug metabolism and cytokine secretion in various cell types.[60–62]

Microfluidic technology offers precise control of fluid flow, and thus enables implementation and control of appropriate shear stresses.

To understand the shear stresses attainable inside the FlexDym™-PC composite devices, a series of flow tests were conducted to correlate the pressure capacity results obtained from the delamination tests to flow rates in the devices. A single channel version of the 3-layered device was developed consisting of a channel of varying widths atop a PC membrane. The design represents geometries and flow characteristics present in typical barrier model cell culture chamber in literature in which there is no flow across the membrane (such as the well-known model developed by Harvard University's Wyss Institute [11,12,63,64]).

The linear relationship between pressure (measured at the device inlet) and the flow rates in the microfluidic setup is presented in **Figure 4.6a**, and **Figure 4.6b** shows the corresponding shear stresses on the membrane in the device. Shear stresses were determined by the following equation describing the wall shear stresses, $\tau_w$, of laminar Newtonian fluids in a closed rectangular geometry:

$$\tau_\omega = \frac{6\mu Q}{bh^2},$$

where μ is the dynamic viscosity of the fluid (water, $8.90 \times 10^{-4}$ Pa·s at 25 °C), Q is the fluid flow rate, b is the channel width and h is the channel height.[65] This approximation of wall shear stress assumes parabolic Poiseuille flow in the microchannel, useful for estimating wall shear stresses in rectangular channels when flow is along the length of the channel and w > h.

Using 500 mbar or less of applied pressure, flow rates up to ~150 μL/min and shear stresses of up to ~140 dyne/cm$^2$ could be achieved (depending on the channel dimensions). Considering that shear stresses desired for in vivo-like cell culture conditions rarely surpass 25 dyne/cm$^2$ , [66] the system could comfortably withstand this relatively low pressure required for such applications, even with the presence of small features.

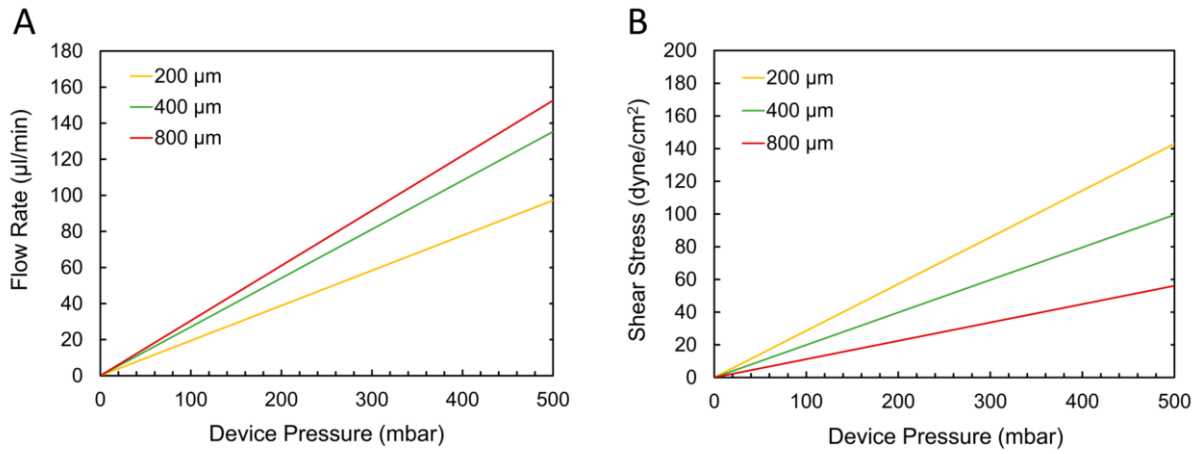


**Figure 4.6**. (a) Flow-pressure correlation in FlexDym™-PC devices from tests measuring the flow rate in a straight microfluidic channel (of width 200, 400 or 800 µm) and corresponding pressure at the channel inlet. Within 500 mBar of pressure applied at the device, flow rates of up to approximately 150 µL/min can be reached. (b) wall shear stresses that can be achieved in each of the example devices, as calculated from the flow rate data in (a), depending on the pressure applied. Shear stresses of up to approximately 140 dyne/cm$^2$ can be generated with pressures of 500 mBar and below. Reproduced from ref.* (see page 1) with permission from MDPI.

It must be noted that the relationships presented above depend on the resistance in the entire microfluidic circuit, which inevitably vary between experimental setups depending on the instruments, devices and tubing used. The flow-pressure correlations are thus not universal but aims to provide aid in translating the pressure-based delamination results into a more practically useful context (many microfluidic cell culture experiments are designed in the context of fluid flow rates or shear stresses rather than pressures) and assist the potential end user in understanding the potential of these devices.

### 4.2.5 Microfluidic cell culture

To ensure that cultured cells could be maintained with the FlexDym™-PC systems, human dermal fibroblasts (HDFs) were cultured within the devices for one week. HDFs were seeded on the top of the PC membrane in the upper channel of the devices. Sustained cell adhesion and spread morphologies were observed for up to one week (**Figure 4.7**), and cells were fixed and stained to visualize actin filaments in cultured cells (**Figure 4.8**). The limited optical transparency of the PC posed some difficulties

in observing cells under bright field illumination, but did not result in problems for fluorescent imaging. Although perfusion conditions may have been preferable to achieve a uniform cell distribution, alignment and proliferation, the static cell culture tests verified that the materials and device configuration could support cells for long term studies.

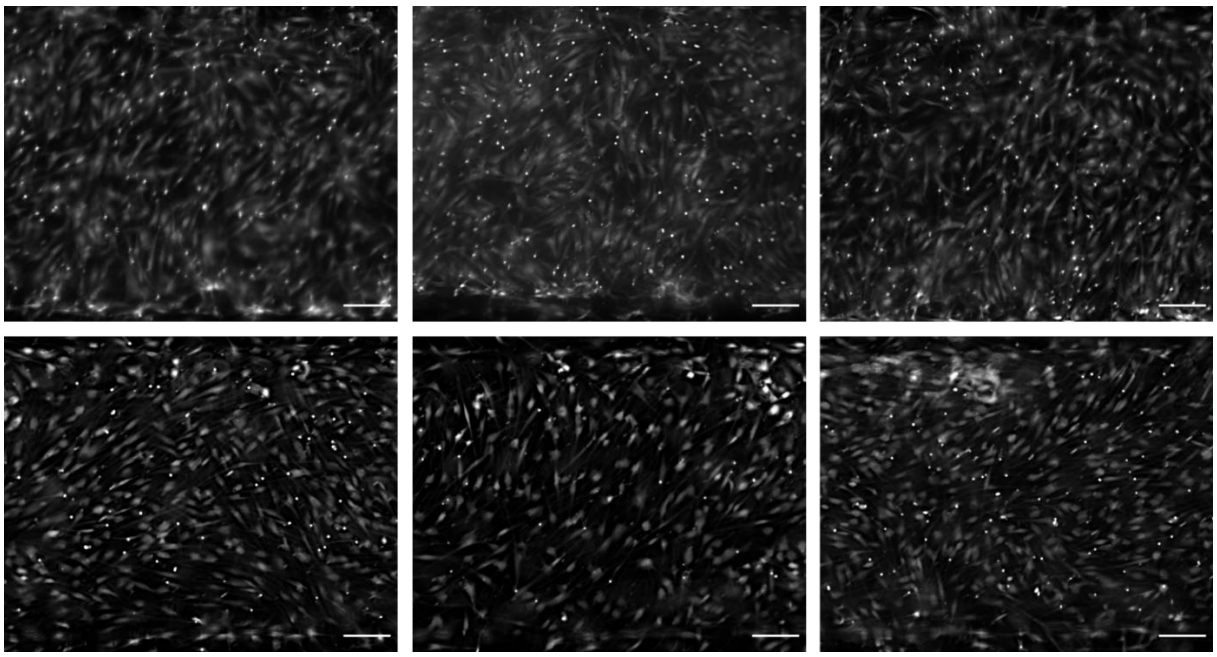

**Figure 4.7**. HDFs cultured in FlexDym™-PC composite devices. HDFs growing atop the PC membrane were stained with Calcein AM and imaged 2 days (top row) and 7 days (bottom row) after seeding. Calcein AM staining verifies that cells remained viable in the devices up to 7 days. Reproduced from ref.* (see page 1) with permission from MDPI.

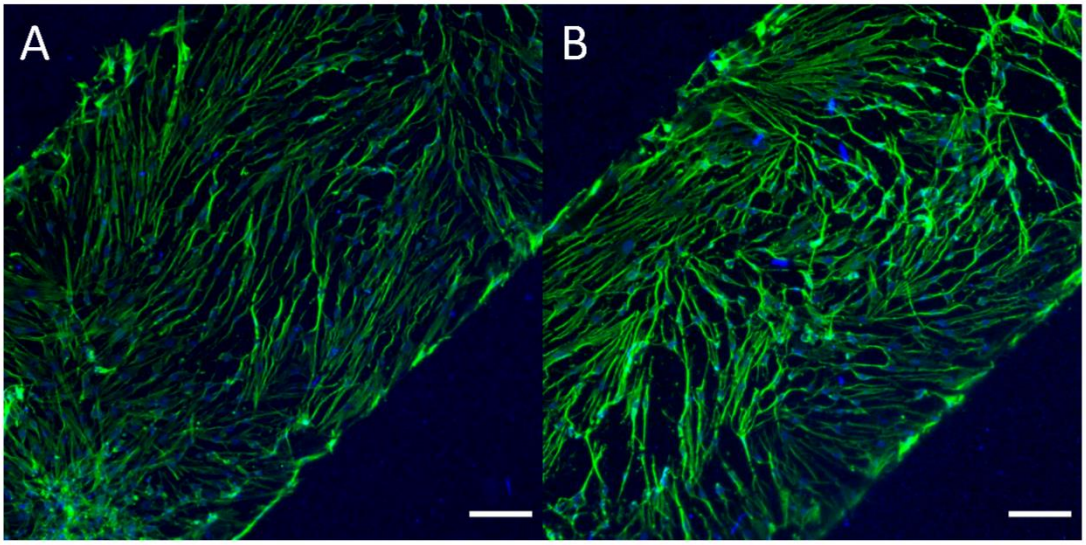


**Figure 4.8**. (A, B) Representative images of HDF cultured in FlexDym™-PC composite devices for 7 days. HDFs presented a primarily spindle geometry, commonly seen when HDFs are cultured to high confluency (due to higher density of cells). HDFs were cultured on top of the PC membrane for 7 days before fixation and staining with 488-Alexa Fluor™ 488 Phalloidin (staining for F-actin, green) and DAPI (nuclear, blue) to demonstrate cell adhesion and maintained presence in static culture within devices up to 1 week. Scale bars represent 150 µm. Reproduced from ref.* (see page 1) with permission from MDPI.

### 4.2.6 Recycling of FlexDym™ polymer

With the rapid expansion of microfluidics, both as a research field and on the commercial market, the questions of sustainability and material waste become increasingly relevant. Microfluidics is contributing to a shift toward smaller, integrated analytical systems that use less material and thus leaving a smaller environmental footprint, but the question of material recycling is something rarely discussed within the microfluidics community. The feasibility of recycling or reuse of microfluidic devices has been evaluated for a number of materials, such as, PMMA [67], perfluoropolyether (PFPE)-based elastomer [68] and polypropylene [69].

Microfluidic devices are generally regarded as disposable devices. For many biological applications disposability is necessary, as reuse or recycling of devices could have serious consequences on safety, health and quality. However, at the prototyping stage in laboratory environments, many rounds of fabrication of large number of devices are often inevitable, and reusing material could contribute to significantly reduced costs and material waste.[70,71] We chose to investigate if material from composite FlexDym™-PC devices that had been used for basic microfluidic cell culture

experiments could be recycled into a new device. Indeed, cell culture use poses additional requirements of cleanliness and sterility that must be addressed.

In an attempt to investigate the feasibility of FlexDym™ material recycling, we developed a protocol to recycle and repurpose material from used composite FlexDym™-PC devices into a new device (**Figure 4.9**). FlexDym™ polymer that had undergone one, two or three cycle(s) of repurposing was referred to as R1, R2 or R3, respectively. Pristine material was referred to as R0.

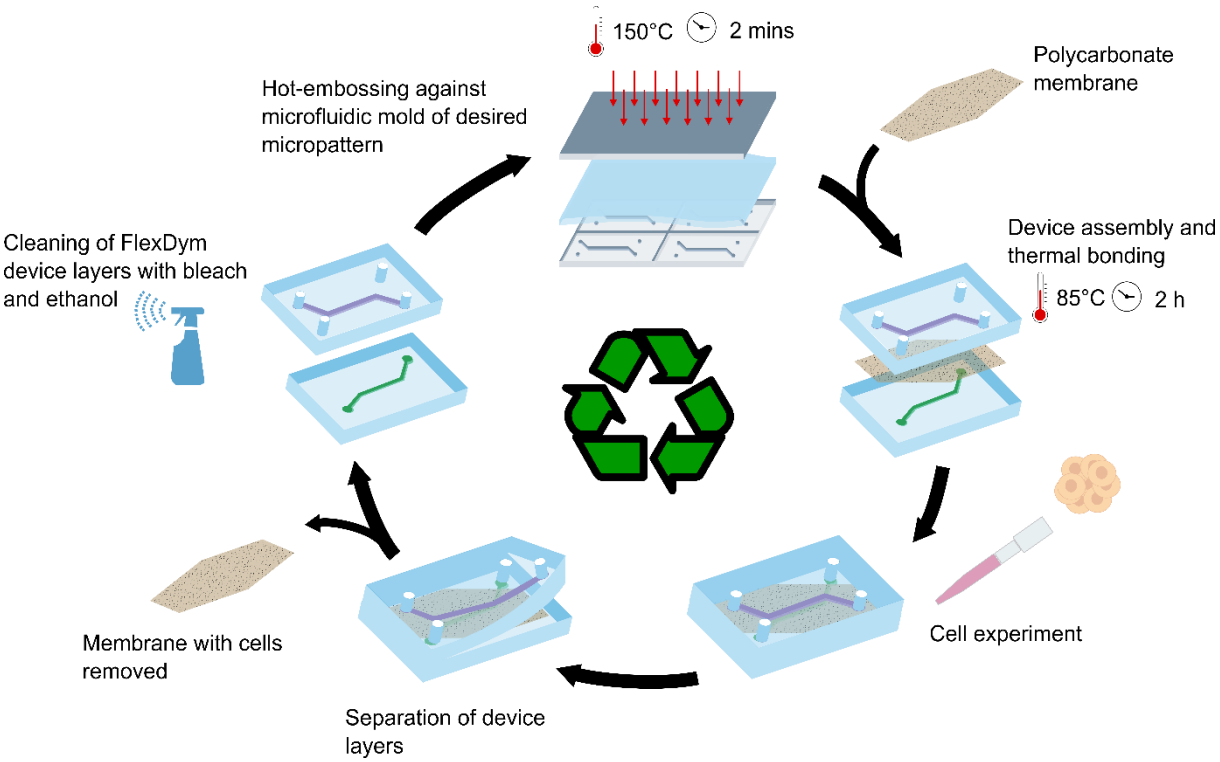


**Figure 4.9**. Schematic overview of the recycling process. A FlexDym™-PC composite device was fabricated starting from pristine FlexDym™ sheets (R0) and PC membranes. The device was used for a cell biological experiment, and subsequently separated and the membrane was removed. The FlexDym™ layers were chemically and physically cleaned with solvent and ultrasound sonication, dried and re-patterned through hot-embossing into a new device (R1-R3).

Thanks to the reversible nature of FlexDym™-PC bonding, the layers could easily be peeled apart with tweezers after the device had been used for a cell experiment. The used membranes were discarded, but could potentially be used for downstream analysis, opening up for analytical techniques that require direct access to cells (such as transmission/scanning electron microscopy, AFM, etc.). Assessing the feasibility of

cell analysis after peeling the devices apart was however outside of the scope of this study.

The FlexDym™ layers were cleaned and chemically sterilized using 10% bleach and 70% ethanol. Although the resistance to solvents of FlexDym™ has not been extensively studied, SEBSs generally have excellent resistance to water, acids and bases but poor resistance to certain organic solvents [72]. A swelling test, consisting of emerging FlexDym™ in different cleaning solvents for 24 hours was therefore performed in order to find a suitable protocol that did not induce material swelling or degradation. As shown in Table 4.1, none of the tested solvents induced any swelling or visible optical degradation.

**Table 4.1. Solvent testing of FlexDym™ material**

| Solvent | Swelling ratio | Visible optical degradation |
|---|---|---|
| 70 % Ethanol | 1 | No |
| 10 % Bleach | 1 | No |
| Isopropanol | 1 | No |
| Aniospray | 1 | No |
| 1M NaOH | 1 | No |

Based on ATCC and biosafety guidelines, 20 min of 10 % bleach treatment followed by 20 min of 70 % ethanol treatment was expected to be a sufficient cleaning procedure.[73] Phase-contrast microscopy was used to verify that no cells remained on the FlexDym™ after the cleaning process. It was not verified whether any biomolecules remained. It was however unlikely that biomolecules would remain active after the high-temperature and high-pressure exposure during the hot-embossing step and the 10 min air plasma treatment for hydrophilization of the channel.[74,75]

After cleaning and drying the FlexDym™ slabs, they could be re-processed by the same procedure as pristine FlexDym™ sheets. Separate pieces and punched access holes completely melted together to form a seamless, uniform block (**Figure 4.10**). A small reduction in thickness was observed after multiple iterations of re-molding, but the quality of the micro-patterning was not compromised. Salmon et al. showed through AFM investigations that, similarly to our findings, re-embossing of FlexDym™ chunks of different thermal history resulted in a uniform block.[58]

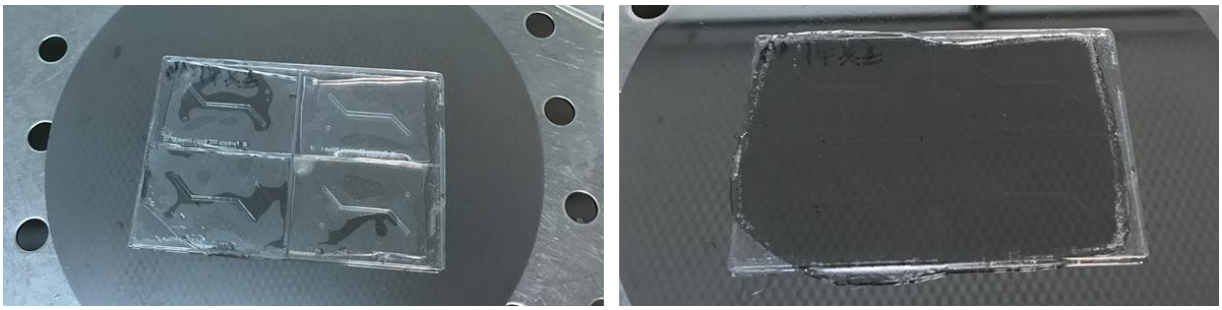

**Figure 4.10**. Re-embossing of FlexDym™. Four recycled FlexDym™ pieces were placed between the microfluidic mold and a metal counter plate for hot-embossing (left). A 2 min hot-embossing cycle at 150 °C resulted in merging of the pieces into one seamless block (right).

New devices were assembled from the repurposed FlexDym™ layers following the same fabrication protocol as used for pristine devices. The cutting steps, where deformed edges were cut off to ensure flatness of the device, resulted in some material loss. However, this material could effectively be collected and reused together with leftover material to mold a new device. This simple remolding procedure of FlexDym™ demonstrates versatility of FlexDym™ as a prototyping material beyond current possibilities with PDMS.

### 4.2.7 Evaluating properties of repurposed FlexDym™

In order to create functional devices from repurposed FlexDym™, it was necessary to investigate if experiments and assays could be conducted with devices fabricated from repurposed FlexDym™ without changing the experimental outcome. As a first step toward testing this, we identified a number of parameters that should remain unaltered (or sufficiently unaltered) in order to not compromise the use of the devices for basic cellular assays: thermal bonding properties, optical transparency, resistance to small molecule absorption, surface hydrophilization through plasma activation and cell culture compatibility.

To evaluate the self-sealing properties after repurposing of FlexDym™ material, we conducted a series of delamination tests. Delamination devices of pristine and repurposed FlexDym™ were tested using gap distances of 1000 µm. A reduction in bonding strength was observed for repurposed FlexDym™ compared to pristine (**Figure 4.11**). It is possible that the reduced bonding strength was attributed to a reduced physical cleanliness as the fabrication took place in an open laboratory space when dust and particles from the environment inevitably contaminate the samples. The bonding strength, however, remained sufficiently high to use the devices under

flow conditions (estimated from flow-pressure correlations, **Figure 4.6a**). We did not evaluate FlexDym™ bonding to other materials, such as PC, which would be necessary to assess the feasibility of using recycled material for hybrid devices.

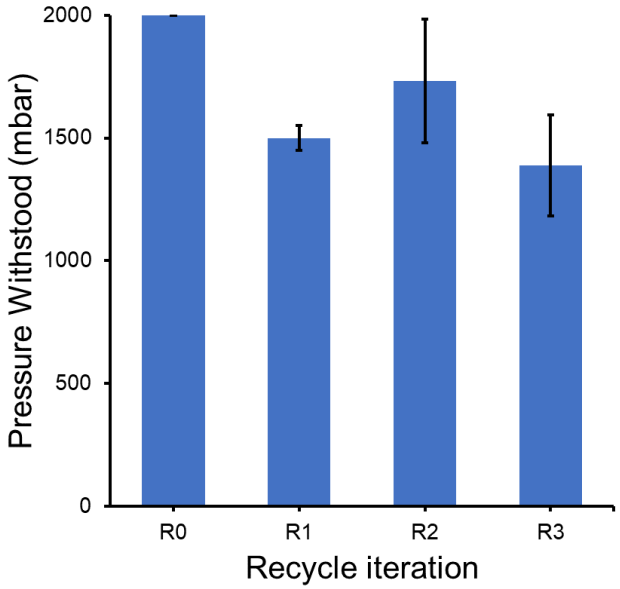


**Figure 4.11.** Evaluation of repurposed FlexDym™ bonding through delamination tests. Delamination devices (1000 µm gap distance) fabricated from repurposed FlexDym™ (R1-R3) showed reduced bonding strength compared to pristine FlexDym™ devices, but readily withstood pressures of > 1000 mbar (n=5 devices per dataset; error bars represent the standard deviation). Maximum test pressure was 2000 mbar.

A significant advantage of FlexDym™ over PDMS is the improved resistance to absorption of small molecules, such as Rhodamine B (as characterized in Chapter 2). To evaluate if the recycling process of FlexDym™ affected the absorption of the dye molecule Rhodamine B, we incubated pristine (R0) and recycled (R1-R3) FlexDym™ with 100 µM Rhodamine B solution (in DI water) for 24 hours. After 24 hours, channels containing rhodamine B were imaged with fluorescent microscopy, generously rinsed with DI water, and re-imaged empty. The line profile corresponding to the fluorescent images are presented in **Figure 4.12**. No widening of the line profile – indicating lateral absorption of the dye – was observed, and the washing effectively removed the fluorescent signal to a barely detectable level for all recycled samples. It was thus concluded that the repurposing did not affect the diffusion of small molecules through the bulk of the material, and devices fabricated from recycled polymer should be equally suitable for experiments involving small soluble molecules as pristine material.

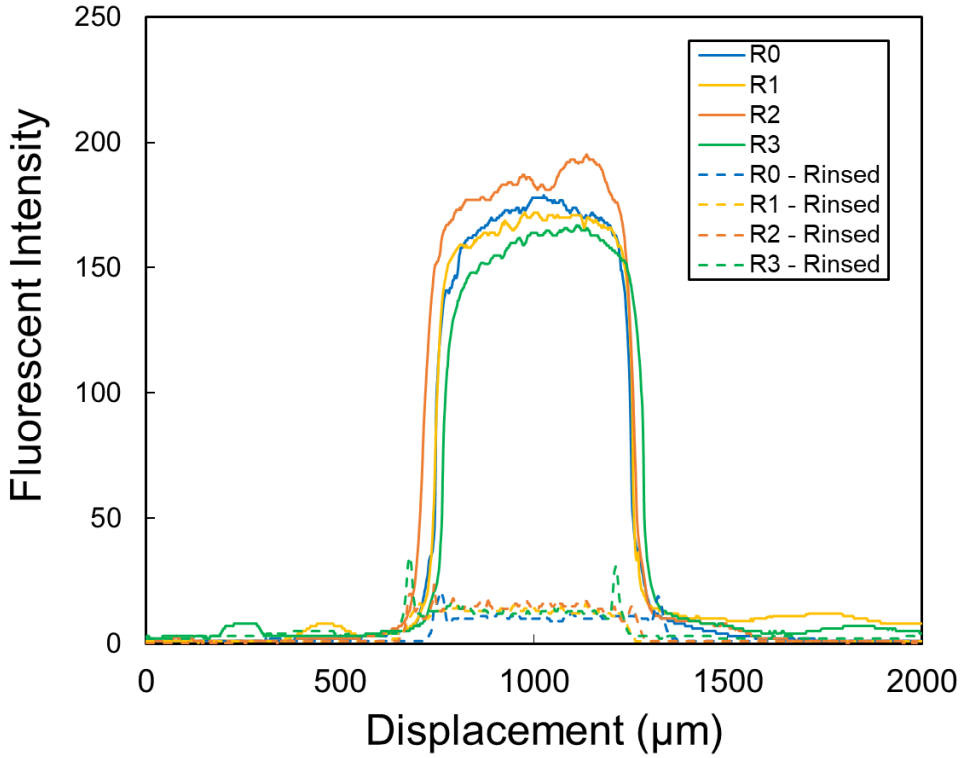


**Figure 4.12.** Rhodamine B uptake in pristine (R0) and repurposed (R1-R3) FlexDym™ microchannels (500 µm x 55 µm). Line profiles correspond to fluorescent images captured of 100 µM Rhodamine B incubated for 24 h in the microfluidic channels (solid lines) and the same channels reimaged after removing the Rhodamine B dye and rinsing the channels with 10 mL DI water (dashed lines).

Hydrophilization of the FlexDym™ surface through oxygen plasma treatment was previously shown to be critical for cell attachment (Chapter 2). In order to evaluate if the wetting behaviours of FlexDym™ were affected by the recycling process, the static contact angle of water (in air) was measured for samples recycled up to 3 iterations (R1-R3). The contact angles before and after plasma treatment are presented in **Figure 4.13**. The recycling process was found to have no impact on the wettability, as no statistical difference ($p > 0.05$) was observed between the static contact angles of recycled and pristine samples. It should be noted that all samples were analysed more than 2 weeks after their last use. Although they had been treated with low power air plasma before cell seeding (multiple times for R2-R3 samples), this time was likely sufficient for recovery to a hydrophobic state. The static contact angles after 10 minutes of oxygen plasma treatment were similarly compared. 10 minutes of oxygen plasma treatment resulted in complete wetting (defined as contact angles < 10 °) for all pristine and recycled samples. The results suggest that recycled FlexDym™ can be hydrophilized through plasma activation to promote cell attachment.

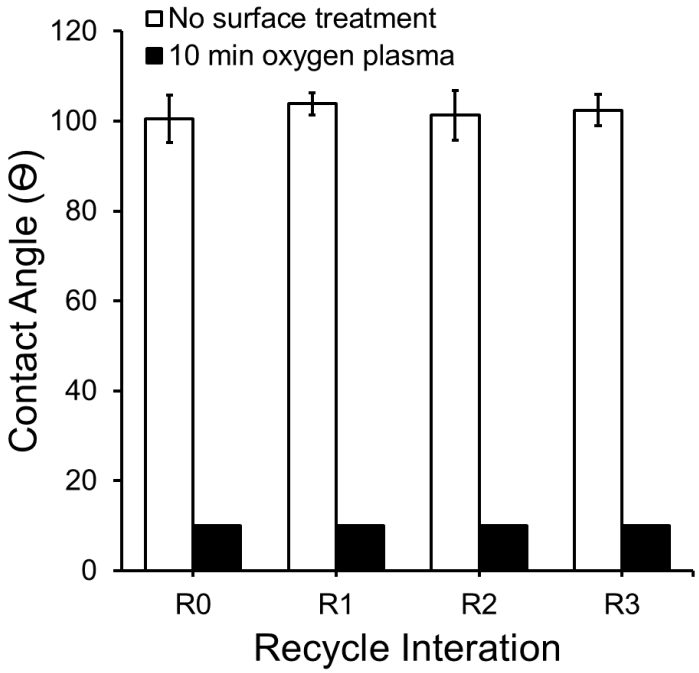


**Figure 4.13.** Surface wettability of repurposed FlexDym™. The static contact angle of water on pristine (R0) and repurposed (R1-R3) FlexDym™ before and after 10 min of oxygen plasma treatment. Oxygen plasma treatment resulted in complete wetting (shown as 10 ° in figure). The values presented are the average values of 5 measurements and error bars represent one standard deviation.

Lastly, HeLa cells were grown in direct contact with recycled FlexDym™ polymer to assess if cell attachment and cell growth could be achieved on recycled material. After 24 hours of culture, the cells on the pristine and recycled (R1-R3) samples were stained with Calcein-AM and propidium iodide to confirm cell attachment and high cell viability (**shown in Figure 4.14.**). While optical properties of the repurposed material were not characterized, the fluorescent imaging confirmed an optical quality that was sufficient for cell imaging by microscopy. The results suggest that recycled material may be feasible for use in basic biological experiments.

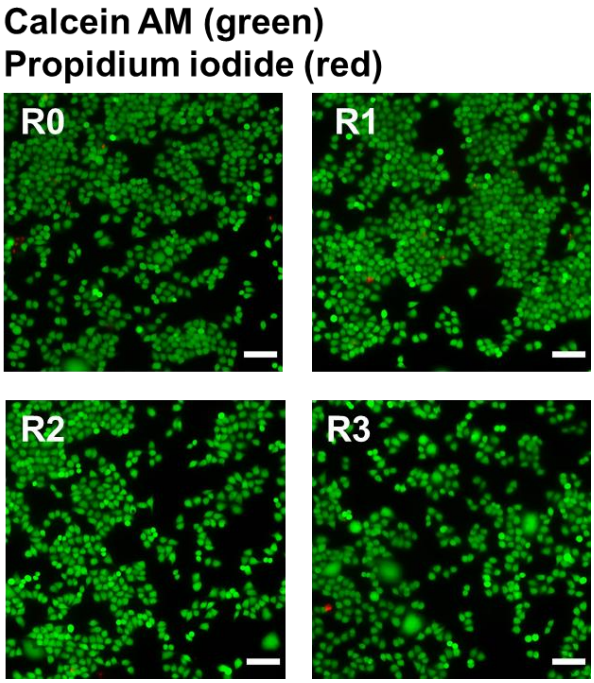


**Figure 4.14.** Fluorescent microscopy images of viable cells stained with calcein AM (green) and dead cells stained with propidium iodide (red), grown on pristine FlexDym™ (R0) and recycled FlexDym™ (R1-R3) for 24 h. Scale bars 100 µm.

While further studies are needed to determine the fitness of recycled FlexDym™ material and whether it can be used for more complex functional assays, this study is a first step toward implementing recycling practices in a microfluidics research laboratory. We demonstrated that FlexDym™ material from membrane-integrated microfluidic devices that had been used for basic cell experiments could be reprocessed multiple times and that the material retained essential functionalities that were critical for use in basic microfluidic cell culture experiments.

## 4.3 Experimental

### 4.3.1 Composite device fabrication

Microfluidic molds for hot embossing of FlexDym™ sheets were fabricated from photolithography using Ordyl® SY300 dry film negative photoresist on borosilicate glass slides, according to protocol in chapter 2. Hot embossing was performed in a vacuum-assisted heat press for 2 minutes at 150 °C and 0.7 bar applied pressure to micropattern FlexDym™ sheets (protocol in chapter 2). A FlexDym™-PC membrane composite device was developed by layering a porous track-etched PC membrane (2

µm pores, 5.6 % porosity, 23 µm thickness, IsoporeTM, Merck KGaA, Darmstadt, Germany) on a micropatterned sheet of FlexDym™, and applying light pressure with tweezers to ensure conformal contact between the surfaces. Light, reversible adhesion instantly occurs between the PC membrane and the FlexDym™ sheet. A second micropatterned sheet of FlexDym™ containing punched access holes was similarly placed on top of the membrane, so that the central channels of the two FlexDym™ layers were in direct superposition. Proper alignment was assured with the help of a stereoscope, and in case of misalignment the reversible adhesive properties of FlexDym™ allowed for separation and correction of layers. Device sealing was achieved by a baking step in a forced convection oven (DKN612C, Yamoto Scientific Co. Ltd., Tokyo, Japan) at 80 °C for 2 hours, without the need for plasma activation or adhesives. Conical FlexDym™ connectors were used to interface the chips with microfluidic tubing.

### 4.3.2 Delamination testing

The microfluidic setup for delamination consisted of an OB1® MK3+ pressure controller (0–2000 ± 0.1 mbar), thermal flow sensor (MFS3, -0–80 µL/min ± 5% m.v.) and capillary pressure sensor (MPS3, -1000–2000 ± 6 mbar) and a valve multiplexer (MUX Distributor) (all microfluidic setup was from Elveflow®, Elvesys SAS, Paris, France). Pressure was applied from the pressure controller to the microfluidic device via a reservoir with water and polytetrafluoroethylene (PTFE) microfluidic tubing (Darwin SAS, Paris, France).

Delamination devices were developed to assess the integrity of the bonding between FlexDym™ and the PC membrane, and the bonding of FlexDym™ to itself. FlexDym™-PC-FlexDym™ delamination devices, containing one micropatterned FlexDym™ sheet (comprising two disconnected channels separated by a gap of varying distances) and one FlexDym ™ sheet without features, separated by a PC membrane, were assembled. Gap distances between 100 and 1000 µm were tested (n=5 per gap distance) to evaluate the effect of the bonding distance on the resulting bond strength. A set of delamination devices lacking PC membranes were analysed, for comparison of the FlexDym™-PC bonding strength with that of FlexDym™-FlexDym™ self-bonding. Delamination tests were similarly conducted on delamination devices (1000 µm gap distance) fabricated from recycled FlexDym™ (R1-R3 and lacking a PC membrane, n=5 for each data set).

Another series of delamination tests were conducted to assess the stability of the device bonding over time, in order to simulate typical use of the devices including

long-term cell culture and repetitive use. Delamination devices of 400 µm gap distance at different time points after fabrication (1, 7 or 14 days post fabrication) were aged at room temperature or in an incubator (Model H2200-H, Benchmark Scientific Inc., Sayreville, NJ, USA) at 37 ˚C and high humidity to simulate cell culture conditions. One-way analysis of variance (ANOVA) was conducted between the six delamination groups to determine if aging time and incubation had a statistically significant impact on delamination pressure. P values of less than 0.05 ($p < 0.05$) were considered statistically significant. Delamination tests were also conducted on FlecDym™-PC devices of gap distance 400 µm to evaluate device stability under long term pressure, tested under static and cyclic pressure conditions. For static tests, devices were subjected to 500 mbar of pressure for 10 hours (n=5), and for cyclic tests, devices were subjected to 10,000 cycles of 0 to 500 mbar pressure at 0.2 Hz (n=5).

The ability of FlexDym™ to form a tight seal to itself and other materials, including glass, tissue culture treated petri dish (polystyrene), PMMA, PDMS and COP, as well as the effect of bonding time and temperature, were characterized through delamination tests. Monolithic or hybrid delamination devices containing one micropatterned layer of FlexDym™ (Eden Tech, Paris, France) of gap distance 1 mm was bonded to a featureless layer of FlexDym™, polystyrene petri dish (Corning Inc., Corning, NY, USA), glass slides (Corning Inc., Corning, NY, USA), PMMA (Perspex®, Lancashire, United Kingdom), COP (Zenonex, Düsseldorf, Germany) or air plasma treated (400 mTorr, 30W, PDC-002, Harrick Plasma, Ithaca, NY, USA) PDMS (10:1, base:crosslinker). Room temperature bonding was performed in ambient conditions, and bonding at elevated temperatures (37 °C and 85 °C) were performed in a forced convection oven. Delamination pressure was characterized from 0 to 2 bar of pressure in steps of 50 mbar.

### 4.3.3 Flow evaluation

A series of flow tests were conducted on FlexDym™-PC-FlexDym™ devices with a single channel of 27 mm length, 55 µm height, and varying width (200, 400, 800 µm). The microfluidic circuit consisted of (i) approximately 50 cm of 0.8 mm inner diameter (ID) PTFE tubing; (ii) a flow sensor with a quartz capillary of 430 µm ID and 3 cm in length (MFS3, -80–80 $\mu L.min^{-1}$ ± 5 % m.v.); (iii) a capillary pressure sensor with an effective ID of 0.8 mm and length of 8 mm (MPS3, - 1000–2000 ± 6 mbar); (iv) the microfluidic channel; and (v) a 5 cm section of polyether ether ketone (PEEK) tubing of 120 µm ID. Pressure and flow rate data in the microfluidic circuit were monitored (n=3 devices per channel width) and the corresponding fluid shear stresses on the PC

membrane surface were calculated to provide a reference of the mechanical conditions achievable within the ranges of pressure that the composite devices could withstand.

### 4.3.4 Microfluidic cell culture

Composite devices comprising two chambers (each of 800 (width) × 110 µm (height) × 27 mm (length)) separated by a PC membrane were fabricated. Devices were sterilized with UV and pre-treated with plasma (BD-20AC laboratory corona treater, Electro-Technic Products, Chicago, IL, US) for 10 seconds to increase hydrophilicity prior to cell culture work. Subsequently, devices were incubated with 10 µg $mL^{-1}$ fibronectin (Millipore Sigma, Burlington, MA, USA) for 1 hour at 37 ˚C. After flushing with 1X PBS supplemented with 1 % penicillin/streptomycin (Gibco®, Thermo Fisher Scientific), the top chamber was manually loaded with 7 µL of HDFs (ATCC, Manassas, VA, USA) at a concentration of 2 × $10^5$ cells $mL^{-1}$ in DMEM (high glucose, GlutaMAXTM supplement, Thermo Fisher Scientific, Waltham, MA, USA) supplemented with 10% FBS (Corning Inc., Corning, NY, USA) and 1% penicillin/streptomycin). Cells were incubated for 12 hours in the devices before exchanging media to remove non-adhered cells. After 48 hours of culture, cells were stained with Calcein AM (4 µM in 1X PBS, Sigma-Aldrich, St. Louis, MO, USA) for 20 minutes, and subsequently imaged with fluorescence microscopy (Zeiss Observer Z1, Carl Zeiss AG, Oberkochen, Germany) to verify the presence and distribution of cells in devices. The same procedure was repeated after 7 days. Cell fixation and staining with Alexa Fluor™ 488 Phalloidin (0.66 µM in 1X PBS, Thermo Fisher Scientific, Waltham, MA, USA) and DAPI (1 µg $mL^{-1}$ in 1X PBS, Sigma-Aldrich, St. Louis, MO, USA) was done after 7 days of cell culture in the top chamber of the devices. Briefly, after flushing the devices with PBS, cells were incubated in 4 % PFA for 15 minutes at room temperature, washed 3 times with PBS and permeabilized with 0.3 % Triton-X (in 1X PBS, Sigma-Aldrich, St. Louis, MO, USA). Cells were then stained with 488 Phalloidin and DAPI for 30 minutes prior to rinsing with PBS and imaging (Nikon C2 Confocal, Nikon, Tokyo, Japan).

### 4.3.5 Recycling process

A protocol to recycle the FlexDym™ layers of a PC membrane-integrated microfluidic device was developed. As a biological experiment, we employed 24 hours of microfluidic cell culture using HeLa cells. After fabrication of FlexDym-PC composite devices, devices were hydrophilized by 10 minutes of air plasma treatment (400 mTorr, 30 W, PDC-002, Harrick Plasma, Ithaca, NY, USA) and incubated with 20

µg.mL$^{-1}$ poly-D-lysine (in DI water, Sigma Aldrich) for 1 hour at 37 °C. After removing the poly-D-lysine coating, channels were flushed with 1X PBS and DMEM before being seeded with HeLa cells 1×10$^6$ cells/mL. Cells were maintained in the devices for 24 hours, before the device layers were separated by carefully peeling off the top FlexDym™ layer and fluid connectors with tweezers. The PC membrane with adhered cells could subsequently be peeled off and discarded. The FlexDym™ layers and connectors were cleaned by soaking them in bleach for 20 minutes, followed by ultrasound bath sonication (Elmasonic S 10, Elma Schmidbauer GmbH, Singen, Germany) in 70 % ethanol for another 20 minutes. Lastly, the layers were generously rinsed in isopropanol, DI water and dried with compressed air and cleaned with scotch tape before being remolded, following the same fabrication protocol as for hot-embossing of pristine FlexDym™. A new PC membrane was used for each recycling iteration. Devices were recycled up to 3 iterations.

To find a suitable sterilization protocol a solvent compatibility test was performed by immersing FlexDym™ pieces containing a microchannel (800 × 55 µm cross section) in five different cleaning solvents, 70 % ethanol, aniospray (Aniospray, Anios, Lille-Hellemmes, France), isopropanol, 1M NaOH solution and 10% bleach (sodium hypochlorite in water, Javel, Paris, France)) for 24 hours. Swelling was determined from determining the "swelling ratio," S=D1/D2, where D1 and D1 are the channel width before and after solvent swelling, respectively. D1 and D2 were determined using an inverted microscope and image analysis. Additionally, qualitative assessment of optical degradation was conducted by visually observing the transparency of pieces before and after solvent swelling.

### 4.3.6 HeLa cell culture

1x1 cm pieces of recycled FlexDym™ and pristine FlexDym™ were cut by scissors and placed in independent wells in a 24-well plate (n=3). Prior to cell culture, the polymer pieces were treated with air plasma for 5 minutes and rinsed with PBS. 0.5 mL of HeLa cells at concentration of 10$^4$ cells/mL were added to each well a top the polymer and incubated in 37 °C/ 5 % $CO_2$ for 24 hours. To assess cell viability after 24 hours of culture, cells were incubated with calcein-AM (GFP, 0.5 µM, Falcon® Corning, Corning, NY, USA) to label living cells and propidium iodide to label dead cells (TRITC, 3µM, Biotium, Fremont, CA, USA) for 30 minutes at 37 °C, after 24 hours. The cells were imaged in warm PBS with a fluorescent microscope (Zeiss Axio Observer Z1, Carl Weiss AG, Oberkonchen, Germany).

### 4.3.7 Rhodamine B absorption assay

Microfluidic devices were fabricated from recycled or pristine FlexDym™, containing a 500 × 55 µm straight microchannel bonded to a flat piece of FlexDym™ (n=3). The channel was filled with 100 mM rhodamine B dye in water (Sigma-Aldrich, St. Louis, MO, USA) and incubated at room temperature for 24 hours. After 24 hours the devices were imaged with the rhodamine B dye in the channel with a fluorescent microscope (Zeiss Axio Observer Z1, Carl Zeiss AG, Oberkochen, Germany). The channel was subsequently washed with 10 mL of DI water for 10 minutes and the device was re-imaged. Light intensity and exposure time were kept constant for all devices and images.

### 4.3.8 Goniometer measurements

Contact angle measurements were performed (according to the procedure outlined in Chapter 2) to compare the static contact angle of water on recycled samples and the effect of oxygen plasma treatment (PDC-002, Harrick Plasma, Ithaca, NY, USA, 10 minutes, 20 sccm, 50 mTorr, 100 W) on the static contact angle. Briefly, a 2 µL drop of DI water was deposited on the polymer surface and the static contact angle was recorded by a drop shape analyser (Krüss, Hamburg, Germany) and analysed using ADVANCE (Krüss, Hamburg, Germany). Contact angles near the limit of complete surface wetting, around 10 ° or less, could not be reliably measured and those samples were defined simply as experiencing “complete wetting” and presented by an arbitrarily chosen value of 10 °. Reported values are averages of 5 measurements. One-way analysis of variance (ANOVA) was applied to compare the difference in contact angle between samples of different recycling history. P values of less than 0.05 ($p < 0.05$) were considered statistically significant.

## 4.4 Conclusion

In this chapter, we demonstrate the use of FlexDym™ for development of a composite PC membrane-integrated microfluidic device. The device is of similar design to membrane-based cell culture platforms in literature, and can be fabricated in under 2.5 hours by means of hot-embossing and sTPE self-sealing. We assessed the device integrity by evaluating the bond between FlexDym™ and the PC membrane through automated delamination tests using a custom-designed delamination setup. The bonding strength measured above 500 mbar for bonding distances of 200 µm and greater, a pressure capacity largely sufficient for applications in microfluidic cell

culture. We confirmed that there was no degradation of bonding strength in cell culture-like conditions or due to long-term pressurization. In addition, we demonstrated that reliable FlexDym™ bonding could be achieved at room temperature for a bonding time as short as 5 minutes, and that FlexDym™ could form a strong bond to various microfluidic materials, including polystyrene, COP and PMMA. The facile bonding procedure demonstrate the versatility of FlexDym™ for the fabrication of composite devices with other materials beyond PC. HDFs could be cultured on the PC membrane over the course of one week, highlighting the potential use of the devices for membrane-based microfluidic cell culture, such as for OOC applications. We further demonstrate a simple recycling process that enables reuse of material from the composite devices multiple times, with the aim to reduce material waste at the prototyping stage. Overall, the work addressed the need for novel materials in microfluidic cell culture[76], by introducing a PDMS-free microfluidic platform, with a geometry commonly used for OOC devices and a fabrication methodology that represents a rapid, facile and transferable solution.


## Acknowledgements

We thank Constantin Edi Tanase at the University of Nottingham for his early-stage feedback on device handling for cell culture. The PANBioRA project has received funding from the European Union's Horizon 2020 research and innovation programme under the grant agreement number 760921.


# 4.5 References


1. Boyden, S. The chemotactic effect of mixtures of antibody and antigen on polymorphonuclear leucocytes. *J. Exp. Med.* **115**, 453–466 (1962).
2. Qi, S. *et al.* ZEB2 Mediates Multiple Pathways Regulating Cell Proliferation, Migration, Invasion, and Apoptosis in Glioma. *PLoS One* **7**, e38842 (2012).
3. Lin, H. *et al.* Air-Liquid Interface (ALI) Culture of Human Bronchial Epithelial Cell Monolayers as an in vitro Model for Airway Drug Transport Studies. *J. Pharm. Sci.* **96**, 341–350 (2007).
4. Harisi, R. *et al.* Differential inhibition of single and cluster type tumor cell migration. *Anticancer Res.* **29**, 2981–2985 (2009).
5. Sheridan, S. D., Gil, S., Wilgo, M. & Pitt, A. B. T.-M. in C. B. Microporous Membrane Growth Substrates for Embryonic Stem Cell Culture and Differentiation. in *Stem Cell Culture* **86**, 29–57 (Academic Press, 2008).
6. Chen, L.-J. *et al.* Microfluidic co-cultures of retinal pigment epithelial cells and vascular

endothelial cells to investigate choroidal angiogenesis. *Sci. Rep.* **7**, 3538 (2017).
7. Henry, O. Y. F. *et al.* Organs-on-chips with integrated electrodes for trans-epithelial electrical resistance (TEER) measurements of human epithelial barrier function. *Lab Chip* **17**, 2264–2271 (2017).
8. Song, J. W. *et al.* Microfluidic Endothelium for Studying the Intravascular Adhesion of Metastatic Breast Cancer Cells. *PLoS One* **4**, e5756 (2009).
9. Achyuta, A. K. H. *et al.* A modular approach to create a neurovascular unit-on-a-chip. *Lab Chip* **13**, 542–553 (2013).
10. Rennert, K. *et al.* A microfluidically perfused three dimensional human liver model. *Biomaterials* **71**, 119–131 (2015).
11. Huh, D. *et al.* Reconstituting organ-level lung functions on a chip. *Science* **328**, 1662–1668 (2010).
12. Jang, K.-J. *et al.* Human kidney proximal tubule-on-a-chip for drug transport and nephrotoxicity assessment. *Integr. Biol.* **5**, 1119–1129 (2013).
13. Kim, H. J. & Ingber, D. E. Gut-on-a-Chip microenvironment induces human intestinal cells to undergo villus differentiation. *Integr. Biol.* **5**, 1130–1140 (2013).
14. Bhatia, S. N. & Ingber, D. E. Microfluidic organs-on-chips. *Nat. Biotechnol.* **32**, 760–772 (2014).
15. Esch, E. W., Bahinski, A. & Huh, D. Organs-on-chips at the frontiers of drug discovery. *Nat. Rev. Drug Discov.* **14**, 248–260 (2015).
16. Moraes, C., Mehta, G., Lesher-Perez, S. C. & Takayama, S. Organs-on-a-Chip: A Focus on Compartmentalized Microdevices. *Ann. Biomed. Eng.* **40**, 1211–1227 (2012).
17. Ronaldson-Bouchard, K. & Vunjak-Novakovic, G. Organs-on-a-Chip: A Fast Track for Engineered Human Tissues in Drug Development. *Cell Stem Cell* **22**, 310–324 (2018).
18. Quirós-Solano, W. F. *et al.* Microfabricated tuneable and transferable porous PDMS membranes for Organs-on-Chips. *Sci. Rep.* **8**, 13524 (2018).
19. Xia, Y. & Whitesides, G. M. SOFT LITHOGRAPHY. *Annu. Rev. Mater. Sci.* **28**, 153–184 (1998).
20. Huh, D. *et al.* Microfabrication of human organs-on-chips. *Nat. Protoc.* **8**, 2135–2157 (2013).
21. Fan, X. *et al.* A microfluidic chip integrated with a high-density PDMS-based microfiltration membrane for rapid isolation and detection of circulating tumor cells. *Biosens. Bioelectron.* **71**, 380–386 (2015).
22. Capulli, A. K. *et al.* Approaching the in vitro clinical trial: engineering organs on chips. *Lab Chip* **14**, 3181–3186 (2014).
23. Chung, H. H., Mireles, M., Kwarta, B. J. & Gaborski, T. R. Use of porous membranes in tissue barrier and co-culture models. *Lab Chip* **18**, 1671–1689 (2018).
24. Apel, P. Track etching technique in membrane technology. *Radiat. Meas.* **34**, 559–566 (2001).
25. Becker, H. & Gärtner, C. Polymer microfabrication technologies for microfluidic systems. *Anal. Bioanal. Chem.* **390**, 89–111 (2008).
26. Young, E. W. K. *et al.* Rapid prototyping of arrayed microfluidic systems in polystyrene for cell-based assays. *Anal. Chem.* **83**, 1408–1417 (2011).
27. Ogończyk, D., Węgrzyn, J., Jankowski, P., Dąbrowski, B. & Garstecki, P. Bonding of microfluidic devices fabricated in polycarbonate. *Lab Chip* **10**, 1324–1327 (2010).
28. Tsao, C. W., Hromada, L., Liu, J., Kumar, P. & DeVoe, D. L. Low temperature bonding of PMMA and COC microfluidic substrates using UV/ozone surface treatment. *Lab Chip* **7**, 499–505 (2007).
29. Brown, L., Koerner, T., Horton, J. H. & Oleschuk, R. D. Fabrication and characterization of poly(methylmethacrylate) microfluidic devices bonded using surface modifications and solvents. *Lab Chip* **6**, 66–73 (2006).
30. Gencturk, E., Mutlu, S. & Ulgen, K. O. Advances in microfluidic devices made from thermoplastics used in cell biology and analyses. *Biomicrofluidics* **11**, 51502 (2017).
31. Sudarsan, A. P., Wang, J. & Ugaz, V. M. Thermoplastic Elastomer Gels: An Advanced Substrate for Microfluidic Chemical Analysis Systems. *Anal. Chem.* **77**, 5167–5173 (2005).
32. Roy, E., Geissler, M., Galas, J. C. & Veres, T. Prototyping of microfluidic systems using a commercial thermoplastic elastomer. *Microfluid. Nanofluidics* **11**, 235–244 (2011).

33. Guillemette, M. D., Roy, E., Auger, F. A. & Veres, T. Rapid isothermal substrate microfabrication of a biocompatible thermoplastic elastomer for cellular contact guidance. *Acta Biomater.* **7**, 2492–2498 (2011).
34. Lachaux, J. *et al.* Thermoplastic elastomer with advanced hydrophilization and bonding performances for rapid (30 s) and easy molding of microfluidic devices. *Lab Chip* **17**, 2581–2594 (2017).
35. Johnston, I. D., McCluskey, D. K., Tan, C. K. L. & Tracey, M. C. Mechanical characterization of bulk Sylgard 184 for microfluidics and microengineering. *J. Micromechanics Microengineering* **24**, 35017 (2014).
36. McDonald, J. C. & Whitesides, G. M. Poly(dimethylsiloxane) as a Material for Fabricating Microfluidic Devices. *Acc. Chem. Res.* **35**, 491–499 (2002).
37. Dewi, B. E., Takasaki, T. & Kurane, I. In vitro assessment of human endothelial cell permeability: effects of inflammatory cytokines and dengue virus infection. *J. Virol. Methods* **121**, 171–180 (2004).
38. Torisawa, Y. *et al.* Microfluidic hydrodynamic cellular patterning for systematic formation of co-culture spheroids. *Integr. Biol.* **1**, 649–654 (2009).
39. Stucki, A. O. *et al.* A lung-on-a-chip array with an integrated bio-inspired respiration mechanism. *Lab Chip* **15**, 1302–1310 (2015).
40. Mireles, M. & Gaborski, T. R. Fabrication techniques enabling ultrathin nanostructured membranes for separations. *Electrophoresis* **38**, 2374–2388 (2017).
41. Ma, S. H., Lepak, L. A., Hussain, R. J., Shain, W. & Shuler, M. L. An endothelial and astrocyte co-culture model of the blood–brain barrier utilizing an ultra-thin, nanofabricated silicon nitride membrane. *Lab Chip* **5**, 74–85 (2005).
42. Temiz, Y., Lovchik, R. D., Kaigala, G. V & Delamarche, E. Lab-on-a-chip devices: How to close and plug the lab? *Microelectron. Eng.* **132**, 156–175 (2015).
43. Chueh, B. *et al.* Leakage-free bonding of porous membranes into layered microfluidic array systems. *Anal. Chem.* **79**, 3504–3508 (2007).
44. Gong, X. *et al.* Wax-bonding 3D microfluidic chips. *Lab Chip* **10**, 2622–2627 (2010).
45. Shiroma, L. S. *et al.* Self-regenerating and hybrid irreversible/reversible PDMS microfluidic devices. *Sci. Rep.* **6**, 26032 (2016).
46. Xie, S. *et al.* Large-Area and High-Throughput PDMS Microfluidic Chip Fabrication Assisted by Vacuum Airbag Laminator. *Micromachines* **8**, (2017).
47. Serra, M. *et al.* A simple and low-cost chip bonding solution for high pressure, high temperature and biological applications. *Lab Chip* **17**, 629–634 (2017).
48. Kim, S., Kim, J., Joung, Y.-H., Choi, J. & Koo, C. Bonding Strength of a Glass Microfluidic Device Fabricated by Femtosecond Laser Micromachining and Direct Welding. *Micromachines* **9**, (2018).
49. Abidin, U., Daud, N. A. S. M. & Le Brun, V. Replication and leakage test of polydimethylsiloxane (PDMS) microfluidics channel. *AIP Conf. Proc.* **2062**, 20064 (2019).
50. Bhattacharya, S., Datta, A., Berg, J. M. & Gangopadhyay, S. Studies on surface wettability of poly(dimethyl) siloxane (PDMS) and glass under oxygen-plasma treatment and correlation with bond strength. *J. Microelectromechanical Syst.* **14**, 590–597 (2005).
51. Eddings, M. A., Johnson, M. A. & Gale, B. K. Determining the optimal PDMS–PDMS bonding technique for microfluidic devices. *J. Micromechanics Microengineering* **18**, 67001 (2008).
52. Mosadegh, B., Bersano-Begey, T., Park, J. Y., Burns, M. A. & Takayama, S. Next-generation integrated microfluidic circuits. *Lab Chip* **11**, 2813–2818 (2011).
53. Kim, S.-J., Lai, D., Park, J. Y., Yokokawa, R. & Takayama, S. Microfluidic Automation Using Elastomeric Valves and Droplets: Reducing Reliance on External Controllers. *Small* **8**, 2925–2934 (2012).
54. Roy, E. Overview of Materials for Microfluidic Applications. in (ed. Pallandre, A.) Ch. 15 (IntechOpen, 2016).
55. El-Ali, J., Sorger, P. K. & Jensen, K. F. Cells on chips. *Nature* **442**, 403–411 (2006).
56. Aran, K., Sasso, L. A., Kamdar, N. & Zahn, J. D. Irreversible, direct bonding of nanoporous

polymer membranes to PDMS or glass microdevices. *Lab Chip* **10**, 548–552 (2010).
57. McDonald, J. C. *et al.* Fabrication of microfluidic systems in poly(dimethylsiloxane). *Electrophoresis* **21**, 27–40 (2000).
58. Salmon, H., Rasouli, M. R., Distasio, N. & Tabrizian, M. Facile engineering and interfacing of styrenic block copolymers devices for low-cost, multipurpose microfluidic applications. *Eng. Reports* **n/a**, e12361 (2021).
59. Drobny, J. G. 5 - Styrenic Block Copolymers. in *Plastics Design Library* (ed. Drobny, J. G. B. T.-H. of T. E.) 161–177 (William Andrew Publishing, 2007).
60. Freund, J. B., Goetz, J. G., Hill, K. L. & Vermot, J. Fluid flows and forces in development: functions, features and biophysical principles. *Development* **139**, 1229–1245 (2012).
61. Rashidi, H., Alhaque, S., Szkolnicka, D., Flint, O. & Hay, D. C. Fluid shear stress modulation of hepatocyte-like cell function. *Arch. Toxicol.* **90**, 1757–1761 (2016).
62. Reneman, R. S., Arts, T. & Hoeks, A. P. G. Wall Shear Stress – an Important Determinant of Endothelial Cell Function and Structure – in the Arterial System in vivo. *J. Vasc. Res.* **43**, 251–269 (2006).
63. Huh, D. *et al.* Acoustically detectable cellular-level lung injury induced by fluid mechanical stresses in microfluidic airway systems. *Proc. Natl. Acad. Sci.* **104**, 18886–18891 (2007).
64. Kim, H. J., Huh, D., Hamilton, G. & Ingber, D. E. Human gut-on-a-chip inhabited by microbial flora that experiences intestinal peristalsis-like motions and flow. *Lab Chip* **12**, 2165–2174 (2012).
65. Kim, L., Vahey, M. D., Lee, H.-Y. & Voldman, J. Microfluidic arrays for logarithmically perfused embryonic stem cell culture. *Lab Chip* **6**, 394–406 (2006).
66. Kim, L., Toh, Y.-C., Voldman, J. & Yu, H. A practical guide to microfluidic perfusion culture of adherent mammalian cells. *Lab Chip* **7**, 681–694 (2007).
67. Wan, A. M. D., Devadas, D. & Young, E. W. K. Recycled polymethylmethacrylate (PMMA) microfluidic devices. *Sensors Actuators, B Chem.* **253**, 738–744 (2017).
68. Liao, S., He, Y., Chu, Y., Liao, H. & Wang, Y. Solvent-resistant and fully recyclable perfluoropolyether-based elastomer for microfluidic chip fabrication. *J. Mater. Chem. A* **7**, 16249–16286 (2019).
69. Sun, H. *et al.* Reliable and reusable whole polypropylene plastic microfluidic devices for a rapid, low-cost antimicrobial susceptibility test. *Lab Chip* **19**, 2915–2924 (2019).
70. Bistulfi, G. Reduce, reuse and recycle lab waste. *Nature* **502**, 170 (2013).
71. Urbina, M. A., Watts, A. J. R. & Reardon, E. E. Labs should cut plastic waste too. *Nature* **528**, 479 (2015).
72. Biron, M. Chapter 4 - Detailed accounts of thermoplastic resins. in (ed. Biron, M. B. T.-T. and T. C.) 217–714 (Elsevier, 2007).
73. Richmond, J. Y. & McKinney, R. W. *Biosafety in microbiological and biomedical laboratories*. (US Government Printing Office, 2009).
74. von Keudell, A. *et al.* Inactivation of Bacteria and Biomolecules by Low-Pressure Plasma Discharges. *Plasma Process. Polym.* **7**, 327–352 (2010).
75. Sakudo, A., Yagyu, Y. & Onodera, T. Disinfection and Sterilization Using Plasma Technology: Fundamentals and Future Perspectives for Biological Applications. *Int. J. Mol. Sci.* **20**, 5216 (2019).
76. Cochrane, A. *et al.* Advanced in vitro models of vascular biology: Human induced pluripotent stem cells and organ-on-chip technology. *Adv. Drug Deliv. Rev.* **140**, 68–77 (2019).

# Chapter 5.
# Conclusions and Outlook

This thesis has presented an evaluation of novel materials and development of new fabrication techniques for prototyping of microfluidic devices. It aimed to assess the utility of sTPE devices for cell biology research through proof-of-concept demonstrations, and, for addressing drawbacks associated with current microfluidic prototyping materials.

In the first chapter, we briefly outlined essential concepts of microfluidics and reviewed materials for microfluidic device fabrication. Current state-of-the-art cell-based microfluidic devices, OOC systems, were introduced. Recent progress, and associated bottlenecks in OOC engineering were discussed to highlight the potential that new fabrication materials can offer toward improved and more transferable microfluidic systems.

Chapter 2 presented the material and microfluidic characterization of two novel sTPE formulations, aimed to fill existing knowledge gaps needed to better understand the potential of sTPE material for microfluidic cell culture uses. Strategies for sTPE microfluidic cell culture, including device fabrication, cell seeding and chip interfacing with microfluidic setup, were developed to promote the adoption of sTPE materials for cell culture studies. The principal subject of characterization was evaluation of cell attachment and cell growth in sTPE microchannels. sTPE materials were demonstrated to disburden the end-user with ECM coating steps and wet-storage after plasma treatment, as are associated with PDMS devices for cell culture use. In addition, reduced absorption of small molecules and excellent biocompatibility make sTPE materials attractive alternatives to PDMS for cell-based microfluidic studies.

Building on the processes developed in chapter 2, chapter 3 and 4 presented proof-of-concept demonstrations of sTPE-based microfluidic cell culture. In chapter 3, we presented a sTPE-based microfluidic system for investigating cardiomyoblast physiology and validated the system against PDMS systems and macro-culture systems. Compared to the PDMS system, sTPE systems demonstrated a more streamlined protocol for cell seeding, reduced media evaporation from the culture chamber and improved compatibility with lipid cellular staining. A microfluidic circuit was developed that enabled fully automated microfluidic assays, as a first step toward high-throughput investigations of heart physiology. In chapter 4, we developed a three-layered composite microfluidic system for membrane-based cell culture, such as barrier OOC studies. Compared to equivalent systems in PDMS, the sTPE system improved on fabrication throughput and transferability across fabrication scales, which could be an important step towards bridging the gap between research laboratories and industry.

Altogether, sTPE materials showed a multitude of properties that makes them attractive alternative materials to PDMS for OOC fabrication. The current use of PDMS in OOC prototyping are among the roadblocks toward full implementation of the technology in the pharmaceutical industry and biology laboratories.

While the pharmaceutical industry often is considered the most important end-user of OOC technology, the OOC community today largely exists within academia and small research laboratories. Therefore, new prototyping materials that can be used in research settings, with potential of direct technology transfer to industrial production, could be valuable for the progression of the field both on a research level and for accelerating technology transfers to industry. A transition from PDMS to sTPE material could represent a feasible next step toward more transferable systems, by keeping fundamental OOC device functionalities based on elastomeric properties (such as stretchable membranes to mimic elastic tissues) while avoiding key PDMS-related hurdles such as poor fabrication throughput, small molecule absorption and fast hydrophobic recovery. To this end, this thesis work could serve as a practical guide for implementation of sTPE materials for cell-based microfluidic studies.

However, further proof-of-concept studies are required to verify the usefulness of sTPE-based OOC systems. Building on the membrane-integrated sTPE device developed in this work, a critical next step would be to demonstrate culture of tissue-specific cell types, e.g., of endothelial-epithelial body barriers, followed by OOC demonstrations such as endothelial cell alignment and functional barrier formation, quantitatively validated by permeability assays, TEER measurements and optical imaging. Benchmarking of results against PDMS models would also be critical to further understand the potential of sTPE materials for OOC fabrication.

Fabrication of thin, porous sTPE membranes would be another valuable development for OOC fabrication that has not yet been attempted. While the flexibility of the PC-FlexDym™ device is limited by the inherent stiffness of PC, an OOC system fabricated completely in sTPE could enable stretching for modelling of mechanically active tissue barriers, such as found for instance in the lung and intestines. The recently developed spin-coat formulation of FlexDym™, FlexDym™SC could be a good candidate for membrane fabrication using similar techniques as used for PDMS membranes.

Given that such demonstrations would be successful, the future role of sTPE materials in OOC engineering would depend on stakeholders in the field to adopt novel materials. Entering the second decade of OOC technology, we are in a stage of exciting developments both on the engineering and biology side, and considerations such as

fabrication scalability, standardization and industry transfer are becoming increasingly important considerations as field matures. Beyond OOC applications, we believe the sTPE materials may present a broad range of bio-applications including, implants, wearables and components in medical devices, such as gaskets and seals.

# Appendix 1

# Application note: How to grow cells in a FlexDym™ microfluidic channel

Application Note

## How to grow cells in a FlexDym™ microfluidic channel

In this application note we describe how to grow adherent cell inside a FlexDym™ microfluidic channel. Chip preparation, cell seeding, medium exchange and on-chip cell imaging will be described.

The microfluidic chip can be interfaced with an OB1 pressure controller to perfuse cells for dynamic cell culture. A variety of flow profiles can be created, including constant flow or intermittent, steady rate or pulsatile, or create a customised profile, e.g. to mimic the cardiac rhythm.


### 1. Chip preparation

Use the Eden Tech connector kit, containing 10 luer lock connectors and 50 double-sided O-ring adhesive stickers, to interface your FlexDym™ microfluidic chip. Follow the step-by-step instructions to position the luer connectors over the fluid access holes of your microfluidic FlexDym™ chip.

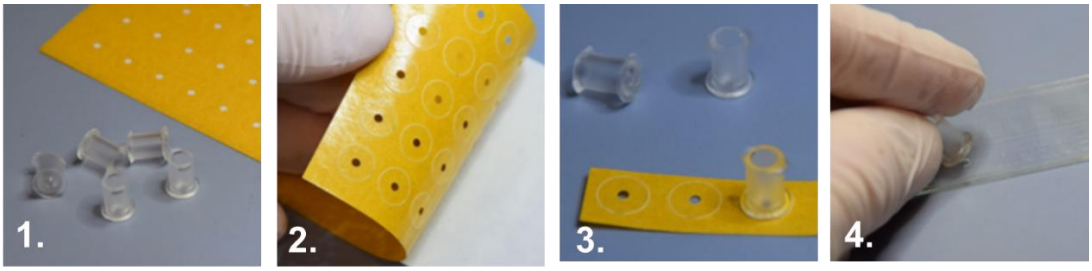

The FlexDym™ is moderately hydrophobic. To promote cell adhesion without the need for chemical or biological coatings and to facilitate filling of the channel we recommend oxygen/air plasma treatment or corona discharge treatment. We recommend 100 W $O_2$ plasma treatment for 5-10 minutes. After hydrophilization, the chip can be stored dry, for instance in a sterile petri dish, for up to 4 days before use.

## 2. Cell seeding

Prepare the cell suspension to desired concertation (e.g. $10^6$ cells/mL). Add 5 µL of cell suspension to the channel with a micropipette. Place the pipette tip close to the bottom before releasing the cell suspension, as show in the figure.

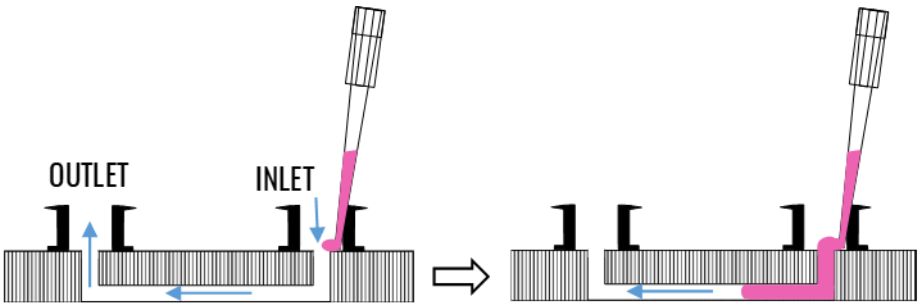


To ensure an even distribution of cell across the channel, it is important to add a volume corresponding to the internal volume of the channel. A too large seeding volume can result in uneven cell distribution and accumulation of cells in the inlet/outlet ports.

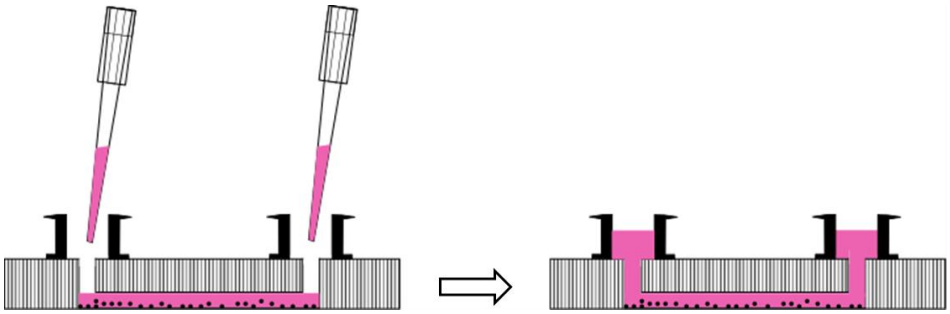

Let the cells settle for 1-2 hours in an incubator before filling up the reservoirs with 50 µL (in each reservoir) of cell-free medium. If medium is added to the reservoirs directly after cell seeding before cells have adhered, cells will be flushed out of the channel. If leaving the cells for too long before filling the reservoirs, the channel may risk drying out due to the very small channel volume.

## 3. Medium exchange

After seeding cells in a microfluidic channel, we recommend to always keep the channel wet. Removing fluid from the channel may lead to the formation and trapping of air bubbles inside the channel. Follow the steps in the figure to refresh medium in the channel. We recommend adding a volume at least three times larger than the channel volume.

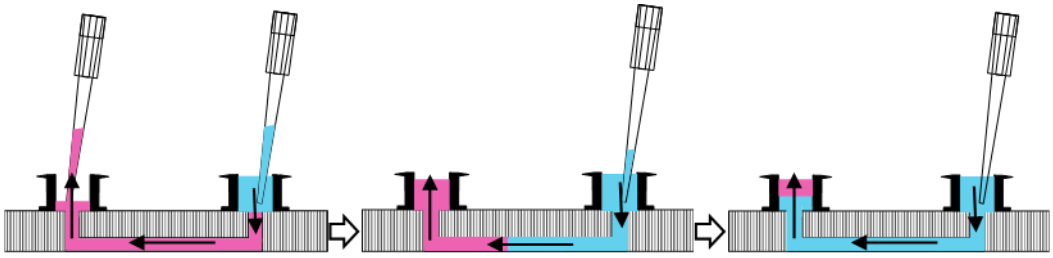

**Continuous medium exchange.**
Old medium is removed from the outlet reservoir and fresh medium is added to the inlet reservoir.

## 4. On-chip cell imaging

FlexDym™ chips are compatible with brightfield, phase-contrast and fluorescent microscopy. The FlexDym™ chip can be place directly on a microscope stage for in situ imaging.

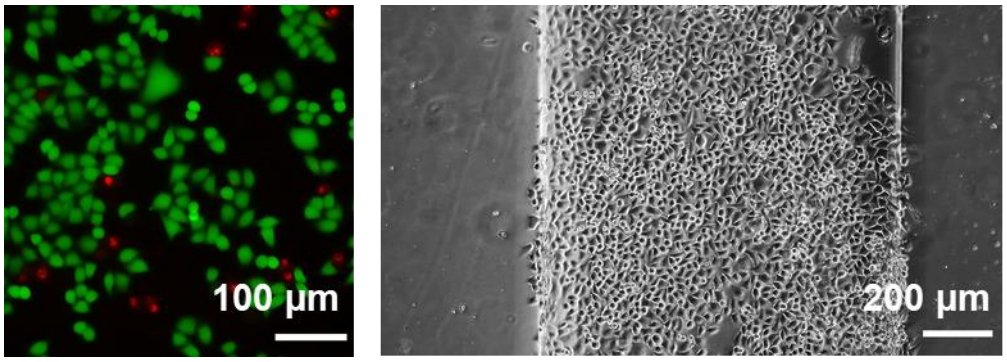


**Live imaging of HeLa cells in FlexDym™ devices.** (left) Fluorescent image showing on-chip LIVE/DEAD assay (green: calcein AM, red: propidium iodide). (right) Phase-contrast image of HeLa cells in a FlexDym™ channel.

## 5. Dynamic cell culture

FlexDym™ chips can be connected to a microfluidic flow control system. Read our application notes on Dynamic cell culture and Microfluidic cell staining for more details on how to culture cells under flow.

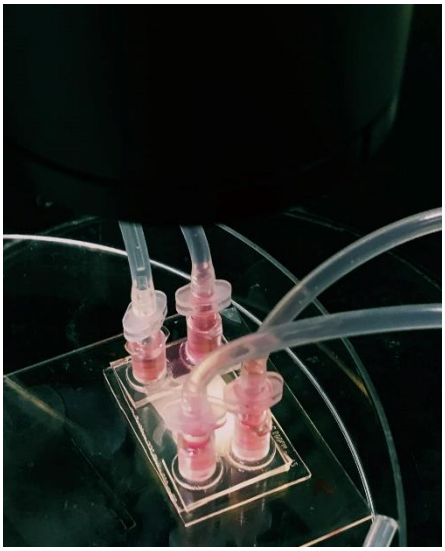

FlexDym chip connected with microfluidic tubing to OB1 flow controller for constant perfusion of medium.

ELVE FLOW an ELVESYS brand

Application Note

# DYNAMIC CELL CULTURE

https://www.elveflow.com/microfluidic-applications/microfluidic-cell-culture/medium-recirculation-for-dynamic-cell-culture/

# Appendix 2

## Application note: Dynamic cell culture and cell staining

## Introduction

In this application note we describe how to stain cells in a microfluidic chip. Stain with the OB1 pressure controller to maintain a precise flow rate of wash buffer and stains over your cells in the perfusion chamber. Automate the sequence to free up your time for multi-stain assays and replicate experiments. Suitable for temperature sensitive stains and small volumes. Read also our application notes about automated cell seeding and microfluidic perfusion for dynamic cell culture.

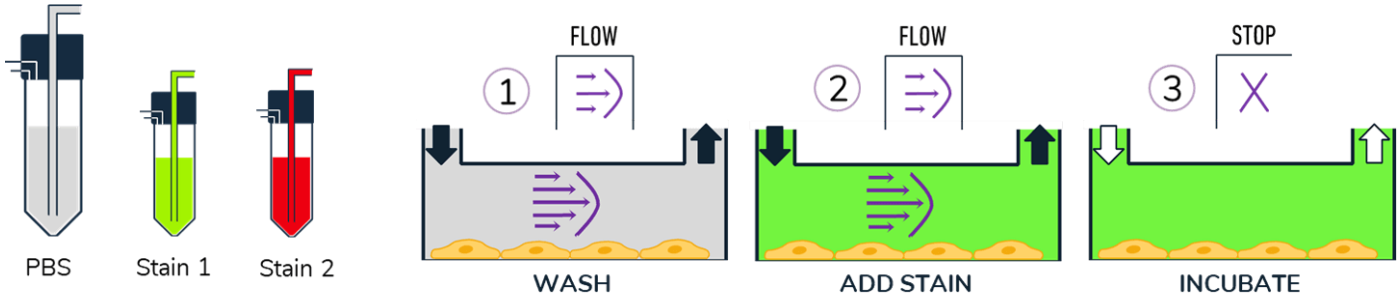

# Applications

- Live cell imaging (e.g. calcium imaging, FISH)
- Drug screening
- Shear stress
- Cell rolling adhesion assay
  - Immune response
  - Cancer invasion and metastasis
- Models of physiology and disease
  - Organs-on-chip
  - Blood vessel formation and occlusion (atherosclerosis)
  - Bone homeostasis and disease (osteoporosis)

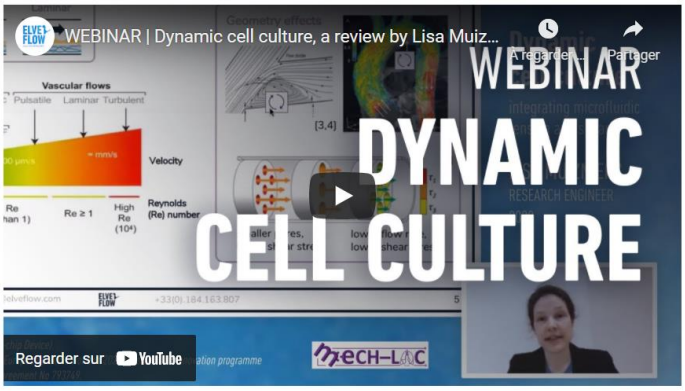


**Watch [the webinar] by our biofluidics application specialist Dr. Lisa Muiznieks about dynamic cell culture!**

https://www.youtube.com/watch?v=O4Hgpw4kN4I&t=5s

# MICROFLUIDIC CELL STAINING

https://www.elveflow.com/microfluidic-applications/microfluidic-cell-culture/how-to-stain-cells-cultured-in-a-microfluidic-chip/

## Setup

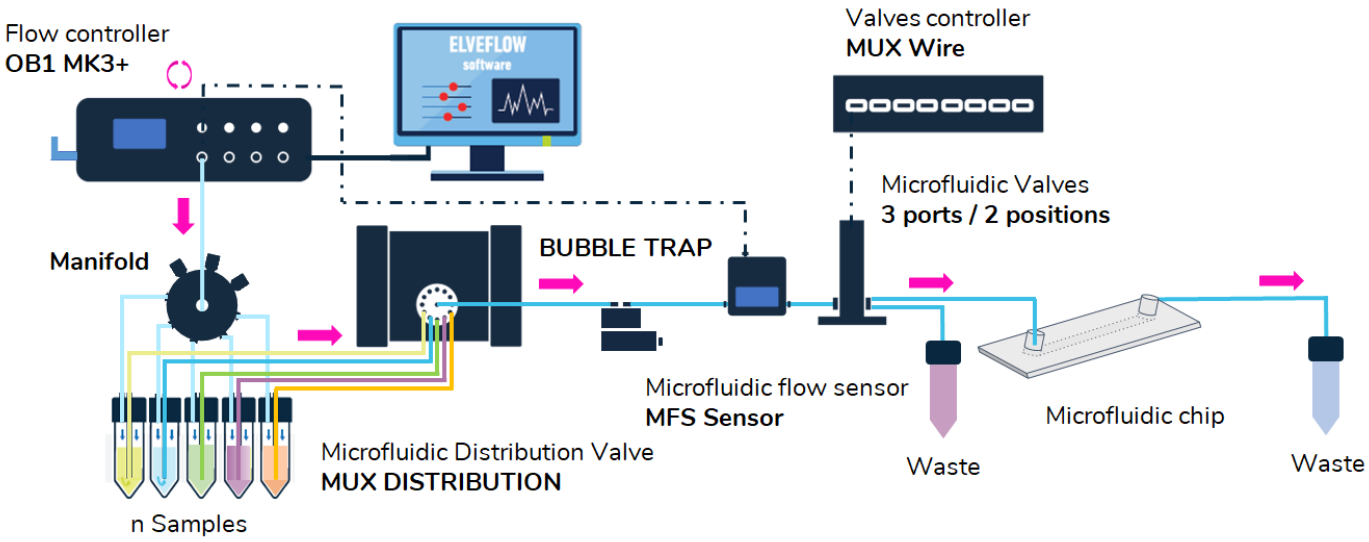


## Materials

### Hardware

1. OB1 flow controller with at least 1 channel 0/2000 mbar
2. 1 x flow sensor MFS3 2.4-80 µL/min
3. 1 x MUX Distribution 10 ports
4. 1 x bubble trap
5. 1 x MUX wire
6. 1 x 3-way valve
7. Kit starter pack Luer Lock + ¼”28 fittings packs
8. n x 15 mL Falcon reservoirs _ S tanks (option 1.5 mL Eppendorf tube _ XS tank)
9. Manifold small or large
10. Microfluidic perfusion chamber chip (IBIDI µSlide I luer)
11. Heated water bath
12. $CO_2$ incubator for incubation
13. Microscope for observation

### Chemicals

1. HeLa cells ($1x10^6$ cells per mL)
2. DMEM high glucose medium, 10% FBS, Penicillin / Streptomycin (100 U/mL; 100 µg/mL)
3. Phosphate Buffered Saline (PBS buffer)
4. Cell stain/s

# Design of the chip

**µ-Slide I Luer**: ibiTreat: #1.5 polymer coverslip, tissue culture treated, sterilized

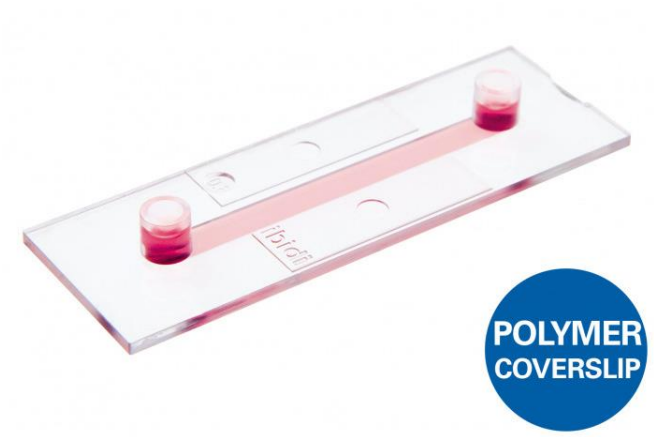


| | |
|---|---|
| Outer dimensions (w x l) | 25.5 x 75.5 mm² |
| Channel length | 50 mm |
| Channel width | 5 mm |
| Adapters | Female Luer |
| Volume per reservoir | 60 µl |
| Growth area | 2.5 cm² |
| Coating area | 5.2 / 5.4 / 5.6 / 5.8 cm² |
| Bottom: ibidi Polymer Coverslip | |

If the microfluidic chip used is non treated, and/or not sterile, here are two steps to prepare the culture chamber:

1. Wash the microfluidic chip with aniosyme (1%, 30 min), rinse thoroughly with water and sterilize using an autoclave or a plasma gun (depending on the chip material).

2. Treat the culture surface with cell adhesion coating (e.g. collagen I or fibronectin).

# Quick Start Guide

### INSTRUMENT CONNECTION

1. Connect your OB1 pressure controller to an external pressure supply using pneumatic tubing, and to a computer using a USB cable. For detailed instructions on OB1 pressure controller setup, please read the "OB1 User Guide".

2. Connect the flow sensor to the OB1 and the 3-way valve to the MUX wire.

3. Connect the MUX Distribution and MUX Wire to your computer.

4. Turn on the OB1 by pressing the power switch.

5. Launch the Elveflow software. The Elveflow Smart Interface's main features and options are covered in the "ESI User Guide". Please refer to those guides for a detailed description.

6. Press Add instrument \ choose OB1 \ set as MK3+, set pressure channels if needed, give a name to the instrument and press OK to save changes. Your OB1 should now be in the list of recognized devices.

7. OB1 calibration is required for the first use. Please refer to the "OB1 User Guide".

8. Add flow sensor: press Add sensor \ select flow sensor \ analog or digital (choose the working range of flow rate for the sensor if you have an analog one), give a name to the sensor, select to which device and channel the sensor is connected and press OK to save the changes. Your flow sensor should be in the list of recognized devices. For details refer to "MFS user guide".

9. Add MUX Distribution: press Add instrument \ choose MUX Distrib/Inj/Rec \ select your instrument, give it a name \ select the MUX version (MUX Distribution 10 here) and press OK to save changes. Your MUX should be in the list of recognized devices.

10. Add MUX wire: press Add instrument \ choose MUX Wire \ select your instrument, give it a name and press OK to save changes. Your MUX should be in the list of recognized devices.

11. Open the OB1, the MUX Distribution and the MUX wire windows.

## PREPARATION OF THE SOLUTIONS

**Tips from the expert.** The idea is to keep everything as STERILE as possible. Every step in this section should be done in the biological safety cabinet (BSC). Wipe down the tanks with aniosyme, then water and air dry in the BSC. An additional step can be added by flushing aniosyme through the tubings that will be used for the experiment.

1. Prepare the warmed medium reservoir and connect the supplied 1/16” OD tubing and the coil tubing 6mm OD to the tank. For more details, refer to the video “Connector for the OB1”. Once connected, place the medium into a heated water bath.

2. Repeat step 2 for all the aqueous solutions you will be using, namely PBS buffer and stain(s).

3. Connect all the coil tubings 6mm OD from the solution tanks to the outer ports of the manifold using 1/4’’-28 thread to 3/32’’ OD barb fittings (black fittings). To the central port of the manifold, connect a coil tubing 6mm OD. Connect the other end of this tubing to the OB1 pressure controller outlet.

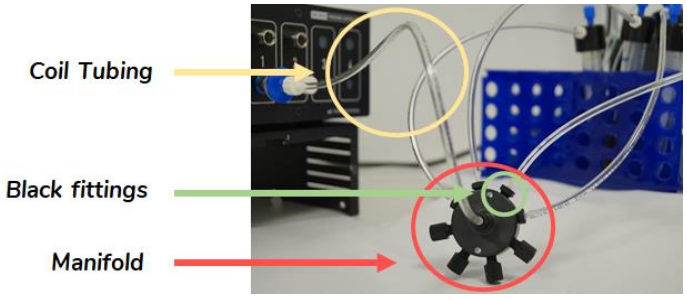


Tips from the expert. If you are not using some ports of the manifold, close them using microfluidic plugs PFA 1/4’’-28 flat-bottom fittings.

## TUBING LENGTH AND VOLUME WORKSHEET

Depending on the installation used with the $CO_2$ incubator and the heated water bath, length of tubing can vary from laboratory to laboratory. Following is a worksheet to record tubing lengths, calculate the total volume of tubing from

the reservoir to the microfluidic chip, and the time it will take to fill the microfluidic chip at the desired flow rate. This worksheet will also provide a guide to the total volume of each reagent needed for an experiment.

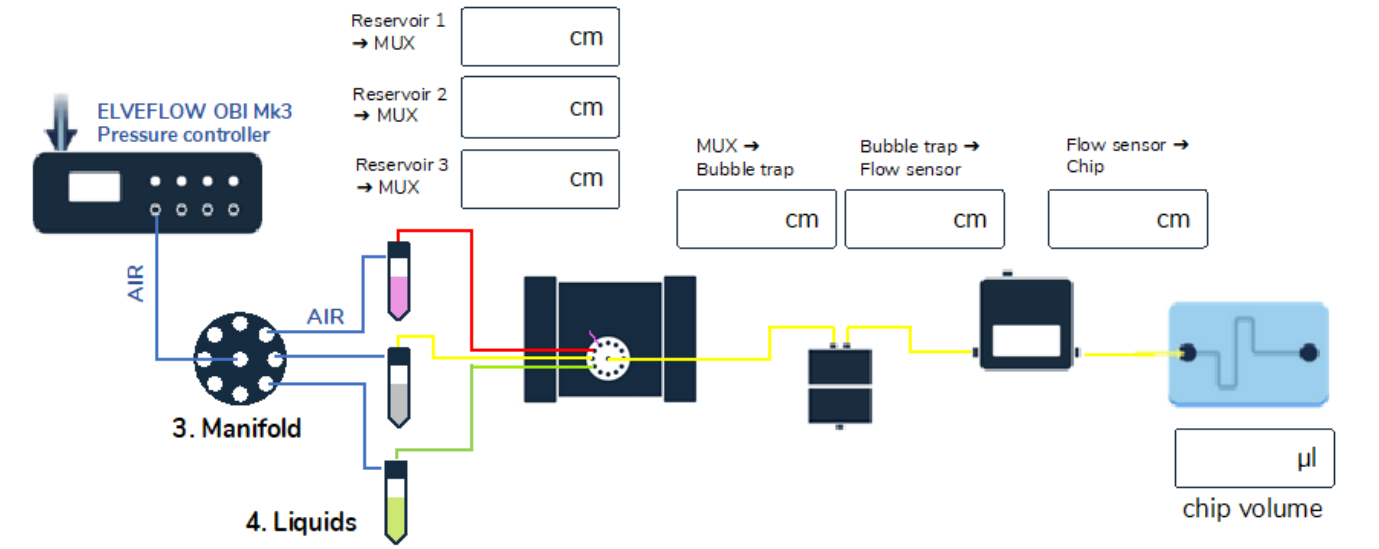


| Tubing volume | Total volume | Flow rate and time worksheet |
|---|---|---|
| Total (liquid) length (cm): | Tubing: | Desired flow rate (µl/ min): |
| Total length (cm → mm): | Chip: | = Flow rate (ml/ h): |
| Tubing radius (mm): | Modules*: | = Flow rate (ml/ 24 h): |
| Volume (☐. r². h) ($mm^3$): [1 $mm^3$ = 1 µl] | TOTAL: | Time required reach end of chip: |

* Module internal volume is likely very small compared to the volume of tubing and the chip, but can be considered for higher precision.

Tips from the expert. If light-sensitive reagents are used, aluminium foil can be wrapped around transparent tubing to minimize light-exposure during the experiment.

Tips from the expert. A low total volume of tubing is desirable to save time and minimize consumption and dilution of reagent, most critically for the distance between the valve and the microfluidic chip. Use a tubing with a small inner diameter such as PTFE tubing OD 1/32 between the valve and the microfluidic chip.

1. Connect the reservoirs containing the solutions to the MUX Distribution inlets by using the supplied 1/16" OD tubing and the 1/4"-28 fittings and add a dead-end block to one of the inlets of the MUX Distribution. For more details, please refer to "User Guide MUX Distribution 12/1".

Tips from the expert. Connect the solutions in the order of injection to optimize the rotation of the valve.

2. Rename the reservoirs in the MUX Distribution window of the ESI.

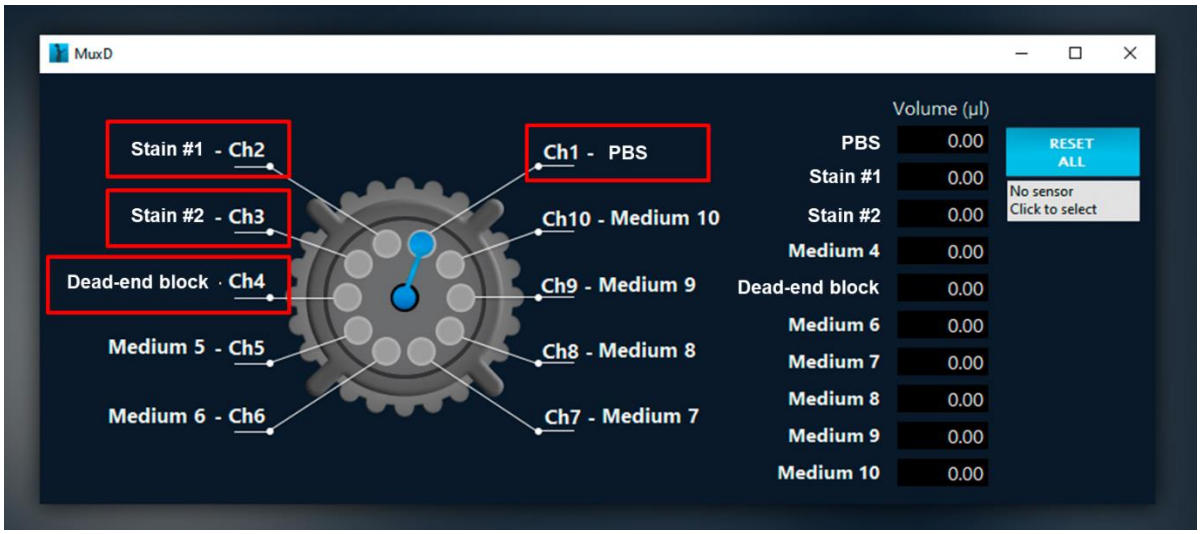


3. At the outlet of the MUX Distribution, connect one end of the supplied 1/16” OD tubing using the 1/4”-28 fitting to a waste reservoir.

4. On the MUX Distribution window, select port #1 (PBS) and set a pressure to fill the tubing with the liquid. Once liquid gets out to the waste, air is completely removed from the system for the medium line.

5. Repeat step 4 for all the different solutions connected to the MUX Distribution by selecting the corresponding port on the MUX Distribution window.

6. Once all the air is removed from the different solution tubing from the MUX Distribution, Connect the tubing from the outlet of the MUX Distribution to the bubble trap. From the outlet of the bubble trap, connect the supplied 1/16” OD tubing using the 1/4”-28 fitting to the inlet of the flow sensor and a tubing from the outlet of the flow sensor to the inlet of the 3-way valve.

Tips from the expert. To finetune the system and to obtain the best performance in terms of flow rate control, a resistance tubing can be added to the system. For more details, please refer to "Flow control tuning".

7. Connect 1/32" OD tubing using the ¼"-28 fitting and a tubing sleeve from the NO (normally open) port to a waste container (this is in order to fill the tubing and remove air before connecting the microfluidic chip containing cells). At the NC (normally closed) port of the valve, connect the supplied 1/16" OD tubing to a waste container.


MUX-wire configuration for flow to chip. 3/2 valve "N.O." (open)


MUX-wire configuration for flow to waste. 3/2 valve "N.C." (closed)


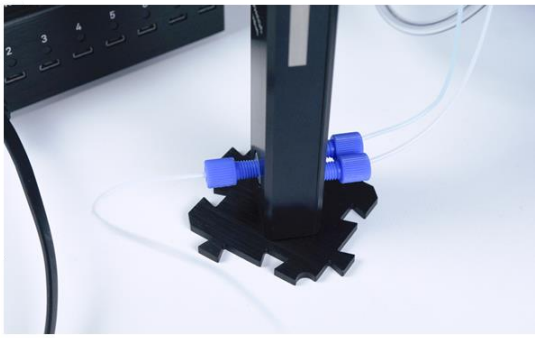

8. On the MUX Wire window, select the configuration NO for the 3-way valve. On the MUX Distribution window, select port #1 (PBS) and set a pressure to fill all the tubing with the liquid. Once liquid gets out to the waste, air is completely removed from the system for the medium line and you can set pressure to zero.

9. You can now carefully connect the microfluidic chip containing cells to the filled tubing coming from the NO port of the valve.

**Tips from the expert.** It is critical to not introduce any air bubbles in the microfluidic chip, especially if the chip contains small channel features as air bubbles tend it get trapped in the chip.

## ON-CHIP CELL STAINING

1. Select port #1 (PBS buffer) on the MUX distributor and switch the valve to NO configuration (to chip) on the MUX wire. Set a low pressure (or flow rate) to flow the buffer inside the microfluidic chip to wash the cells (e.g., one chip volume).

---

2. Select port #2 (stain #1) on the MUX distributor and switch the valve to NC configuration (to waste) on the MUX wire. Set a high pressure (or flow rate) to push the staining solution up until the valve. Set a low pressure (or flow rate) and switch the valve to NO configuration (to chip) on the MUX wire. Fill the microfluidic chip with staining solution.

**Tips from the expert.** It is not necessary to fill the entire system with a precious staining solution. After a short injection, PBS (or buffer of choice) can be used to push the staining solution from the MUX distributor to the chip.

It is important to calculate or measure the filling time of the system in order to optimize the timing steps in order to minimizing waste of reagents.

---

3. Once the microfluidic chip filled, stop the flow by switching to port #4 (dead-end channel) on the MUX Distribution window and set a zero pressure (or flow rate) on the OB1 window.

**Tips from the expert.** Switching to a dead-end channel rather than turning off the pressure prevents back flow, in order to ensure that the staining solution remains inside the microfluidic chip.

---

4. Incubate for the required amount of time.

---

5. Repeat step 1, 2, 3 and 4 for all the different stains needed for the experiment.

6. Select port #1 (PBS buffer) and set a pressure (or flow rate) to flow the buffer inside the microfluidic chip to wash the cells.

7. Select port #4 (dead-end channel) on the MUX Distribution window and set a zero pressure (or flow rate) on the OB1 window.

8. The cells inside the microfluidic chip are ready to be imaged under the microscope.

### GENERAL CLEANING OF SETUP

1. Flush lines and modules with water, then aniosyme (1%). Rinse thoroughly with water. Do a final flush with ethanol and air dry (flush air from an empty reservoir).

2. Change fluidic tubing between experiments and use sterile reservoirs for new experiments. Periodically replace the Bubble Trap membrane.

### AUTOMATED CELL STAINING

*The following steps can be implemented to automatise the flow control and liquid switching of the cell staining.*

1. To create a sequence, click on the top middle button “Create Sequence” on the main window of the ESI software: a new window will appear.

2. Back to the OB1 window: set up the desired flow rate or pressure for your experiment and save the configuration by clicking on “Config”. Repeat for all flow rates or pressure values that will be used throughout the experiment. Remember to save a “0” pressure or flow rate configuration. For more details, refer to the “ESI User Guide”.

3. Similarly, in the MUX wire window: save configurations for each valve position, NC (normally closed) and NO (normally open) by clicking on “Config”.

Tips from the expert. Automated cell seeding and staining should be performed using microfluidics valves to avoid loss of reagents and clogging of the system.

4. Back on the sequence window: on the left side of the window, click on the green “OB1” box (a line “OB1: Select instrument” appears in the middle part), on the right side, select the instrument (your OB1 pressure controller should appear when clicking on “Instrument”) and “load a configuration” saved previously.

5. On the left side of the sequence window, click on the purple “DIST” box (a new line “DIST: Select Instrument” appears): select your instrument and write in the box “Valve position” the desired port’s number corresponding to the needed solution.

Tips from the expert. You can also choose the type of rotation of the MUX Distribution for your convenience (shortest, clockwise or counterclockwise).

6. On the left side of the sequence window, click on the purple “MUX” box (a new line “MUX: Select Instrument” appears): select your instrument and load your valve configuration corresponding to the needed solution (normally closed or normally open).

7. On the left side of the sequence window, click on the “Clock” box (a new line with a time frame appears): set a desired duration.

8. Create your fluid injection sequence based on the procedures outlined in step 4-7.

   Option: on the left side of the sequence window, click on the “GO” box. This step will allow you to repeat your sequence: choose the “target step” (2 if you want to repeat the all sequence without changing the OB1 configuration) and “time” for how many times you want this to repeat.

**9.** On the left side of the sequence window, click on the blue “END” box (a new line “END” appears). This means that your sequence is over.

***10.*** Following is an example of sequences for the cell staining with two stains:

a) Rinse cells with PBS.

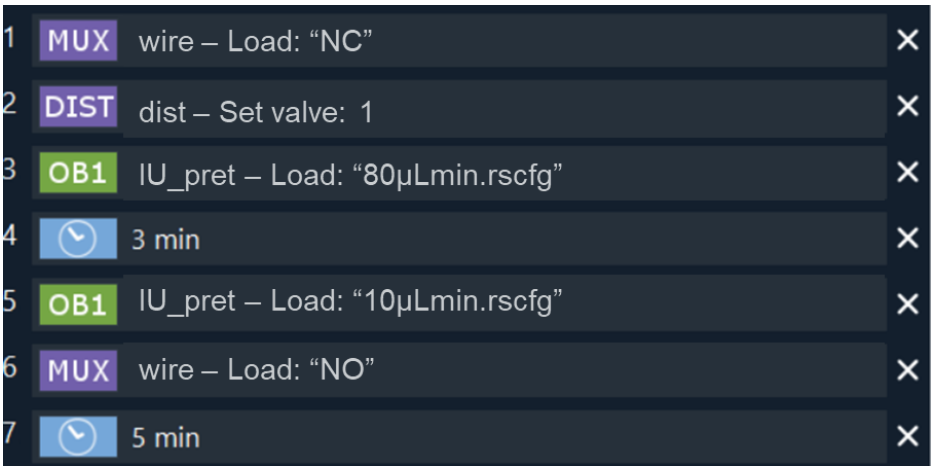


b) Fill chip with stain #1 and incubate for 30 min.

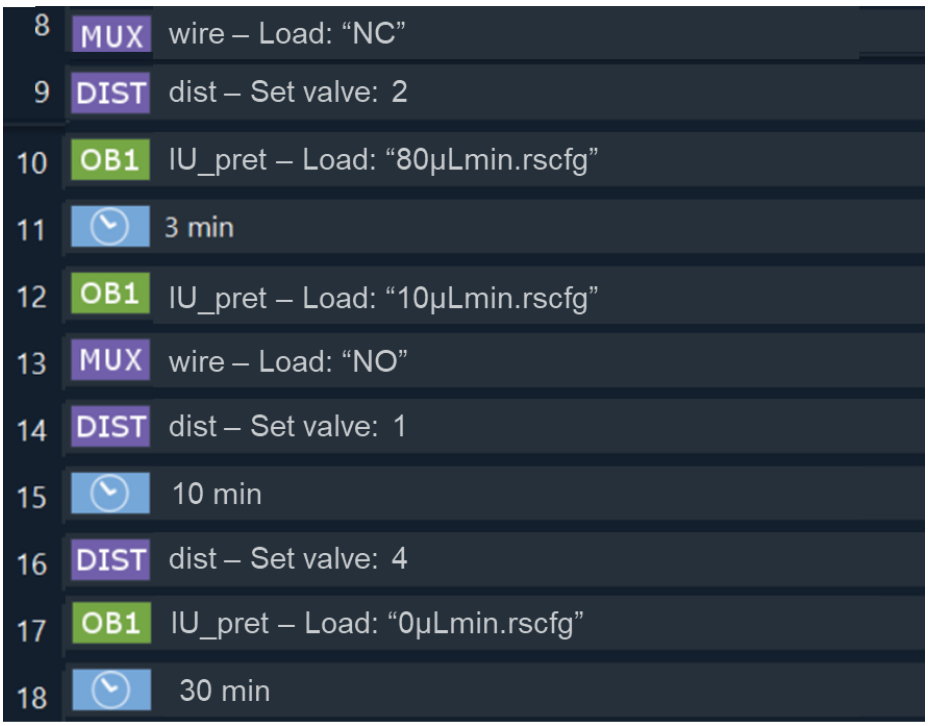


c) Repeat step (a) to rinse cell with PBS.

d) Fill chip with stain #2 and incubate for 30 min.

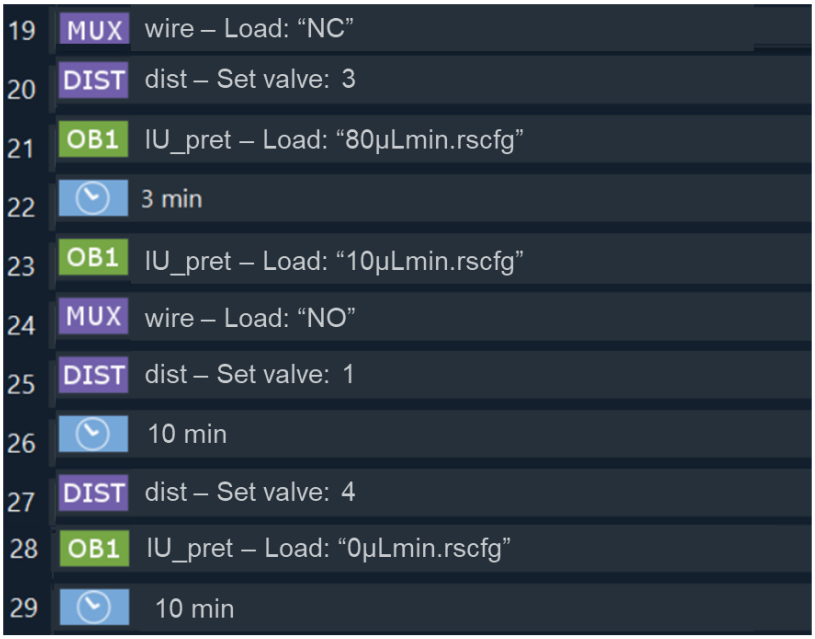


e) Repeat step (a) to rinse cell with PBS.

*f)* Chip is ready for imaging.

## Results

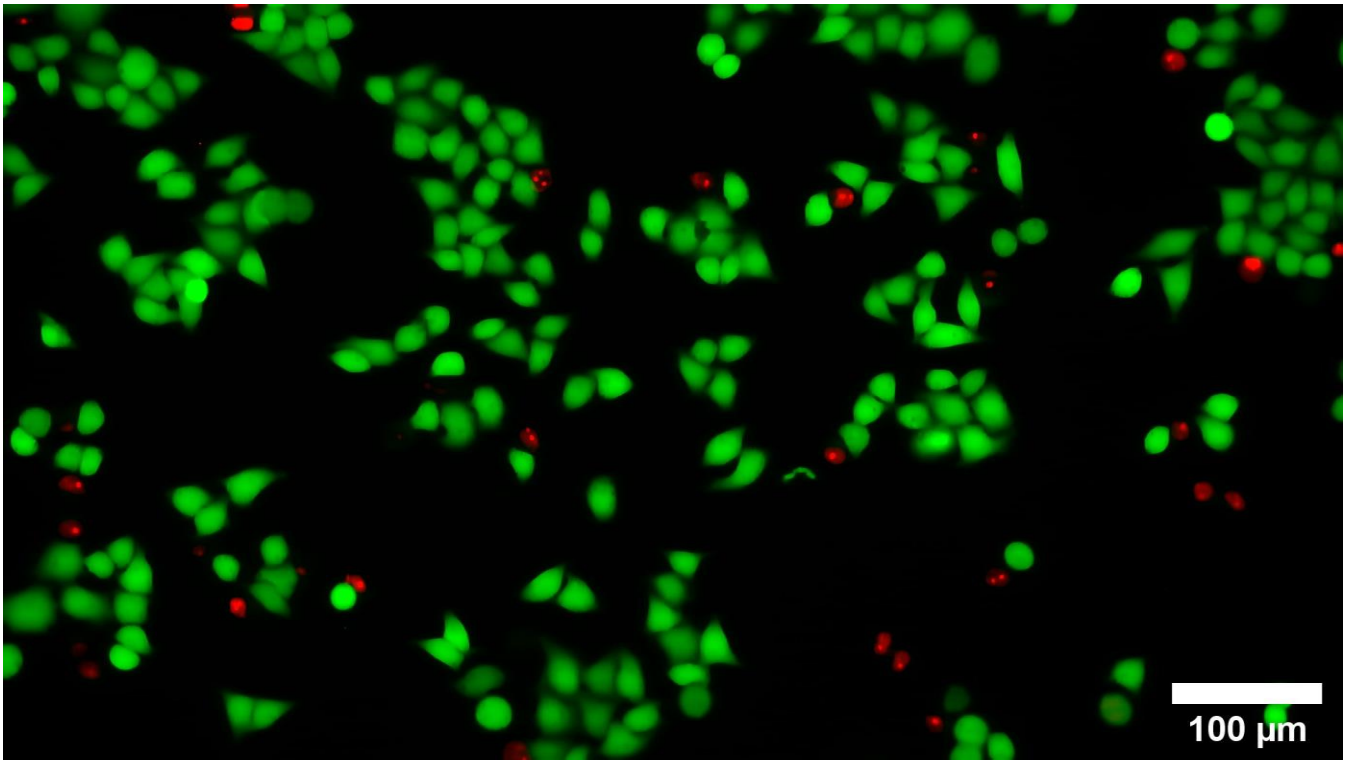


LIVE/DEAD staining of HeLa cells (Calcein AM and propodium iodide, merged image)

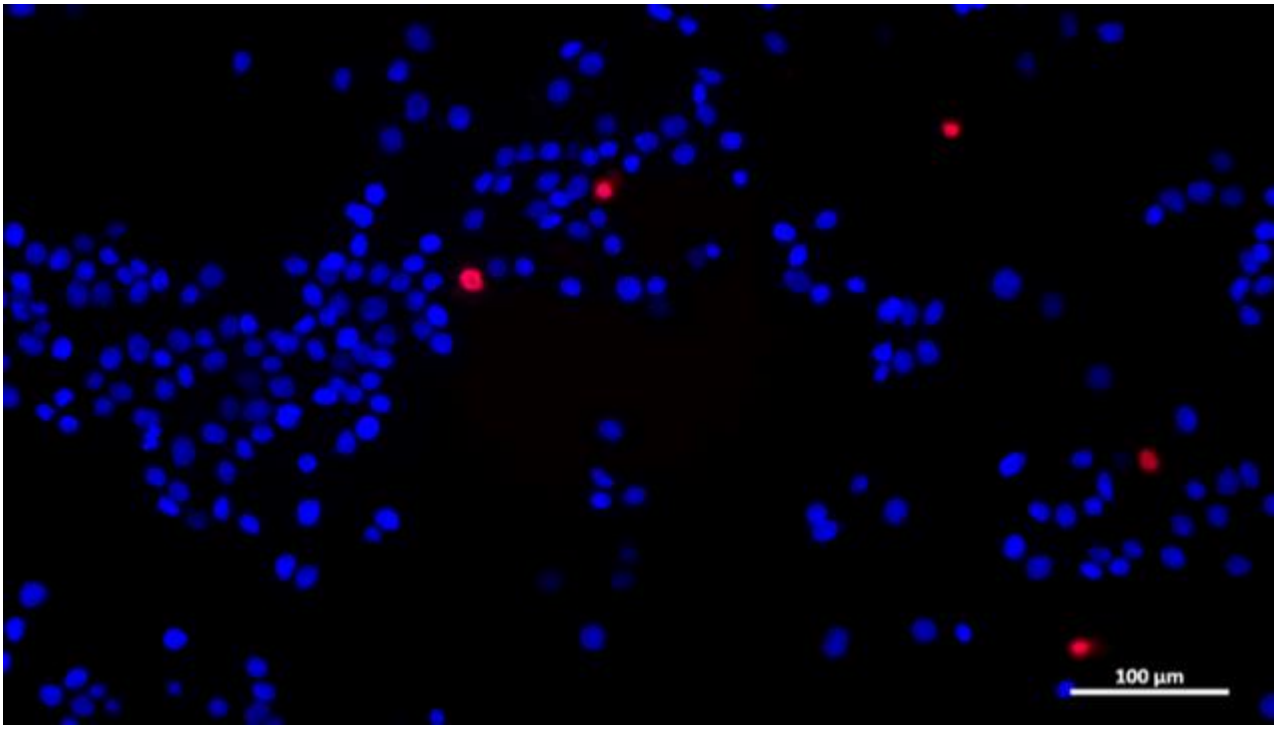


LIVE/DEAD staining of MCF7 cells (Hoechst 33342 and propodium iodide, merged image)

## Acknowledgements

This application note is part of a project that has received funding from the European Union's Horizon 2020 research and innovation programme under grant agreement No 766007.

## Troubleshooting

***I'm having trouble keeping the flow rate steady.***
Check the height of the OB1, reservoir chip and exit (waste container). Adjust the Flow Sensor feedback to increase the pressure required to maintain constant flow rate. Adding more resistance tubing will also provide more tolerance for small changes and differences in height.

***How do I know when the stain has reached my chip? Options to speed up the flow of stain to my chip?***
Measure and cut each piece of tubing in a precise round number length. Calculate volume of lines ($\pi$r2h) and set a constant flow rate, then use a timer, or program the ESI sequence scheduler.

# Résumé

## 1. Introduction

La "microfluidique" désigne les phénomènes physiques et le domaine de recherche impliquant la manipulation de fluides dans des géométries à l'échelle du micron.[1] Dans la recherche biologique et médicale, le potentiel des techniques microfluidiques pour améliorer le débit des analyses, la consommation d'échantillons et de réactifs, les capacités d'automatisation, ainsi que pour apporter de nouvelles fonctionnalités au-delà des techniques conventionnelles est évident. [2]

L'utilisation de la technologie microfluidique pour la recherche biomédicale a connu une croissance importante au cours des deux dernières décennies. Les « organes-sur-puce» (OOC) sont des systèmes microphysiologiques qui visent à reproduire les aspects structurels et fonctionnels des tissus et organes humains, en utilisant la technologie microfluidique.[3] Ces modèles in vitro avancés intègrent des cellules humaines vivantes sur une puce microfluidique et régulent des paramètres clés, tels que les gradients de concentration, les contraintes de cisaillement, les interfaces tissulaires et les architectures de type organe, au moyen de la microfluidique et de la microtechnique. Diverses fonctions organiques humaines ont été modélisées à l'aide de la technologie OOC, notamment les poumons, l'intestin, le cœur, les reins, les os et le cerveau (**Figure 1**). L'intérêt croissant pour les systèmes OOC est largement motivé par leur potentiel d'intégration dans le développement de médicaments, en passant par leur découverte précoce, jusqu'au dépistage préclinique, aux tests et à l'application de nouveaux médicaments, comblant ainsi le fossé entre les études animales et les essais cliniques impliquant des sujets humains.
Les systèmes OOC présentent deux caractéristiques déterminantes : ils sont constitués de plusieurs types de cellules qui ont une disposition tridimensionnelle, physiologiquement pertinente, et ils incorporent des forces biomécaniques (telles que l'étirement des tissus ou les forces de cisaillement hémodynamiques) pertinentes pour le tissu en question. [4]

L'un des principaux défis de l'ingénierie des OOC est de trouver des matériaux appropriés pour la fabrication des dispositifs.[5] Ce défi s'étend largement au-delà des OOC pour inclure la microfluidique dans les essais à base de cellules. Le choix des matériaux utilisés pour créer un dispositif microfluidique est essentiel pour sa

fonction finale. Un matériau donné doit être évalué sous deux angles : ses propriétés et ses procédés de fabrication. Ce dernier point est particulièrement important lorsque des géométries complexes sont souhaitées. Les premiers dispositifs microfluidiques ont été fabriqués en verre ou en silicium, adoptant directement les techniques de microfabrication de l'industrie des semi-conducteurs. C'est à la suite de l'introduction de dispositifs microfluidiques à base de PDMS et de son procédé de fabrication associé, la lithographie douce (**Figure 1**), par Whitesides et ses collaborateurs dans les années 90 (plusieurs années après les premiers dispositifs en verre et en silicium), que le domaine de la microfluidique a connu sa percée.[6,7]

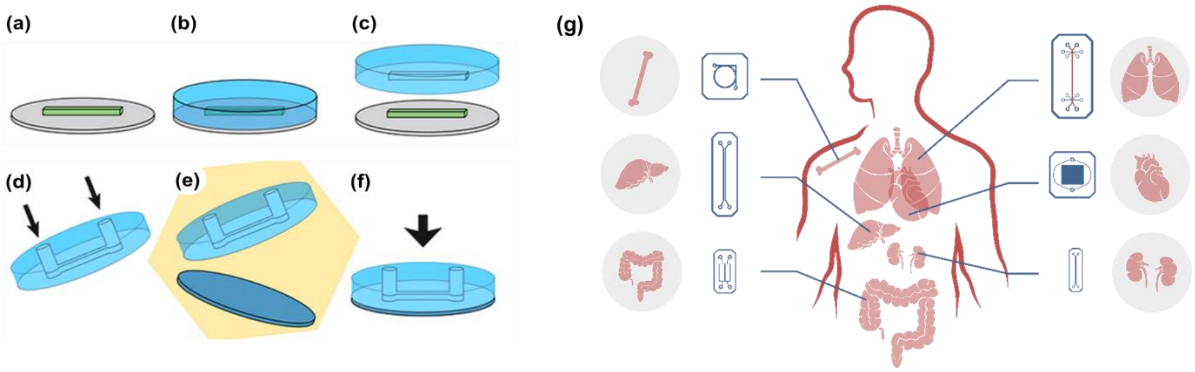


**Figure 1.** Lithographie douce au PDMS. Le procédé, partant d'un moule microfluidique (a), comprend les étapes suivantes : (b) coulée de PDMS sur le moule microfluidique, (c) libération de la réplique de PDMS, (d) poinçonnage de trous pour l'interface fluide, (e) activation de surface par plasma des deux composants du dispositif (PDMS et une lame de verre) et (f) collage du dispositif en plaçant les surfaces activées par plasma en contact conforme. Adapté de Velve-Casquillas et al.[8] avec la permission d'Elsevier. (d) Illustration de systèmes d'organes humains sur puce (OOC), notamment des modèles d'os, de foie, d'intestin, de poumon, de cœur et de rein sur puce.

Actuellement, le polydiméthylsiloxane (PDMS) est le matériau de fabrication le plus largement adopté pour la recherche microfluidique et OOC.[5] Grâce à sa faible rigidité ajustable, à sa manipulation facile et à son processus de moulage abordable, les dispositifs en PDMS de structures complexes peuvent être réalisés sans équipement ou savoir-faire spécialisé.[6] Le PDMS est également biocompatible, perméable aux gaz et possède d'excellentes propriétés optiques. Ces aspects en font un matériau de choix pour les études biologiques, en particulier lorsque l'évaluation par microscopie à fluorescence est nécessaire.[9–11] Cependant, le PDMS présente un certain nombre d'inconvénients. Bien que la fabrication de dispositifs en PDMS soit facile, le processus en plusieurs étapes ne se prête pas bien à une mise à l'échelle industrielle.[12] En outre, l'absorption de petites molécules hydrophobes dans le matériau [13] est problématique dans les applications qui impliquent des facteurs solubles, tels que les petits médicaments, les colorants et les composés de signalisation cellulaire.[14] De

même, on a observé que la nature hydrophobe du PDMS, qui entraîne une adsorption non spécifique des biomolécules à sa surface, réduit les performances du système pour ce qui concerne la séparation et la bio-détection.[15] Une technique courante pour rendre la surface du PDMS hydrophile est l'activation de surface par plasma. Cependant, en raison de la mobilité de la chaîne polymère, la surface du PDMS retrouve rapidement un état hydrophobe.[16] Les problèmes mentionnés ci-dessus peuvent être résolus avec des matériaux plus inertes tels que les thermoplastiques durs, comme le polystyrène, le polycarbonate ou les copolymères d'oléfines cycliques [17–19]. Cependant, avec des modules de traction de l'ordre de 1 à 4 GPa pour ces matériaux [20], le processus de fabrication devient moins accessible, nécessitant des moules coûteux et des instruments spécialisés.

Le besoin de nouveaux matériaux autres que le PDMS pour la fabrication d'OOC a été largement reconnu, et s'applique également à d'autres applications biomédicales des dispositifs microfluidiques.[4,21] Des procédures de prototypage transférables et une meilleure adoption des concepts de fabrication évolutive, de normalisation et d'intégration des systèmes au stade du prototypage pourraient aider à combler le fossé entre le monde universitaire et l'industrie.[22] Une catégorie particulièrement prometteuse de nouveaux matériaux émergents est celle des élastomères thermoplastiques (sTPE). sTPE promet de combiner l'aspect de prototypage simple du PDMS avec la transférabilité de la fabrication des thermoplastiques.[25–27] L'un de ces matériaux, un copolymère séquencé styrénique flexible, a récemment été commercialisé sous le nom de FlexDym™ et a démontré des propriétés favorables à la fabrication de dispositifs microfluidiques.[28] Il est optiquement transparent et présente un faible module de traction d'environ 1 MPa, permettant un gaufrage souple à haute résolution pour créer des dispositifs de structures microfluidiques complexes. Un deuxième fluoropolymère thermoplastique, Fluoroflex, a été développé par les créateurs de Flexdym™ avec des applications microfluidiques en chimie en tête. Fluoroflex se comporte de manière similaire à son polymère frère à base de polystyrène en termes de traitement.[29]

*L'objectif de ce projet de doctorat industriel est d'évaluer le potentiel de deux nouvelles formulations de sTPE : FlexDym™ et Fluoroflex en tant que matériaux pour le prototypage de dispositifs microfluidiques dans le contexte d'études de culture cellulaire, comme une étape vers la mise en œuvre dans la technologie OOC, au moyen de la caractérisation des matériaux et des microfluidiques et d'études de preuve de concept.*

## 2. Résultats et discussions

Nous avons évalué le potentiel de deux nouveaux matériaux sTPE, FlexDym™ et Fluoroflex, comme matériaux de prototypage pour les dispositifs de culture cellulaire microfluidique au moyen d'études de caractérisation des matériaux et de preuve de concept. L'étude sert de première étape vers l'évaluation de leur aptitude à la fabrication de OOC.

### I. Évaluation du sTPE pour les applications dans les études microfluidiques pour culture cellulaire

La première section présente la caractérisation matérielle et microfluidique de FlexDym™ et Fluroflex pour des applications dans la culture cellulaire microfluidique. La caractérisation des matériaux visait à combler les lacunes existantes en matière de connaissances nécessaires pour mieux comprendre le potentiel des matériaux sTPE pour les utilisations de culture cellulaire microfluidique. Les systèmes microfluidiques à base d'élastomères thermoplastiques souples (sTPE) ont déjà été utilisés pour la culture cellulaire microfluidique [26,30]. Cependant, il y a eu peu de données publiées associées au Flexdym™ et à sa mise en œuvre pour des systèmes de culture cellulaire. Les dispositifs Fluoroflex ont été développés pour des applications de microfluidique en chimie à base de gouttelettes.[29] Il n'y a cependant pas eu de démonstrations antérieures utilisant Fluoroflex pour des applications biologiques.

Nous avons démontré que FlexDym™ et Fluoroflex, sont bien adaptés à la fabrication de dispositifs microfluidiques avec des applications en biologie cellulaire telles que les études OOC. Les deux matériaux offrent une méthodologie de fabrication simplifiée qui permet un prototypage économique et rapide des dispositifs microfluidiques. Contrairement aux procédures de lithographie douce du PDMS, le traitement du sTPE est transférable à travers les échelles de fabrication, ce qui pourrait constituer une étape importante pour combler le fossé entre les laboratoires de recherche et l'industrie.[31]

Les matériaux sTPE ont montré une excellente biocompatibilité (**Figure 2**). Le FlexDym™ a pu être efficacement hydrophilisé par un traitement au plasma d'oxygène qui a montré une stabilité prolongée par rapport au PDMS, mais pas au-delà de 7 jours. Une étape de traitement au plasma de faible puissance de 2 minutes était suffisante pour favoriser la fixation des cellules. Le traitement au plasma de

Fluoroflex a montré une réduction minimale de l'hydrophobie de la surface, mais les cellules ont pu adhérer et se développer sur les surfaces natives de Fluoroflex.

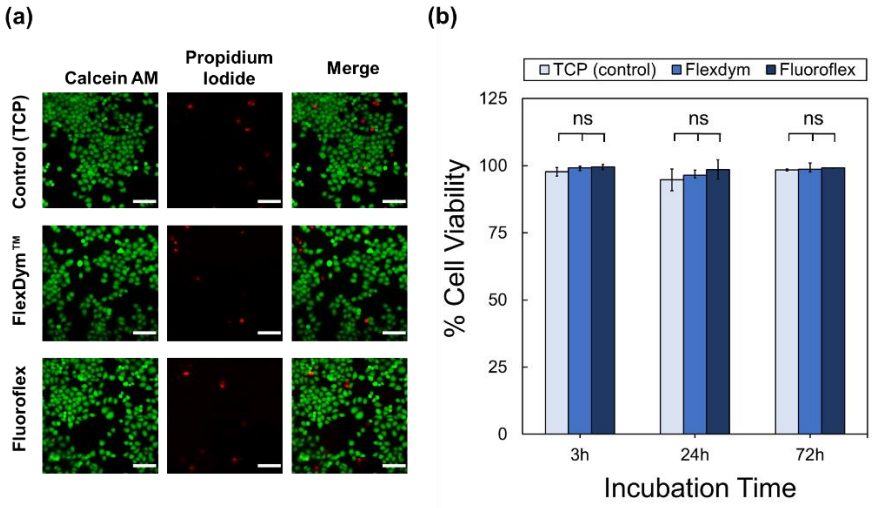


**Figure 2.** Coloration et quantification de la viabilité cellulaire LIVE/DEAD des cellules HeLa. (a) Images de microscopie fluorescente de cellules viables colorées par la calcéine AM (vert) et de cellules mortes colorées par l'iodure de propidium (rouge) sur les substrats TCP (contrôle), FlexDym™ et Fluoroflex après 24 heures d'incubation. Barres d'échelle 200 µm. (b) Une viabilité cellulaire élevée (> 90%) a été observée pour les cellules cultivées sur TCP, FlexDym™ (FD) et Fluorflex (FF) après 3, 24 et 72 heures d'incubation. Ns indique l'absence de différence statistique ($p > 0,05$, $n = 3$ pour chaque ensemble de données, les barres d'erreur représentent un écart-type).

De plus, il a été démontré que les dispositifs sTPE étaient adaptés aux expériences de culture cellulaire dynamique sur puce. Nous avons présenté des procédures complètes pour réaliser une culture cellulaire dynamique dans des dispositifs sTPE, y compris l'interfaçage de la puce avec l'instrumentation de contrôle du flux, l'ensemencement des cellules dans des dispositifs microfluidiques et la culture sur puce sous perfusion constante de milieux de culture. Il a été démontré que les dispositifs FlexDym™ et Fluoroflex pouvaient supporter la culture de cellules HeLa dans des canaux microfluidiques fermés jusqu'à 5 jours, une première étape importante vers la mise en œuvre des matériaux pour les études cellulaires microfluidiques basées sur la perfusion et les études OOC (**Figure 3.**).

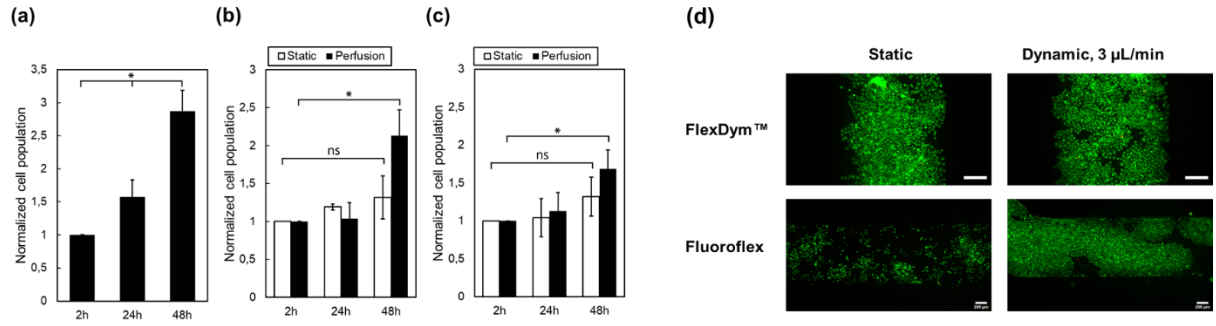


**Figure 3.** Culture de cellules HeLa dans des conditions de perfusion statiques et dynamiques. (a) Prolifération des cellules HeLa dans une macro-culture de méthode standard (plaques à 6 puits). Prolifération des cellules HeLa dans des dispositifs microfluidiques de (b) FlexDym™ et (c) Fluoroflex dans des conditions statiques et dynamiques. Ns indique aucune différence statistique, * indique une différence statistique ($p > 0,05$, $n = 3$ pour chaque ensemble de données, les barres d'erreur représentent l'erreur standard). (d) Images représentatives, obtenues par microscopie à fluorescence, de cellules HeLa cultivées dans les dispositifs FlexDym™ et Fluoroflex, dans des conditions statiques et sous perfusion constante de milieux à 3 µL/min, pendant 5 jours. Les cellules viables sont colorées avec de la calcéine AM (vert) et les cellules mortes sont colorées avec de l'iodure de propidium (rouge). Les barres d'échelle représentent 200 µm.

Dans la quête de matériaux flexibles, optiquement transparents et offrant des possibilités de fabrication faciles, FlexDym™ et Fluroflex sont des candidats prometteurs pour une large gamme de bio-essais microfluidiques, y compris la technologie OOC.

## II. Plate-forme microfluidique en élastomère thermoplastique pour le traitement combinatoire automatisé des cellules cardiaques

Cette section décrit la conception et l'évaluation de la preuve de concept d'un dispositif microfluidique à base de sTPE et d'une plateforme de contrôle automatisé des fluides pour les études à haut débit de la physiologie des cardiomyoblastes. Nous avons évalué la fixation durable des cellules de cardiomyoblastes dans les dispositifs sTPE par rapport aux dispositifs PDMS et nous avons effectué un traitement au palmitate sur puce. Dans les cardiomyoblastes transfectés avec (Caveolin-3) Cav-3-GFP et (Apolipoprotein O) ApoO, des effets physiologiques d'apoptose et de production de ROS ont été observés (**Figure 4**). Il a été suggéré que l'expression de Caveolin-3 (Cav-3) est positivement corrélée au stress métabolique induit par l'ApoO.[32] À notre connaissance, c'est la première fois qu'un effet physiologique sur les cellules a été observé dans des dispositifs microfluidiques à base de FlexDym™. Par rapport au système PDMS, les systèmes sTPE ont démontré un protocole plus rationalisé pour l'ensemencement des cellules, une évaporation réduite des milieux

de la chambre de culture et une meilleure compatibilité avec la coloration cellulaire des lipides.

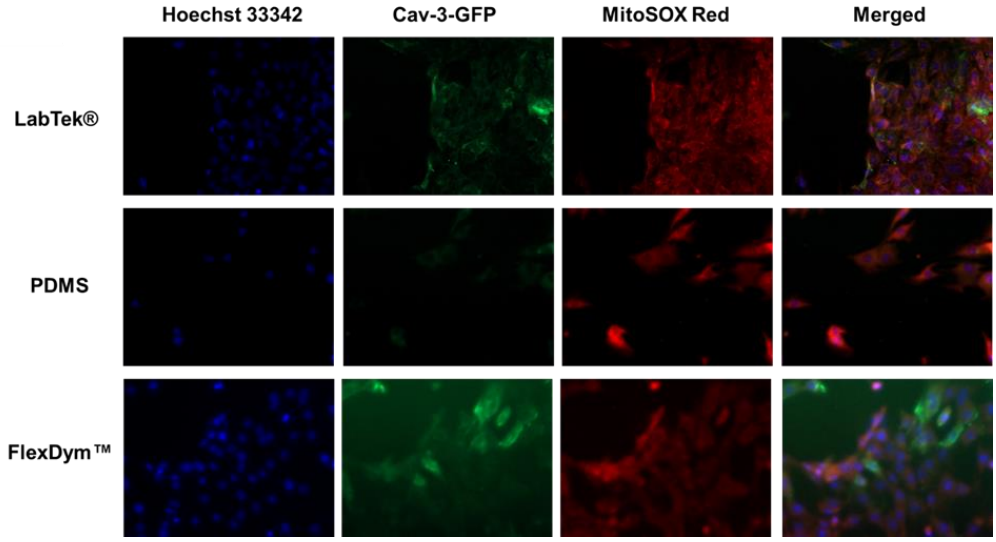


**Figure 4.** Traitement au palmitate des cellules ApoO Cav-3 dans des dispositifs microfluidiques. (a) L'apoptose cellulaire, indiquée par des flèches, a été déterminée par la coloration des noyaux au Hoechst 33342. (b) Images fluorescentes représentatives des cellules Cav-3 ApoO après traitement au palmitate dans des dispositifs LabTek®, PDMS et FlexDym™, montrant les noyaux (bleu), Cav-3 (vert) et le superoxyde dans les mitochondries (rouge). Grossissement de 20X.

Nous avons également développé un circuit microfluidique pour la livraison contrôlée à haut débit de facteurs solubles aux dispositifs FlexDym™ (**Figure 5**). La plateforme a été mise en œuvre dans un laboratoire de biologie, et pouvait effectivement traiter 10 dispositifs simultanément avec la capacité de parallélisation supplémentaire. Un protocole entièrement automatisé a été développé et validé pour le traitement d'une nuit avec du palmitate et la coloration ultérieure avec deux sondes fluorescentes et les étapes de lavage sans intervention de l'utilisateur. Le circuit microfluidique doté de capacités d'automatisation est très polyvalent, et le moment et la durée de l'apport fluidique peuvent être ajustés à la demande. L'approche "plug-and-play" que nous présentons dans ce chapitre représente une solution accessible pour l'injection séquentielle qui est compatible avec les puces microfluidiques disponibles dans le commerce et peut être facilement intégrée dans un laboratoire de biologie. Cette configuration est donc idéale à des fins de prototypage et pourrait potentiellement contribuer à rendre la microfluidique plus accessible au-delà des laboratoires de recherche spécialisés en microfluidique.

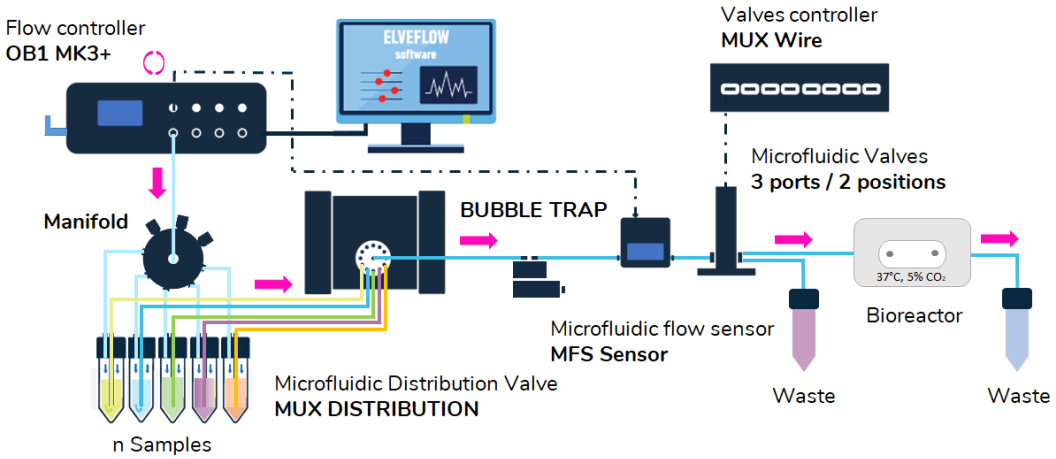


**Figure 5.** Schéma d'une plateforme microfluidique de contrôle de flux pour l'injection séquentielle de fluides, composée d'un contrôleur de pression OB1 (non visible sur la figure), de réservoirs de fluides, d'une vanne rotative, d'un capteur de flux, d'un piège à bulles, d'une vanne 2/3 voies et d'une puce microfluidique sTPE. La puce microfluidique contenant les cellules se trouve dans un incubateur de culture cellulaire dont la température (37°C) et le niveau de CO2 (5%) sont contrôlés.

## III. Fabrication rapide de dispositifs microfluidiques en élastomère thermoplastique intégrés à une membrane

Les propriétés élastiques et thermoplastiques des matériaux Flexdym™ ont été exploitées pour créer une étanchéité réversible aux matériaux thermoplastiques par des méthodes simples. Ce travail décrit la fabrication rapide d'un système microfluidique pour la culture de cellules à base de membranes, composé d'une membrane poreuse en polycarbonate disponible dans le commerce, suspendue entre deux microcanaux Flexdym™. Il a été démontré que les systèmes de culture cellulaire à membrane sont utiles pour modéliser les barrières tissulaires, comme dans le cas de la technologie émergente des organes sur puce, qui a suscité beaucoup d'attention pour sa valeur potentielle dans la découverte de médicaments et la modélisation des maladies [33–35]. Grâce à l'utilisation de l'embossage à chaud, de l'auto-scellage assisté par la chaleur et de composants exclusivement disponibles sur le marché, le protocole développé améliore la vitesse, la simplicité et la transférabilité de la fabrication, par rapport aux systèmes équivalents en PDMS (**Figure 5**).

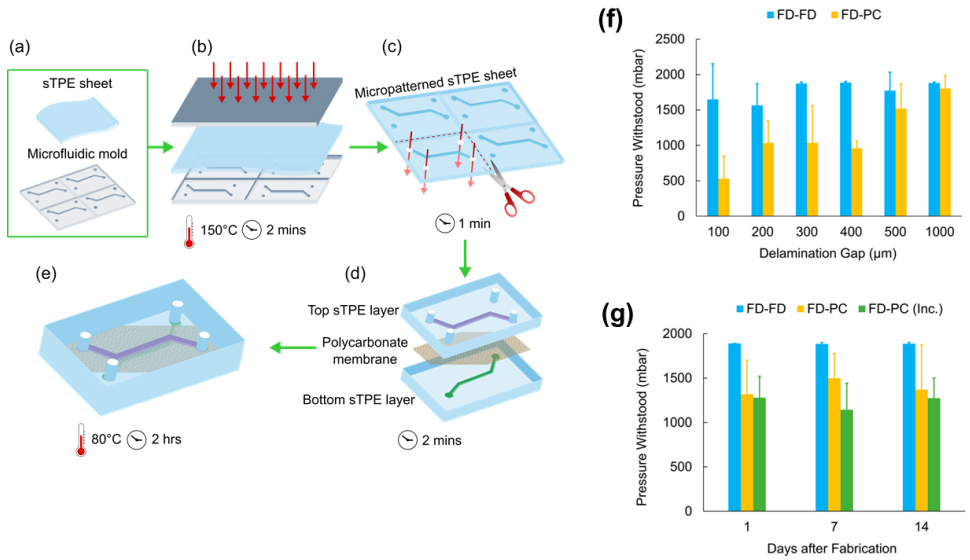


**Figure 6.** Microfabrication d'un dispositif composite FlexDym-PC comprenant les étapes suivantes : (a) une feuille de sTPE et un moule microfluidique, (b) gaufrage à chaud, (c) découpe et poinçonnage de trémies d'accès, (d) assemblage du dispositif, et, (e) collage thermique du dispositif. (f) Évaluation du collage FlexDym™-polycarbonate (FD-PC) et FlexDym™- FlexDym™ (FD-FD) par le biais d'un essai de délamination sous pression de dispositifs présentant des distances d'écartement de 100 à 1000 µm. Les dispositifs FD-PC présentent une force de collage réduite par rapport au collage FD-FD, mais résistent de manière fiable à des pressions de 500 mbar à des distances d'écartement de 200 µm et plus. (g) Test de délamination sous pression des dispositifs FD-FD et FD-PC (distance fixe de 400 µm) à 1, 7 et 14 jours après la fabrication. Un ensemble supplémentaire de dispositifs FD-PC a été vieilli dans des conditions d'incubation à 37 °C et à humidité élevée (Inc.), ce qui n'a révélé aucun impact significatif sur l'étanchéité du dispositif en raison du temps écoulé après la fabrication ou des conditions d'incubation (n=5 dispositifs par ensemble de données ; les barres d'erreur représentent un écart type). Reproduit de la réf.* (voir page 1) avec la permission de MDPI.

Nous avons évalué l'intégrité du dispositif en évaluant la liaison entre le FlexDym™ et la membrane PC par des tests de délamination automatisés à l'aide d'une configuration de délamination conçue sur mesure. La force de collage mesurée était supérieure à 500 mbar pour des distances de collage de 200 µm et plus, une capacité de pression largement suffisante pour les applications de culture cellulaire microfluidique (**Figure 6**). Nous avons confirmé qu'il n'y avait aucune dégradation de la force de collage dans des conditions de culture cellulaire ou en raison d'une pressurisation à long terme. En outre, nous avons démontré qu'un collage fiable du FlexDym™ pouvait être réalisé à température ambiante pour un temps de collage aussi court que 5 minutes, et que le FlexDym™ pouvait former une liaison solide avec divers matériaux microfluidiques, notamment le polystyrène, le COP et le PMMA. La procédure de collage facile démontre la polyvalence de FlexDym™ pour la fabrication de dispositifs composites avec d'autres matériaux que le PC.

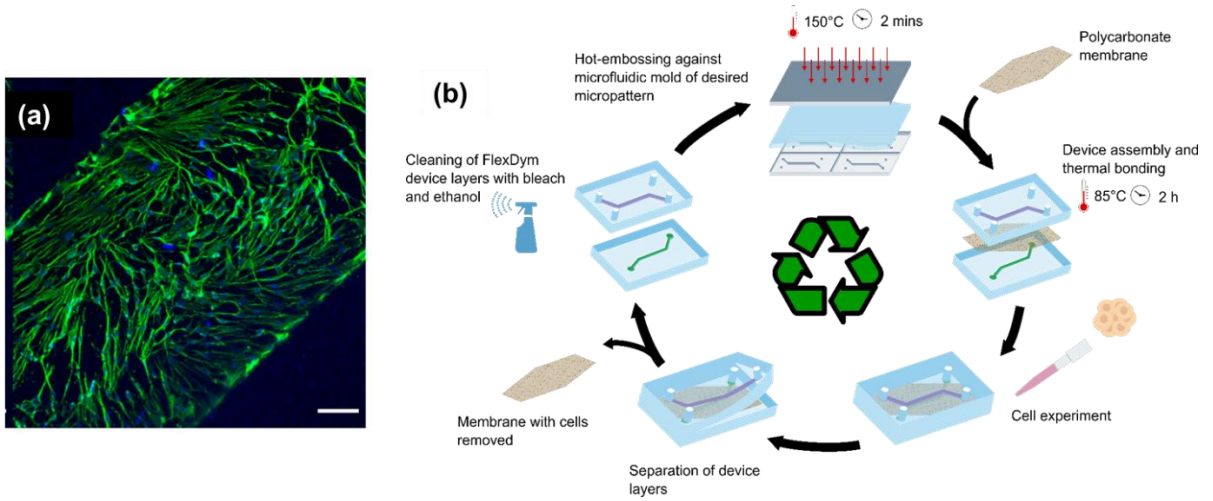


**Figure 7.** (a) Image représentative de fibroblastes dermiques humains (HDF) cultivés dans des dispositifs composites FlexDym™-PC pendant 7 jours. Les HDF ont été cultivées sur le dessus de la membrane PC pendant 7 jours avant d'être fixées et colorées avec de la phalloïdine 488-Alexa Fluor™ 488 (coloration de la F-actine, en vert) et du DAPI (nucléaire, en bleu) pour démontrer l'adhésion cellulaire et la présence maintenue en culture statique dans les dispositifs jusqu'à 1 semaine. Les barres d'échelle représentent 150 µm. Reproduit de la réf.* (voir page 1) avec la permission de MDPI. (b) Aperçu schématique du processus de recyclage. Un dispositif composite FlexDym™-PC a été fabriqué à partir de feuilles FlexDym™ vierges (R0) et de membranes PC. Le dispositif a été utilisé pour une expérience de biologie cellulaire, puis séparé et la membrane a été retirée. Les couches de FlexDym™ ont été nettoyées chimiquement et physiquement à l'aide d'un solvant et d'une sonication par ultrasons, séchées et remodelées par gaufrage à chaud dans un nouveau dispositif.

Des fibroblastes dermiques humains ont pu être cultivés sur la membrane PC pendant une semaine, soulignant l'utilisation potentielle des dispositifs pour la culture cellulaire microfluidique sur membrane, comme pour les applications OOC (**Figure 7**). Nous démontrons également un processus de recyclage simple qui permet de réutiliser plusieurs fois les matériaux des dispositifs composites, dans le but de réduire les déchets de matériaux au stade du prototypage (**Figure 7**). Dans l'ensemble, ce travail répond au besoin de nouveaux matériaux pour la culture cellulaire microfluidique [36], en introduisant une plateforme microfluidique sans PDMS, avec une géométrie couramment utilisée pour les dispositifs OOC et une méthodologie de fabrication qui représente une solution rapide, facile et transférable.

## 3. Conclusion générale

Cette thèse a présenté une évaluation de nouveaux matériaux et le développement de nouvelles techniques de fabrication pour le prototypage de dispositifs microfluidiques. Elle visait à évaluer l'utilité des dispositifs sTPE pour la recherche en biologie cellulaire par des démonstrations de preuve de concept, et à remédier aux inconvénients associés aux matériaux actuels de prototypage microfluidique.

Dans l'ensemble, les matériaux sTPE présentent une multitude de propriétés qui en font une alternative intéressante au PDMS pour la fabrication d'OOC. Cependant, d'autres études de preuve de concept sont nécessaires pour vérifier l'utilité des systèmes OOC à base de sTPE. L'utilisation actuelle du PDMS pour le prototypage d'OOC fait partie des obstacles à la mise en œuvre complète de cette technologie dans l'industrie pharmaceutique et les laboratoires de biologie. De nouveaux matériaux de prototypage pouvant être utilisés dans le cadre de la recherche, avec un potentiel de transfert technologique direct vers la production industrielle, pourraient être précieux pour la progression du domaine tant au niveau de la recherche que pour accélérer les transferts technologiques vers l'industrie.

# 4. Références


1. Venkatesan, S., Jerald, J., Asokan, P. & Prabakaran, R. A Comprehensive Review on Microfluidics Technology and its Applications. in *Lecture Notes in Mechanical Engineering* 235–245 (Springer Singapore, 2020).
2. Franke, T. A. & Wixforth, A. Microfluidics for Miniaturized Laboratories on a Chip. *ChemPhysChem* **9**, 2140–2156 (2008).
3. Convery, N. & Gadegaard, N. 30 years of microfluidics. *Micro Nano Eng.* **2**, 76–91 (2019).
4. Low, L. A., Mummery, C., Berridge, B. R., Austin, C. P. & Tagle, D. A. Organs-on-chips: into the next decade. *Nat. Rev. Drug Discov.* **20**, 345–361 (2021).
5. Probst, C., Schneider, S. & Loskill, P. High-throughput organ-on-a-chip systems: Current status and remaining challenges. *Curr. Opin. Biomed. Eng.* **6**, 33–41 (2018).
6. Duffy, D. C., McDonald, J. C., Schueller, O. J. & Whitesides, G. M. Rapid Prototyping of Microfluidic Systems in Poly(dimethylsiloxane). *Anal. Chem.* **70**, 4974–4984 (1998).
7. McDonald, J. C. *et al.* Fabrication of microfluidic systems in poly(dimethylsiloxane). *Electrophoresis* **21**, 27–40 (2000).
8. Velve-Casquillas, G., Le Berre, M., Piel, M. & Tran, P. T. Microfluidic tools for cell biological research. *Nano Today* **5**, 28–47 (2010).
9. Deguchi, S., Hotta, J., Yokoyama, S. & Matsui, T. S. Viscoelastic and optical properties of four different PDMS polymers. *J. Micromechanics Microengineering* **25**, 97002 (2015).
10. Mata, A., Fleischman, A. J. & Roy, S. Characterization of polydimethylsiloxane (PDMS) properties for biomedical micro/nanosystems. *Biomed. Microdevices* **7**, 281–293 (2005).
11. Merkel, T. C., Bondar, V. I., Nagai, K., Freeman, B. D. & Pinnau, I. Gas sorption, diffusion, and permeation in poly(dimethylsiloxane). *J. Polym. Sci. Part B Polym. Phys.* **38**, 415–434 (2000).
12. Capulli, A. K. *et al.* Approaching the in vitro clinical trial: engineering organs on chips. *Lab Chip* **14**, 3181–3186 (2014).
13. Toepke, M. W. & Beebe, D. J. PDMS absorption of small molecules and consequences in microfluidic applications. *Lab Chip* **6**, 1484–1486 (2006).
14. Roman, G. T., Hlaus, T., Bass, K. J., Seelhammer, T. G. & Culbertson, C. T. Sol-gel modified poly(dimethylsiloxane) microfluidic devices with high electroosmotic mobilities and hydrophilic channel wall characteristics. *Anal. Chem.* **77**, 1414–1422 (2005).
15. Shin, S., Kim, N. & Hong, J. W. Comparison of Surface Modification Techniques on Polydimethylsiloxane to Prevent Protein Adsorption. *BioChip J.* **12**, 123–127 (2018).
16. Eddington, D. T., Puccinelli, J. P. & Beebe, D. J. Thermal aging and reduced hydrophobic recovery of polydimethylsiloxane. *Sensors Actuators B Chem.* **114**, 170–172 (2006).
17. Ogończyk, D., Węgrzyn, J., Jankowski, P., Dąbrowski, B. & Garstecki, P. Bonding of microfluidic devices fabricated in polycarbonate. *Lab Chip* **10**, 1324–1327 (2010).
18. Tsao, C. W., Hromada, L., Liu, J., Kumar, P. & DeVoe, D. L. Low temperature bonding of PMMA and COC microfluidic substrates using UV/ozone surface treatment. *Lab Chip* **7**, 499–505 (2007).
19. Young, E. W. K. *et al.* Rapid prototyping of arrayed microfluidic systems in polystyrene for cell-based assays. *Anal. Chem.* **83**, 1408–1417 (2011).
20. Gencturk, E., Mutlu, S. & Ulgen, K. O. Advances in microfluidic devices made from thermoplastics used in cell biology and analyses. *Biomicrofluidics* **11**, 51502 (2017).
21. Campbell, S. B. *et al.* Beyond Polydimethylsiloxane: Alternative Materials for Fabrication of Organ-on-a-Chip Devices and Microphysiological Systems. *ACS Biomater. Sci. Eng.* (2020).
22. Becker, H. Mind the gap! *Lab Chip* **10**, 271–273 (2010).
23. Singh, M. *et al.* 3D printed conformal microfluidics for isolation and profiling of biomarkers from whole organs. *Lab Chip* **17**, 2561–2571 (2017).
24. Wang, Y. I. & Shuler, M. L. UniChip enables long-term recirculating unidirectional perfusion with gravity-driven flow for microphysiological systems. *Lab Chip* **18**, 2563–2574 (2018).
25. Brassard, D. *et al.* 3D thermoplastic elastomer microfluidic devices for biological probe immobilization. *Lab Chip* **11**, 4099–4107 (2011).

26. Guillemette, M. D., Roy, E., Auger, F. A. & Veres, T. Rapid isothermal substrate microfabrication of a biocompatible thermoplastic elastomer for cellular contact guidance. *Acta Biomater.* **7**, 2492–2498 (2011).
27. Roy, E. *et al.* From cellular lysis to microarray detection, an integrated thermoplastic elastomer (TPE) point of care Lab on a Disc. *Lab Chip* **15**, 406–416 (2015).
28. Lachaux, J. *et al.* Thermoplastic elastomer with advanced hydrophilization and bonding performances for rapid (30 s) and easy molding of microfluidic devices. *Lab Chip* **17**, 2581–2594 (2017).
29. McMillan, A. H. *et al.* Self-sealing thermoplastic fluoroelastomer enables rapid fabrication of modular microreactors. *Nano Sel.* **n/a**, (2021).
30. Borysiak, M. D. *et al.* Simple replica micromolding of biocompatible styrenic elastomers. *Lab Chip* **13**, 2773–2784 (2013).
31. Ramadan, Q. & Zourob, M. Organ-on-a-chip engineering: Toward bridging the gap between lab and industry. *Biomicrofluidics* **14**, 41501 (2020).
32. Caubère, C. Molecular and functional interactions between Apolipoprotein O and Caveolin 3 in the heart.Implication in the development of metabolic disorder-associated cardiomyopathy. in (2013).
33. Chan, C. Y. *et al.* Accelerating drug discovery via organs-on-chips. *Lab Chip* **13**, 4697–4710 (2013).
34. Jodat, Y. A. *et al.* Human-Derived Organ-on-a-Chip for Personalized Drug Development. *Curr. Pharm. Des.* **24**, 5471–5486 (2018).
35. Dellaquila, A., Thomée, E. K., McMillan, A. H. & Lesher-Pérez, S. C. Chapter 4 - Lung-on-a-chip platforms for modeling disease pathogenesis. in (eds. Hoeng, J., Bovard, D. & Peitsch, M. C. B. T.-O.) 133–180 (Academic Press, 2020).
36. Cochrane, A. *et al.* Advanced in vitro models of vascular biology: Human induced pluripotent stem cells and organ-on-chip technology. *Adv. Drug Deliv. Rev.* **140**, 68–77 (2019).

Emma THOMÉE

# Development of thermoplastic elastomer microfluidic systems for bio-applications


## Résumé

Depuis son apparition, la technologie microfluidique s'est révélée être un outil puissant en biologie. La manipulation de fluides dans des géométries à l'échelle du micron avec un contrôle fluidique de précision permet l'analyse de cellules cultivées à un débit amélioré et à un coût réduit. Il est nécessaire de trouver de nouveaux matériaux pour le prototypage de dispositifs microfluidiques au-delà du polydiméthylsiloxane (PDMS), afin de combler le fossé entre la microfluidique dans des contextes de recherche à petite échelle et la production industrielle à grande échelle. Les inconvénients associés aux dispositifs en PDMS pour les applications de biologie cellulaire et les organes-sur-puce encouragent la transition vers d'autres matériaux de fabrication. Cette thèse présente une évaluation de nouveaux élastomères thermoplastiques souples et le développement de nouvelles techniques de fabrication pour le prototypage de dispositifs microfluidiques pour des applications biomédicals. Nous démontrons l'utilité des élastomères thermoplastiques souples pour la fabrication transférable de systèmes microfluidiques pour la biologie cellulaire.


**Mots clés :** microfluidique, élastomère thermoplastique, lab-on-a-chip, micro dispositifs biomédicaux, organe-sur-puce


## Résumé en anglais

Since its emergence, microfluidic technology has been demonstrated to be a powerful tool in biology and the life sciences. Manipulation of fluids in micron-scale geometries with precision fluidic control enables analysis of cultured cells at improved throughput and reduced cost. However, there is a need for new materials for microfluidic device prototyping, beyond polydimethylsiloxane (PDMS), to bridge the gap between microfluidics in small-scale research settings and large-scale industrial production. Drawbacks associated with PDMS devices for cell biological applications and organ-on-a-chip are further encouraging a transition to alternative fabrication materials. This thesis presents an evaluation of novel soft thermoplastic elastomers and the development of new fabrication techniques for prototyping of microfluidic devices for bio-applications. We demonstrate the utility of soft thermoplastic elastomers for rapid and transferable device fabrication of microfluidic systems for cell biology research.


**Keywords:** microfluidics, thermoplastic elastomer, lab-on-a-chip, biomedical microdevices, organ-on-a-chip